Metabolic characterization and viable delivery of *Akkermansia muciniphila* for its future application

Kees C. H. van der Ark

Metabolic characterization and viable delivery of *Akkermansia muciniphila* for its future application

Kees C.H. van der Ark

Thesis committee

Promotor

Prof. Dr Willem M. de Vos

Professor of Microbiology

Wageningen University & Research

Co-promotor

Dr Clara Belzer

Assistant professor, Laboratory of Microbiology

Wageningen University & Research

Other members

Prof. Dr E.J. Smid, Wageningen University & Research

Dr N. Juge, Institute of Food Research, Norwich, United Kingdom

Dr H.J.M. Harmsen, University of Groningen

Dr M. Derrien, Danone, Paris, France

This research was conducted under the auspices of the Graduate School VLAG (Advanced studies in Food Technology, Agrobiotechnology, Nutrition and Health Sciences)

Metabolic characterization and viable delivery of *Akkermansia muciniphila* for its future application

Kees C.H. van der Ark

Thesis

submitted in fulfilment of the requirements for the degree of doctor

at Wageningen University

by the authority of the Rector Magnificus,

Prof. Dr A.P.J. Mol,

in the presence of the

Thesis Committee appointed by the Academic Board

to be defended in public

on Monday 22 January 2018

at 4 p.m. in the Aula.

Kees C.H. van der Ark

Metabolic characterization and viable delivery of *Akkermansia muciniphila* for its future application,

236 pages.

PhD thesis, Wageningen University, Wageningen, the Netherlands (2018)

With references, with summaries in English and Dutch

DOI: 10.18174/427507

ISBN: 978-94-6343-825-4

Table of content

Chapter 1. General introduction and thesis outline 7

Chapter 2. More than just a gut feeling: Constraint-based genome-scale metabolic models for predicting functions of human intestinal microbes 39

Chapter 3. Model-driven design of a minimal medium for *Akkermansia muciniphila* confirms mucus adaptation. 69

Chapter 4. The influence of an animal component free medium on cell morphology and therapeutic efficacy of *Akkermansia muciniphila* 97

Chapter 5. Adaptation of *Akkermansia muciniphila* to the oxic-anoxic interface of the mucus layer 125

Chapter 6. Encapsulation of the therapeutic microbe *Akkermansia muciniphila* in a double emulsion enhances survival in simulated gastric conditions 171

Chapter 7. General Discussion 199

Summary 225

Samenvatting 228

About the author 231

Acknowledgements 232

List of Publications 234

Overview of Completed training activities 235

CHAPTER 1

General introduction and thesis outline

General Introduction

This thesis deals with the physiology, growth and application strategy of *Akkermansia muciniphila* (Figure 1). This intestinal bacterium lives in the colon of most humans and mammals, and degrades the mucus that is produced by the specialised epithelial goblet cells of the host. *A. muciniphila* is highly specialised in degrading mucus, hence the species name muciniphila, which loosely translates as 'loving mucin'. The genus name *Akkermansia* derives from Dr. Antoon Akkermans, who was leading the Microbial Ecology group of the Laboratory of Microbiology at Wageningen University at the time *A. muciniphila* was isolated and published (Derrien, et al., 2004). Here an introduction is provided into the role of the intestinal microbiota in health and disease with specific attention for *A. muciniphila*, its properties and impact. In addition, an overview is provided of approaches on how to grow and deliver this intestinal microbe for their application in model animals or human studies.

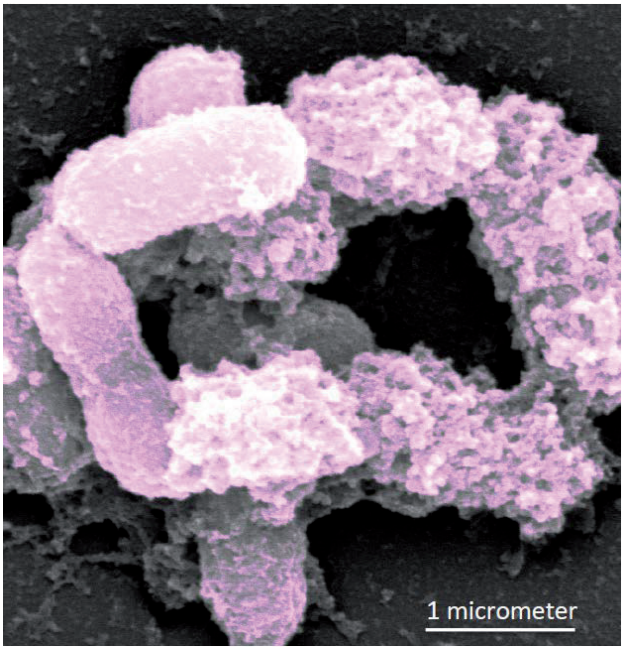

Figure 1. Image of *A. muciniphila* obtained by scanning electron microscopy (Image by Laura Huuskonen).

The role of the faecal microbiota in health and disease

The human colon can be considered as a very densely populated bioreactor. The density of microbial cells can reach 10^{11} cells per gram of faeces for members of the *Bacteria* and 10^{10}

cells per gram of faeces for that of *Archaea*. The amount of eukaryotic cells is approximately 100-1000 fold lower than bacteria and includes protozoa, fungi and multicellular helminths (Berg, 1996, Sender, et al., 2016, Hugon, et al., 2017). It is estimated that the amount of bacteria is similar to the amount of cells in an average human body (Sender, et al., 2016).

The number of cultured microbial species from the gut has been reviewed and found to reach over 1000 (Rajilic-Stojanovic and de Vos, 2014). This number will rapidly increase by the recent isolation of hundreds of new candidate species by high throughput methods (Browne, et al., 2016, Lagier, et al., 2016). The number of prokaryotic species in the gut based on systematic mining of 16S rRNA gene libraries was recently estimated to amount to approximately 2500 (Ritari, et al., 2015). This would suggest that over half of the bacterial gut species have already been cultured. The intestine of a single adult has been estimated to contain at least 500 different bacterial species (Sears, 2005, Steinhoff, 2005). The presence and absence of species is influenced by many different factors, including diet, age, host genomics, use of antibiotics and the environment in general (Greenhalgh, et al., 2016). Colonisation in early life is influenced by the delivery mode, diet and the environment of the baby, including the presence of siblings (Martin, et al., 2016). Early colonizers are mainly species of *Bifidobacteria, Bacteroides* and *Lactobacillus.* This early life event has a lasting influence on the immune system (Gensollen, et al., 2016).

Correlations between gut microbial species composition and a variety of disorders have been described and include many gut-related diseases (Joossens, et al., 2011, Marchesi, et al., 2016), metabolic diseases (Vrieze, et al., 2010) and more recently also brain-related diseases, such as autism and schizophrenia (Dinan, et al., 2013, Zhou and Foster, 2015). However, the causal relationships between changes in the microbiota and the onset and subsequent stages of associated diseases have rarely been addressed (de Vos and de Vos, 2012).

Even though it is debatable what a healthy microbiota composition is (Clemente, et al., 2012), it is possible to treat diseases using faecal microbiota transplantations (FMT), as was already described in scientific literature in 1958 (Eiseman, et al., 1958). Earlier practices of FMT in humans have been documented in the Chinese Djongji dynasty in the fourth century (de Vos, 2013, Zhang, et al., 2013a). This treatment has demonstrated exceptional good results in case of recurrent *Clostridium difficile* infection, showing a therapeutic effect in 90% of the recipients (van Nood, et al., 2013). FMT has also been tested for other diseases and

syndromes, including inflammatory bowel disease (IBD), diabetes and metabolic syndrome, but with lower success rates (Gupta, et al., 2016). Upon FMT, the microbiota of the recipient changes, resulting in a mixture of donor and recipient derived strains (Li, et al., 2016). Initially, it resembles the microbial composition of the donor, but it deviates to an alternative but usually stable composition of either predominantly recipient strains or a mixture of donor and recipient strains (Weingarden, et al., 2015, Li, et al., 2016). The application of FMT and the relations found between changes in the microbiota and diseases calls for mechanistic insights, which can only be obtained with the study of cultured microbes. Therefore, it is important to obtain cultured representatives of all species, and preferably even strains, as will be discussed below (Hugon, et al., 2017) (Figure 2).

It was shown in mouse models that changes or interventions in the microbial composition may have influences on host metabolism and psychology (Dinan, et al., 2013, Plovier, et al., 2017). In addition, alterations and interventions in the gut ecosystem may cause diseases, as was discovered in the Nobel Prize winning case of *Helicobacter pylori,* which can cause ulcerative colitis (Marshall and Warren, 1984, Ahmed, 2005). The influence of bacteria on host health can differ between strains, as was shown for the influence of *F. prausnitizii* in mice (Rossi, et al., 2015, Song, et al., 2016) and the well-described differences between probiotic strains in human (Hill, et al., 2014). So, to study the causal relationships between bacterial species and compositions in general, we need to culture not only all species, but preferably multiple strains per species.

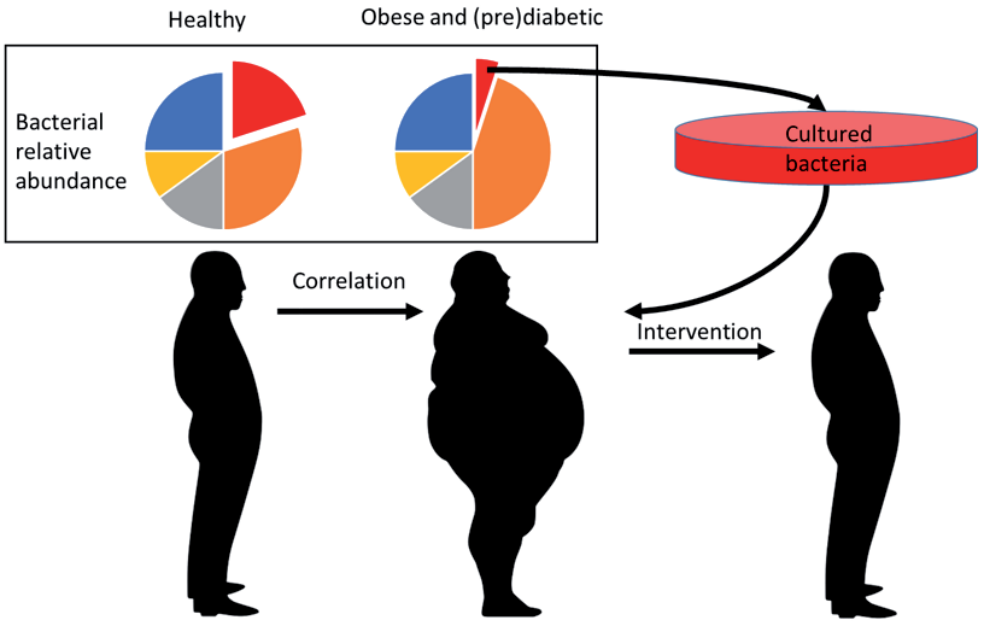

Figure 2. Correlations between bacterial relative abundances and metabolic status can be observed. Cultured representatives of species negatively correlating with disease should be obtained for intervention studies to study the causality.

The niche of *Akkermansia muciniphila* in the colon

The high number species described to be present in the microbiota live in complex microbial-ecologic networks with high competition for nutrients, usually from our diet. There are different ecosystems along the length of the colon, including the caecum, the crypts, the mucus layer and the ascending, transverse and descending colon (Donaldson, et al., 2016). Along the length of the colon, there is a gradient of compounds that are indigestible for humans, but for which the bacteria compete. Therefore, it is important for species to fully utilize the potential of the niche they live in.

An important niche in the colon that is largely independent of our diet is the mucus layer (Figure 3A). It serves as a barrier between the host and the intestinal microbiota, thereby protecting the host, facilitates the flux of digest in the intestine, and provides nutrients to mucolytic bacteria. Studies in mouse and recently also human have shown that the mucus layer can be divided into two separate layers, namely the firm mucus layer and the loose mucus layer (Johansson, et al., 2011, Johansson, et al., 2014). The loose mucus layer is the

result of proteolytic cleavage of the mucins that form the firm mucus layer (Figure 3B). The mucus dependency of *A. muciniphila* locates this bacterium close to the host in the loose mucus layer, leaving only the firm mucus layer as a border between host and bacteria. The mucus layer in the colon measures up to several hundred micrometers, which protects the host against invading bacteria and thereby infections (Hansson, 2012). *A. muciniphila* is commonly found throughout the colonic mucus layer, but has also been found to be present in ileum mucosal biopsies (Wang, et al., 2005). The close proximity to the host could result in direct influences of human metabolic processes on the growth of *A. muciniphila.* Firstly, the host requires oxygen for cells to grow. The oxygen diffuses through the mucus layer into the colon (Figure 3A). This poses challenges and opportunities for a bacterium characterized as strictly anaerobic, such as *A. muciniphila*. Secondly, the host mucus provides nearly all the nutrients that are required by *A. muciniphila*. This results in a nutrient availability that is mainly dependent on host mucin secretion, and not host dietary intake. The presence of mucus throughout the intestine (Donaldson, et al., 2016) would allow colonisation by *A. muciniphila* also in the small intestine. The main constituent of mucus is mucin (Figure 3C). This glycosylated protein consists of a threonine, proline and serine-rich peptide backbone, which is abundantly decorated with O-linked glycans (Figure 3D). Both the glycan and amino acids from the peptide backbone are used by *A. muciniphila.* The uptake of L-threonine by *A. muciniphila* and other mucolytic bacteria during growth in mice was demonstrated by the incorporation of stable isotope (^{13}C and ^{15}N) labelled L-threonine into the bacterial cell. The labelled L-threonine was dosed intravenously and rapidly incorporated in intestinal mucus as this is the fastest dividing tissue in the body, after which bacteria were visualised with fluorescent in situ hybridisation and high-resolution secondary ion mass spectrometry imaging. It was shown that *A. muciniphila* effectively incorporated host-protein derived amino acids *in vivo* (Berry, et al., 2013).

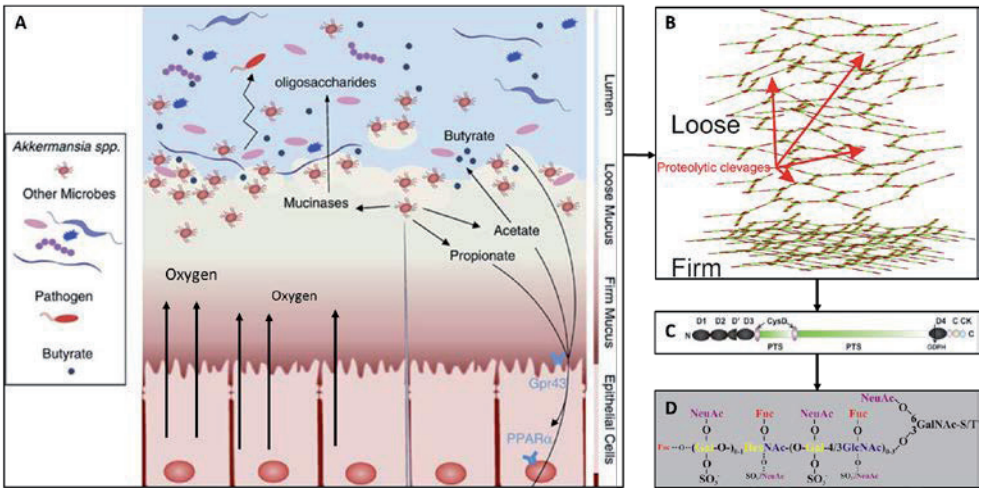

Figure 3. The niche of *A. muciniphila*. (A) Specialized goblet cells secrete mucus that covers the intestinal cells to form the loose and firm mucus layer. Moreover, an oxygen gradient is formed between the epithelial cell and the anaerobic intestinal lumen. *A. muciniphila* resides in this mucus layer and metabolises the mucus to produce and export acetate and propionate. Sugars released by mucinases facilitate the production of butyrate by other bacteria (adapted from (Belzer and de Vos, 2012). (B) The firm mucus layer is composed of linked mucin molecules. Proteolytic cleavages opens this structure to form the loose mucus layer, image from (Johansson, et al., 2011). (C) One mucin molecule is comprised of a C-terminal region and N-terminal region that enclose cysteine rich domains and PTS-domains. The cysteine rich domains form sulphur bridges and the PTS domains are heavily O-linked glycosylated (picture after (Johansson, et al., 2011). (D) Composition of O-linked glycans attached to proline or serine residues in the PTS domain of the mucin molecule (Johansson, et al., 2011).

The mucosal glycans contain a plethora of sugars residues that differ between the types of mucin. The colonic mucin MUC2 contains mannose, N-acetylglucosamine (GlcNAc), N-acetylgalactosamine (GalNAc), galactose and fucose. In addition to the sugars, a glycan can be capped by sulphate and sialic acid residues (Johansson, et al., 2011).

The genome of *A. muciniphila* ATCC BAA-835 is a circular genome of 2.7 Mbp coding for 2,176 protein coding genes, of which 65% was assigned a putative function (van Passel, et al., 2011). A total of 61 genes was annotated to be potentially involved in mucus degradation, including glycosyl hydrolases, sialidases, proteases and sulfatases. This number was later expanded to 78 putative mucus-degrading enzymes (Ouwerkerk, 2016a). *A. muciniphila* is predicted to encode 11 sulfatase and 2 sialidase genes that could be capable of desulfonating and detaching the sialic acid residues from the mucus molecules. *A. muciniphila* cell extract shows sulfatase activity on purified hog gastric mucus (Derrien, et al., 2004). The desulfonation and detachment of sialic acids of mucins makes the glycan groups accessible for *A. muciniphila* (van Passel, et al., 2011, Tailford, et al., 2015).

The degradation of mucosal glycans is not only important for the growth of the mucolytic bacteria, but also releases sugars that can be used by other colonic residents (Derrien, et al., 2004). It was proposed that the released sugars combined with acetate produced by *A. muciniphila* stimulate growth of butyrate producing-bacteria and thereby also the butyrate production (Belzer and de Vos, 2012). This hypothesis was strengthened after the addition of mucus to the *in vitro* intestinal model SHIME, resulting in the M-SHIME model (Van den Abbeele, et al., 2013). The amount of butyrate producing bacteria was increased by the addition of mucus. This interaction was studied in more detail by co-culturing *A. muciniphila* with different butyrate-producing bacteria. This showed that medium containing mucus supported the production of butyrate by co-cultures, while either of the species in pure culture on the same medium did not result in butyrate production (Belzer et al., 2017).

This example of interactions between species shows that gut ecology is difficult to predict. Even when we focus on the ecology of only one niche within the colon, it is still difficult to mechanistically understand what the implications of changes are. In addition, for each species, there are many strains, which vary between individuals. Each strain could have a different influence on the host (Rossi, et al., 2015), so it is important to understand the differentiation between strains of one species, and investigate the role of a strain in its niche.

Strains and species of the family *Akkermansiaceae*

A. muciniphila was the first cultured representative of the *Verrucomicrobiae* phylum from the intestinal microbiota and is found throughout lifetime in the colon in humans (Collado, et al., 2007, Derrien, et al., 2008). In mammals it is the only cultured species, although DNA sequences have been found that could be assigned to species of the *Spartobacteria* family in otters (Ouwerkerk, 2016a). One different species has been isolated from a python and termed *Akkermansia glycaniphila* (Ouwerkerk, et al., 2016b, Ouwerkerk, et al., 2017b). The 16S rRNA gene of *A. glycaniphila* is only 94.4% similar to that of *A. muciniphila*, and its genome shares 79.7% similarity with that of *A. muciniphila*. The growth substrates are like those of *A. muciniphila*. In a recent study, a total of 22 *A. muciniphila* strains were isolated from faecal samples of Chinese adults, which could be grouped in 12 different clusters based on the enterobacterial repetitive intergenic consensus DNA fingerprinting method (Guo, et al., 2016). Different strains of *A. muciniphila* were also isolated from many mammals. Many strains are derived from mice, but isolates have also been obtained from horse, pig, echidna,

apes and elephant (Lagkouvardos, et al., 2016, Ouwerkerk, 2016a). The phylogenetic differentiation of the strains does not follow the phylogeny of the mammals, indicating that the bacteria colonized the gut after the mammals diversified (Derrien, et al., 2010, Ouwerkerk, 2016a).

The isolated *A. muciniphila* species seem to be very conserved among all mammals, including humans. The average genomic nucleotide identity between human isolates is 97.6% and only small differences in genomic organization were observed, including an inversion and two rearrangements (Ouwerkerk, 2016a). Mammalian isolated show a somewhat higher dissimilarity of up to 93.9% genomic nucleotide identity (Ouwerkerk, 2016a). All strains showed highly similar annotations for genes involved in mucus degradation, with a maximum of 3 out of 78 mucus degrading enzymes possibly missing in the chimpanzee isolates. Considering the high similarity between all strains, we focus for the remainder of this thesis only on the type strain *A. muciniphila* strain ATCC BAA-835^T.

The physiology of *Akkermansia muciniphila* strain ATCC BAA-835^T

A. muciniphila is an oval shaped Gram-negative bacterium, and the only cultured representative of the Verrucromicrobiae in the human gut. The typical size of *A. muciniphila* cells is 0.5-1 μm, and the cells appear as either single cells or as diplococci (Derrien, et al., 2004). Like many anaerobic members of the microbiota, *A. muciniphila* was described as a fermentative bacterium that produces short chain fatty acids (SCFA). The definition of fermentation requires the anaerobic degradation of substrates, in which the substrate functions as both electron acceptor and electron donor. When oxygen is used for respiration as well, a bacterium cannot be considered to be fully fermentative. For respiration, a functional electron transport pathway is required, which transports electrons released from sugar degradation, via NADH and membrane-associated quinones to a cytochrome. The cytochrome finally reduces oxygen to water (Willey, 2008).

The substrates used for fermentative degradation can be derived from colonic mucus, since *A. muciniphila* is capable of utilizing mucus as sole carbon, nitrogen and energy source (Derrien, et al., 2004). Predictions on the degradation of monosaccharides released from mucins were done by the interpretation of a genome-scale metabolic model (GEM) obtained for *A. muciniphila* (Ottman, et al., 2017a).

In short, a GEM is a collection of all reactions that are the result of genome annotation. With the addition of model constrains, localisation of the reaction, estimated energy requirements and the determination of biomass composition, the information can be used for a stoichiometric model of metabolism (Baart and Martens, 2012). The model for *A. muciniphila* allowed the prediction on consumption rates of sugars and production rates of SCFAs (Ottman, et al., 2017a). The model accurately predicted the degradation of galactose, fucose and GlcNAc, but did not predict the degradation of GalNAc or the conversion of oxygen (Figure 4).

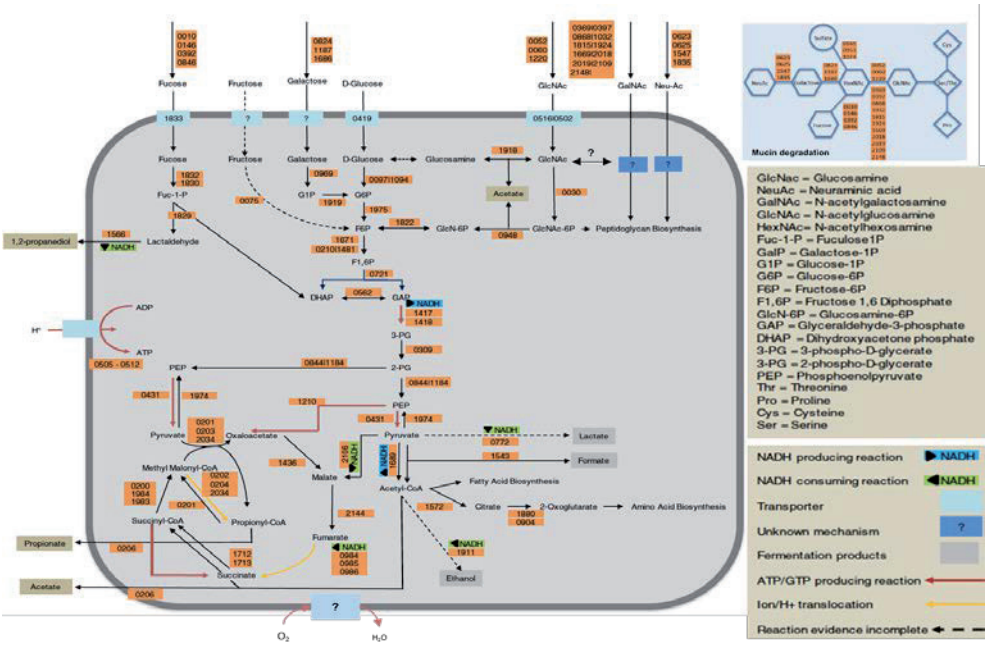

Figure 4. Metabolic overview of *A. muciniphila*. The overview shows the degradation of mucin (top right) and mucosal sugars. The degradation of GalNAc and reduction of oxygen are indicated with a question mark, indicating gaps in the model. Image adapted from (Ottman, et al., 2017a).

The biomass objective function in this model includes all building blocks of the cell (Feist and Palsson, 2010). Combined with the reactions to make these building blocks and the sugar consumption rates, it can also be predicted what the growth rate of the bacterium is. Finally, by summarizing all requirements, it can be predicted what components are essential for growth, which can be used in the definition of a minimal growth medium.

The first interpretation of the *A. muciniphila* model for the composition of a defined medium, showed that L-threonine is essential for growth. This was caused by the absence of a pathway for the synthesis of this amino acid. Moreover, it was predicted that the addition of simple sugars would be sufficient to support growth. These predictions were partly confirmed by growth experiments, in which it was shown that *A. muciniphila* can degrade many sugars, including glucose, GlcNAc, GalNAc and fucose. Additionally, it was shown that the addition of L-threonine increased growth rate and yield (Ottman, et al., 2017a). Still, the addition of undefined components such as large amounts of casein tryptone and mucus, or the use of rich media such as Columbia broth or brain- heart infusion (BHI) broth was needed to obtain growth (Derrien, et al., 2004, Ottman, et al., 2017a). These additions resulted in media with undefined composition that could not fully confirm the predictions obtained from the GEM and hence necessitated the development of a minimal medium.

Besides the metabolic capacities of *A. muciniphila,* it also has some other features that influence its physiology or application. *A. muciniphila* has been found to be sensitive to several antibiotics, including penicillins, macrolides and tetracyclines, but resistant to some others, including fluoroquinoles, aminoglycosides and glycopeptides (Ouwerkerk, 2016a). However, inspection of the genome sequence did not reveal antibiotic resistance genes that are linked to known genetically transferrable elements (Gomez-Gallego, et al., 2016). Recently, another *A. muciniphila* strain was shown to be resistant to fluoroquinol and glycopeptide antibiotics, such as vancomycin and ofloxacin, in the context a broad-spectrum antibiotic isolation procedure on Columbia agar blood plates (Dubourg, et al., 2017).

Akkermansia in health and disease

The relative abundance of gut bacteria has been the main mode of studying the effect of health, disease, genetics and diet on the microbiota composition. In many of these studies, a high relative abundance of *A. muciniphila* has been associated with health or negatively correlated with a disease. For example, in patients suffering acute appendicitis, a negative correlation was found for the abundance of *A. muciniphila* (Swidsinski, et al., 2011). Many other negative correlations have been found between the relative abundance of *A. muciniphila* and a dozen of diseases, including obesity, type 2 diabetes, metabolic syndrome and colonic inflammations and autism in a small-cohort study (Wang, et al., 2011) (see Table 1 for an overview and references).

Table 1. Studies (observational or interventional) related to metabolic disorder and intestinal disorder in which a differential *Akkermansia* abundance was observed. Updated from (Derrien, et al., 2017).

Target **population**	**Study (observational or intervention)**	**Groups (number of individuals)**	**Microbiota analysis approach**	**Samples analysed time**	***Akkermansia* population**	**References**
Obese women	Observational	Obese women (n = 53)	Whole shotgun metagenomic	Stool	Negatively associated with markers for insulin resistance or dyslipidaemia	(Brahe, et al., 2015)
				One time point		
Elite athletes	Observational	Elite athletes high BMI (n = 40)	16S rRNA sequencing	Stool	Higher proportions in athletes and in low	(Clarke, et al., 2014)
		Healthy males Low BMI ≤25 (n = 23)		One time point	BMI control group	
		Healthy males high BMI (n = 23)				
Infants of overweight and normal-weight mothers	Observational	Lean (n = 16)	qPCR	Stool	Decreased prevalence in infants of normal-weight mothers and of mothers with normal weight gain during pregnancy	(Collado, et al., 2010)
		Overweight mothers (n = 26)	FISH-FCM	Infants (1, 6 months)		
		Infants (1, 6 months)				

Lean and overweight lactating women	Observational	Lean women (n = 34) Overweight women (n = 22)	qPCR	Breast milk (after delivery, 1 and 6 months later)	Trend towards increased prevalence in breast milk (1 month after delivery) from overweight mothers	(Collado, et al., 2012)
Overweight and obese adults	6-week calorie restriction (CR) and 6-week follow up	Overweight (n = 11) Obese (n = 38)	qPCR Metagenomic	Stool Baseline (T0) After CR (T = 6 weeks) After weight stabilisation (T = 12 weeks)	At baseline, *A. muciniphila* MGS was inversely related to fasting glucose, waist-to-hip ratio, and subcutaneous adipocyte diameter. Subjects with higher level of *A. muciniphila* at baseline had greater improvement in insulin sensitivity markers and other clinical parameters after CR	(Dao, et al., 2016)
Lean, overweight and obese adults	Observational	Lean (n = 10) Overweight (n = 10) Obese (n = 10)	16S rRNA sequencing	Stool One time point	*Akkermansia* negatively correlated with BMI	(Escobar, et al., 2014)

Lean, overweight and obese children(4–5 years)	Observational	Lean (n = 20)	qPCR, T-RFLP	Stool	Decrease in obese/overweight children	(Karlsson, et al., 2012)
		Overweight, obese (n = 20)		One time point		
Obese women	8-week of impact of 4 g of Ephedra sinica extract/day	Obese women (n = 7)	16S rRNA sequencing	Stool	Positive association of Akkermansia with weight loss	(Kim, et al., 2014)
				2 samples/subject (before and after Ephedra sinica extract intake)		
T2D and healthy individuals	Observational	T2D (n = 71)	Whole shotgun metagenomic	Stool	Increase in T2D	(Qin, et al., 2012)
		Healthy controls (n = 74)		One time point		
Overweight individuals	1-week fasting program and 6-week probiotic intervention	Overweight adults (n = 13)	qPCR	Stool	Increase between T1 and T3	(Remely, et al., 2015)
				Before fasting (T1)		
				During fasting (T2)		

				After 6-week probiotic intervention (T3)		
Obese individuals	16-week weight reduction diet	Obese individuals (n = 33)	qPCR	Stool	Increase after weight reduction	(Remely, et al., 2015)
				Before, during and after intervention		
Normal weight and overweight pregnant women (24 weeks)	Observational	Normal weight (n = 34)	qPCR	Stool	No difference between normal and overweight Decrease in excessive weight gain	(Santacruz, et al., 2010)
		Overweight (n = 16)		One time point		
Adult women	Observational	Lean (n = 17)	qPCR	Stool	Trend to increase prevalence in lean individuals	(T, et al., 2013)
		Obese (n = 50)		One time point		
Lean, morbidly obese post-gastric-bypass surgery human subjects	Gastric bypass	Normal weight (n = 3)	16S rRNA sequencing	Stool	Increase after bariatric surgery	(Zhang, et al., 2009)
		Morbidly obese(n = 3)		One time point	Low in obese	

		Post-gastric-bypass surgery (n = 3)				
Normal glucose tolerance (NGT), Prediabetes (PD) and newly diagnosed T2D subjects	Observational	NGT (n = 44)	16S rRNA sequencing	Stool	Decrease in Pre-DM and T2D	(Zhang, et al., 2013b)
		Pre-DM (n = 64)		One time point		
		T2D (n = 13)				
Diabetics with and without metformin medication	Observational	T2D no metformin (n=14)	16S rRNA sequencing	Stool	Higher in T2D with metformin compared to other groups	(de la Cuesta-Zuluaga, et al., 2017)
		T2D with metformin (n=14)		One time point		
		matched controls (n=84)				
T2D patients	4 month double-blinded intervention with metformin	Metformin (n=22)	Whole shotgun metagenomic	Stool	Higher in metformin treatment	(Wu, et al., 2017)
		Placebo (n=18)		Before and after intervention		

Alcoholic steatohepatitis (ASH) patients	Observational	ASH (n=21)	16S rRNA sequencing	Stool	Decrease with ASH severity	(Grander, et al., 2017)
		Severe ASH (n=15)		One time point		
		Non-obese healthy individuals (n=16)				
Overweight men and women	12-week double-blinded polyphenol intervention	Obese males (n=18)	qPCR	Stool	not affected	(Most, et al., 2017)
		Obese females (n=19)		Before and after intervention		
Crohn's disease patients	Cross over dietary intervention	Crohn's disease patients (n=9)	qPCR	Stool	Increased abundance on Australian (higher FODMAP) diet	(Halmos, et al., 2016)
				Pooled samples of each stage (habitual diet, low FODMAP, high FODMAP)		
Monozygotic twins with subclinical metabolic disorders	Observational	Twins (n=40 individuals)	Whole shotgun metagenomic	Stool, two time points	Negatively correlated with BMI, insulin levels and fasting blood sugar	(Yassour, et al., 2016)

However, also the opposite has been observed, where a high *A. muciniphila* relative abundance was found to be correlated with overweight and colorectal cancer in humans and allergic diarrhoea in mice (Collado, et al., 2010, Sonoyama, et al., 2010, Weir, et al., 2013, Wang, et al., 2017). The increase of *A. muciniphila* in colorectal cancer patients could be induced by the low caloric intake of these patients. A low caloric intake is generally associated with a higher abundance of *A. muciniphila* due to its independence of host diet. Recently, *A. muciniphila* has also been co-isolated from a blood culture with *Enterococcus faecium* and *E. coli* in a woman with severe diarrhoea (Dubourg, et al., 2017). This suggests that *A. muciniphila* can survive in the blood stream in severe cases of intestinal barrier disruption. The studies in which correlations are described, both positive and negative, indicate that *A. muciniphila* has a profound influence on human health.

To move from case reports and correlations to causalities and mechanistic insight, live cells of *A. muciniphila* were administered to mice fed a high fat diet. The mice receiving the live but not the autoclaved bacteria showed a decrease in body weight gain when compared to the control group (Everard, et al., 2013). In follow-up studies it was shown that the same or an even stronger effect can be achieved by pasteurizing the cells before administration. Finally, a purified outer membrane protein was administered to the mice that mimicked the effect of a whole cell supplement (Plovier, et al., 2017). Additionally, it was shown *in vitro* that an *A. muciniphila* outer membrane complex could modulate the immune response. The effect was traced back to a single pili-associated protein encoded by the DNA at locus Amuc_1100 (Ottman, et al., 2017b). Such mechanistic studies are needed for the definition and final use of therapeutic microbes.

Growing therapeutic microbes

Probiotics have been marketed worldwide, with different regulations imposed for marketing in the European Union, Japan, Canada and the USA. Regulations for marketing probiotics differ from safety regulations only in the USA, to scientifically proven functionality in the European Union (Kumar, et al., 2015). The value of the probiotic market is still increasing worldwide (Solanki, et al., 2013, Grand-View-Research, 2016). Most probiotic strains are lactic acid bacteria or Bifidobacteria or combinations thereof. *E. coli* Nissle and *S. boulardii* are also marketed as probiotics (Table 2). In the past decade, the interest for the interaction between human health and the microbiota has led to the discovery of potential therapeutic

bacteria. Note that these bacteria are not termed probiotics, because their use or intended use is to treat or prevent diseases and disorders, although they could be employed as next generation probiotics. These bacteria are not within the same families as the original probiotics, but include various intestinal anaerobes (Table 2). Like some of the previously marketed *Lactobacilli* and *Bifidobacteria* (Talwalkar and Kailasapathy, 2003, Talwalkar and Kailasapathy, 2004), all these gut-derived bacteria are anaerobic and thus mostly very sensitive to the exposure to oxygen. This poses great challenges for growing these bacteria, upscaling to large scale cultivation and maintaining viability of the bacteria up to delivery in the colon.

Small-scale laboratory cultures have been obtained for all species described in Table 2. In case of *F. prausnitzii*, a minimal medium was defined based on the metabolic map of the microbe, in which undefined compounds such as yeast extract and casitone were replaced by defined compounds, mainly amino acids (Heinken, et al., 2014). This modification of the medium reduced the growth rate from 0.32 h^{-1} to 0.13 h^{-1}. A defined medium was also used to grow and study *Intesnimonas butyriciproducens,* exposing a new pathway for butyrate production with the degradation of fructoselysin. The growth rate on this Amadori product as sole carbon source was 0.04 h^{-1}, and when supplemented with acetate 0.06 h^{-1}. When lysine is used as carbon source, the growth speed was 0.1 h^{-1} (Bui, et al., 2015).

Such a defined medium has not been obtained for *A. muciniphila* before, even though it has been used as supplement or treatment in multiple studies. For this purpose it was grown on multiple complex media, including mucus based medium (Ouwerkerk, et al., 2017a), tryptone-based medium, BHI medium (Derrien, et al., 2004, Ottman, 2017), and on solid chocolate agar (Grander, et al., 2017).

Table 2. Potential next generation probiotics or therapeutic microbes, which are isolated from human. Adapted from (O'Toole, et al., 2017).

Organism	Disease target	Level of evidence	Study type	Reference
***Bacteroides xylanisolvens* DSM 23694**	Cancer	Medium: safety in humans has been established while levels of TFα-specific IgM have been shown to be elevated in humans	Human	(Ulsemer, et al., 2016)
***Bacteroides ovatus* D-6**	Cancer	Low to medium: increases levels of murine TFα-specific IgM and IgG	Preclinical in mice	(Ulsemer, et al., 2013)
***Bacteroides dorei* D8**	Heart disease	Low: depletion of cholesterol in vitro	Preclinical in vitro	(Gerard, et al., 2007)
***Bacteroides fragilis* ZY-312**	Clearance of infectious agents	Low: data only in vitro	Preclinical in vitro	(Deng, et al., 2016)
***Bacteroides acidifaciens* JCM 10556(T)**	Clearance of infectious agents	Low to medium: increases IgA levels in the large intestine of gnotobiotic mice	Preclinical in mice	(Yanagibashi, et al., 2013)
***Clostridium butyricum* MIYAIRI 588**	Multiple targets including cancer, inflammation and infectious agents	Low to medium: evidence gathered for claims in human and animals trials	Human	(Hosomi, et al., 1982, Kobashi, et al., 1983, Takeda, et al., 1983, Kuroiwa, et al., 1990, Murayama, et al., 1995, Seki, et al., 2003, Takahashi, et al., 2004, Shimbo, et al., 2005, Kohiruimaki, et al., 2008, Nakanishi and Tanaka, 2010, Woo, et al., 2011, Sato, et al., 2012, Seo, et al., 2013, Shinnoh, et al., 2013, Weng, et al., 2015, Chen, et al., 2016, Isa, et al., 2016, Yasueda, et al., 2016)
Faecalibacterium prausnitzii	Mainly IBD but also asthma, eczema and type 2 diabetes	Low to medium: mainly focused animal models of colitis and in associative studies	Preclinical in mice and *in vitro*	(Rossi, et al., 2015, Simonyte Sjodin, et al., 2016, Song, et al., 2016)
Eubacterium hallii L2-7	Type 2 diabetes	Medium: correlations in human FMT and animal-based efficacy	Preclinical in mice	(Udayappan, et al., 2016)
Akkermansia muciniphila Muc^T	Metabolic disorders, obesity, type 2 diabetes	Medium: Correlations in human and animal based efficacy	Human phase 1 and preclinical in mice	(Everard, et al., 2013, Plovier, et al., 2017)

***Intestinimonas butyriciproducens* AF211**	reduction of Advanced Glycation Endproducts (AGEs) in people with Metabolic syndrome and type 2 diabetes	Very low: based on butyrate production only	Ongoing preclinical in mice	(Bui, et al., 2015) Caelus Health BV

Formulation of therapeutic microbes

A final challenge in using anaerobic bacteria as therapeutic microbes or probiotics is the downstream processing and subsequent formulation of the product. Many of the conventional marketed probiotics are formulated in yoghurt or similar dairy drinks. For most therapeutic microbes, these formulations are too acidic and the diffusion of oxygen would be too high for survival. Additionally, free suspension of bacteria in dairy products provides no protection against gastro-intestinal conditions, such as the high acidity in the stomach, high oxygen concentrations in the upper intestinal tract and exposure to bile.

The formulation of probiotics has influence on the efficacy of the bacteria (Govender, et al., 2014, Sanders, et al., 2014), so the same can be assumed for therapeutic microbes. Therefore, it is very important to not only study the physiology and host-microbe interaction of therapeutic microbes, but also find a way to deliver the cells in an appropriate way. The possibilities to deliver viable bacteria depend on the resistance of these bacteria against processing techniques. Techniques that are currently employed to deliver the bacteria include lyophilisation and different encapsulation methods. The encapsulation methods aim at protecting the bacteria, while lyophilisation inactivates the bacteria. Protection in double emulsion systems, by extrusion and encapsulation in starch has been employed successfully to protect probiotic bacteria (Mattila-Sandholm, et al., 2002, Pimentel-Gonzalez, et al., 2009, Solanki, et al., 2013, Govender, et al., 2014).

Aim and thesis outline

The introduction above describes the complexity of the gut microbiota and the potential role of *A. muciniphila* in this ecosystem. The application of molecular tools, such as 16S rRNA amplicon sequencing as well as metagenomic insight, has been important in describing the species abundance in the gut and supporting a correlation between the abundance of specific bacteria, their genes and diseases (Le Chatelier, et al., 2013). However, correlations are not sufficient to provide causal relationships or a mechanistically understanding that precedes the identification of potential therapeutic agents for the use of intervention studies and the cure of diseases. Hence, it is the aim of the present study to identify and solve some of the physiological, growth and delivery bottlenecks that limit application studies of *A. muciniphila.* The studies are essential to determine causality and identify mechanistic explanations for host-microbe interactions. To obtain causal relationships and test hypothesized mechanisms, it is important to be able to culture bacteria and study their possible phenotypes. In **chapter 2** we describe the use of GEMs to predict possible growth media, phenotypes and species interactions.

The use of GEMs as discussed in chapter 2 has been applied in **chapter 3**, in which we describe the development of a minimal medium to grow *A. muciniphila.* This resulted in a further refining of the GEM of *A. muciniphila.*

The development of the minimal medium directly resulted in the optimization of a food-grade growth medium for therapeutic applications, as described in **chapter 4.** We studied the influence of this growth medium on gene expression and cell morphology of *A. muciniphila*. Finally, we compared the efficacy of cells grown on this newly developed medium with cells grown on the previously tested mucus medium in preclinical mice trials.

The niche of *A. muciniphila* is reflected in its known physiology and genetics, by its arsenal of mucus degrading enzymes and ability to utilize the mucosal sugars. The mucus lining the epithelial cells does not prevent oxygen form diffusing into the gut. This results in recurrent oxygen exposure to *A. muciniphila.* It is expected that this is not beneficial for strictly anaerobic bacteria. We investigated the influence of low oxygen concentrations on *A. muciniphila,* and showed that *A. muciniphila* is capable of respiring oxygen as presented in **chapter 5.**

To deliver viable *A. muciniphila* to the host, we employed a double emulsion system as will be discussed in **chapter 6**. The protective capabilities of a double water-in-oil-in-water emulsion was tested in an *in vitro* gastric system.

Finally, the relevance of the findings described in this thesis will be discussed in **chapter 7**, with a future perspective about the possible applications of *A. muciniphila* as a therapeutic microbe.

References

1 Ahmed, N. (2005) 23 years of the discovery of Helicobacter pylori: is the debate over?, *Ann Clin Microbiol Antimicrob* **4**: 17.
2 Baart, G.J., and Martens, D.E. (2012) Genome-scale metabolic models: reconstruction and analysis, *Methods Mol Biol* **799**: 107-126.
3 Belzer, C., and de Vos, W.M. (2012) Microbes inside-from diversity to function: the case of Akkermansia, *Isme Journal* **6**: 1449-1458.
4 Belzer, C.C., L.W.; Aalvink, S.; Chamlagain, B.; Piironen, V.; Knol, J.; de Vos, W.M. (2017) Microbial metabolic networks at the mucus layer lead to diet-independent butyrate and vitamin B12 production by intestinal symbionts *Mbio* **In Press**.
5 Berg, R.D. (1996) The indigenous gastrointestinal microflora, *Trends Microbiol* **4**: 430-435.
6 Berry, D., Stecher, B., Schintlmeister, A., Reichert, J., Brugiroux, S., Wild, B., et al. (2013) Host-compound foraging by intestinal microbiota revealed by single-cell stable isotope probing, *Proc Natl Acad Sci U S A* **110**: 4720-4725.
7 Brahe, L.K., Le Chatelier, E., Prifti, E., Pons, N., Kennedy, S., Hansen, T., et al. (2015) Specific gut microbiota features and metabolic markers in postmenopausal women with obesity, *Nutr Diabetes* **5**: e159.
8 Browne, H.P., Forster, S.C., Anonye, B.O., Kumar, N., Neville, B.A., Stares, M.D., et al. (2016) Culturing of 'unculturable' human microbiota reveals novel taxa and extensive sporulation, *Nature* **533**: 543-+.
9 Bui, T.P.N., Ritari, J., Boeren, S., de Waard, P., Plugge, C.M., and de Vos, W.M. (2015) Production of butyrate from lysine and the Amadori product fructoselysine by a human gut commensal, *Nature Communications* **6**.
10 Chen, J.C., Lee, W.J., Tsou, J.J., Liu, T.P., and Tsai, P.L. (2016) Effect of probiotics on postoperative quality of gastric bypass surgeries: a prospective randomized trial, *Surg Obes Relat Dis* **12**: 57-61.
11 Clarke, S.F., Murphy, E.F., O'Sullivan, O., Lucey, A.J., Humphreys, M., Hogan, A., et al. (2014) Exercise and associated dietary extremes impact on gut microbial diversity, *Gut* **63**: 1913-1920.
12 Clemente, J.C., Ursell, L.K., Parfrey, L.W., and Knight, R. (2012) The impact of the gut microbiota on human health: an integrative view, *Cell* **148**: 1258-1270.
13 Collado, M.C., Derrien, M., Isolauri, E., de Vos, W.M., and Salminen, S. (2007) Intestinal integrity and Akkermansia muciniphila, a mucin-degrading member of the intestinal microbiota present in infants, adults, and the elderly, *Appl Environ Microbiol* **73**: 7767-7770.
14 Collado, M.C., Isolauri, E., Laitinen, K., and Salminen, S. (2010) Effect of mother's weight on infant's microbiota acquisition, composition, and activity during early infancy: a prospective follow-up study initiated in early pregnancy, *Am J Clin Nutr* **92**: 1023-1030.
15 Collado, M.C., Laitinen, K., Salminen, S., and Isolauri, E. (2012) Maternal weight and excessive weight gain during pregnancy modify the immunomodulatory potential of breast milk, *Pediatr Res* **72**: 77-85.
16 Dao, M.C., Everard, A., Aron-Wisnewsky, J., Sokolovska, N., Prifti, E., Verger, E.O., et al. (2016) Akkermansia muciniphila and improved metabolic health during a dietary intervention in obesity: relationship with gut microbiome richness and ecology, *Gut* **65**: 426-436.
17 de la Cuesta-Zuluaga, J., Mueller, N.T., Corrales-Agudelo, V., Velasquez-Mejia, E.P., Carmona, J.A., Abad, J.M., and Escobar, J.S. (2017) Metformin Is Associated With Higher Relative Abundance of Mucin-Degrading Akkermansia muciniphila and Several Short-Chain Fatty Acid-Producing Microbiota in the Gut, *Diabetes Care* **40**: 54-62.
18 de Vos, W.M. (2013) Fame and future of faecal transplantations--developing next-generation therapies with synthetic microbiomes, *Microbial Biotechnology* **6**: 316-325.
19 de Vos, W.M., and de Vos, E.A. (2012) Role of the intestinal microbiome in health and disease: from correlation to causation, *Nutr Rev* **70 Suppl 1**: S45-56.
20 Deng, H., Li, Z., Tan, Y., Guo, Z., Liu, Y., Wang, Y., et al. (2016) A novel strain of Bacteroides fragilis enhances phagocytosis and polarises M1 macrophages, *Sci Rep* **6**: 29401.

21 Derrien, M., Belzer, C., and de Vos, W.M. (2017) Akkermansia muciniphila and its role in regulating host functions, *Microb Pathog* **106**: 171-181.
22 Derrien, M., Collado, M.C., Ben-Amor, K., Salminen, S., and de Vos, W.M. (2008) The Mucin degrader Akkermansia muciniphila is an abundant resident of the human intestinal tract, *Appl Environ Microbiol* **74**: 1646-1648.
23 Derrien, M., van Passel, M.W., van de Bovenkamp, J.H., Schipper, R.G., de Vos, W.M., and Dekker, J. (2010) Mucin-bacterial interactions in the human oral cavity and digestive tract, *Gut Microbes* **1**: 254-268.
24 Derrien, M., Vaughan, E.E., Plugge, C.M., and de Vos, W.M. (2004) Akkermansia muciniphila gen. nov., sp nov., a human intestinal mucin-degrading bacterium, *Int J Syst Evol Microbiol* **54**: 1469-1476.
25 Dinan, T.G., Stanton, C., and Cryan, J.F. (2013) Psychobiotics: a novel class of psychotropic, *Biol Psychiatry* **74**: 720-726.
26 Donaldson, G.P., Lee, S.M., and Mazmanian, S.K. (2016) Gut biogeography of the bacterial microbiota, *Nature Reviews Microbiology* **14**: 20-32.
27 Dubourg, G., Cornu, F., Edouard, S., Battaini, A., Tsimaratos, M., and Raoult, D. (2017) First isolation of Akkermansia muciniphila in a blood-culture sample, *Clin Microbiol Infect*.
28 Eiseman, B., Silen, W., Bascom, G.S., and Kauvar, A.J. (1958) Fecal enema as an adjunct in the treatment of pseudomembranous enterocolitis, *Surgery* **44**: 854-859.
29 Escobar, J.S., Klotz, B., Valdes, B.E., and Agudelo, G.M. (2014) The gut microbiota of Colombians differs from that of Americans, Europeans and Asians, *BMC Microbiol* **14**: 311.
30 Everard, A., Belzer, C., Geurts, L., Ouwerkerk, J.P., Druart, C., Bindels, L.B., et al. (2013) Cross-talk between Akkermansia muciniphila and intestinal epithelium controls diet-induced obesity, *Proc Natl Acad Sci U S A* **110**: 9066-9071.
31 Feist, A.M., and Palsson, B.O. (2010) The biomass objective function, *Curr Opin Microbiol* **13**: 344-349.
32 Gensollen, T., Iyer, S.S., Kasper, D.L., and Blumberg, R.S. (2016) How colonization by microbiota in early life shapes the immune system, *Science* **352**: 539-544.
33 Gerard, P., Lepercq, P., Leclerc, M., Gavini, F., Raibaud, P., and Juste, C. (2007) Bacteroides sp. strain D8, the first cholesterol-reducing bacterium isolated from human feces, *Appl Environ Microbiol* **73**: 5742-5749.
34 Govender, M., Choonara, Y.E., Kumar, P., du Toit, L.C., van Vuuren, S., and Pillay, V. (2014) A review of the advancements in probiotic delivery: Conventional vs. non-conventional formulations for intestinal flora supplementation, *AAPS PharmSciTech* **15**: 29-43.
35 Grand-View-Research (2016) Probiotics Market Analysis By Application (Probiotic Foods & Beverages (Dairy Products, Non-Dairy Products, Cereals, Baked Food, Fermented Meat Products, Dry Food), Probiotic Dietary Supplements (Food Supplements, Nutritional Supplements, Specialty Nutrients, Infant Formula), Animal Feed Probiotics), By End-Use (Human Probiotics, Animal Probiotics) And Segment Forecast To 2024 (Summary). Grand View Research, Inc. 85.
36 Grander, C., Adolph, T.E., Wieser, V., Lowe, P., Wrzosek, L., Gyongyosi, B., et al. (2017) Recovery of ethanol-induced Akkermansia muciniphila depletion ameliorates alcoholic liver disease, *Gut*.
37 Greenhalgh, K., Meyer, K.M., Aagaard, K.M., and Wilmes, P. (2016) The human gut microbiome in health: establishment and resilience of microbiota over a lifetime, *Environ Microbiol* **18**: 2103-2116.
38 Guo, X., Zhang, J., Wu, F., Zhang, M., Yi, M., and Peng, Y. (2016) Different subtype strains of Akkermansia muciniphila abundantly colonize in southern China, *J Appl Microbiol* **120**: 452-459.
39 Gupta, S., Allen-Vercoe, E., and Petrof, E.O. (2016) Fecal microbiota transplantation: in perspective, *Therap Adv Gastroenterol* **9**: 229-239.
40 Halmos, E.P., Christophersen, C.T., Bird, A.R., Shepherd, S.J., Muir, J.G., and Gibson, P.R. (2016) Consistent Prebiotic Effect on Gut Microbiota With Altered FODMAP Intake in Patients with Crohn's Disease: A Randomised, Controlled Cross-Over Trial of Well-Defined Diets, *Clin Transl Gastroenterol* **7**: e164.

41 Hansson, G.C. (2012) Role of mucus layers in gut infection and inflammation, *Curr Opin Microbiol* **15**: 57-62.
42 Heinken, A., Khan, M.T., Paglia, G., Rodionov, D.A., Harmsen, H.J., and Thiele, I. (2014) Functional metabolic map of Faecalibacterium prausnitzii, a beneficial human gut microbe, *J Bacteriol* **196**: 3289-3302.
43 Hill, C., Guarner, F., Reid, G., Gibson, G.R., Merenstein, D.J., Pot, B., et al. (2014) Expert consensus document. The International Scientific Association for Probiotics and Prebiotics consensus statement on the scope and appropriate use of the term probiotic, *Nat Rev Gastroenterol Hepatol* **11**: 506-514.
44 Hosomi, M., Tanida, N., and Shimoyama, T. (1982) The role of intestinal bacteria in gallstone formation in animal model. A study on biliary lipid composition and bile acid profiles in bile, small intestinal contents and feces of clostridium butyricum Miyairi No. 588 monocontaminated mice, *Gastroenterol Jpn* **17**: 316-323.
45 Hugon, P., Lagier, J.C., Colson, P., Bittar, F., and Raoult, D. (2017) Repertoire of human gut microbes, *Microb Pathog* **106**: 103-112.
46 Isa, K., Oka, K., Beauchamp, N., Sato, M., Wada, K., Ohtani, K., et al. (2016) Safety assessment of the Clostridium butyricum MIYAIRI 588(R) probiotic strain including evaluation of antimicrobial sensitivity and presence of Clostridium toxin genes in vitro and teratogenicity in vivo, *Hum Exp Toxicol* **35**: 818-832.
47 Johansson, M.E., Gustafsson, J.K., Holmen-Larsson, J., Jabbar, K.S., Xia, L., Xu, H., et al. (2014) Bacteria penetrate the normally impenetrable inner colon mucus layer in both murine colitis models and patients with ulcerative colitis, *Gut* **63**: 281-291.
48 Johansson, M.E., Larsson, J.M., and Hansson, G.C. (2011) The two mucus layers of colon are organized by the MUC2 mucin, whereas the outer layer is a legislator of host-microbial interactions, *Proc Natl Acad Sci U S A* **108 Suppl 1**: 4659-4665.
49 Joossens, M., Huys, G., Cnockaert, M., De Preter, V., Verbeke, K., Rutgeerts, P., et al. (2011) Dysbiosis of the faecal microbiota in patients with Crohn's disease and their unaffected relatives, *Gut* **60**: 631-637.
50 Karlsson, C.L., Onnerfalt, J., Xu, J., Molin, G., Ahrne, S., and Thorngren-Jerneck, K. (2012) The microbiota of the gut in preschool children with normal and excessive body weight, *Obesity (Silver Spring)* **20**: 2257-2261.
51 Kim, B.S., Song, M.Y., and Kim, H. (2014) The anti-obesity effect of Ephedra sinica through modulation of gut microbiota in obese Korean women, *J Ethnopharmacol* **152**: 532-539.
52 Kobashi, K., Takeda, Y., Itoh, H., and Hase, J. (1983) Cholesterol-lowering effect of Clostridium butyricum in cholesterol-fed rats, *Digestion* **26**: 173-178.
53 Kohiruimaki, M., Ohtsuka, H., Tanami, E., Kitagawa, M., Masui, M., Ando, T., and Kawamura, S. (2008) Effects of active egg white product/ Clostridium butyricum Miyairi 588 additive on peripheral leukocyte populations in periparturient dairy cows, *J Vet Med Sci* **70**: 321-323.
54 Kumar, H., Salminen, S., Verhagen, H., Rowland, I., Heimbach, J., Banares, S., et al. (2015) Novel probiotics and prebiotics: road to the market, *Curr Opin Biotechnol* **32**: 99-103.
55 Kuroiwa, T., Kobari, K., and Iwanaga, M. (1990) [Inhibition of enteropathogens by Clostridium butyricum MIYAIRI 588], *Kansenshogaku Zasshi* **64**: 257-263.
56 Lagier, J.C., Khelaifia, S., Alou, M.T., Ndongo, S., Dione, N., Hugon, P., et al. (2016) Culture of previously uncultured members of the human gut microbiota by culturomics, *Nat Microbiol* **1**.
57 Lagkouvardos, I., Pukall, R., Abt, B., Foesel, B.U., Meier-Kolthoff, J.P., Kumar, N., et al. (2016) The Mouse Intestinal Bacterial Collection (miBC) provides host-specific insight into cultured diversity and functional potential of the gut microbiota, *Nat Microbiol* **1**: 16131.
58 Le Chatelier, E., Nielsen, T., Qin, J., Prifti, E., Hildebrand, F., Falony, G., et al. (2013) Richness of human gut microbiome correlates with metabolic markers, *Nature* **500**: 541-546.
59 Li, S.S., Zhu, A., Benes, V., Costea, P.I., Hercog, R., Hildebrand, F., et al. (2016) Durable coexistence of donor and recipient strains after fecal microbiota transplantation, *Science* **352**: 586-589.

60 Marchesi, J.R., Adams, D.H., Fava, F., Hermes, G.D., Hirschfield, G.M., Hold, G., et al. (2016) The gut microbiota and host health: a new clinical frontier, *Gut* **65**: 330-339.
61 Marshall, B.J., and Warren, J.R. (1984) Unidentified curved bacilli in the stomach of patients with gastritis and peptic ulceration, *Lancet* **1**: 1311-1315.
62 Martin, R., Makino, H., Cetinyurek Yavuz, A., Ben-Amor, K., Roelofs, M., Ishikawa, E., et al. (2016) Early-Life Events, Including Mode of Delivery and Type of Feeding, Siblings and Gender, Shape the Developing Gut Microbiota, *PLoS One* **11**: e0158498.
63 Mattila-Sandholm, T., Myllärinen, P., Crittenden, R., Mogensen, G., Fondén, R., and Saarela, M. (2002) Technological challenges for future probiotic foods, *International Dairy Journal* **12**: 173-182.
64 Most, J., Penders, J., Lucchesi, M., Goossens, G.H., and Blaak, E.E. (2017) Gut microbiota composition in relation to the metabolic response to 12-week combined polyphenol supplementation in overweight men and women, *Eur J Clin Nutr*.
65 Murayama, T., Mita, N., Tanaka, M., Kitajo, T., Asano, T., Mizuochi, K., and Kaneko, K. (1995) Effects of orally administered Clostridium butyricum MIYAIRI 588 on mucosal immunity in mice, *Vet Immunol Immunopathol* **48**: 333-342.
66 Nakanishi, S., and Tanaka, M. (2010) Sequence analysis of a bacteriocinogenic plasmid of Clostridium butyricum and expression of the bacteriocin gene in Escherichia coli, *Anaerobe* **16**: 253-257.
67 O'Toole, P.W., Marchesi, J.R., and Hill, C. (2017) Next-generation probiotics: the spectrum from probiotics to live biotherapeutics, *Nat Microbiol* **2**: 17057.
68 Ottman, N., Davids, M., Suarez-Diez, M., Boeren, S., Schaap, P.J., Martins Dos Santos, V.A.P., et al. (2017a) Genome-scale model and omics analysis of metabolic capacities of Akkermansia muciniphila reveal a preferential mucin-degrading lifestyle, *Appl Environ Microbiol*.
69 Ottman, N., Reunanen, J., Meijerink, M., Pietila, T.E., Kainulainen, V., Klievink, J., et al. (2017b) Pili-like proteins of Akkermansia muciniphila modulate host immune responses and gut barrier function, *PLoS One* **12**: e0173004.
71 Ouwerkerk, J.P. (2016a) Akkermansia species : phylogeny, physiology and comparative genomics. Wageningen: Wageningen University.
72 Ouwerkerk, J.P., Aalvink, S., Belzer, C., and de Vos, W.M. (2016b) Akkermansia glycaniphila sp. nov., an anaerobic mucin-degrading bacterium isolated from reticulated python faeces, *Int J Syst Evol Microbiol* **66**: 4614-4620.
73 Ouwerkerk, J.P., Aalvink, S., Belzer, C., and De Vos, W.M. (2017a) Preparation and preservation of viable Akkermansia muciniphila cells for therapeutic interventions, *Benef Microbes* **8**: 163-169.
74 Ouwerkerk, J.P., Koehorst, J.J., Schaap, P.J., Ritari, J., Paulin, L., Belzer, C., and de Vos, W.M. (2017b) Complete Genome Sequence of Akkermansia glycaniphila Strain PytT, a Mucin-Degrading Specialist of the Reticulated Python Gut, *Genome Announc* **5**.
75 Pimentel-Gonzalez, D.J., Campos-Montiel, R.G., Lobato-Calleros, C., Pedroza-Islas, R., and Vernon-Carter, E.J. (2009) Encapsulation of Lactobacillus rhamnosus in double emulsions formulated with sweet whey as emulsifier and survival in simulated gastrointestinal conditions, *Food Research International* **42**: 292-297.
76 Plovier, H., Everard, A., Druart, C., Depommier, C., Van Hul, M., Geurts, L., et al. (2017) A purified membrane protein from Akkermansia muciniphila or the pasteurized bacterium improves metabolism in obese and diabetic mice, *Nat Med* **23**: 107-113.
77 Qin, J., Li, Y., Cai, Z., Li, S., Zhu, J., Zhang, F., et al. (2012) A metagenome-wide association study of gut microbiota in type 2 diabetes, *Nature* **490**: 55-60.
78 Rajilic-Stojanovic, M., and de Vos, W.M. (2014) The first 1000 cultured species of the human gastrointestinal microbiota, *FEMS Microbiol Rev* **38**: 996-1047.
79 Remely, M., Hippe, B., Geretschlaeger, I., Stegmayer, S., Hoefinger, I., and Haslberger, A. (2015) Increased gut microbiota diversity and abundance of Faecalibacterium prausnitzii and Akkermansia after fasting: a pilot study, *Wien Klin Wochenschr* **127**: 394-398.
80 Remely, M., Tesar, I., Hippe, B., Gnauer, S., Rust, P., and Haslberger, A.G. (2015) Gut microbiota composition correlates with changes in body fat content due to weight loss, *Benef Microbes* **6**: 431-439.

81 Ritari, J., Salojarvi, J., Lahti, L., and de Vos, W.M. (2015) Improved taxonomic assignment of human intestinal 16S rRNA sequences by a dedicated reference database, *Bmc Genomics* **16**.
82 Rossi, O., Khan, M.T., Schwarzer, M., Hudcovic, T., Srutkova, D., Duncan, S.H., et al. (2015) Faecalibacterium prausnitzii Strain HTF-F and Its Extracellular Polymeric Matrix Attenuate Clinical Parameters in DSS-Induced Colitis, *PLoS One* **10**: e0123013.
83 Sanders, M.E., Klaenhammer, T.R., Ouwehand, A.C., Pot, B., Johansen, E., Heimbach, J.T., et al. (2014) Effects of genetic, processing, or product formulation changes on efficacy and safety of probiotics, *Ann N Y Acad Sci* **1309**: 1-18.
84 Santacruz, A., Collado, M.C., Garcia-Valdes, L., Segura, M.T., Martin-Lagos, J.A., Anjos, T., et al. (2010) Gut microbiota composition is associated with body weight, weight gain and biochemical parameters in pregnant women, *Br J Nutr* **104**: 83-92.
85 Sato, S., Nagai, H., and Igarashi, Y. (2012) Effect of probiotics on serum bile acids in patients with ulcerative colitis, *Hepatogastroenterology* **59**: 1804-1808.
86 Sears, C.L. (2005) A dynamic partnership: celebrating our gut flora, *Anaerobe* **11**: 247-251.
87 Seki, H., Shiohara, M., Matsumura, T., Miyagawa, N., Tanaka, M., Komiyama, A., and Kurata, S. (2003) Prevention of antibiotic-associated diarrhea in children by Clostridium butyricum MIYAIRI, *Pediatr Int* **45**: 86-90.
88 Sender, R., Fuchs, S., and Milo, R. (2016) Revised Estimates for the Number of Human and Bacteria Cells in the Body, *PLoS Biol* **14**: e1002533.
89 Seo, M., Inoue, I., Tanaka, M., Matsuda, N., Nakano, T., Awata, T., et al. (2013) Clostridium butyricum MIYAIRI 588 improves high-fat diet-induced non-alcoholic fatty liver disease in rats, *Dig Dis Sci* **58**: 3534-3544.
90 Shimbo, I., Yamaguchi, T., Odaka, T., Nakajima, K., Koide, A., Koyama, H., and Saisho, H. (2005) Effect of Clostridium butyricum on fecal flora in Helicobacter pylori eradication therapy, *World J Gastroenterol* **11**: 7520-7524.
91 Shinnoh, M., Horinaka, M., Yasuda, T., Yoshikawa, S., Morita, M., Yamada, T., et al. (2013) Clostridium butyricum MIYAIRI 588 shows antitumor effects by enhancing the release of TRAIL from neutrophils through MMP-8, *Int J Oncol* **42**: 903-911.
92 Simonyte Sjodin, K., Vidman, L., Ryden, P., and West, C.E. (2016) Emerging evidence of the role of gut microbiota in the development of allergic diseases, *Curr Opin Allergy Clin Immunol* **16**: 390-395.
93 Solanki, H.K., Pawar, D.D., Shah, D.A., Prajapati, V.D., Jani, G.K., Mulla, A.M., and Thakar, P.M. (2013) Development of microencapsulation delivery system for long-term preservation of probiotics as biotherapeutics agent, *Biomed Res Int* **2013**.
94 Solanki, H.K., Pawar, D.D., Shah, D.A., Prajapati, V.D., Jani, G.K., Mulla, A.M., and Thakar, P.M. (2013) Development of microencapsulation delivery system for long-term preservation of probiotics as biotherapeutics agent, *Biomed Res Int* **2013**: 620719.
95 Song, H., Yoo, Y., Hwang, J., Na, Y.C., and Kim, H.S. (2016) Faecalibacterium prausnitzii subspecies-level dysbiosis in the human gut microbiome underlying atopic dermatitis, *J Allergy Clin Immunol* **137**: 852-860.
96 Sonoyama, K., Ogasawara, T., Goto, H., Yoshida, T., Takemura, N., Fujiwara, R., et al. (2010) Comparison of gut microbiota and allergic reactions in BALB/c mice fed different cultivars of rice, *Br J Nutr* **103**: 218-226.
97 Steinhoff, U. (2005) Who controls the crowd? New findings and old questions about the intestinal microflora, *Immunol Lett* **99**: 12-16.
98 Swidsinski, A., Dorffel, Y., Loening-Baucke, V., Theissig, F., Ruckert, J.C., Ismail, M., et al. (2011) Acute appendicitis is characterised by local invasion with Fusobacterium nucleatum/necrophorum, *Gut* **60**: 34-40.
99 T, F.S.T., Grzeskowiak, L.M., Salminen, S., Laitinen, K., Bressan, J., and Gouveia Peluzio Mdo, C. (2013) Faecal levels of Bifidobacterium and Clostridium coccoides but not plasma lipopolysaccharide are inversely related to insulin and HOMA index in women, *Clin Nutr* **32**: 1017-1022.
100 Tailford, L.E., Owen, C.D., Walshaw, J., Crost, E.H., Hardy-Goddard, J., Le Gall, G., et al. (2015) Discovery of intramolecular trans-sialidases in human gut microbiota suggests novel mechanisms of mucosal adaptation, *Nat Commun* **6**: 7624.

101 Takahashi, M., Taguchi, H., Yamaguchi, H., Osaki, T., Komatsu, A., and Kamiya, S. (2004) The effect of probiotic treatment with Clostridium butyricum on enterohemorrhagic Escherichia coli O157:H7 infection in mice, *FEMS Immunol Med Microbiol* **41**: 219-226.
102 Takeda, Y., Itoh, H., and Kobashi, K. (1983) Effect of Clostridium butyricum on the formation and dissolution of gallstones in experimental cholesterol cholelithiasis, *Life Sci* **32**: 541-546.
103 Talwalkar, A., and Kailasapathy, K. (2003) Metabolic and biochemical responses of probiotic bacteria to oxygen, *Journal of Dairy Science* **86**: 2537-2546.
104 Talwalkar, A., and Kailasapathy, K. (2004) The role of oxygen in the viability of probiotic bacteria with reference to L. acidophilus and Bifidobacterium spp, *Curr Issues Intest Microbiol* **5**: 1-8.
105 Udayappan, S., Manneras-Holm, L., Chaplin-Scott, A., Belzer, C., Herrema, H., Dallinga-Thie, G.M., et al. (2016) Oral treatment with Eubacterium hallii improves insulin sensitivity in db/db mice **2**: 16009.
106 Ulsemer, P., Henderson, G., Toutounian, K., Loffler, A., Schmidt, J., Karsten, U., et al. (2013) Specific humoral immune response to the Thomsen-Friedenreich tumor antigen (CD176) in mice after vaccination with the commensal bacterium Bacteroides ovatus D-6, *Cancer Immunol Immunother* **62**: 875-887.
107 Ulsemer, P., Toutounian, K., Kressel, G., Goletz, C., Schmidt, J., Karsten, U., et al. (2016) Impact of oral consumption of heat-treated Bacteroides xylanisolvens DSM 23964 on the level of natural TFalpha-specific antibodies in human adults, *Benef Microbes* **7**: 485-500.
108 Van den Abbeele, P., Belzer, C., Goossens, M., Kleerebezem, M., De Vos, W.M., Thas, O., et al. (2013) Butyrate-producing Clostridium cluster XIVa species specifically colonize mucins in an in vitro gut model, *ISME J* **7**: 949-961.
109 van Nood, E., Vrieze, A., Nieuwdorp, M., Fuentes, S., Zoetendal, E.G., de Vos, W.M., et al. (2013) Duodenal infusion of donor feces for recurrent Clostridium difficile, *N Engl J Med* **368**: 407-415.
110 van Passel, M.W., Kant, R., Zoetendal, E.G., Plugge, C.M., Derrien, M., Malfatti, S.A., et al. (2011) The genome of Akkermansia muciniphila, a dedicated intestinal mucin degrader, and its use in exploring intestinal metagenomes, *PLoS One* **6**: e16876.
111 Vrieze, A., Holleman, F., Zoetendal, E.G., de Vos, W.M., Hoekstra, J.B., and Nieuwdorp, M. (2010) The environment within: how gut microbiota may influence metabolism and body composition, *Diabetologia* **53**: 606-613.
112 Wang, L., Christophersen, C.T., Sorich, M.J., Gerber, J.P., Angley, M.T., and Conlon, M.A. (2011) Low relative abundances of the mucolytic bacterium Akkermansia muciniphila and Bifidobacterium spp. in feces of children with autism, *Appl Environ Microbiol* **77**: 6718-6721.
113 Wang, M., Ahrne, S., Jeppsson, B., and Molin, G. (2005) Comparison of bacterial diversity along the human intestinal tract by direct cloning and sequencing of 16S rRNA genes, *FEMS Microbiol Ecol* **54**: 219-231.
114 Wang, X., Wang, J., Rao, B., and Deng, L. (2017) Gut flora profiling and fecal metabolite composition of colorectal cancer patients and healthy individuals, *Exp Ther Med* **13**: 2848-2854.
115 Weingarden, A., Gonzalez, A., Vazquez-Baeza, Y., Weiss, S., Humphry, G., Berg-Lyons, D., et al. (2015) Dynamic changes in short- and long-term bacterial composition following fecal microbiota transplantation for recurrent Clostridium difficile infection, *Microbiome* **3**: 10.
116 Weir, T.L., Manter, D.K., Sheflin, A.M., Barnett, B.A., Heuberger, A.L., and Ryan, E.P. (2013) Stool Microbiome and Metabolome Differences between Colorectal Cancer Patients and Healthy Adults, *PLoS One* **8**: e70803.
117 Weng, H., Endo, K., Li, J., Kito, N., and Iwai, N. (2015) Induction of peroxisomes by butyrate-producing probiotics, *PLoS One* **10**: e0117851.
118 Willey, J.M.S., L M; Woolverton, C J (2008) *Prescott, Harley, and Klein's Microbiology*: McGraw-Hill, 1088.
119 Woo, T.D., Oka, K., Takahashi, M., Hojo, F., Osaki, T., Hanawa, T., et al. (2011) Inhibition of the cytotoxic effect of Clostridium difficile in vitro by Clostridium butyricum MIYAIRI 588 strain, *J Med Microbiol* **60**: 1617-1625.

120 Wu, H., Esteve, E., Tremaroli, V., Khan, M.T., Caesar, R., Manneras-Holm, L., et al. (2017) Metformin alters the gut microbiome of individuals with treatment-naive type 2 diabetes, contributing to the therapeutic effects of the drug, *Nat Med* **23**: 850-858.
121 Yanagibashi, T., Hosono, A., Oyama, A., Tsuda, M., Suzuki, A., Hachimura, S., et al. (2013) IgA production in the large intestine is modulated by a different mechanism than in the small intestine: Bacteroides acidifaciens promotes IgA production in the large intestine by inducing germinal center formation and increasing the number of IgA+ B cells, *Immunobiology* **218**: 645-651.
122 Yassour, M., Lim, M.Y., Yun, H.S., Tickle, T.L., Sung, J., Song, Y.M., et al. (2016) Sub-clinical detection of gut microbial biomarkers of obesity and type 2 diabetes, *Genome Medicine* **8**: 17.
123 Yasueda, A., Mizushima, T., Nezu, R., Sumi, R., Tanaka, M., Nishimura, J., et al. (2016) The effect of Clostridium butyricum MIYAIRI on the prevention of pouchitis and alteration of the microbiota profile in patients with ulcerative colitis, *Surg Today* **46**: 939-949.
124 Zhang, F.M., Wang, H.G., Wang, M., Cui, B.T., Fan, Z.N., and Ji, G.Z. (2013a) Fecal microbiota transplantation for severe enterocolonic fistulizing Crohn's disease, *World J Gastroenterol* **19**: 7213-7216.
125 Zhang, H., DiBaise, J.K., Zuccolo, A., Kudrna, D., Braidotti, M., Yu, Y., et al. (2009) Human gut microbiota in obesity and after gastric bypass, *Proc Natl Acad Sci U S A* **106**: 2365-2370.
126 Zhang, X., Shen, D., Fang, Z., Jie, Z., Qiu, X., Zhang, C., et al. (2013b) Human gut microbiota changes reveal the progression of glucose intolerance, *PLoS One* **8**: e71108.
127 Zhou, L., and Foster, J.A. (2015) Psychobiotics and the gut-brain axis: in the pursuit of happiness, *Neuropsychiatr Dis Treat* **11**: 715-723.

CHAPTER 2

More than just a gut feeling: Constraint-based genome-scale metabolic models for predicting functions of human intestinal microbes

Kees C.H. van der Ark*, Ruben G.A. van Heck*, Vitor A. P. Martins Dos Santos, Clara Belzer and Willem M. de Vos

(*) Contributed equally

This chapter was previously published as:

More than just a gut feeling: Constraint-based genome-scale metabolic models for predicting functions of human intestinal microbes, *Microbiome, 2017, 5:78* **Kees C.H. van der Ark***, Ruben G.A. van Heck*, Vitor A. P. Martins Dos Santos, Clara Belzer, Willem M. de Vos (2017)

Abstract

The human gut is colonized with a myriad of microbes, with substantial interpersonal variation. This complex ecosystem is an integral part of the gastrointestinal tract and plays a major role in the maintenance of homeostasis. Its dysfunction has been correlated to a wide array of diseases, but the understanding of causal mechanisms is hampered by the limited amount of cultured microbes, poor understanding of phenotypes, and the limited knowledge about interspecies interactions. Genome-scale metabolic models (GEMs) have been used in many different fields, ranging from metabolic engineering to the prediction of interspecies interactions. We provide showcase examples for the application of GEMs for gut microbes and focus on (i) the prediction of minimal, synthetic or defined media, (ii) the prediction of possible functions and phenotypes, and (iii) the prediction of interspecies interactions. All three applications are key in understanding the role of individual species in the gut ecosystem as well as the role of the microbiota as a whole. Using GEMs in the described fashions has led to designs of minimal growth media, an increased understanding of microbial phenotypes and their influence on the host immune system, and dietary interventions to improve human health. Ultimately, an increased understanding of the gut ecosystem will enable targeted interventions in gut microbial composition to restore homeostasis and appropriate host-microbe crosstalk.

Understanding the gut microbiome

The human gut is colonized since birth with complex microbial communities, mainly consisting of bacteria with millions of unique genes that show substantial interpersonal variation in adult life (Qin, et al., 2010). This complex ecosystem – the gut microbiome– is an integral part of the gastrointestinal tract (GIT) and is intrinsically involved in the maintenance of body homeostasis. Aberrations in the microbial composition have been correlated to a wide array of diseases, ranging from obesity to diabetes, and from inflammatory bowel disease to autism (Flint, et al., 2012, Zhou and Foster, 2015). These correlations have spawned interest in developing strategies to improve human health by rationally steering this composition and thereby the function of the gut microbiome (El-Semman, et al., 2014, Kelly, et al., 2014). This approach has been greatly stimulated by the success of transplantations of faecal microbiota, which showed that 'bugs-can-beat-drugs' in fighting recurrent *Clostridium difficile* infections (van Nood, et al., 2013). However, rationally steering microbiome composition and function requires a thorough understanding of the causal mechanisms underpinning these correlations. Thus far, this understanding has been hampered by (i) the gap between the number cultured gut bacteria and sequenced gut bacteria, (ii) the poor phenotypic characterization of the majority of gut microbes, and (iii) the limited understanding of the interactions of microbes with each other as well as their host. As in other areas of research, the deployment of descriptive and predictive mathematical models has the potential to provide insights that ultimately enable to overcome these limitations. In this review we will discuss the use of genome-scale constraint-based metabolic models for an increased understanding of the gut microbiome and its role in gut homeostasis and (dys)function.

GEnome-scale metabolic Models (GEMs) in gut microbiota research

GEMs are mathematical representations of the knowledge on an organism's metabolic capacity and have been previously applied in bacterial systems for a variety of purposes, including the design of cultivation media, phenotypic characterizations, metabolic engineering, drug discovery, and to study interspecies interactions. For an overview of common GEM applications we would like to refer to these reviews (Feist and Palsson, 2008, Oberhardt, et al., 2009).

Strong developments in both GEMs and gut microbiome research are bound to facilitate moving from correlation studies to gaining mechanistic insights. GEMs can integrate knowledge on the metabolism of one or more gut microbes and predict how this metabolic system functions in different niches in the gut. The gut environment includes nutrient gradients both along the length of the GIT, as well as along the mucosal gradient and villi, and have strong effects on the microbial function (Espey, 2013, Ridlon, et al., 2014). GEMs provide a valuable framework for the integrated study of gut function as they enable the generation of testable hypotheses that can lead to novel insights into causal relationships between the gut microbiome and human health. Considerable progress in these relations has been obtained with the short chain fatty acids (SCFAs) that are produced as main bacterial metabolites in the colon, as illustrated for butyrate, an established functional compound (Hamer, et al., 2008, Smith, et al., 2013). The impact of SCFAs on metabolic health has been reviewed recently (Puddu, et al., 2014). In a model system it was found that acetate is secreted by *Bifidobacterium adolescentis* L2-32, taken up by *Faecalibacterium prausnitzii* A2-165 and used to produce butyrate from sugar. This enabled the prediction of *F. prausnitzii* acetate requirements for butyrate production and how this relates to its low abundance in cases of Crohn's disease (El-Semman, et al., 2014), showing how an observed correlation can possibly be explained mechanistically using GEMs.

In the remainder of this review we will discuss the use of GEMs in gut microbiota research and how GEMs can advance gut research towards the understanding of gut homeostasis and (dys)function. We will focus on the metabolic reactions of the microbes in the gut, on their growth, on their interactions and on the metabolites produced. These are either primary products of microbial metabolism or breakdown products of our diets or host compounds, having a plethora of functions, ranging from SCFAs that fuel enterocytes and have specific signalling and immune functions, to vitamins and other host growth-promoting compounds (Zoetendal and de Vos, 2014). Most of these metabolites cannot be easily detected in the human GIT as these are taken up by the host and processed in the liver. Since GEMs stochiometrically represent all metabolic reactions in a microbe or microbial community, such models enable to estimate the production of these transient metabolites, estimate their distributions within the global metabolic network and provide hypotheses for the metabolic interactions among gut microbes and of those with their host. Moreover, GEMs are instrumental in optimizing growth of GIT microbes in laboratory conditions and hence are

relevant for the production of biomolecules that are involved in host signalling, such as TLR ligands or specific functional proteins (Ottman, 2015, Quevrain, et al., 2016). First, we briefly describe the process of genome-scale metabolic reconstruction and its implications for network modelling. Secondly, we describe applications of GEMs for gut microbiome research that enable: (i) selecting minimal and defined growth media for previously cultured as well as not yet cultured gut microbes, (ii) predicting growth and phenotypes of gut microbes and their influence on health and disease, and (iii) modelling co-cultures and multispecies interactions of gut microbes and the human host (Figure 1).

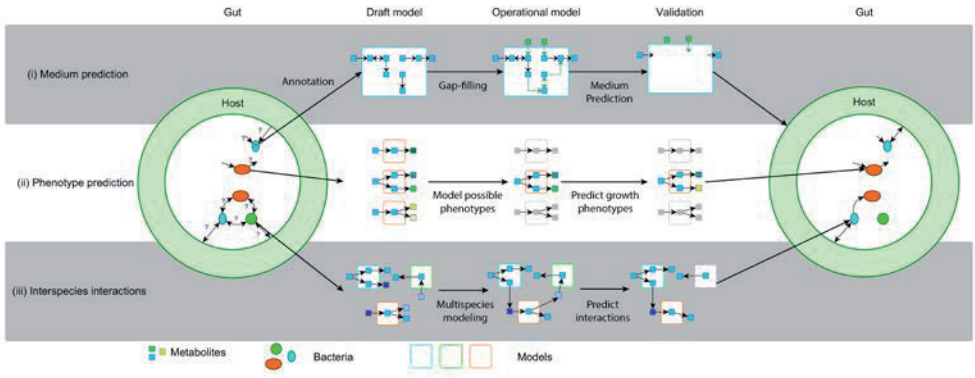

Figure 1. Simplified overview of the use of GEM to increase understanding of the metabolic interactions in the gut microbiome. Individual species require metabolites (squares) to grow. These metabolites can be predicted by GEMs, which results in medium and growth (rate) prediction (i, top). The possible solution the bacteria use to metabolize these metabolites can change under different conditions (ii, middle), which leads to altered interactions between bacteria (iii, bottom)

Genome-scale metabolic reconstruction and network modelling

The basis of GEM construction is the genome annotation of the microbe of interest since this predicts the enzymes a microbe encodes, and thereby provides a list of chemical reactions the microbe can perform. This list of chemical reactions forms the draft metabolic model, which is often far from complete (Thiele and Palsson, 2010). Typically, there are missing reactions due to incorrect, missing, or low-quality annotations, even for well-studied organisms (Orth and Palsson, 2012). Moreover, our knowledge of the biochemical pathways is often insufficient, with unknown conversions still being discovered (Bui, et al., 2015). These missing reactions – also called gaps – severely limit the possibilities for GEM analyses, as parts of the metabolic network are not connected. Therefore, gap-filling algorithms are used to predict the presence of additional reactions that can be obtained from reaction

databases such as KEGG (Kanehisa, et al., 2014) or Metacyc (Caspi, et al., 2014) and to connect disconnected parts of the network (Orth and Palsson, 2010, Thiele and Palsson, 2010). Thereby, these algorithms provide hypotheses on enzymes that were missed in the genome annotation. In some cases, a corresponding gene, not initially annotated as such, is identified and the genome annotation is improved. In the remaining cases, the reactions become 'orphan reactions', e.g., reactions that are thought to occur in the microbe based on existing pathways of other microbes but that have not been linked to any genes. The addition of orphan reactions might lead to erroneous model predictions, but is often essential to obtain a functioning GEM and facilitates targeted gene identification (Orth and Palsson, 2010, Thiele and Palsson, 2010). Model construction and gap-filling algorithms have been extensively described elsewhere (Orth and Palsson, 2010, Thiele and Palsson, 2010, O'Brien, et al., 2015).

After gap-filling, GEMs are expected to be able to sustain in silico growth of the modelled organism. Growth is modelled as the formation of biomass in a complex organism-specific reaction involving a large number of biomass precursors such as DNA, RNA, proteins, lipids, ATP, NADPH, and various small molecules. The use of biomass precursors in bacterial GEMs has recently been thoroughly explored resulting in a shortlist of universally essential, as well as organism-specific biomass precursors (Xavier, et al., 2017). If all of these precursors can be formed in the right ratios the GEM predicts that growth is possible. The most common way to predict growth phenotypes is through Flux Balance Analysis (FBA) (Orth, et al., 2010). FBA determines an optimal flux distribution for the production of biomass components while adhering to several types of constraints: (i) mass-balance constraints; the production and consumption of intracellular metabolites cancels out, (ii) thermodynamic feasibility constraints; reactions can only operate in thermodynamically feasible directions, and (iii) capacity constraints; fluxes through reactions are bounded to biologically feasible ranges. Capacity constraints are also used to define the medium conditions by directly defining which metabolites can be imported. Thereby, GEMs can be easily modified to simulate growth phenotypes in a wide range of different experimental conditions.

GEMs are typically evaluated by comparing predicted growth phenotypes for both wild type and mutant strains to the available experimental data. This experimental data usually consists

of growth measurements for a large number of media containing different carbon, nitrogen, phosphorus and sulphur sources. For the comparison, both the experimental data and the GEM predictions are discretized to the two states 'growth' and 'no growth'. This binary discretization leads to two different types of inconsistencies: (i) growth predicted by the GEM but not experimentally found, and (ii) growth that is experimentally validated but not predicted by the GEM. In the first case, the GEM overestimates the microbe's abilities, suggesting it may include reactions that the microbe cannot perform. In contrast, the other case suggests that the GEM is missing reactions. This comparison can thus be used to evaluate both the annotation and the gap-filling process that underlie the GEM construction. For example, if the removal of a single reaction from the GEM results in a large improvement of GEM predictions, this suggests that this reaction was erroneously added and should be considered for removal. This process of using experimental data to find incorrect GEM predictions and subsequently making changes to the GEM has also been combined into algorithms, such as GrowMatch (Kumar and Maranas, 2009), that will make a minimal number of changes to a GEM while maximizing its coherence to experimental data.

The established manual GEM reconstruction process ultimately results in high-quality GEMs, but is extremely time-consuming (Thiele and Palsson, 2010). The advent of high throughput sequencing and concurrent rapid increase in available biological data warrants a faster approach, which is provided by the RAVEN toolbox (Agren, et al., 2013) and the ModelSEED approach (Henry, et al., 2010). In both cases, the process of genome annotation, draft GEM construction and gap-filling has been fully automated, although extensive manual curation remains necessary to sustain a high quality (Henry, et al., 2010, Agren, et al., 2013). This curation process has recently been streamlined for gut microbes specifically as part of the AGORA metabolic GEM resource (Magnusdottir, et al., 2017). A distinguishing feature of the AGORA GEM resource is the semi-automatic curation of ModelSEED GEMs where corrections that are manually applied to a single GEM are propagated to the GEMs of other gut microbes. This semi-automatic curation both speeds up the curation process and finally results in more uniform and higher quality GEMs.

Use of GEMs to design defined culture media

The basis of classic microbiology is the ability to culture bacteria in a pure culture on a well-defined medium. Such a well-defined medium is required for detailed metabolic analyses,

growth optimization and finally also in a feedback loop with the GEM itself to optimize the metabolic model. Moreover, well-defined media devoid of animal-derived compounds will be needed when intestinal microbes that are therapeutically effective are to be cultured and used in therapeutic settings. An example is the recently developed medium for *Akkermansia muciniphila* that was used for a human safety study [61]. Finally, obtaining pure cultures is essential for intervention studies to investigate host-microbe interactions and to use the beneficial bacteria as potential therapeutic microbes. Pure cultures have been successfully obtained for over 1000 different gut species (Rajilic-Stojanovic and de Vos, 2014), which was recently expanded by high throughput culturing approaches (Lagier, et al., 2016, Abdallah, et al., 2017). However, as it has been predicted that there are at least two to three times more different gut species, a significant number of gut microbes remain uncultured and inaccessible for study in isolation (Ritari, et al., 2015). A number of known not-yet cultured candidates have been listed in a 'most wanted' list (Fodor, et al., 2012), which highlights the need for culturing of gut microbes. Among these targets are *Oscillospira* spp. that are receiving considerable attention (Mackie, et al., 2003, Cuiv, et al., 2015, Konikoff and Gophna, 2016). A major issue in the culturing of these microbes is the lack of suitable growth media. Growth media are often based on the ecosystem a microbe naturally occurs in, but the gut is extremely complex with many different nutrients, highly variable nutrient levels, and many interspecies interactions. Here we first describe the challenges in the use of GEMs for the design of defined media, and then how GEMs have been successfully used for the design of defined media and how similar approaches can be used to design suitable defined media for not-yet cultured bacteria.

There are three main challenges in the use of GEMs for the design of defined growth media: (i) The *in silico* biomass composition is an influential aspect of the GEM as it defines all metabolites required for growth (Xavier, et al., 2017) . The omission of even a single metabolite in this composition can prevent the GEM from predicting an essential media supplement. However, the biomass composition cannot be fully determined *in silico* and relies on the availability of organism-specific experimental data. As this is not available for many gut microbes, automatic model generation procedures rely on heuristics to estimate the biomass components that are required for each organism (Henry, et al., 2010, Magnusdottir, et al., 2017). We highly recommend evaluating a given biomass composition generated from automatically generated GEMs according to the guidelines recently set out in a thorough

evaluation of biomass compositions (Xavier, et al., 2017) prior to gap-filling and media design. (ii) The gap-filling step in GEM construction typically relies on the introduction of known biochemical reactions to complement the metabolic network of the modelled microbe (Orth and Palsson, 2010). In particular, reactions are often added such that the GEM predicts *in silico* growth in a pre-defined medium, which is not directly suitable if no chemically defined medium is known for the microbe or if the microbe uses not previously characterized reactions. Hence, all gap-filling reactions should be carefully individually inspected and corresponding genes need to be identified to support the procedure. (iii) GEMs do not capture the non-linear link between concentrations of medium components and the speed with which microbes can import them. Hence, GEM-based medium design is limited to predicting which compounds need to be present and cannot be used to determine optimal concentrations.

Despite these challenges, GEMs have proven to be useful in the design of chemically defined growth media , as has been shown for the lactic acid bacterium *Lactobacillus plantarum* WCFS1 (Teusink, et al., 2005). Lactic acid bacteria are important in many industrial food processes and some are marketed as probiotics (Teusink and Smid, 2006). Therefore, the GEMs of lactic acid bacteria are used to study their metabolic capabilities and behavior in fermentation processes (Teusink, et al., 2006, Wegkamp, et al., 2010), as well as their probiotic functions (Saulnier, et al., 2011, dos Santos, et al., 2013). The GEM of *Lactobacillus plantarum* WCFS1 was automatically constructed based on its genome sequence and subsequently extensively manually curated (Kleerebezem, et al., 2003, Teusink, et al., 2005). The GEM was then used to predict the essentiality of 36 compounds in a chemically defined growth medium. The GEM predictions were correct for 29/36 (81%) of the compounds, but were incorrect for the vitamins folate, thiamine, and vitamin B6, as well as for the amino acids arginine, glutamate, isoleucine, and tryptophan. The incorrect predictions pinpointed errors in both the GEM construction process and in the experimental procedures, and also pinpointed distinct metabolic features of *L. plantarum WCFS1,* for example: (i) The incomplete folate biosynthesis pathway in the GEM was in part due to a missing EC number for a correctly annotated gene, as well as no reactions in Metacyc for another EC number. (ii) The GEM lacked a complete isoleucine biosynthesis pathway, but growth was observed in the isoleucine omission experiment. This turned out to be a result of isoleucine contamination in the other amino acids. (iii) A missing reaction for thiamine biosynthesis was assigned to a gene involved in molybdopterin biosynthesis. In

Enterobacteria these reactions are carried out by two paralogs, but it appears that both reactions are carried out by a single enzyme in *L. plantarum* (Teusink, et al., 2005). These results clearly illustrate how a GEM-driven systematic evaluation of medium compositions can increase the understanding of a microbe's metabolism.

A GEM of a different lactic acid bacterium, *Lactococcus lactis* IL1403, was constructed and used to remove all non-essential metabolites from a rich medium in order to design a minimal medium for physiological studies (Oliveira, et al., 2005). This exercise in medium design not only resulted in a minimal medium, but also allowed for careful comparisons between *in silico* predictions and experimental data to understand their differences. The GEM predicted that arginine, methionine and valine are essential for growth, and that either glutamate or glutamine is required additionally. However, recent single amino acid omission experiments have led to the conclusion that arginine, asparagine, histidine, methionine, serine, isoleucine, leucine, and valine are essential medium components for *L. lactis*, and that glutamate and glutamine are not (Aller, et al., 2014). At first glance this might incorrectly seem like poor performance by the GEM. However, the agreements and disagreements between predictions and experiments can be summarized in three points: (i) they agree on the essentiality of arginine, methionine, valine and the non-essentiality of the ten amino acids not previously mentioned, (ii) they do not evaluate glutamate and glutamine in the same manner - the GEM predicts that one of them is required, whereas the experiment indicates that either one can be omitted, but that glutamine cannot be omitted if the concentration of glutamate is additionally reduced to 10% of the normal concentration - and (iii) they disagree on the essentiality of asparagine, histidine, isoleucine, leucine, and serine, but also disagree on the meaning of 'essential'. In the *L. lactis* IL1403 GEM a compound was essential if its omission reduced the specific growth rate below 0.01/h. In the omission experiment a compound was considered essential if the final OD dropped below 40% of the final OD in the rich medium. This introduces a certain level of ambiguity and, for example, if the experimental threshold would instead be at 20%, asparagine and serine would not have been considered essential.

The ability to culture pathogens and probiotics is important to study them in isolation and to determine their role in the gut microbiome. Therefore, a GEM was used to design a minimal growth medium for *Staphylococcus aureus* N315, a pathogen that frequently infects hospitalized patients (Becker and Palsson, 2005). The GEM predicted that several amino

acids were essential, but *in vivo* experiments indicated otherwise. Later on, an updated GEM predicted that *S. aureus* N315 has no intrinsic auxotrophies for amino acids, but that some particular isolates do require some amino acids (Heinemann, et al., 2005). This discrepancy between the updated GEM and the experimental results for the isolates was explained by the repression of amino acid synthesizing genes. The repression could be relieved by progressively eliminating the amino acids from the medium, supporting the GEM prediction that *S. aureus* can indeed synthesize these amino acids. This study showed how a GEM can aid in omitting nutrients from a known defined medium.

These three case studies show that GEMs are a good starting point for designing minimal media. In fact, the ability of GEMs to design growth media was recently emphasized by the development of the Minimal Environmental TOol (MENTO) (Zarecki, et al., 2014). MENTO predicts the minimal medium requirements for an organism based on its GEM, and was used to study broad nutritional trends in over 2500 automatically generated ModelSEED (Henry, et al., 2010) models. For three well-characterized organisms, the predictions based on the ModelSEED models were also compared to the predictions based on manually curated models. The comparison indicated that the ModelSEED models are more pessimistic growth predictors, but have a similar accuracy (Zarecki, et al., 2014). Nonetheless, the authors indicate that while the ModelSEED models are suitable for studying broad nutritional trends, one should be careful in interpreting results for any specific organism. A ModelSEED model thus requires manual curation before using it to predict suitable minimal growth media.

Such a manually curated ModelSEED GEM was recently used for minimal medium design for *F. prausnitzii*, a prevalent and potential beneficial gut microbe that is commonly grown on the chemically undefined YCFAG medium (Heinken, et al., 2014). The automatically generated ModelSEED GEM was first manually curated such that it correctly captured the known biochemistry and physiology of *F. prausnitzii*. This curation involved changing the biomass reaction, updating reaction directionalities, adding species-specific pathways, and filling gaps. The curated GEM was then used to predict a chemically defined growth medium called CDM1. CDM1 did, however, not facilitate *in vitro* growth and was subsequently supplemented with additional nutrients to form an extended medium CDM2, which did facilitate *in vitro* growth. The researchers then used LC-MS to identify what metabolites in CDM2 are net consumed, and what metabolites are net produced. The metabolite

consumption and production data was then used to improve the GEM and the corresponding genome annotation. Ultimately, the researchers were able to design a refined and chemically defined medium CDM3 that facilitated both *in silico* and *in vitro* growth, albeit that growth was still rather poor and unreliable (Heinken, et al., 2014).

The requirement for manual curation of ModelSEED (Henry, et al., 2010) GEMs prior to media design has been substantially reduced due to the presence of 773 semi-automatically curated GEMs of relevant gut microbes (Rajilic-Stojanovic and de Vos, 2014, Bauer, et al., 2015) in the AGORA GEM resource (Magnusdottir, et al., 2017). These GEMs have been curated collectively such that any issues addressed in one GEM are also directly addressed in others. Although further microbe-specific manual curation may still be required for many microbes, some AGORA GEMs may also be directly suitable for media design. As a showcase, the AGORA GEM of *Bacteroides caccae* ATCC 34185 was successfully used to design the first chemically defined medium supporting *in vitro* growth for this gut microbe (Magnusdottir, et al., 2017).

Metagenomic studies (Nielsen, et al., 2014) and single-cell genomics (Lasken, 2012, Kolinko, et al., 2015) of gut bacteria have already yielded genomes that could be used to create draft GEMs. However, the available biochemical information to turn draft GEMs into functional GEMs for uncultured bacteria is limited. To gain more insight in secreted metabolites and available nutrients in the gut, imaging mass spectrometry can be applied (Rath, et al., 2012). These uptake and secretion patterns can be incorporated into GEMs. We encourage the use of GEMs to predict minimal or defined media on which the microbes of interest can be cultured. Combined with additional ecological and genomic markers, such as temperature, antibiotic resistance and spore formation, it should be possible to culture more bacterial species (Figure 2). The next steps are in predicting how varying environments result in different phenotypes.

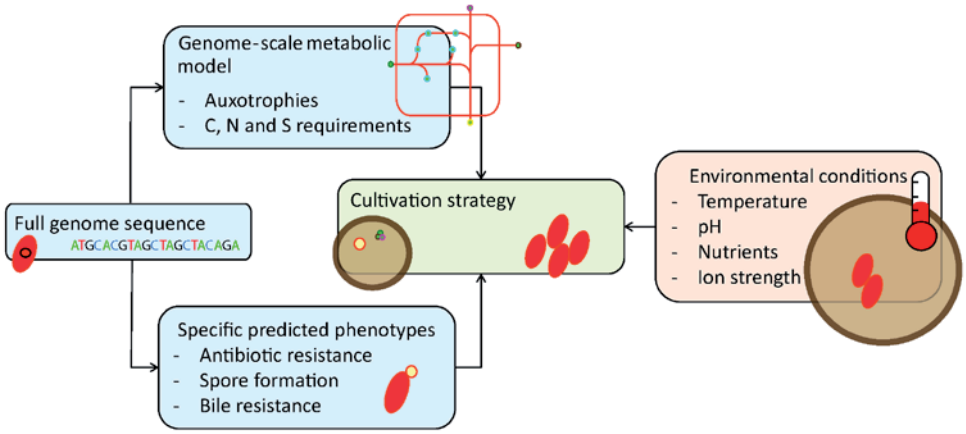

Figure 2. Suggested cultivation strategy. The initial cultivation strategy of a microbe can be optimised by thorough analysis of its genome and isolation conditions. The genome contains information on metabolic pathways, as represented in GEMs, that inform on auxotrophies and suitable carbon, nitrogen, and sulphur sources. In addition, the genome annotation can reveal additional considerations such as antibiotic or bile resistance, or the ability to form spores. The isolation condition of a microbe, for example the human gut, provides information on suitable environmental conditions such as temperature, pH, and ion strength.

Phenotype prediction

Most microbes have versatile and complex metabolic pathways. Often, many alternative pathways are available for the conversion of the available substrate to all biomass components. GEMs can be used to explore all possible phenotypes for a wild type or mutant strain in a given environment. In addition, GEMs can be used to interpret experimental data that is difficult to directly connect to metabolic rates, such as transcriptomics and proteomics data. GEMs, which are ultimately based on genotypes, are thus a means to explore possible phenotypes in a wide range of different experimental conditions. The ability to predict how different microbial phenotypes result from different environments can ultimately have consequences for human health. For example, GEMs may be able to identify the conditions under which conditional pathogens become pathogenic (Oberhardt, et al., 2008), or, in contrast, when therapeutic bacteria or probiotics may convey their beneficial properties (Ventura, et al., 2009, Saulnier, et al., 2011).

A main challenge in the use of GEMs for the prediction of phenotypes of gut microbes is that these models are –traditionally – restricted to metabolic activities. They do not explicitly

include regulation nor the synthesis of mRNAs or individual proteins. Hence, GEMs can accurately predict growth phenotypes that are related to the optimal conversion of substrates to biomass components (Lewis, et al., 2010), but do not directly predict the synthesis of secondary metabolites and proteins involved in, crucial processes such as microbe-microbe signalling, microbe-host communication (Guo, et al., 2017, Plovier, et al., 2017) and inflammation (Quevrain, et al., 2016). Such predictions rely on the integration of ~omics data or regulatory networks, as highlighted by several of the following examples.

GEM-driven exploration of the metabolic capacities of pathogens has been explanatory for pathogenic phenotypes. For example, a GEM was used to predict virulence of *Salmonella* in a mouse model system. The GEM describes a very versatile metabolism that enables *Salmonella* to utilize 31 host nutrients, allowing it to grow fast within the host cell. The GEM predicted the pathogenicity of phenotypes and was accurate in 92% of the cases (Steeb, et al., 2013). In addition, it was found that the metabolic capabilities of *Salmonella* show similarities in host dependency for growth substrates and biosynthesis to other pathogens. Like *Salmonella*, other pathogens are also capable of degrading purine nucleosides, pyrimidine nucleosides, fatty acids, glycerol, arginine, N-acetylglucosamine, glucose and gluconate. Similarly, it was hypothesized that comparisons of metabolic patterns between *Pseudomonas aeruginosa* and non-pathogenic relatives could yield insight into opportunistic pathogenic phenotypes of this species (Oberhardt, et al., 2008), as has later been done successfully for *Burkholderia* species (Bartell, et al., 2014). The metabolic model for the pathogenic *P. aeruginosa* also showed a versatile metabolic pattern and accounted for virulence inducing pathways, such as exopolysaccharide alginate synthesis (Ramsey and Wozniak, 2005).

In more recent research, highly quantitative proteomics and metabolic measurements were used to impose pH-dependent constraints on the GEM of *Enterococcus faecalis,* a human gut pathogen (Großeholz, et al., 2016). The pH-dependent constrained GEM accurately predicted growth rate, proton pump activity by ATPase and a metabolic shift from mixed acid fermentation to homolactic fermentation. However, discrepancies were found between expression of lactate dehydrogenase and lactate production, which emphasized that constrains based on solely proteomic measurements are not sufficient for an accurate phenotype prediction.

Transcriptomics and proteomics experiments aim to discover what an organism is doing, but the data is often difficult to analyse because there are no one-to-one relationships between expression levels, protein quantities, enzyme activities, and fluxes (Hoppe, 2012, Rocca, et al., 2015). GEMs can aid in elucidating the metabolic activities from these data by visualising the data on a metabolic map or by predicting metabolic fluxes (Machado and Herrgård, 2014, Weaver, et al., 2014, King, et al., 2015, Zhang, et al., 2017). For example, transcriptomics data of two strains of *Lactobacillus reuteri,* with potentially opposite effects on the human immune system, were analysed by visualising the data on two GEMs. The analysis revealed that both strains produce vitamins, essential amino acids, and mucosal binding proteins, but that they differed in their production of potential inducers of tumour necrosis factor (Saulnier, et al., 2011). The prediction of metabolic fluxes from ~omics data relies on the concept that, on average, gene expression levels are a proxy for fluxes. The GEM then predicts a flux distribution that matches the trends in the expression data, while accounting for mass balance, thermodynamics, and capacity constraints. Several such methods have been developed in the last few years, and have been extensively summarised and evaluated recently (Machado and Herrgård, 2014). The evaluation did not result in a clear best-performing method, and none of the methods actually outperforms parsimonious FBA (Lewis, et al., 2010), which does not require any ~omics data as input. However, the evaluation conditions were limited to minimal media where the optimization of the conversion of substrates to biomass seems a suitable growth strategy. It remains to be seen how these various methods compare when microbes actively synthesize secondary metabolites *in situ* or in rich media.

A different approach to find out what an organism is doing, rather than what it can do, is by combining GEMs with other models, such as regulatory networks (Chandrasekaran and Price, 2013, Faria, et al., 2014, Kim and Reed, 2014). The regulatory networks of well-studied species such as *E. coli, M. tuberculosis* and *M. genitalium* have been elucidated and incorporated in metabolic models (Chandrasekaran and Price, 2010, Karr, et al., 2012, Carrera, et al., 2014, Kim and Lun, 2014). Based on these model organisms, attempts have been made to automate the incorporation of regulatory networks into GEMs (Novichkov, et al., 2013), also especially aiming at less well-characterized species (Chandrasekaran and Price, 2010). These models incorporate the influence of environmental factors on the behaviour of the modelled organism, which may be extremely relevant for microbes residing in a dynamic environment such as the human gut.

These examples show how GEMs can be used to explore possible phenotypes, and to predict actual phenotypes based on ~omics data or regulatory models. However, we highlight the need for a thorough evaluation on methods for the integration of ~omics data and regulatory networks with GEMs to predict the phenotypes of gut bacteria *in vitro* and ultimately *in vivo*. This will be an important stepping-stone in predicting the role of bacteria under different gastrointestinal conditions, on which also other microbial species have a big influence.

GEM predictions on interspecies interactions

Within the gut microbiome there are numerous microbial interactions and networks. Three types of simple multispecies interactions have been described and modelled before: mutualism, commensalism, competition and neutralism (Klitgord and Segre, 2010, Freilich, et al., 2011, McCloskey, et al., 2013). GIT-colonizing microbial species often depend on each other for growth signals and substrates or compete for the metabolites, thus this ecosystem is ideal for the modelling of interspecies interactions and using interspecies interactions predictions to gain a mechanistic insight into this ecosystem (Borenstein, 2012, Ji and Nielsen, 2015). Interactions between microbes have been modelled on different phylogenetic levels, ranging from strains (Tzamali, et al., 2011) to species (Salimi, et al., 2010, Sun, et al., 2010) and ecosystem communities (Levy and Borenstein, 2013). The challenges in multispecies modelling are briefly described below, followed by examples of successful GEM-based multispecies modelling approaches that are also summarized in Figure 3.

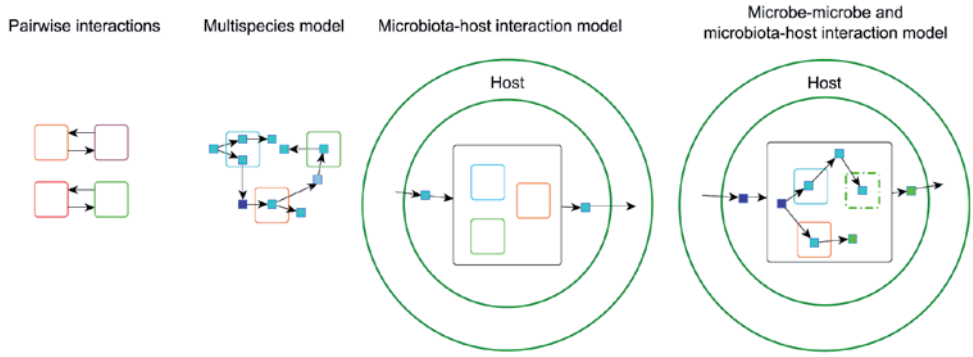

Figure 3. Modes of interspecies interactions as modelled before. Pairwise interactions only account for two species to share metabolites. Multispecies models allow sharing of metabolites between more than two species. Microbiota-host interaction models lump all the microbial species into one meta-model and model the interaction with the host. Microbe-microbe and microbiota-host interactions are multilevel models that take into account microbial interactions and interactions with the host.

Multispecies modelling using GEMs is complicated through the aforementioned phenotype prediction challenge regarding secondary metabolites, but also by two other challenges: (i) The vast majority of GEM analysis methods rely on a steady-state assumption, but microbial interactions via signalling molecules are inherently dynamic. (ii) Flux prediction methods are based on computational optimization with regards to a single metabolic goal, usually the maximization of biomass production; a reasonable goal for an individual microbial species. However, when multiple microbes are modelled simultaneously it is not a reasonable assumption that all work together to maximize total biomass production. The examples discussed hereafter provide a rough overview of different approaches that have been taken to minimize or circumvent these issues.

The pioneering work in GEM-based multispecies modelling was directly combining two GEMs for the mutualistic bacterium *Desulfovibrio vulgaris* and archaeon *Methanococcus maripaludis S2* into a single model with a shared extracellular environment (Stolyar, et al., 2007). In this ecologically relevant syntrophic relationship, *D. vulgaris* ferments lactate, and *M. maripaludis* consumes the fermentation products formate, dihydrogen and acetate. In this work, the aforementioned issue on optimizing for biomass production was evaluated by applying distinct weights to the different types of biomass. In other words, the mathematical optimization would prioritize one type of biomass over the other in order to explore how this would affect overall flux predictions. The predicted biomass production for *D. vulgaris* was practically independent of the relative weights, whereas the *M. maripaludis* biomass production increased if it received higher weights. This is due to the sequential nature of the interaction between these bacteria, where *D. vulgaris* effectively 'feeds' *M. maripaludis.* However, this approach is not suitable if the community members exhibit cross-feeding or substrate competition.

A similar approach was taken to identify media that stimulate commensal or mutualistic relationships between each possible pair of seven well-known microbes (Klitgord and Segre, 2010). This number was rapidly expanded to 118 species coupled in 6.903 pairs driven by automated curation of over a hundred GEMs (Freilich, et al., 2011). The latter study not only focused on cooperation, but also specifically on identifying media that induce competition between pairs of microbes. It was found that competition was generally 'won' by species that grew fast on versatile media, such as *E. coli,* while cooperation was more evident in

Clostridia species that were able to degrade lignin and cellulose, which releases free sugars to other bacteria. This type of macromolecule degradation is highly important in degradation of host dietary compounds and thus directly relates to gut health.

Instead of looking into the details of the interactions between a few species, GEMs have also been used to elucidate general properties of the co-occurrence of microbes. Specifically, there are two main mechanisms driving species co-occurrence: (i) habitat filtering: microbes occupy a similar nutritional niche and compete, and (ii) species assortment: microbes have complementary metabolisms and cooperate. A recent study aimed to identify which of these two mechanisms is the driving force behind the co-occurrence of microbes in the human gut (Levy and Borenstein, 2013). Therefore, they automatically generated 154 GEMs based on KEGG (Feng, et al., 2012, Kanehisa, et al., 2014) for gut microbes whose co-occurrences were determined based on a gut metagenome dataset containing measurements from 124 individuals. These GEMs were used to determine metabolic competition and complementarity indices between each pair of species based on network topology, thereby circumventing the need for optimization based on an ambiguous multispecies metabolic goal. As the species co-occurrence was best explained via the metabolic competition index, the authors concluded that habitat filtering is the main driving force behind species co-occurrence in the human gut. In an other recent study, GEMs were used to study species co-occurrence based on 261 microbial species in 1297 communities from diverse habitats (Zelezniak, et al., 2015). The GEMs were used to calculate both the resource competition and interaction potential within these communities based on network topology. Resource competition was significantly higher in the 1297 communities versus random assemblies, indicating that habitat filtering was again identified as the main driving force behind community composition. However, there were also 7221 sub-communities of up to 4 co-occurring species within the larger communities. Within these sub-communities, the interaction potential – defined as the difference in minimal number of metabolites required for growth between a non-interacting and a cooperating community - was significantly higher than in full communities and random assemblies.

In order to understand how gut communities form and change, it is also important to consider spatial and temporal effects. The novel modelling framework COMETS (Harcombe, et al., 2014) - Computation of Microbial Ecosystems in Time and Space – simulates multiple GEMs

on a lattice over time using dynamic FBA (Mahadevan, et al., 2002), which is based on simulating dynamics using successive steady-state optimizations. COMETS does not require any prior information on how the modelled microbes interact, but nonetheless captures interesting and non-intuitive spatiotemporal dynamics of multispecies interactions. For example, it correctly predicted that the slowest-growing microbe of a three-species ecosystem would also ultimately be the most-prevalent one, and that the growth rate of a colony with a mutualistic partner can be improved by placing a competing colony in between them. COMETS has also been used to study how robust competing and mutualistic interactions are to genetic perturbations. Specifically, it has been possible to predict the effects of gene knockouts on a synthetic community of *Escherichia coli* and *Salmonella enterica* (Harcombe, 2010) on competition-inducing and mutualism-inducing growth media (Chubiz, et al., 2015). Interestingly, the community was more robust to genetic perturbations in *E. coli* under cooperative conditions, but more robust to genetic perturbations in *S. enterica* under competing conditions (Chubiz, et al., 2015). These results highlight that GEMs can mechanistically explain the intriguing interactions of multispecies interactions.

A conceptually similar framework is BacArena (Bauer, et al., 2017). BacArena also uses a dynamic form of FBA simulations to model microbes over time, but simulates individual microbes across a 2D grid (Bauer, et al., 2017) rather than microbial communities on a lattice as in COMETS (Harcombe, et al., 2014). Of particular interest is the application of BacArena to the seven species SIHUMI community representative of a simplified human gut (Becker, et al., 2011). Initial simulations excluding glycan production in the lumen resulted in a community dominated by *E.* coli. However, as a mucus glycan gradient was imposed using diffusion on the 2D grid, the glycan-degrading *Bacteroides thetaiotamicron* became dominant in the mucosal layer, while the lumen represented a more varied community still dominated by *E.coli*.

A multispecies interaction of particular interest is the interaction between gut microbes and their host. The host is not only an important environmental factor for gut microbes, but is also metabolically active itself. Additionally, host behaviour such as diet intake has a great and reproducible influence on the microbiota composition (Flint, et al., 2017). GEMs have been created for hosts of particular interest, such as mouse (Sigurdsson, et al., 2010) and human (Thiele, et al., 2013), and have even been trimmed down to tissue-specific GEMs,

including a GEM for colon-derived tissue (Browne, et al., 2016). The human Recon 2.04 GEM was adapted to be not only tissue specific but context specific as well. Transcriptome data obtained from inflamed mucosal tissue in IBD data was used to generate new GEMs (Hasler, et al., 2016). Subsequent combination of this data with bacterial expression data showed uncoupling of host-microbe metabolic interactions in IBD patients. The mouse GEM (Sigurdsson, et al., 2010) was recently used to study how different diets and the presence of the gut microbe *Bacteroides thetaiotaomicron* affect its metabolism (Heinken, et al., 2014). A *B. thetaiotaomicron* model was constructed using ModelSEED (Henry, et al., 2010) and, after manual curation, was linked to the mouse GEM via a shared lumen compartment. Although a single microbe is not directly representative of the gut community, the combined GEM mechanistically explained how both organisms benefit from the mutualism, correctly predicted how the interaction affects biofluid metabolome composition, and even described how gut microbes can rescue hosts with lethal gene deletions (Heinken, et al., 2014).

Host-microbe interactions have also been modelled using a single 'supra-organism model' (Borenstein, 2012) to represent all gut microbes simultaneously, thereby also avoiding optimization-related issues with multiple microbial biomass types. These GEMs don't focus on individual microbes or their interactions, but rather on the interaction of the community with the environment or host. Such a GEM was used together with metagenomics data to study how host-microbe interactions differ in case of obesity or inflammatory bowel disease (IBD) (Greenblum, et al., 2012). This revealed a differential expression of enzyme groups expressed by the complete microbiota between diseased and healthy people, without investigating the roles of individual species or their interactions. The differences were found in the upregulation of membrane transport and downregulation of vitamin metabolism, nucleotide metabolism and transcription. This study suggests that the differences in enzyme expression originate from an altered interaction between the microbes and their environment. They are the result of a change in the environment of the bacteria and do not come from a change in core metabolic processes. By combining previous approaches of modelling interspecies interactions and considering the whole microbiota as one entity, a predictive tool for dietary interventions was created (Shoaie, et al., 2015). The tool, CASINO - Community And Systems-level Interactive and Optimization - predicts dietary interventions based on interactions between the host, the microbiota and the applied diet. CASINO was used to model the interactions of four microbes in two synthetic communities that differed by a single

microbe. It correctly predicted the produced metabolites, including essential amino acids, and the contribution of each species to the production of each metabolite. CASINO was then used to predict the impact of a dietary intervention in 44 individuals, based on relative abundances of the most prevalent microbes in each individual before and after the intervention. The predicted production of SCFAs and amino acids mostly matched the *in vivo* measurements. Finally, CASINO was used to design a beneficial diet for subjects with a poor microbiota composition (Shoaie, et al., 2015).

The use of GEMs to predict multispecies interactions and to study the influence of perturbations in environmental factors and communities is a valuable asset in microbiota function prediction. In this way it can be predicted how individual species contribute to healthy and diseased conditions. The increase in tools for the prediction of multispecies interactions highlights the importance of this application. Moreover, these predictions were instrumental in the prediction of diets to improve the metabolic function of gut microbiota (Shoaie, et al., 2015). Ultimately, this research will lead to increased understanding of the interactions of the gut microbiota and its host, and on its role in gut homeostasis and (dys)function, and it will ultimately pave to way to improve human health using specific gut microbes or dietary interventions.

Conclusion and perspectives

After a few decades of characterizing gut microbiota composition many gut microbes have been sequenced (Peterson, et al., 2009, Qin, et al., 2010). Over 200 of these genome sequences have been used to generate GEMs, in most cases by automated tools (Henry, et al., 2010, Caspi, et al., 2014). These GEMs have been used to predict growth phenotypes of single microbes and communities in laboratory and *in vivo* settings.

Here, we reviewed three ways in which GEMs contribute in elucidating gut microbiome function. We described how GEMs are used to: (i) culture bacteria, (ii) predict bacterial phenotypes under changing conditions, and (iii) study the interactions both among the bacterial species and with their host.

We have shown that recent advances in automated generation of GEMs (Henry, et al., 2010, Magnusdottir, et al., 2017), single-cell genomics (Blainey, 2013), metagenomics (Gill, et al., 2006, Qin, et al., 2010) and metatranscriptomics (Bailly, et al., 2007, Maurice, et al., 2013,

Baldrian and Lopez-Mondejar, 2014) can increase the availability and accuracy of GEMs. Metagenomics as well as single-cell genomics will yield more genome sequences of microbes that can be used for generating GEMs. Moreover, developments in single molecule sequencing will allow for closed genomes that are in the end the golden standard to be used for generating GEMs. These GEMs will contribute in understanding how both uncultured and cultured bacteria live and behave in complex ecosystems (Ji and Nielsen, 2015). *In vivo* or *in vitro* validation of GEM predictions and subsequent GEM updates remain key in improving GEM quality and ultimately understanding the complex gut ecosystem.

GEMs allow understanding *why* species are present and *what* they do, instead of *who* they are, as was the focus in the last decades. We expect that GEMs will contribute to elucidate the mechanisms behind known probiotics, as well as in identifying new probiotics, and understanding the role of different bacteria in complex ecosystems. Ultimately, GEMs can contribute to the design of controlled interventions that steer gut composition and activity to improve human health.

References

1 Abdallah, R.A., Beye, M., Diop, A., Bakour, S., Raoult, D., and Fournier, P.E. (2017) The impact of culturomics on taxonomy in clinical microbiology, *Antonie Van Leeuwenhoek*.

2 Agren, R., Liu, L., Shoaie, S., Vongsangnak, W., Nookaew, I., and Nielsen, J. (2013) The RAVEN toolbox and its use for generating a genome-scale metabolic model for Penicillium chrysogenum, *Plos Computational Biology* **9**: e1002980.

3 Aller, K., Adamberg, K., Timarova, V., Seiman, A., Feštšenko, D., and Vilu, R. (2014) Nutritional requirements and media development for Lactococcus lactis IL1403, *Applied Microbiology and Biotechnology* **98**: 5871-5881.

4 Bailly, J., Fraissinet-Tachet, L., Verner, M.C., Debaud, J.C., Lemaire, M., Wesolowski-Louvel, M., and Marmeisse, R. (2007) Soil eukaryotic functional diversity, a metatranscriptomic approach, *Isme Journal* **1**: 632-642.

5 Baldrian, P., and Lopez-Mondejar, R. (2014) Microbial genomics, transcriptomics and proteomics: new discoveries in decomposition research using complementary methods, *Applied Microbiology and Biotechnology* **98**: 1531-1537.

6 Bartell, J.A., Yen, P., Varga, J.J., Goldberg, J.B., and Papin, J.A. (2014) Comparative metabolic systems analysis of pathogenic Burkholderia, *Journal of Bacteriology* **196**: 210-226.

7 Bauer, E., Laczny, C.C., Magnusdottir, S., Wilmes, P., and Thiele, I. (2015) Phenotypic differentiation of gastrointestinal microbes is reflected in their encoded metabolic repertoires, *Microbiome* **3**: 55.

8 Bauer, E., Zimmermann, J., Baldini, F., Thiele, I., and Kaleta, C. (2017) BacArena: Individual-based metabolic modeling of heterogeneous microbes in complex communities, *PLoS Comput Biol* **13**: e1005544.

9 Becker, N., Kunath, J., Loh, G., and Blaut, M. (2011) Human intestinal microbiota: characterization of a simplified and stable gnotobiotic rat model, *Gut Microbes* **2**: 25-33.

10 Becker, S.A., and Palsson, B.Ø. (2005) Genome-scale reconstruction of the metabolic network in Staphylococcus aureus N315: an initial draft to the two-dimensional annotation, *BMC microbiology* **5**: 1.

11 Blainey, P.C. (2013) The future is now: single-cell genomics of bacteria and archaea, *FEMS Microbiol Rev* **37**: 407-427.

12 Borenstein, E. (2012) Computational systems biology and in silico modeling of the human microbiome, *Briefings in Bioinformatics* **13**: 769-780.

13 Browne, H.P., Forster, S.C., Anonye, B.O., Kumar, N., Neville, B.A., Stares, M.D., et al. (2016) Culturing of 'unculturable' human microbiota reveals novel taxa and extensive sporulation, *Nature* **533**: 543-+.

14 Bui, T.P.N., Ritari, J., Boeren, S., de Waard, P., Plugge, C.M., and de Vos, W.M. (2015) Production of butyrate from lysine and the Amadori product fructoselysine by a human gut commensal, *Nature Communications* **6**.

15 Carrera, J., Estrela, R., Luo, J., Rai, N., Tsoukalas, A., and Tagkopoulos, I. (2014) An integrative, multi-scale, genome-wide model reveals the phenotypic landscape of Escherichia coli, *Molecular Systems Biology* **10**.

16 Caspi, R., Altman, T., Billington, R., Dreher, K., Foerster, H., Fulcher, C.A., et al. (2014) The MetaCyc database of metabolic pathways and enzymes and the BioCyc collection of Pathway/Genome Databases, *Nucleic Acids Res* **42**: D459-D471.

17 Chandrasekaran, S., and Price, N.D. (2013) Metabolic Constraint-Based Refinement of Transcriptional Regulatory Networks, *Plos Computational Biology* **9**.

18 Chandrasekaran, S., and Price, N.D. (2010) Probabilistic integrative modeling of genome-scale metabolic and regulatory networks in Escherichia coli and Mycobacterium tuberculosis, *Proceedings of the National Academy of Sciences of the United States of America* **107**: 17845-17850.

19 Chubiz, L.M., Granger, B.R., Segre, D., and Harcombe, W.R. (2015) Species interactions differ in their genetic robustness, *Front Microbiol* **6**.

20 Cuiv, P.O., Smith, W.J., Pottenger, S., Burman, S., Shanahan, E.R., and Morrison, M. (2015) Isolation of Genetically Tractable Most-Wanted Bacteria by Metaparental Mating, *Sci Rep* **5**: 13282.

21 dos Santos, F.B., de Vos, W.M., and Teusink, B. (2013) Towards metagenome-scale models for industrial applications—the case of Lactic Acid Bacteria, *Current Opinion in Biotechnology* **24**: 200-206.
22 El-Semman, I.E., Karlsson, F.H., Shoaie, S., Nookaew, I., Soliman, T.H., and Nielsen, J. (2014) Genome-scale metabolic reconstructions of Bifidobacterium adolescentis L2-32 and Faecalibacterium prausnitzii A2-165 and their interaction, *BMC Syst Biol* **8**: 41.
23 Espey, M.G. (2013) Role of oxygen gradients in shaping redox relationships between the human intestine and its microbiota, *Free Radical Biology and Medicine* **55**: 130-140.
24 Faria, J.P., Overbeek, R., Xia, F.F., Rocha, M., Rocha, I., and Henry, C.S. (2014) Genome-scale bacterial transcriptional regulatory networks: reconstruction and integrated analysis with metabolic models, *Briefings in Bioinformatics* **15**: 592-611.
25 Feist, A.M., and Palsson, B.O. (2008) The growing scope of applications of genome-scale metabolic reconstructions using Escherichia coli, *Nat Biotechnol* **26**: 659-667.
26 Feng, X., Xu, Y., Chen, Y., and Tang, Y.J. (2012) MicrobesFlux: a web platform for drafting metabolic models from the KEGG database, *BMC Syst Biol* **6**: 94.
27 Flint, H.J., Duncan, S.H., and Louis, P. (2017) The impact of nutrition on intestinal bacterial communities, *Curr Opin Microbiol* **38**: 59-65.
28 Flint, H.J., Scott, K.P., Louis, P., and Duncan, S.H. (2012) The role of the gut microbiota in nutrition and health, *Nat Rev Gastroenterol Hepatol* **9**: 577-589.
29 Fodor, A.A., DeSantis, T.Z., Wylie, K.M., Badger, J.H., Ye, Y., Hepburn, T., et al. (2012) The "most wanted" taxa from the human microbiome for whole genome sequencing, *Plos One* **7**: e41294.
30 Freilich, S., Zarecki, R., Eilam, O., Segal, E.S., Henry, C.S., Kupiec, M., et al. (2011) Competitive and cooperative metabolic interactions in bacterial communities, *Nat Commun* **2**: 589.
31 Gill, S.R., Pop, M., DeBoy, R.T., Eckburg, P.B., Turnbaugh, P.J., Samuel, B.S., et al. (2006) Metagenomic analysis of the human distal gut microbiome, *Science* **312**: 1355-1359.
32 Greenblum, S., Turnbaugh, P.J., and Borenstein, E. (2012) Metagenomic systems biology of the human gut microbiome reveals topological shifts associated with obesity and inflammatory bowel disease, *Proceedings of the National Academy of Sciences of the United States of America* **109**: 594-599.
33 Großeholz, R., Koh, C.-C., Veith, N., Fiedler, T., Strauss, M., Olivier, B., et al. (2016) Integrating highly quantitative proteomics and genome-scale metabolic modeling to study pH adaptation in the human pathogen Enterococcus faecalis **2**: 16017.
34 Guo, C.J., Chang, F.Y., Wyche, T.P., Backus, K.M., Acker, T.M., Funabashi, M., et al. (2017) Discovery of Reactive Microbiota-Derived Metabolites that Inhibit Host Proteases, *Cell* **168**: 517-526 e518.
35 Hamer, H.M., Jonkers, D., Venema, K., Vanhoutvin, S., Troost, F.J., and Brummer, R.J. (2008) Review article: the role of butyrate on colonic function, *Alimentary Pharmacology & Therapeutics* **27**: 104-119.
36 Harcombe, W. (2010) Novel Cooperation Experimentally Evolved between Species, *Evolution* **64**: 2166-2172.
37 Harcombe, W.R., Riehl, W.J., Dukovski, I., Granger, B.R., Betts, A., Lang, A.H., et al. (2014) Metabolic Resource Allocation in Individual Microbes Determines Ecosystem Interactions and Spatial Dynamics, *Cell Reports* **7**: 1104-1115.
38 Hasler, R., Sheibani-Tezerji, R., Sinha, A., Barann, M., Rehman, A., Esser, D., et al. (2016) Uncoupling of mucosal gene regulation, mRNA splicing and adherent microbiota signatures in inflammatory bowel disease, *Gut*.
39 Heinemann, M., Kümmel, A., Ruinatscha, R., and Panke, S. (2005) In silico genome-scale reconstruction and validation of the Staphylococcus aureus metabolic network, *Biotechnol Bioeng* **92**: 850-864.
40 Heinken, A., Khan, M.T., Paglia, G., Rodionov, D.A., Harmsen, H.J., and Thiele, I. (2014) Functional metabolic map of Faecalibacterium prausnitzii, a beneficial human gut microbe, *Journal of Bacteriology* **196**: 3289-3302.

41 Henry, C.S., DeJongh, M., Best, A.A., Frybarger, P.M., Linsay, B., and Stevens, R.L. (2010) High-throughput generation, optimization and analysis of genome-scale metabolic models, *Nat Biotechnol* **28**: 977-U922.
42 Hoppe, A. (2012) What mRNA Abundances Can Tell us about Metabolism, *Metabolites* **2**: 614-631.
43 Ji, B., and Nielsen, J. (2015) From next-generation sequencing to systematic modeling of the gut microbiome, *Front Genet* **6**: 219.
44 Kanehisa, M., Goto, S., Sato, Y., Kawashima, M., Furumichi, M., and Tanabe, M. (2014) Data, information, knowledge and principle: back to metabolism in KEGG, *Nucleic Acids Research* **42**: D199-D205.
45 Karr, J.R., Sanghvi, J.C., Macklin, D.N., Gutschow, M.V., Jacobs, J.M., Bolival, B., Jr., et al. (2012) A whole-cell computational model predicts phenotype from genotype, *Cell* **150**: 389-401.
46 Kelly, C.R., Ihunnah, C., Fischer, M., Khoruts, A., Surawicz, C., Afzali, A., et al. (2014) Fecal microbiota transplant for treatment of Clostridium difficile infection in immunocompromised patients, *Am J Gastroenterol* **109**: 1065-1071.
47 Kim, J., and Reed, J.L. (2014) Refining metabolic models and accounting for regulatory effects, *Current Opinion in Biotechnology* **29**: 34-38.
48 Kim, M.K., and Lun, D.S. (2014) Methods for integration of transcriptomic data in genome-scale metabolic models, *Computational and Structural Biotechnology Journal* **11**: 59-65.
49 King, Z.A., Drager, A., Ebrahim, A., Sonnenschein, N., Lewis, N.E., and Palsson, B.O. (2015) Escher: A Web Application for Building, Sharing, and Embedding Data-Rich Visualizations of Biological Pathways, *Plos Computational Biology* **11**: e1004321.
50 Kleerebezem, M., Boekhorst, J., van Kranenburg, R., Molenaar, D., Kuipers, O.P., Leer, R., et al. (2003) Complete genome sequence of Lactobacillus plantarum WCFS1, *Proceedings of the National Academy of Sciences* **100**: 1990-1995.
51 Klitgord, N., and Segre, D. (2010) Environments that Induce Synthetic Microbial Ecosystems, *Plos Computational Biology* **6**.
52 Kolinko, S., Richter, M., Glockner, F.O., Brachmann, A., and Schuler, D. (2015) Single-cell genomics of uncultivated deep-branching magnetotactic bacteria reveals a conserved set of magnetosome genes, *Environ Microbiol*.
53 Konikoff, T., and Gophna, U. (2016) Oscillospira: a Central, Enigmatic Component of the Human Gut Microbiota, *Trends in Microbiology* **24**: 523-524.
54 Kumar, V.S., and Maranas, C.D. (2009) GrowMatch: an automated method for reconciling in silico/in vivo growth predictions, *PLoS Comput Biol* **5**: e1000308.
55 Lagier, J.C., Khelaifia, S., Alou, M.T., Ndongo, S., Dione, N., Hugon, P., et al. (2016) Culture of previously uncultured members of the human gut microbiota by culturomics, *Nat Microbiol* **1**: 16203.
56 Lasken, R.S. (2012) Genomic sequencing of uncultured microorganisms from single cells, *Nature Reviews Microbiology* **10**: 631-640.
57 Levy, R., and Borenstein, E. (2013) Metabolic modeling of species interaction in the human microbiome elucidates community-level assembly rules, *Proc Natl Acad Sci U S A* **110**: 12804-12809.
58 Lewis, N.E., Hixson, K.K., Conrad, T.M., Lerman, J.A., Charusanti, P., Polpitiya, A.D., et al. (2010) Omic data from evolved E. coli are consistent with computed optimal growth from genome-scale models, *Mol Syst Biol* **6**: 390.
59 Machado, D., and Herrgård, M. (2014) Systematic evaluation of methods for integration of transcriptomic data into constraint-based models of metabolism, *PLoS Comput Biol* **10**: e1003580.
60 Mackie, R.I., Aminov, R.I., Hu, W., Klieve, A.V., Ouwerkerk, D., Sundset, M.A., and Kamagata, Y. (2003) Ecology of uncultivated Oscillospira species in the rumen of cattle, sheep, and reindeer as assessed by microscopy and molecular approaches, *Appl Environ Microbiol* **69**: 6808-6815.
61 Magnusdottir, S., Heinken, A., Kutt, L., Ravcheev, D.A., Bauer, E., Noronha, A., et al. (2017) Generation of genome-scale metabolic reconstructions for 773 members of the human gut microbiota, *Nat Biotechnol* **35**: 81-89.

62 Mahadevan, R., Edwards, J.S., and Doyle, F.J. (2002) Dynamic flux balance analysis of diauxic growth in Escherichia coli, *Biophysical journal* **83**: 1331-1340.
63 Maurice, C.F., Haiser, H.J., and Turnbaugh, P.J. (2013) Xenobiotics Shape the Physiology and Gene Expression of the Active Human Gut Microbiome, *Cell* **152**: 39-50.
64 McCloskey, D., Palsson, B.Ø., and Feist, A.M. (2013) Basic and applied uses of genome-scale metabolic network reconstructions of Escherichia coli, *Molecular Systems Biology* **9**: 661.
65 Nielsen, H.B., Almeida, M., Juncker, A.S., Rasmussen, S., Li, J.H., Sunagawa, S., et al. (2014) Identification and assembly of genomes and genetic elements in complex metagenomic samples without using reference genomes, *Nat Biotechnol* **32**: 822-828.
66 Novichkov, P.S., Kazakov, A.E., Ravcheev, D.A., Leyn, S.A., Kovaleva, G.Y., Sutormin, R.A., et al. (2013) RegPrecise 3.0-A resource for genome-scale exploration of transcriptional regulation in bacteria, *Bmc Genomics* **14**.
67 O'Brien, Edward J., Monk, Jonathan M., and Palsson, Bernhard O. (2015) Using Genome-scale Models to Predict Biological Capabilities, *Cell* **161**: 971-987.
68 Oberhardt, M.A., Palsson, B.O., and Papin, J.A. (2009) Applications of genome-scale metabolic reconstructions, *Molecular Systems Biology* **5**: 320.
69 Oberhardt, M.A., Puchalka, J., Fryer, K.E., Martins dos Santos, V.A., and Papin, J.A. (2008) Genome-scale metabolic network analysis of the opportunistic pathogen Pseudomonas aeruginosa PAO1, *J Bacteriol* **190**: 2790-2803.
70 Oliveira, A.P., Nielsen, J., and Förster, J. (2005) Modeling Lactococcus lactis using a genome-scale flux model, *BMC microbiology* **5**: 1.
71 Orth, J.D., and Palsson, B. (2012) Gap-filling analysis of the i JO1366 Escherichia coli metabolic network reconstruction for discovery of metabolic functions, *BMC Syst Biol* **6**: 1.
72 Orth, J.D., and Palsson, B.Ø. (2010) Systematizing the generation of missing metabolic knowledge, *Biotechnology and bioengineering* **107**: 403-412.
73 Orth, J.D., Thiele, I., and Palsson, B.Ø. (2010) What is flux balance analysis?, *Nature Biotechnology* **28**: 245-248.
74 Ottman, N.A. (2015) Host immunostimulation and substrate utilization of the gut symbiont Akkermansia muciniphila. Wageningen: Wageningen University.
75 Peterson, J., Garges, S., Giovanni, M., McInnes, P., Wang, L., Schloss, J.A., et al. (2009) The NIH Human Microbiome Project, *Genome Res* **19**: 2317-2323.
76 Plovier, H., Everard, A., Druart, C., Depommier, C., Van Hul, M., Geurts, L., et al. (2017) A purified membrane protein from Akkermansia muciniphila or the pasteurized bacterium improves metabolism in obese and diabetic mice, *Nat Med* **23**: 107-113.
77 Puddu, A., Sanguineti, R., Montecucco, F., and Viviani, G.L. (2014) Evidence for the Gut Microbiota Short-Chain Fatty Acids as Key Pathophysiological Molecules Improving Diabetes, *Mediators of Inflammation*.
78 Qin, J.J., Li, R.Q., Raes, J., Arumugam, M., Burgdorf, K.S., Manichanh, C., et al. (2010) A human gut microbial gene catalogue established by metagenomic sequencing, *Nature* **464**: 59-U70.
79 Quevrain, E., Maubert, M.A., Michon, C., Chain, F., Marquant, R., Tailhades, J., et al. (2016) Identification of an anti-inflammatory protein from Faecalibacterium prausnitzii, a commensal bacterium deficient in Crohn's disease, *Gut* **65**: 415-425.
80 Rajilic-Stojanovic, M., and de Vos, W.M. (2014) The first 1000 cultured species of the human gastrointestinal microbiota, *Fems Microbiology Reviews* **38**: 996-1047.
81 Ramsey, D.M., and Wozniak, D.J. (2005) Understanding the control of Pseudomonas aeruginosa alginate synthesis and the prospects for management of chronic infections in cystic fibrosis, *Mol Microbiol* **56**: 309-322.
82 Rath, C.M., Alexandrov, T., Higginbottom, S.K., Song, J., Milla, M.E., Fischbach, M.A., et al. (2012) Molecular analysis of model gut microbiotas by imaging mass spectrometry and nanodesorption electrospray ionization reveals dietary metabolite transformations, *Anal Chem* **84**: 9259-9267.
83 Ridlon, J.M., Kang, D.J., Hylemon, P.B., and Bajaj, J.S. (2014) Bile acids and the gut microbiome, *Current Opinion in Gastroenterology* **30**: 332-338.

84 Ritari, J., Salojarvi, J., Lahti, L., and de Vos, W.M. (2015) Improved taxonomic assignment of human intestinal 16S rRNA sequences by a dedicated reference database, *Bmc Genomics* **16**.
85 Rocca, J.D., Hall, E.K., Lennon, J.T., Evans, S.E., Waldrop, M.P., Cotner, J.B., et al. (2015) Relationships between protein-encoding gene abundance and corresponding process are commonly assumed yet rarely observed, *ISME J* **9**: 1693-1699.
86 Salimi, F., Zhuang, K., and Mahadevan, R. (2010) Genome-scale metabolic modeling of a clostridial co-culture for consolidated bioprocessing, *Biotechnology Journal* **5**: 726-738.
87 Saulnier, D.M., Santos, F., Roos, S., Mistretta, T.-A., Spinler, J.K., Molenaar, D., et al. (2011) Exploring metabolic pathway reconstruction and genome-wide expression profiling in Lactobacillus reuteri to define functional probiotic features, *Plos One* **6**: e18783.
88 Shoaie, S., Ghaffari, P., Kovatcheva-Datchary, P., Mardinoglu, A., Sen, P., Pujos-Guillot, E., et al. (2015) Quantifying Diet-Induced Metabolic Changes of the Human Gut Microbiome, *Cell Metabolism* **22**: 320-331.
89 Sigurdsson, M.I., Jamshidi, N., Steingrimsson, E., Thiele, I., and Palsson, B.Ø. (2010) A detailed genome-wide reconstruction of mouse metabolism based on human Recon 1, *BMC Syst Biol* **4**: 1.
90 Smith, P.M., Howitt, M.R., Panikov, N., Michaud, M., Gallini, C.A., Bohlooly, Y.M., et al. (2013) The microbial metabolites, short-chain fatty acids, regulate colonic Treg cell homeostasis, *Science* **341**: 569-573.
91 Steeb, B., Claudi, B., Burton, N.A., Tienz, P., Schmidt, A., Farhan, H., et al. (2013) Parallel exploitation of diverse host nutrients enhances Salmonella virulence, *PLoS Pathog* **9**: e1003301.
92 Stolyar, S., Van Dien, S., Hillesland, K.L., Pinel, N., Lie, T.J., Leigh, J.A., and Stahl, D.A. (2007) Metabolic modeling of a mutualistic microbial community, *Molecular systems biology* **3**: 92.
93 Sun, J., Haveman, S.A., Bui, O., Fahland, T.R., and Lovley, D.R. (2010) Constraint-based modeling analysis of the metabolism of two Pelobacter species, *BMC Syst Biol* **4**.
94 Teusink, B., and Smid, E.J. (2006) Modelling strategies for the industrial exploitation of lactic acid bacteria, *Nature Reviews Microbiology* **4**: 46-56.
95 Teusink, B., van Enckevort, F.H.J., Francke, C., Wiersma, A., Wegkamp, A., Smid, E.J., and Siezen, R.J. (2005) In silico reconstruction of the metabolic pathways of Lactobacillus plantarum: Comparing predictions of nutrient requirements with those from growth experiments, *Appl Environ Microbiol* **71**: 7253-7262.
96 Teusink, B., Wiersma, A., Molenaar, D., Francke, C., de Vos, W.M., Siezen, R.J., and Smid, E.J. (2006) Analysis of growth of Lactobacillus plantarum WCFS1 on a complex medium using a genome-scale metabolic model, *Journal of Biological Chemistry* **281**: 40041-40048.
97 Thiele, I., and Palsson, B.Ø. (2010) A protocol for generating a high-quality genome-scale metabolic reconstruction, *Nature Protocols* **5**: 93-121.
98 Thiele, I., Swainston, N., Fleming, R.M., Hoppe, A., Sahoo, S., Aurich, M.K., et al. (2013) A community-driven global reconstruction of human metabolism, *Nature Biotechnology* **31**: 419-425.
99 Tzamali, E., Poirazi, P., Tollis, I.G., and Reczko, M. (2011) A computational exploration of bacterial metabolic diversity identifying metabolic interactions and growth-efficient strain communities, *BMC Syst Biol* **5**.
100 van Nood, E., Vrieze, A., Nieuwdorp, M., Fuentes, S., Zoetendal, E.G., de Vos, W.M., et al. (2013) Duodenal infusion of donor feces for recurrent Clostridium difficile, *N Engl J Med* **368**: 407-415.
101 Ventura, M., O'Flaherty, S., Claesson, M.J., Turroni, F., Klaenhammer, T.R., van Sinderen, D., and O'Toole, P.W. (2009) Genome-scale analyses of health-promoting bacteria: probiogenomics, *Nature Reviews Microbiology* **7**: 61-U77.
102 Weaver, D.S., Keseler, I.M., Mackie, A., Paulsen, I.T., and Karp, P.D. (2014) A genome-scale metabolic flux model of Escherichia coli K-12 derived from the EcoCyc database, *BMC Syst Biol* **8**: 79.

103 Wegkamp, A., Teusink, B., De Vos, W., and Smid, E. (2010) Development of a minimal growth medium for Lactobacillus plantarum, *Letters in applied microbiology* **50**: 57-64.
104 Xavier, J.C., Patil, K.R., and Rocha, I. (2017) Integration of Biomass Formulations of Genome-Scale Metabolic Models with Experimental Data Reveals Universally Essential Cofactors in Prokaryotes, *Metab Eng* **39**: 200-208.
105 Zarecki, R., Oberhardt, M.A., Reshef, L., Gophna, U., and Ruppin, E. (2014) A novel nutritional predictor links microbial fastidiousness with lowered ubiquity, growth rate, and cooperativeness, *Plos Computational Biology* **10**: e1003726.
106 Zelezniak, A., Andrejev, S., Ponomarova, O., Mende, D.R., Bork, P., and Patil, K.R. (2015) Metabolic dependencies drive species co-occurrence in diverse microbial communities, *Proceedings of the National Academy of Sciences* **112**: 6449-6454.
107 Zhang, S.W., Gou, W.L., and Li, Y. (2017) Prediction of metabolic fluxes from gene expression data with Huber penalty convex optimization function, *Mol Biosyst* **13**: 901-909.
108 Zhou, L., and Foster, J.A. (2015) Psychobiotics and the gut-brain axis: in the pursuit of happiness, *Neuropsychiatr Dis Treat* **11**: 715-723.
109 Zoetendal, E.G., and de Vos, W.M. (2014) Effect of diet on the intestinal microbiota and its activity, *Current Opinion in Gastroenterology* **30**: 189-195.

CHAPTER 3

Model-driven design of a minimal medium for *Akkermansia muciniphila* confirms mucus adaptation

Kees C.H. van der Ark, Steven Aalvink, Maria Suarez-Diez, Peter J. Schaap, Willem M. de Vos and Clara Belzer

(A revised manuscript accepted for publication)

Abstract

The abundance of the human intestinal symbiont *Akkermansia muciniphila* has found to be inversely correlated with several diseases, including metabolic syndrome and obesity. *A. muciniphila* is known to use mucin as sole carbon and nitrogen source. To study the physiology and the potential for therapeutic applications of this bacterium, we designed a defined minimal medium. The composition of the medium was based on the genome-scale metabolic model of *A. muciniphila* and the composition of mucin. Our results indicate that *A. muciniphila* does not code for GlmS, the enzyme that mediates the conversion of fructose-6-phosphate (Fru6P) to glucosamine-6-phosphate (GlcN6P), which is essential in peptidoglycan formation. The only annotated enzyme that could mediate this conversion is Amuc-NagB on locus Amuc_1822. We found that Amuc-NagB was unable to form GlcN6P from Fru6P at physiological conditions, while it efficiently catalyzed the reverse reaction. To overcome this inability, N-acetylglucosamine needs to be present in the medium for *A. muciniphila* growth. With these findings the genome scale-metabolic model was updated and used to accurately predict growth of *A. muciniphila* on synthetic media. The finding that *A. muciniphila* has a necessity for GlcNAc, which is present in mucin further prompts the adaptation to its mucosal niche.

Introduction

Akkermansia muciniphila is a mucin-degrading bacterium that is present in the intestinal tract of a majority of people (Derrien, et al., 2008). On average the relative abundance of *A. muciniphila* is 0.1-4% in human fecal samples (Derrien, et al., 2008, Png, et al., 2010, Lyra, et al., 2012). Inverse correlations have been reported between the relative abundance of *A. muciniphila* and diseases and disorders such as metabolic syndrome, autism and obesity (Derrien, et al., 2008, Wang, et al., 2011, Derrien, et al., 2016, Gomez-Gallego, et al., 2016). In humans it was shown that weight loss interventions and gastric bypass surgery in obese people, increase the abundance of *A. muciniphila* (Liou, et al., 2013, Anhe, et al., 2015, Dao, et al., 2015). Moreover, in a series of preclinical interventions in mice it was shown that *A. muciniphila* reversed diet induced metabolic fat-mass gain and insulin resistance (Everard, et al., 2013, Plovier, et al., 2017) possibly due to outer membrane produced pili (Ottman, et al., 2017a, Plovier, et al., 2017).

A. muciniphila was first isolated by using purified hog gastric mucus as sole carbon and nitrogen source (Derrien, et al., 2004). In addition to the degradation of intestinal mucins, *A. muciniphila* was shown to be closely associated to colonic epithelial cells producing these mucins (Derrien, et al., 2011). The adaptation to this niche is exemplified by the capabilities of *A. muciniphila* to utilize low concentrations of oxygen present in the mucus layer (Ouwerkerk, et al., 2016), even though it was previously characterized as a strictly anaerobic bacterium (Derrien, et al., 2004). The efficient use of mucin by *A. muciniphila* was shown in an *in vitro* intestinal model and upon addition of mucus, *A. muciniphila* abundance showed over 10.000 fold increase, the highest ever observed in this model (Van Herreweghen, et al., 2017).

The mucin in the mucus layer lining the intestinal track is composed of a peptide backbone abundantly decorated with O-linked glycans (Johansson, et al., 2011, Thomsson, et al., 2012). The peptide backbone is rich in threonine, serine, cysteine and proline, while the glycans are composed of a plethora of sugar groups that contain mannose, galactose, fucose and N-acetylhexosamines such as N-acetylglucosamine (GlcNAc), and N-acetylgalactosamine (GalNAc). Some fecal microbiota species are known to have mucolytic activities (Variyam and Hoskins, 1981). Glycosidases needed to degrade polysaccharides have been isolated from the supernatant of cultures of *Bifidobacterium* and *Ruminococcus spp* (Hoskins, et al.,

1985). These bacteria were supposed to be a distinct subpopulation of the normal fecal microbiota based on their glycosidase activity. The involvement of glycosidases in mucolytic activity has since been described for multiple species, including *Bacteroides* species and *A. muciniphila* (Tailford, et al., 2015). The subsequent degradation of polysaccharides and monosaccharides is a common feature in bacteria, as they are similar to diet derived sugars and used in fermentation (Chen, et al., 2002, Pereira and Berry, 2017). *A. muciniphila* is capable of fermenting some of the monosaccharides including galactose, fucose, glucose, GlcNAc and GalNAc, which have been reported to be used for both energy generation and as carbon source (Desai, et al., 2016, Ottman et al., 2017b). However, the degradation of these sugars is only possible in the presence of mucin or large amounts of a tryptic digest of casein (Desai, et al., 2016, Ottman et al., 2017b).

The genome-encoded metabolic potential of *A. muciniphila* has been previously exploited to design a genome scale model of its metabolism (van Passel, et al., 2011, Ottman et al., 2017b). Extensive model curation and evaluation led to the prediction of an auxotrophy for L-threonine as well as predictions regarding the production of the short chain fatty acids (SCFA) acetate and propionate. The production of these SCFAs was confirmed by growth experiments, however in deviating ratios compared to the predictions. The addition of L-threonine to the growth media did increase growth, but its essentiality for growth was not confirmed due to the presence of the partially undefined casein hydrolysate in the medium (Ottman et al., 2017b).

To better understand the physiological properties of *A. muciniphila* it is essential to have a defined minimal medium for growth. Such a medium can also be the basis for the application of *A. muciniphila* as a therapeutic microbe since the medium components should be defined and preferably of non-animal origin before clinical tests can be conducted. Here, we present a completely defined and minimal medium that supports growth of this beneficial microbe. We confirmed that the amino acid L-threonine is essential for growth and observed that the addition of either GlcNAc or GalNAc was essential for the growth of *A. muciniphila.* Furthermore, we discovered *A. muciniphila* does not code for a functional GlmS and hence requires the exogenously added GlcNAc or GalNAc not only for fermentation, but also for peptidoglycan formation.

Materials and Methods

Culturing *A. muciniphila,* optical density and HPLC

A. muciniphila was grown in anaerobic bottles containing 10 ml medium as described before (Derrien, et al., 2004), supplemented with 6 g/l of L-threonine and 25 mM sugar, as indicated in Table S1. Growth was determined by measuring the optical density at 600 nm. High-pressure liquid chromatography (HPLC) was used to determine sugar consumption and SCFA production, as described before (Derrien, et al., 2004, Ouwerkerk, et al., 2016, Ottman et al., 2017b). Glucosamine (GlcN) concentration was determined by reagent free ion chromatography using a Dionex™ ICS-5000 (Thermo Scientific, Sunnyville, CA, USA), with a Dionex CarboPac PA20 Analytic column and 20mM NaOH as eluent. Further settings were according to manufacturer's application note.

Identification of GlmS and NagB homologues in *A. muciniphila*

Escherichia coli K12 NagB (NP_415204.1) and GlmS (NP_418185.1) amino acid sequences were used to identify enzymes that can mediate the formation of GlcN6P from Fru6P in *Akkermansia* (taxid:239934). This was done by selecting best bidirectional blastp (protein-protein BLAST) hits between both genomes (Altschul, et al., 1990). Analysis was performed on February 10, 2017.

Enzyme expression and purification

The *A. muciniphila* gene NagB on locus Amuc_1822 (AMUC_RS09725) was amplified using the forward primer 5'-ATAGAGGTACCATGATCGGGGTGGAAAGT-3' and the reverse primer 5'-TATGCCCTAGGTTA**ATGGTGGTGGTGATGATG**AAGGAGGGAAGCAGCCC-3', adding a C-terminal His-tag (bold in primer sequence) and restriction sites (underlined in primer sequence). Genomic DNA from *A. muciniphila* ATCC BAA-835 was used as template. The purified amplicon and vector pCDF-1b (Novagen, Merck Milipore, Darmstadt, Germany) were digested using enzymes XmaIJ (Thermo Fisher Scientific) and KpnI HF (New England Biolabs) in Tango buffer (Thermo Fisher Scientific) for 1.5 hours at 37˚C. The DNA was purified again and ligated with 3:1 ratio (insert:vector) using T4 ligase (manufacturers protocol, Thermo Fisher Scientific). Competent *Escherichia coli* DH10B (manufacturers protocol, New England Biolabs) were transformed with 2 µL ligation mixture and plated on LB agar with 50 ug/mL spectinomycin. A selected colony was grown in 10 mL

liquid LB until an OD600 of 1 after which plasmids were purified. *E. coli* BL21 (DE3) (manufacturers protocol, New England Biolabs) was transformed with 1µL plasmid containing 60 ug/mL DNA, and 100 µL was plated on LB agar with 50 ug/mL spectinomycin. The transformed strain was grown in 250 mL liquid LB medium with 50 ug/mL spectinomycin until an OD600 of 0.5-1 after which is was induced with 1 mM IPTG for 4 hours at 37˚C. The bacteria were collected by centrifugation at 5.000 g for 10 minutes and suspended in lysis buffer (50 mM Tris-HCl pH 7.5, 200 mM NaCl, 1 mM $MgCl_2$, 5 mM DTT, 1 mM PMSF). The cells were lysed by three passages in a French Press (15.000 psi, Pressure Cell Homogeniser, Stansted Fluid Power Ltd., Essex, UK). The lysate was cleared by centrifugation for 10 minutes at 16.000g. The proteins were purified using a nickel column (manufacturers protocol, Ni-NTA Agarose, Qiagen GmbH, Hilden, Germany). Purified fractions were dialyzed against 1 L of buffer A (25 mM KH_2PO_4/K_2HPO_4, pH 7.0, 0.5 mM PMSF, 1 mM DTT, 1 mM EDTA). Purity of the enzymes was checked using SDS-PAGE. Enzyme concentration was determined by BCA protein assay (manufacturers protocol, Thermo Fisher Scientific).

Enzyme assays

Enzyme assays were performed as described before (Kwiatkowska-Semrau, et al., 2015). Shortly, 1.5 mL tubes were filled with the buffer and substrates as indicated in Table S3. The enzymes were added last, after which the tubes were vortexed shortly and incubated at 37˚C for exactly 3 minutes. Subsequently, the tubes were placed at 99˚C for 1 minute and cooled on ice. To acetylate GlcN6P, 100 µL of 10% acetic acid in acetone and 200 µL of a saturated $NaHCO_3$ solution were added, after which the samples were incubated for 3 minutes at 20˚C and 3 minutes at 99˚C. The samples were cooled on ice again, after which 200 µL of a 0.8 M potassium tetraborate hexahydrate solution was added. The samples were incubated for 3 minutes at 99˚C and cooled on ice. Finally, 800 µL of these solution were added to 5 mL of reagent A (1 g of 4-dimethylaminobenzaldehyde in 100 mL of glacial acetic acid to which 1.5 mL 37% HCl is added). The samples were incubated at 37˚C for 30 minutes, after which the absorbance was measured at 585 nm (manufacturer). The Km and Vmax values were determined by plotting the obtained data on a Lineweaver-Burk plot (Burk, et al., 1934).

Genome-scale constraint based metabolic model

The genome scale constraint based model of *A. muciniphila* AkkMuc_588 reported previously (Ottman et al., 2017b) was used to assess growth potential on different media. The core of the model is $\boldsymbol{S}$ the stoichiometric matrix. $\boldsymbol{S}$ is an $m \times n$ matrix, where n is the number of metabolites and m is the number of reactions in the model, 734 and 745 respectively. Entries of $\boldsymbol{S}$ represent the stoichiometric coefficients of each metabolite in each reaction. In addition to reactions describing metabolic interconversions and transport, the model also contain reactions that describe the media composition and the uptake and secretion potential of the organism, these are the so-called exchange reactions. The usual convention, (followed in the *A. municiniphila* model) is to represent uptake and production as negative and positive fluxes through the exchange reactions respectively. The model was used to simulate steady state as, in such situation, production of intracellular metabolites equals consumption and the model was used to identify sets of reactions (or pathways) that carry flux in such a case. Moreover, flux balance analysis (FBA) can be used to identify optimal (maximal or minimal) theoretical values for selected objectives such as biomass synthesis or metabolite uptake or production (Orth, et al., 2010).

Model simulations were performed by simulating the experimentally tested media. Unlimited secretion was allowed for metabolites in the media by setting the upper bounds of the corresponding exchange reactions to 1000. Abundant metabolites in the media such as water, P, Mn, Mg, Fe, Cu, Co, Cl, H_2O_2, sulfate and dimethylbenzimidazole, were set to be non-limiting by setting the lower bounds of the corresponding exchange reactions to -1000. Simulations involving threonine media supplementation were performed with a limited maximal possible uptake of 1. For all the tested sugars a range of uptake rates between 0 and 10 were tested. Arbitrary units (a.u.) were used in all simulations. FBA and model simulations were performed using Python version 2.7.12 (Python, 2017) the COBRApy library (version 0.4.1) (Ebrahim, et al., 2013) and Gurobi solver (Gurobi Optimizer Version 6.5.1 linux64) (Gurobi, 2016).

Results and Discussion

GlcNAc is essential for *A. muciniphila* growth

A. muciniphila was isolated using porcine gastric mucus and it was shown that this complex substrate could serve as the sole nitrogen and carbon source (Derrien, et al., 2004). Limited

growth was also observed when large amounts of tryptone, a tryptic digest of casein, were added as nitrogen source in combination with monosaccharides (Ottman et al., 2017b). This can be due to the presence of either amino acids or glycans in both complex substrates. Hence, the dependency of *A. muciniphila* on exogeneous nitrogen-containing compounds and sugars was tested in a series of growth experiments (Figure 1). The amino sugars tested (GlcNAc, GalNAc and GlcN) in these experiments were selected based on their presence in mucin glycans. We tested the essentiality of L-threonine by omitting it in the medium in the presence of ammonium and other amino acids, which resulted in no growth. This amino acid was selected based on the *A. muciniphila* genome scale constraint based model of metabolism, referred to as 'the model' hereafter (Ottman et al., 2017b). The final composition of the minimal medium is mineral CP medium (Derrien, et al., 2004) without ammonium chloride and added L-threonine and GlcNAc or GalNAc.

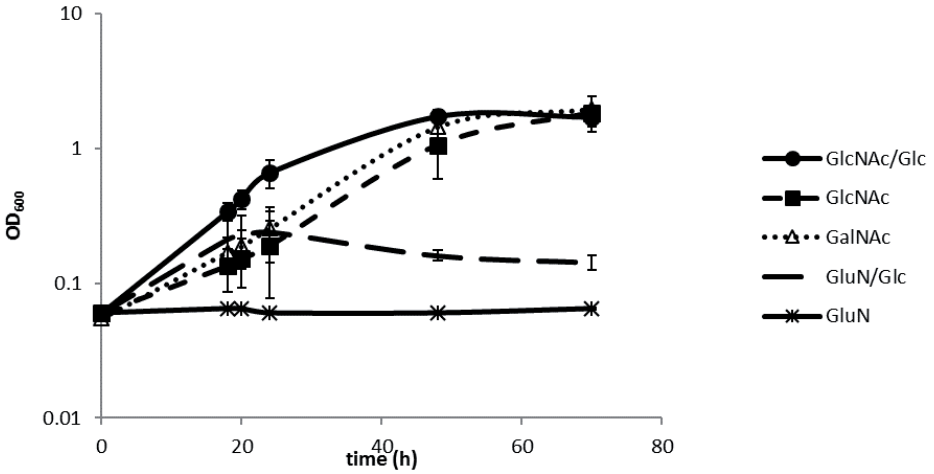

Figure 1. Growth of *A. muciniphila* on CP medium supplemented with L-threonine and different sugars. All sugars were supplemented to a total of 25mM. The negative control was supplemented with GlcNAc/glucose and not inoculated. The data shown are averages of 3 biological replicates and two technical duplicates for each.

A growth rate of 0.056 h^{-1} was observed for medium containing 25mM GlcNAc, and a value of 0.084 h^{-1} was found for growth on 25mM GalNAc (Table 1). The growth rate was increased from 0.056 h^{-1} to 0.122 h^{-1} when half of the GlcNAc was replaced by an equimolar amount of glucose. The final density of the cells is similar for growth on GlcNAc, GalNAc and GlcNAc/glucose, (Figure 1). When GlcN was used as substrate, growth was only observed with the addition of glucose, at a very low growth rate of 0.005 h^{-1}.

Table 1 Growth rate per hour (μ) of *A. muciniphila* on different sugars, with 6 g/L L-Thr

Sugars	μ (h^{-1})	SD
GlcNAc/Glc	0.122	0.036
GlcNAc	0.056	0.023
GalNAc	0.084	0.014
GlcN/Glc	0.005	0.004
GlcN	-0.001	0.002
Fru	0.000	0.000
Glc	0.000	0.000
Neg. control	0.000	0.000

The consumption and production of metabolites by *A. muciniphila* after growth were measured by HPLC and used to obtain insight in the pathways operating (Figure 2). This analysis showed that the consumption rates of glucose and GlcNAc were the same when both were present in the growth medium (Figure 2A). In case of GlcNAc and GalNAc degradation by *A. muciniphila*, the ratio of acetate and propionate production was the same, between 1.5:1 and 2:1 (Figure 2B,C). Combination of GlcNAc and glucose in the medium leads to a 1:1 ratio (Figure 2A). Degradation of glucose in the presence of GlcN produced acetate and propionate in a 1:2 ratio, GlcN as a sole carbon source was not able to sustain growth, nevertheless is degraded albeit in low amounts and did not contribute to SCFA production (Figure 2D,E). This level of SCFA production on glucose was in line with the predictions by the model (Ottman et al., 2017b), but not with previous findings in growth experiments where an acetate to propionate ratio of 1:1 was found (Ottman et al., 2017b). The accurate determination of SCFA production on monosaccharides needed the minimal medium described here since on complex and undefined media with mucus or casein hydrolysate such measurements were inaccurate.

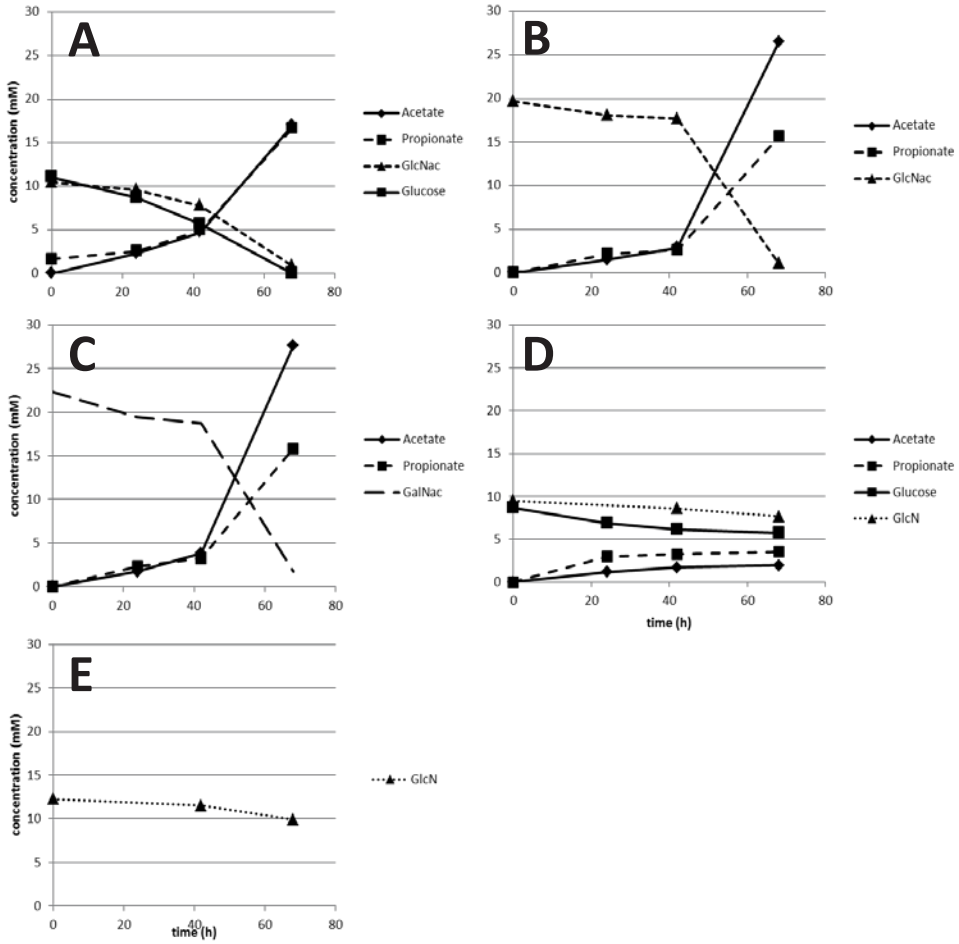

Figure 2. SCFA production and degradation of sugars. The degradation of GlcNAc and glucose results in a 1:1 ratio of acetate and propionate (A). The degradation of GlcNAc and GalNAc results in similar acetate and propionate ratios of 1.5:1 to 2:1 (B, C). The production of acetate and propionate on glucose and GlcN is in a 1:2 ratio (D). GlcN is still degraded when not supplemented with glucose, but no SCFA production was observed (E).

The production of SCFA after degradation of the acetylated aminosugars GlcNAc and GalNAc indicated that these compounds are degraded for the generation of energy in addition to their possible use for the formation of peptidoglycan. A ratio of 1.5:1 to 2:1 is in line with previous findings (Ottman et al., 2017b). The metabolic model predicts a 5:4 ratio, which slightly lower than the measured value (Ottman et al., 2017b). The early stagnation of growth on GlcN and glucose while there is some production of SCFA shows that the cells are active and alive, but limited in growth. This shows again that either GlcNAc or GalNAc is essential for growth in terms of biomass formation.

Although it has been suggested that *A. muciniphila* is able to degrade GalNAc (Ottman et al., 2017b) the previous metabolic reconstruction of *A. muciniphila* contained no GalNAc degradation pathways due to the current lack of reference degradation pathways in the MetaCyc database (Caspi, et al., 2014). The growth of *A. muciniphila* on GalNAc could possibly be explained by an isomerizing step from UDP-GalNAc to UDP-GlcNAc, mediated by the enzyme UDP-glucose 4-epimerase encoded on locus Amuc_1125 (AMUC_RS06020) (Thoden, et al., 2001, Bernatchez, et al., 2005, van Passel, et al., 2011). The growth of *A. muciniphila* on GlcN in combination with glucose could be due to acetylation of GlcN6P (Figure 3). This acetate group is known to be donated by acetyl-CoA, which can only be formed if a sugar is degraded first. Due to this constraint, the growth may be slower because it requires glucose to form acetyl-CoA. Additionally, from the metabolic model point of view, growth on GlcN is only impaired by the lack of a transport mechanism as we could not identify a gene in the *A. muciniphila* genome that would code for a transporter for GlcN. Therefore, it be could that the transport of GlcN to the cytoplasm is limited to transportation by other sugars transporters and thereby very inefficient.

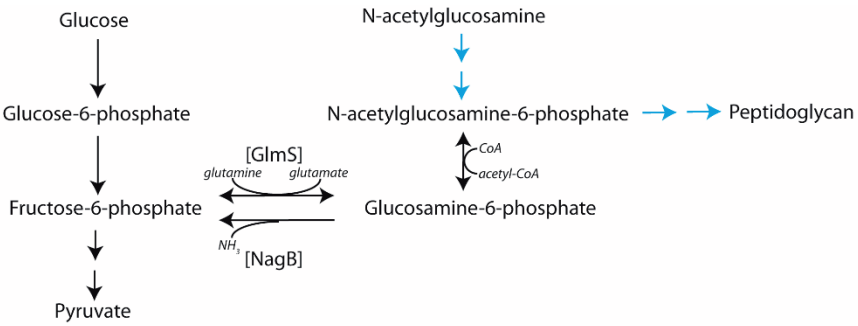

Figure 3. Schematic representation of sugar phosphorylation and conversion of phosphorylated sugars and formation of peptidoglycans. Co-metabolites are depicted when appropriate in italic, enzymes between square brackets [], arrows represent directionality, multiple arrows indicate multiple conversions. Blue arrows indicate the proposed Akkermansia GlcNAc shortcut for peptidoglycan formation.

The results indicated that amino sugars (GlcNAc, GalNAc and limited on GlcN) could support growth of *A. muciniphila,* but not glucose or fructose (Table S1). This suggested that *A. muciniphila might* lack the ability to aminate fructose-6-phospgate (Fru6P) to form glucosamine-6-phosphate (GlcN6P), which is an essential step in peptidoglycan synthesis (Barreteau, et al., 2008, Durand, et al., 2008), (Figure 3). This reaction is catalyzed by the enzyme GlmS (see below), which mediates the attachment of an amino group donated by glutamine to Fru6P to form GlcN6P (Durand, et al., 2008). This phosphorylated sugar is

subsequently converted to N-acetylglucosamine-6-phosphate after the addition of an acetate group and isomerized to N-acetylglucosamine-1-phosphate (Barreteau, et al., 2008), (Figure 3). The enzyme GlmS is essential in all peptidoglycan forming bacteria (Milewski, 2002) and *Escherichia coli* glms mutants are only viable if the growth medium is supplemented with GlcNAc (Wu and Wu, 1971). This indicates that the GlcNAc can be phosphorylated and used for peptidoglycan synthesis directly by *A. muciniphila*, an *Akkermansia* GlcNAc shortcut (Figure 3).

Genomic analysis of *A. muciniphila* for the identification of glucosamine-6-phosphate deaminase

We mined the *A. muciniphila* genome to identify genes encoding enzymes mediating conversions between Fru6P and GlcN6P. This lead to the finding that the genome of *A. muciniphila* does not code for a gene with high similarity to a characterized GlmS, see Table S5. The highest identity to *E. coli* GlmS was a von Willebrand factor type A domain protein (KXT50996.1) with an identity of 26% and an E-value of 0.68. There is also no gene homologues to GlmS from *Verrucomicrobium spinosum*, the type strain for Verrucromicrobiae, and thus a relative of *A. muciniphila*. Therefore, we consider *A. muciniphila* does not code for GlmS. The gene that encodes for glucosamine-6-phosphate deaminase (CDB55261.1) on locus amuc_1822 (AMUC_RS09725) is the only candidate gene that expresses an enzyme which could mediate the reaction between GlcN6P and Fru6P. No homologues were found in the *A. muciniphila* genome. The analogue in *E. coli* is named NagB. The directionality of this enzyme from different organisms is ambiguous (Vincent, et al., 2005). It has been found to predominantly mediate the reaction in the deaminating direction, but aminating activity has been found as well (Tanaka, et al., 2005, Kwiatkowska-Semrau, et al., 2015). Hence, we focused our attention to the kinetic characterization of the *A. muciniphila* NagB homologue.

Enzyme assays confirm the deamination properties of glucosamine-6-phosphate deaminase

We observed that *A. muciniphila* was not able to metabolise fructose and does not grow on glucose, while GlcN supports growth, although very limited, (Table 1). To assess the capabilities of *A. muciniphila* to convert fructose-6-phosphate (Fru6P) into glucosamine-6-phosphate (GlcN6P) and vice versa, we overproduced the only possible candidate enzyme,

termed Amuc-NagB, encoded by gene amuc_1822 (AMUC_RS09725) in *E. coli* BL21 (DE3) with a C-terminal His-tag and purified it to apparent homogeneity as a 33-kDa protein (Figure S2). The purified Amuc-NagB was assayed for conversions in both the aminating and deaminating direction and with all possible substrates involved (Table S2).

We found that the enzyme Amuc-NagB can mediate the reaction combining Fru6P and NH4 to produce GlcN6P, with Km values for Fru6P and NH4 of 5.5 ± 0.9 mM and 41.3 ± 12.8 mM respectively (Table 2), as calculated based on triplicate assays, one of which one is represented in a Lineweaver-Burk plot (Figure 4). However, the Km of GlcN6P value for the deaminating direction is much lower at 2.4 ± 0.2 mM, see Figure 4 and Table 2. The addition of GlcNAc6P as possible allosteric activator had no significant influence on the Km values ($p > 0.05$). On top of this, the activity of the purified Amuc-NagB on Fru6P with glutamine was measured to determine the possibility for this enzyme to mediate the conversion of Fru6P + glutamine → GlcN6P + glutamate [EC 2.6.1.16]. No activity was found using these substrates. Additional controls using enzyme without substrates and substrate without enzyme also showed no activity (Table S8).

Table 2 Enzyme kinetics of *A. muciniphila* NagB with and without GlcNAc6P. The addition of 0.25 mM GlcNAc6P as activator has no influence on the kinetics of the enzyme.

	Km (mM)		
Activator: GlcNAc6P (mM)	0 (n=3)	25 (n=2)	p-value
NH4	41.3 ± 12.8	50.6 ± 10.5	0.54
Fru6P	5.5 ± 0.9	8.4 ± 2.7	0.48
GlcN6P	2.4 ± 0.2	2.1 ± 0.8	0.75

The Km value of 41.3 mM for NH4 is high, but ammonium is not toxic at this concentration (Figure S3), and these concentrations are described to be present in the gut (Macfarlane, et al., 1986, Macfarlane, et al., 1992). The ammonium present in the gut diffuses through the cell to almost equilibrium (Muller, et al., 2006), so the required ammonium concentration for the aminating direction could take place as such in the *A. muciniphila* cells. However, the Km value of Fru6P at 5.5 mM is rather high, this compound is described to be toxic in these amounts in many bacteria (Kadner, et al., 1992). Additionally, the Km value of GlcN6P is lower at 2.4 mM. GlcN6P is the only compound involved in the deaminating direction (Table 2, Table S8).

The kinetic values found for Amuc-NagB are in line with previously characterized NagB-like enzymes (Calcagno, et al., 1984), except for the absence of the need for an allosteric activator. In all cases GlcNAc6P is described as an allosteric activator (Alvarez-Anorve, et al., 2005, Alvarez-Anorve, et al., 2016). Our results clearly show that the overexpressed Amuc-NagB is not allosterically activated by GlcNAc6P (Table 2). Considering the kinetic values of Amuc-NagB, it is unlikely for the aminating reaction to occur at physiological conditions, as also postulated before (Calcagno, et al., 1984). We assume an alternative route to synthesize phosphorylated amino glucoses (GlcN6P, GlcN1P, GlcNAc6P and GlcNAc1P) is taking place, which is provided by the addition of non-phosphorylated GlcNAc or GalNAc to the growth medium. We propose that GlcNAc can be used by *A. muciniphila* to form peptidoglycan intermediates and ultimately peptidoglycan via the *Akkermansia* GlcNAc shortcut (Figure 3).

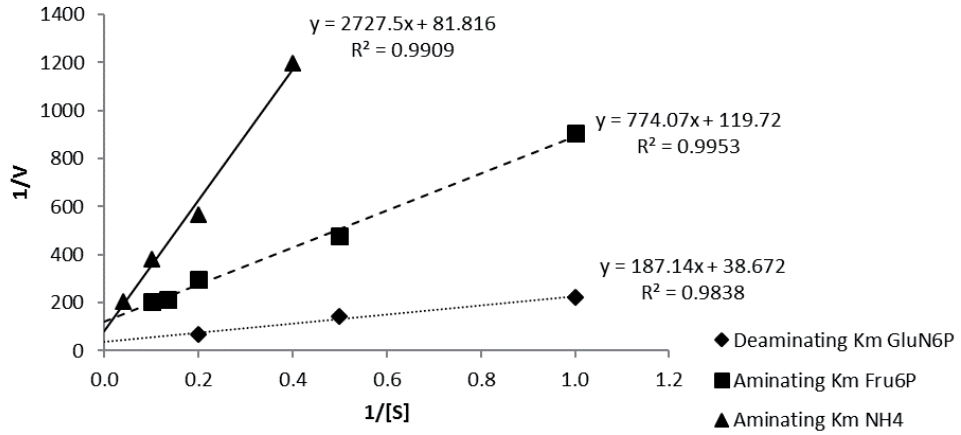

Figure 4. Lineweaver-Burk plot to determine the Km values of NH4 (triangles), Fru6P (squares) and GlcN6P (diamonds). The Km value is determined based on the trend line according to Lineweaver and Burk (Lineweaver, et al., 1934). The figure shows one of the three replicates. Formulas, trend line and R2 were obtained by Microsoft Excel 2010.

Optimization of the *A. muciniphila* genome-scale constraint-based model of metabolism

The growth on different sugars was compared with predictions from the *A. muciniphila* model as presented before (Ottman et al., 2017b). The initial version of the model (AkkMuc_588 v1) predicted growth on all sugars testes, except GlcN, as discussed above. This is in discrepancy with growth in minimal medium and can be explained by the absence of GlmS, that was assumed to be present in the model due to the use of gap filling algorithms (Table 3). Based on these findings, the model was adjusted by deleting the reaction Fru6P +

Glutamine → GlcN6P + Glutamate [EC 2.6.1.16]. This yielded correct growth predictions for glucose and GlcNAc. The adjusted model (AkkMuc_588 v2) still did not predict growth on GalNAc. This was solved by the additional annotation of UDP-glucose 4-epimerase on locus Amuc_1125 (AMUC_RS06020) as UDP-GlcNAc 4-epimerase and which supports the formation of UDP-GalNAc from GalNAc as discussed above. The epimerase has previously shown to bidirectional mediate the conversion of UDP-glucose to UDP-galactose and UDP-GlcNAc to UDP-GalNAc in both bacteria and human (Thoden, et al., 2001, Bernatchez, et al., 2005). The improved version of the model contains 748 reactions describing conversions among 737 metabolites and can be found in SBML and table (xls) formats in the supplementary information.

Qualitative predictions by the adjusted model (AkkMuc_588 v2) showed higher similarity to our laboratory experiments than the original model (Table 3). The only small difference between the model and laboratory experiments is the growth on a medium containing GlcN and glucose. While the model predicts no growth a growth rate of 0.005 h^{-1} was observed in the laboratory experiment. This could be caused by a limited uptake of GlcN, even though there is no GlcN transporter annotated. Simulations with an *in silico* generated mutant with a hypothetical GlcN transporter show that absence of this transporter is the sole reason for the lack of growth predicted for this sugar. This small uptake could explain the low growth rate in the presence of both GlcN and glucose, thereby providing full agreement between the model qualitative predictions and the experimental results. Nevertheless the role of glucose remains unclear, as from the experiments we see that it would be essential to enable this possible low uptake rate.

Table 3. Growth comparison between in vitro and in silico analyses.

Sugar 1	**Sugar 2**	AkkMuc_588 v1 **(y/n)**	AkkMuc_588 v2 **(y/n)**	AkkMuc_588 v2 **(au)**	**Lab (μ) (h^{-1})**
Glucose	GlcN	y	n	0	0.005
GlcN		n	n	0	0
GlcNAc		y	y	0.09	0.056
GlcNAc	Glucose	y	y	0.13	0.122
GalNAc		y	y	0.09	0.084
Glucose		y	n	0	0

Concluding, we have shown that GlcNAc or GalNAc with the addition of L-threonine are essential for growth of *A. muciniphila.* The dependency on GlcNAc or GalNAc is caused by the absence of a gene coding for GlmS, which mediates the aminating reaction from Fru6P to GlcN6P with glutamine as amino donor (Figure 3), while Amuc-NagB was shown to be NagB indeed. The absence of GlmS enzyme and the presence of GlcNAc in the ecological niche of *A. muciniphila* resulted in an alternative pathway for peptidoglycan formation.

This finding supported the development of a growth medium that allows the use of *A. muciniphila* in pre-clinical and phase I clinical trials. Additionally, a minimal medium can be used for detailed physiological studies, and manipulation. With this information we adjusted an existing genome-scale metabolic model by deleting the reaction mediated by GlmS. This yielded a more accurate prediction of growth possibilities and growth rate by the metabolic model compared to the previous version of the model. The development of the defined minimal medium for *A. muciniphila* was based on gathered knowledge about this species and contributed to a better understanding of this organism and it evolutionary adaptation to mucin components.

References

1 Altschul, S.F., Gish, W., Miller, W., Myers, E.W., and Lipman, D.J. (1990) Basic local alignment search tool, *J Mol Biol* **215**: 403-410.

2 Alvarez-Anorve, L.I., Calcagno, M.L., and Plumbridge, J. (2005) Why does Escherichia coli grow more slowly on glucosamine than on N-acetylglucosamine? Effects of enzyme levels and allosteric activation of GlcN6P deaminase (NagB) on growth rates, *J Bacteriol* **187**: 2974-2982.

3 Alvarez-Anorve, L.I., Gaugue, I., Link, H., Marcos-Viquez, J., Diaz-Jimenez, D.M., Zonszein, S., et al. (2016) Allosteric Activation of Escherichia coli Glucosamine-6-Phosphate Deaminase (NagB) In Vivo Justified by Intracellular Amino Sugar Metabolite Concentrations, *J Bacteriol* **198**: 1610-1620.

4 Anhe, F.F., Roy, D., Pilon, G., Dudonne, S., Matamoros, S., Varin, T.V., et al. (2015) A polyphenol-rich cranberry extract protects from diet-induced obesity, insulin resistance and intestinal inflammation in association with increased Akkermansia spp. population in the gut microbiota of mice, *Gut* **64**: 872-883.

5 Barreteau, H., Kovac, A., Boniface, A., Sova, M., Gobec, S., and Blanot, D. (2008) Cytoplasmic steps of peptidoglycan biosynthesis, *FEMS Microbiol Rev* **32**: 168-207.

6 Bernatchez, S., Szymanski, C.M., Ishiyama, N., Li, J., Jarrell, H.C., Lau, P.C., et al. (2005) A single bifunctional UDP-GlcNAc/Glc 4-epimerase supports the synthesis of three cell surface glycoconjugates in Campylobacter jejuni, *J Biol Chem* **280**: 4792-4802.

7 Burk, D., Lineweaver, H., and Horner, C.K. (1934) The Specific Influence of Acidity on the Mechanism of Nitrogen Fixation by Azotobacter, *J Bacteriol* **27**: 325-340.

8 Calcagno, M., Campos, P.J., Mulliert, G., and Suastegui, J. (1984) Purification, molecular and kinetic properties of glucosamine-6-phosphate isomerase (deaminase) from Escherichia coli, *Biochim Biophys Acta* **787**: 165-173.

9 Caspi, R., Altman, T., Billington, R., Dreher, K., Foerster, H., Fulcher, C.A., et al. (2014) The MetaCyc database of metabolic pathways and enzymes and the BioCyc collection of Pathway/Genome Databases, *Nucleic Acids Res* **42**: D459-471.

10 Chen, H.C., Chang, C.C., Mau, W.J., and Yen, L.S. (2002) Evaluation of N-acetylchitooligosaccharides as the main carbon sources for the growth of intestinal bacteria, *FEMS Microbiol Lett* **209**: 53-56.

11 Dao, M.C., Everard, A., Aron-Wisnewsky, J., Sokolovska, N., Prifti, E., Verger, E.O., et al. (2015) Akkermansia muciniphila and improved metabolic health during a dietary intervention in obesity: relationship with gut microbiome richness and ecology, *Gut*.

12 Derrien, M., Belzer, C., and de Vos, W.M. (2016) Akkermansia muciniphila and its role in regulating host functions, *Microb Pathog*.

13 Derrien, M., Collado, M.C., Ben-Amor, K., Salminen, S., and de Vos, W.M. (2008) The Mucin degrader Akkermansia muciniphila is an abundant resident of the human intestinal tract, *Appl Environ Microbiol* **74**: 1646-1648.

14 Derrien, M., Van Baarlen, P., Hooiveld, G., Norin, E., Muller, M., and de Vos, W.M. (2011) Modulation of Mucosal Immune Response, Tolerance, and Proliferation in Mice Colonized by the Mucin-Degrader Akkermansia muciniphila, *Front Microbiol* **2**: 166.

15 Derrien, M., Vaughan, E.E., Plugge, C.M., and de Vos, W.M. (2004) Akkermansia muciniphila gen. nov., sp. nov., a human intestinal mucin-degrading bacterium, *Int J Syst Evol Microbiol* **54**: 1469-1476.

16 Desai, M.S., Seekatz, A.M., Koropatkin, N.M., Kamada, N., Hickey, C.A., Wolter, M., et al. (2016) A Dietary Fiber-Deprived Gut Microbiota Degrades the Colonic Mucus Barrier and Enhances Pathogen Susceptibility, *Cell* **167**: 1339-1353 e1321.

17 Durand, P., Golinelli-Pimpaneau, B., Mouilleron, S., Badet, B., and Badet-Denisot, M.A. (2008) Highlights of glucosamine-6P synthase catalysis, *Arch Biochem Biophys* **474**: 302-317.

18 Ebrahim, A., Lerman, J.A., Palsson, B.O., and Hyduke, D.R. (2013) COBRApy: COnstraints-Based Reconstruction and Analysis for Python, *BMC Syst Biol* **7**: 74.

19 Everard, A., Belzer, C., Geurts, L., Ouwerkerk, J.P., Druart, C., Bindels, L.B., et al. (2013) Cross-talk between Akkermansia muciniphila and intestinal epithelium controls diet-

induced obesity, *Proceedings of the National Academy of Sciences of the United States of America* **110**: 9066-9071.
20 Gomez-Gallego, C., Pohl, S., Salminen, S., De Vos, W.M., and Kneifel, W. (2016) Akkermansia muciniphila: a novel functional microbe with probiotic properties, *Benef Microbes* **7**: 571-584.
21 Gurobi (2016) Optimizer Reference Manual.
22 Hoskins, L.C., Agustines, M., McKee, W.B., Boulding, E.T., Kriaris, M., and Niedermeyer, G. (1985) Mucin degradation in human colon ecosystems. Isolation and properties of fecal strains that degrade ABH blood group antigens and oligosaccharides from mucin glycoproteins, *J Clin Invest* **75**: 944-953.
23 Johansson, M.E., Larsson, J.M., and Hansson, G.C. (2011) The two mucus layers of colon are organized by the MUC2 mucin, whereas the outer layer is a legislator of host-microbial interactions, *Proc Natl Acad Sci U S A* **108 Suppl 1**: 4659-4665.
24 Kadner, R.J., Murphy, G.P., and Stephens, C.M. (1992) Two mechanisms for growth inhibition by elevated transport of sugar phosphates in Escherichia coli, *J Gen Microbiol* **138**: 2007-2014.
25 Kwiatkowska-Semrau, K., Czarnecka, J., Wojciechowski, M., and Milewski, S. (2015) Heterogeneity of quaternary structure of glucosamine-6-phosphate deaminase from Giardia lamblia, *Parasitol Res* **114**: 175-184.
26 Lineweaver, H., Burk, D., and Deming, W.E. (1934) The Dissociation Constant of Nitrogen-Nitrogenase in Azotobacter, *Journal of the American Chemical Society* **56**: 225-230.
27 Liou, A.P., Paziuk, M., Luevano, J.M., Jr., Machineni, S., Turnbaugh, P.J., and Kaplan, L.M. (2013) Conserved shifts in the gut microbiota due to gastric bypass reduce host weight and adiposity, *Sci Transl Med* **5**: 178ra141.
28 Lyra, A., Forssten, S., Rolny, P., Wettergren, Y., Lahtinen, S.J., Salli, K., et al. (2012) Comparison of bacterial quantities in left and right colon biopsies and faeces, *World J Gastroenterol* **18**: 4404-4411.
29 Macfarlane, G.T., Cummings, J.H., and Allison, C. (1986) Protein degradation by human intestinal bacteria, *J Gen Microbiol* **132**: 1647-1656.
30 Macfarlane, G.T., Gibson, G.R., and Cummings, J.H. (1992) Comparison of fermentation reactions in different regions of the human colon, *J Appl Bacteriol* **72**: 57-64.
31 Milewski, S. (2002) Glucosamine-6-phosphate synthase--the multi-facets enzyme, *Biochim Biophys Acta* **1597**: 173-192.
32 Muller, T., Walter, B., Wirtz, A., and Burkovski, A. (2006) Ammonium toxicity in bacteria, *Curr Microbiol* **52**: 400-406.
33 Orth, J.D., Thiele, I., and Palsson, B.O. (2010) What is flux balance analysis?, *Nat Biotechnol* **28**: 245-248.
34 Ottman, N., Reunanen, J., Meijerink, M., Pietila, T.E., Kainulainen, V., Klievink, J., et al. (2017a) Pili-like proteins of Akkermansia muciniphila modulate host immune responses and gut barrier function, *PLoS One* **12**: e0173004.
35 Ottman, N.D., M.; Suarez-Diez, M.; Boeren, S.; Schaap, P.J.; Martins dos Santos V.A.P.; Smidt, H.; Belzer, C.; de Vos W.M. (2017b) Genome-scale model and omics analysis of metabolic capacities of Akkermansia muciniphila reveal a preferential mucin-degrading lifestyle, *Appl Environ Microbiol*.
36 Ouwerkerk, J.P., van der Ark, K.C., Davids, M., Claassens, N.J., Robert Finestra, T., de Vos, W.M., and Belzer, C. (2016) Adaptation of Akkermansia muciniphila to the oxic-anoxic interface of the mucus layer, *Appl Environ Microbiol*.
37 Pereira, F.C., and Berry, D. (2017) Microbial nutrient niches in the gut, *Environ Microbiol* **19**: 1366-1378.
38 Plovier, H., Everard, A., Druart, C., Depommier, C., Van Hul, M., Geurts, L., et al. (2017) A purified membrane protein from Akkermansia muciniphila or the pasteurized bacterium improves metabolism in obese and diabetic mice, *Nat Med* **23**: 107-113.
39 Png, C.W., Linden, S.K., Gilshenan, K.S., Zoetendal, E.G., McSweeney, C.S., Sly, L.I., et al. (2010) Mucolytic bacteria with increased prevalence in IBD mucosa augment in vitro utilization of mucin by other bacteria, *Am J Gastroenterol* **105**: 2420-2428.
40 Python (2017) Python Software Foundation. In: *Python Language reference*.

41 Tailford, L.E., Crost, E.H., Kavanaugh, D., and Juge, N. (2015) Mucin glycan foraging in the human gut microbiome, *Front Genet* **6**: 81.
42 Tanaka, T., Takahashi, F., Fukui, T., Fujiwara, S., Atomi, H., and Imanaka, T. (2005) Characterization of a novel glucosamine-6-phosphate deaminase from a hyperthermophilic archaeon, *J Bacteriol* **187**: 7038-7044.
43 Thoden, J.B., Wohlers, T.M., Fridovich-Keil, J.L., and Holden, H.M. (2001) Human UDP-galactose 4-epimerase. Accommodation of UDP-N-acetylglucosamine within the active site, *J Biol Chem* **276**: 15131-15136.
44 Thomsson, K.A., Holmen-Larsson, J.M., Angstrom, J., Johansson, M.E., Xia, L., and Hansson, G.C. (2012) Detailed O-glycomics of the Muc2 mucin from colon of wild-type, core 1- and core 3-transferase-deficient mice highlights differences compared with human MUC2, *Glycobiology* **22**: 1128-1139.
45 Van Herreweghen, F., Van den Abbeele, P., De Mulder, T., De Weirdt, R., Geirnaert, A., Hernandez-Sanabria, E., et al. (2017) In vitro colonisation of the distal colon by Akkermansia muciniphila is largely mucin and pH dependent, *Benef Microbes* **8**: 81-96.
46 van Passel, M.W., Kant, R., Zoetendal, E.G., Plugge, C.M., Derrien, M., Malfatti, S.A., et al. (2011) The genome of Akkermansia muciniphila, a dedicated intestinal mucin degrader, and its use in exploring intestinal metagenomes, *PLoS One* **6**: e16876.
47 Variyam, E.P., and Hoskins, L.C. (1981) Mucin degradation in human colon ecosystems. Degradation of hog gastric mucin by fecal extracts and fecal cultures, *Gastroenterology* **81**: 751-758.
48 Vincent, F., Davies, G.J., and Brannigan, J.A. (2005) Structure and kinetics of a monomeric glucosamine 6-phosphate deaminase: missing link of the NagB superfamily?, *J Biol Chem* **280**: 19649-19655.
49 Wang, L., Christophersen, C.T., Sorich, M.J., Gerber, J.P., Angley, M.T., and Conlon, M.A. (2011) Low relative abundances of the mucolytic bacterium Akkermansia muciniphila and Bifidobacterium spp. in feces of children with autism, *Appl Environ Microbiol* **77**: 6718-6721.
50 Wu, H.C., and Wu, T.C. (1971) Isolation and characterization of a glucosamine-requiring mutant of Escherichia coli K-12 defective in glucosamine-6-phosphate synthetase, *J Bacteriol* **105**: 455-466.

Availability of data and material

The genome-scale metabolic model of *Akkermansia muciniphila* AkkMuc_588_v2 is available as supplementary material together with a list of the changes respect to the previous version. Supplementary file contains the AkkMuc_588_v2 model in SBML level 2 and in table (xls) format. The file also contains documentation indicating the changes respect to the previous version. Finally, to ease model reutilization we have included a Python script to perform growth simulations on different media. The script requires the COBRApy library (and has been tested with version 0.4.1) (Ebrahim, et al., 2013) and an LP solver such as Gurobi (Gurobi, 2016).

Supplementary Figures and Tables

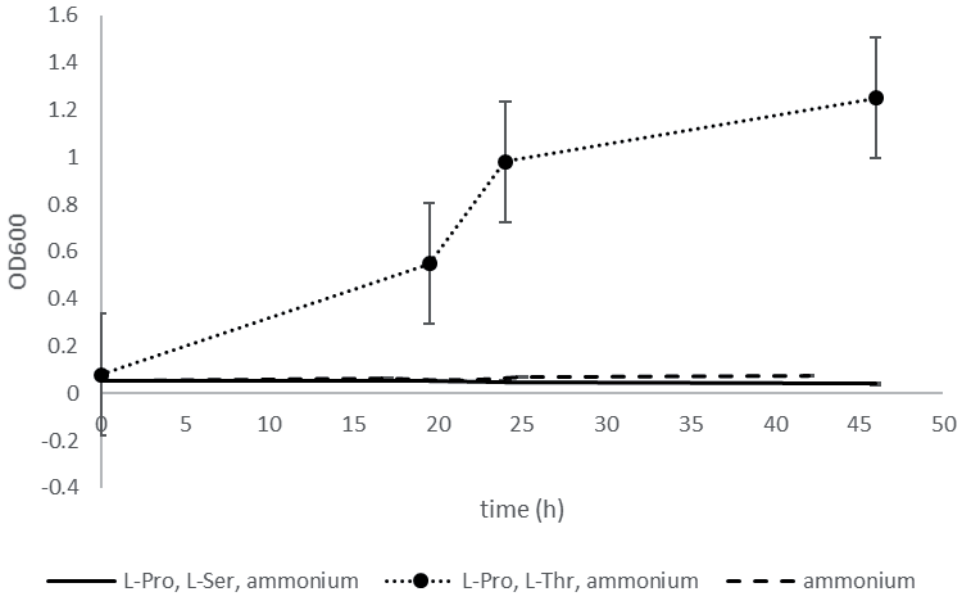

Figure S1. Growth of *A. muciniphila* on CP medium supplemented with 25 mM of each glucose and GlcNAc. As nitrogen source was added 4 g/L of L-proline and either L-serine or L-threonine. In all bottles 0.3 g/L NH_4Cl was added. Growth was only observed with the addition of L-threonine.

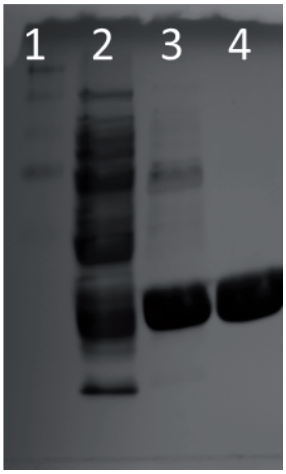

Figure S2. SDS-PAGE gel of overexpressed protein purification using a Ni-column. In lane 1: marker, lane 2: E. coli BL21-Amuc_1822 CFE, lane 3: wash flow through, lane 4: purified protein amuc_1822.

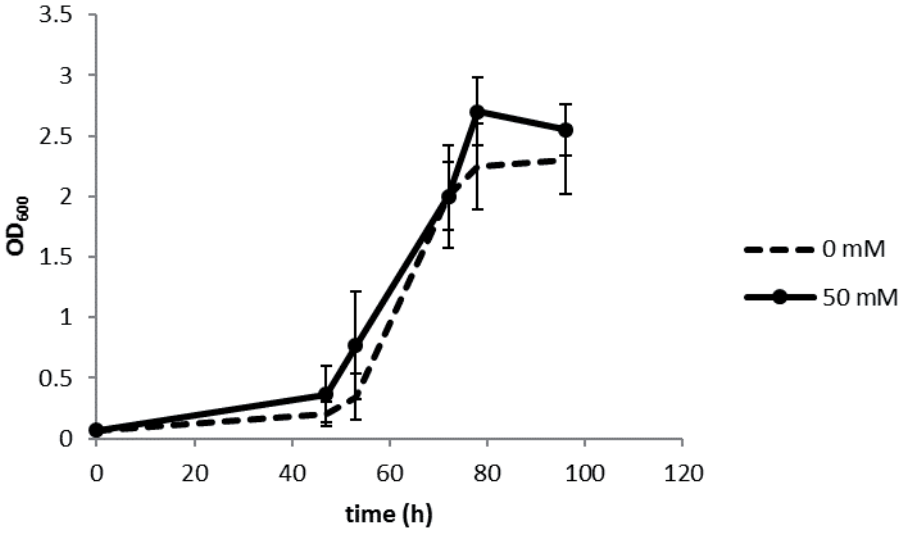

Figure S3. Growth of *A. muciniphila* on CP medium supplemented with 25mM GlcNAc, 6g/L Thr and 0mM or 50mM NH_4Cl.

Table S1. Composition of tested media. The indicated compounds are added to CP medium without ammonium (Derrien, et al., 2004).

Carbon source		
Glucose (mM)	**GlcNAc (mM)**	**Other sugars (mM)**
12.5	12.5	
0	0	
0	25	
12.5	12.5	
0	0	
0	25	
12.5	0	12.5 GlcN
0	0	25 GalNAc
0	0	25 GlcN
12.5	0	12.5 GlcN
0	0	25 Fru

Table S2. Determination of protein concentrations by BCA assay used for enzyme assays. The BSA was used for a standard curve. The enzyme was diluted 5 times and 40 times to determine the protein concentration.

BSA (ug/mL)	**590nm**	**450nm**	**OD590/450**
0	0.45	0.74	0.61
1	0.46	0.75	0.61
5	0.50	0.73	0.69
10	0.57	0.70	0.81
50	0.97	0.54	1.78
100	1.31	0.42	3.14
5 × diluted Amuc-NagB	1.82	0.29	6.28
40× diluted Amuc-NagB	0.78	0.62	1.25
Concentration Amuc-NagB (mg/mL)			SD
1.10			0.04

Table S3. Overview of substrates used in enzyme assay.

		Substrates (mM)			Activator[1] (mM)	Enzyme (µL)
	# tube	Fru6P	NH4	GlcN6P	(GlcNAC-6P)	
AMINATING	1	15	50		0.25	5
	2	10	50		0.25	5
	3	7.5	50		0.25	5
	4	5	50		0.25	5
	5	2	50		0.25	5
	6	1	50		0.25	5
	7	20	50		0.25	5
	8	20	25		0.25	5
	9	20	10		0.25	5
	10	20	5		0.25	5
	11	20	2.5		0.25	5
DEAMINATING	12*			15	0.25	1
	13*			10	0.25	1
	14*			7.5	0.25	1
	15			5	0.25	1
	16			2	0.25	1
	17			1	0.25	1
Standard curve	18			0		
	19			0.5		
	20			1		
	21			2		
Control GlcNAC6P	22				0.25	

[1] *Added in 2 out of 5 replicates. * Not used in determination of Km.*

Table S4. BlastP of Escherichia coli K12 NagB (NP_415204.1) against Akkermansia (taxid:239934). All hits are shown.

Description	Max score	Total score	Query cover	E value	Ident	Accession
glucosamine-6-phosphate deaminase [Akkermansia muciniphila CAG:154]	177	177	92%	5.00E-55	40%	CDB55261.1
MULTISPECIES: glucosamine-6-phosphate deaminase [*Akkermansia*]	176	176	92%	8.00E-55	40%	WP_067570388.1
glucosamine-6-phosphate deaminase [*Akkermansia glycaniphila*]	175	175	87%	2.00E-54	42%	WP_067775984.1
glucosamine-6-phosphate deaminase [*Akkermansia muciniphila*]	175	175	90%	1.00E-53	41%	WP_065529150.1
glucosamine-6-phosphate deaminase [*Akkermansia muciniphila*]	175	175	90%	1.00E-53	41%	WP_012420854.1
glucosamine-6-phosphate deaminase [*Akkermansia sp.* CAG:344]	172	172	92%	3.00E-53	39%	CDD98135.1
glucosamine-6-phosphate deaminase [*Akkermansia muciniphila*]	173	173	90%	5.00E-53	40%	WP_031931289.1
hypothetical protein HMPREF3038_03217 [*Akkermansia* sp. KLE1797]	24.6	24.6	4%	7.8	73%	KXT46402.1

Table S5. BlastP of *A muciniphila* NagB (CDB55261.1) against all sequence except Akkermansia (taxid:239934). Top 5 hits are shown.

Description	Max score	Total score	Query cover	E value	Ident	Accession
glucosamine-6-phosphate deaminase [*Rubritalea squalenifaciens* DSM 18772]	354	354	82%	3.00E-120	67%	SHJ43774.1
glucosamine-6-phosphate deaminase [*Rubritalea marina*]	319	319	81%	2.00E-106	61%	WP_018969388.1
glucosamine-6-phosphate deaminase [*Capnocytophaga canis*]	317	317	79%	2.00E-100	60%	WP_042008125.1
Glucosamine-6-phosphate deaminase [*Flavobacterium aquidurense*]	305	305	80%	2.00E-99	56%	KQB39432.1
glucosamine-6-phosphate deaminase [*Capnocytophaga canis*]	314	314	79%	2.00E-99	59%	WP_042347886.1

Table S6. BlastP of Escherichia coli K12 GlmS (NP_418185.1) against Akkermansia (taxid:239934). All hits are shown.

Description	Max score	Total score	Query cover	E value	Ident	Accession
von Willebrand factor type A domain protein [*Akkermansia* sp. KLE1797]	32	32	17%	0.68	26%	KXT50996.1

MULTISPECIES: hypothetical protein [*Akkermansia*]	32	32	17%	0.71	26%	WP_067570323.1
queuine tRNA-ribosyltransferase [*Akkermansia muciniphila* CAG:154]	29.3	29.3	4%	3.9	40%	CDB55386.1
tRNA guanosine(34) transglycosylase Tgt [*Akkermansia* sp. 54_46]	29.3	29.3	4%	4.2	40%	OLA88015.1
tRNA-guanine(34) transglycosylase [*Akkermansia muciniphila*]	29.3	29.3	4%	4.2	40%	WP_031930139.1
tRNA guanosine(34) transglycosylase Tgt [*Akkermansia muciniphila*]	29.3	29.3	4%	4.4	40%	WP_012419333.1

Table S7. BlastP of Verrucromicrobium spinosum GlmS (WP_009962724.1) against *Akkermansia muciniphila*. All hits are shown.

Description	Max score	Total score	Query cover	E value	Ident	Accession
tRNA-guanine(34) transglycosylase [*Akkermansia muciniphila*]	30	30	5%	0.83	42%	WP_031930139.1

tRNA guanosine(34) transglycosylase Tgt [*Akkermansia muciniphila*]	30	30	5%	0.84	42%	WP_012419333.1
hypothetical protein [*Akkermansia muciniphila*]	27.3	27.3	11%	6	25%	WP_065529387.1

Table S8. Control reactions for enzyme assay of *A. muciniphila* NagB. The amount of GlcN6P formed is not above 0.01 mM in 10 minutes.

Content assay	OD_{585}	GlcN6P (mM)
10 mM Fru6P + 10mM glutamine 5 uL Enzyme	0.006	0.01
50 mM NH4Cl + 7,5mM Fru6P	0.000	0.00
5 uL Enzyme	0.000	0.00

CHAPTER 4

The influence of an animal component free medium on cell morphology and therapeutic efficacy of *Akkermansia muciniphila*

Kees C. H. van der Ark, Steven Aalvink, Laura Huuskonen, Hubert Plovier, Patrice Cani, Clara Belzer and Willem M. de Vos

The *in vivo* experiment described in this chapter was previously published in:

A purified membrane protein from Akkermansia muciniphila or the pasteurized bacterium improves metabolism in obese and diabetic mice, *Nature medicine, 2017,* **23**: 107-113.Plovier, H., Everard, A., Druart, C., Depommier, C., Van Hul, M., Geurts, L., Chilloux, J., Ottman, N., Duparc, T., Lichtenstein, L., Myridakis, A., Delzenne, N. M., Klievink, J., Bhattacharjee, A., **van der Ark, C. H**., Aalvink, S., Martinez, L. O., Dumas, M., Maiter, D., Loumaye, A., Hermans, M. P., Thissen, J.-P., Belzer, C., de Vos, W. M. and Cani, P. D.

Abstract

Presence of the symbiont *Akkermansia muciniphila* in the intestinal microbiota is associated with a healthy metabolic status. Previous studies have shown that administration of a daily dose of cells of *A. muciniphila* cultured on a mucus-based medium is able to protect mice from diet-induced obesity. Based on a recently developed genome-scale metabolic model, we designed an improved growth medium for *A. muciniphila* that was free from animal-derived components. The medium composition was based on the discovery that N-acetylglucosamine is essential for the growth of *A. muciniphila*. Moreover, to increase growth rate, we supplemented the synthetic growth medium with a plant protein hydrolysate, resulting in significant growth rate increase. We showed that *A. muciniphila* cells grown on this synthetic medium had a similar effect on mice compared to mucus-grown cells. To investigate the impact of the newly designed synthetic medium on the functionality of *A. muciniphila*, we compared the global gene expression of mucus and synthetic medium-grown cells by transcriptome analysis. The results revealed no major effects on the expression of household functions or genes involved in the production of the type IV pili, including that coding for the biologically active protein Amuc_1100 that was found to be not significantly increased during growth on the synthetic medium. However, we observed various genes involved in cell morphology to be significantly upregulated in the synthetic medium, including that coding for the cell-shape determining protein MreB. Detailed cell analysis by quantitative phase-contrast and electron microscopy analysis revealed morphological changes of cells grown in the synthetic medium, mainly by elongation. In conclusion, we designed, tested and validated a medium free from animal components that showed improved growth and cell size but did not affect the efficacy of *A. muciniphila* in therapeutic applications.

Introduction

Cultivating bacteria has been the core focus for microbiologists since the discovery of the first pure culture in 1878 to show cause-effect relations (Santer, 2010). This provided the foundation for present day studies that showed that the ability to grow bacteria in pure culture allows for detailed studies of their metabolism, morphology, genetics and interactions with other bacteria, bacteriophages, and other organisms. Even in times of rapidly expanding methods of genomic and other molecular techniques to detect and characterize bacteria, there is the need to culture bacteria for physiological characterization and intervention studies. The recently developed high-throughput culture techniques have been helpful in cultivating more bacterial species from the intestinal tract (Nichols, et al., 2010, Lagier, et al., 2016). Culturing these intestinal bacteria is of specific interest since these may directly affect human health or are influenced by the health status of humans. One of these bacteria is the mucus-degrading intestinal symbiont *Akkermansia muciniphila.* This bacterium was isolated using pig gastric mucus as sole carbon and nitrogen source, supplemented with vitamins and minerals (Derrien, et al., 2004). Next to inverse correlations with several diseases based on relative abundances (Swidsinski, et al., 2011, Wang, et al., 2011, Derrien, et al., 2016), *A. muciniphila* was also shown to be effective in preventing metabolic disorders during intervention studies (Derrien, et al., 2016). When administered by intestinal gavage in mice, *A. muciniphila* was able to reduce weight gain in diet-induced obesity (Everard, et al., 2013). The estimated amount of bacterial species in the gut is around 2500 based on 16S rRNA sequencing data (Ritari, et al., 2015). These intestinal bacteria could potentially be used as biomarkers or serve as therapeutic agents. The diseases that are associated with the abundance, presence or absence of bacterial species in the gut vary from inflammatory gut, metabolic and immune disorders to even psychological aberrations (Dinan, et al., 2013, Guinane and Cotter, 2013, Hur and Lee, 2015). Especially bacterial species that show an inversed correlation with the occurrence or severity of diseases are of interest for further development as therapeutic microbes. At present, several gut microbiota members have been identified that show such inverse correlations or, alternatively, show an increase in relative abundance upon treatment of the disease, including butyrate-producing bacteria such as *Faecalibacterium prausnitzii, Clostridium butyricum, Eubacterium hallii* and *Intestimonas butyriciproducens* (Bui, et al., 2015, Kanai, et al., 2015, Quevrain, et al., 2016, Udayappan, et al., 2016), but also the previously mentioned *Akkermansia muciniphila* (Everard, et al., 2013, Derrien, et al., 2016).

To allow application as food supplements in humans, therapeutic microbes should meet the safety regulations of novel foods and when health claims are made should live up to similar requirements as nowadays probiotics have in EU countries (Hill, et al., 2014, Kumar, et al., 2015, Gomez-Gallego, et al., 2016). Regulations concerning pharmaceuticals are stricter and require large dossiers of preclinical testing and successful human trials. When *A. muciniphila* would be marketed as a new therapeutic microbe, the development of an animal component-free medium and further safety studies are required according to the novel food regulation of the EU (Gomez-Gallego, et al., 2016).

Probiotic bacteria are usually lactic acid bacteria, and can therefore tolerate a low pH and potentially oxygen (Higuchi, et al., 2000, Andriantsoanirina, et al., 2013). The growth media of these bacteria are based on complex media containing yeast extract, beef extract and tryptone (Chang and Liew, 2013), but successful growth on minimal and animal component free media have also been reported (Heenan, et al., 2002, Mattila-Sandholm, et al., 2002, Teusink, et al., 2006, Heinken, et al., 2014). Most of the potential therapeutic microbes (*F. prausnitzii, E. hallii, I. butyriciproducens* and *A. muciniphila*) are strictly anaerobic or able to tolerate small amounts of oxygen. *A. muciniphila* can use only small amounts of oxygen for respiration (Flint, et al., 2007, Khan, et al., 2012, Bui, et al., 2015, Ouwerkerk, et al., 2016b). This could pose technical challenges in large-scale production. We have previously shown that that *A. muciniphila* requires the addition of N-acetylglucosamine (GlcNAc) or N-acetylgalactosamine (GalNAc) for growth since this bacterium is unable to synthesize the peptidoglycan building block uridine diphosphate (UDP)-GlcNAc via the amination of fructose-6-phosphate to glucosamine-6-phosphate (van der Ark, et al., 2017). This finding was the basis for further development of a synthetic medium for cultivation of *A. muciniphila* suited for therapeutic applications with significant growth rate and yield. The impact of the optimized synthetic medium was analysed by characterizing the global gene expression and morphology.

Materials and methods

A. muciniphila culturing

A. muciniphila was grown in carbonate buffered mineral medium as described previously (Derrien, et al., 2004, Ouwerkerk, et al., 2017), but without the addition of mucus. The mucus was replaced with either soy peptone or a combination of L-proline and L-threonine as nitrogen source and GlcNAc and glucose as carbon source.

In the text, the media are referred to as 'soy medium' and 'PT medium' when equimolar amounts of glucose and GlcNAc are used, to a total of 25 mM in case of the PT medium and 25 mM for soy medium. When deviating sugar concentrations were used, it is mentioned in the text. Mucus medium always refers to medium in which 0.5% hog gastric mucus (Sigma) was used as described before (Derrien, et al., 2004).

Preparation of *A. muciniphila* for preclinical trials

A. muciniphila was grown in soy medium or mucus medium, after which the bacteria were collected essentially as described before (Everard, et al., 2013, Ouwerkerk, et al., 2017), with the adjustments described following. Bacteria were collected at the end of the growth phase (OD600 of 1.5-2 for soy medium or OD of 1 for mucus medium). All subsequent steps were executed in a sterile environment, at ambient air and at 4˚C or on ice. The bacteria were centrifuged at 10,000 g for 10 minutes. The supernatant was discarded, after which the pelleted cells were suspended in sterile PBS (manufacturer salt). Centrifugation was repeated, and cells were suspended again in sterile PBS. After a third centrifugation, cells were suspended in 1/10 of the original culture volume of sterile anaerobic PBS containing 25% glycerol and 0.05% L-cysteine-HcCl. Aliquots of 1 mL were made in 10 mL anaerobic bottles containing N_2/CO_2 80/20 (v/v) at 1.8 atm and stored immediately at -80˚C. Determination of Cfu's in the aliquots and preparation for gavage was done exactly as described before (Ouwerkerk, et al., 2017).

Mice trials and analyses

Mice were given daily gavages of 1.5×10^8 CFU *A. muciniphila* grown on either mucus medium or soy medium, or received a daily placebo, for 4 weeks. The gavages and measurements were performed in a non-blinded fashion. The mice were male C57BL/6J of

10 weeks old (Charles River, L'Arbresle, France). Food was freely available throughout the experiment, which was a chow diet (AIN93Mi, Research diet, New Brunswick, NJ, USA) during acclimatisation of all mice and for the control diet (ND) group, and a high-fat diet (HFD) (60% fat and 20% carbohydrates (kcal/100g) D12492i, Research diet, New Brunswick, NJ, USA) for the experimental groups. Body weight gain, food and water consumption were determined once a week. Body composition for fat mass detection was determined using 7.5 MHz time domain-nuclear magnetic resonance (TD-NMR) (LF50 Minispec, Bruker, Rheinstetten, Germany).

Mice were excluded when abnormal behaviour was shown, or tissue abnormalities where found during necropsy and sampling. All mouse experiments were approved by and performed in accordance with the guidelines of the local ethics committee. Housing conditions were specified by the Belgian Law of May 29, 2013, regarding the protection of laboratory animals (agreement number LA1230314). Further details of the mice experiments were described before, including description of statistical analyses (Plovier, et al., 2017).

Light microscopy, electron microscopy and cell size analysis

To determine the size of the bacteria, three soy medium cultures and two mucus medium cultures were visualised using phase-contract microscopy (microscope model). Cells on the image were analysed using ImageJ (version 1.51f). Scale was set using the scale bar on the microscopy image, selecting analyse, scale in Image J. The cell length was measured by selecting the longest diameter within the cell. Cells were individually measured, after which the data was analysed using Excel 2016. Scanning electron microscopy was performed on soy medium grown *A. muciniphila* at an OD600 of 1.3 as described before (Ouwerkerk, et al., 2016a).

RNA sequencing

Samples for RNA sequencing were obtained at late exponential phase of cultures grown in soy medium and mucus medium. RNA isolation and sequencing was performed as described before (Ouwerkerk, et al., 2016b), with in this case duplicates of both soy and mucus medium. Sequencing was performed at Baseclear BV, the Netherlands. Gene annotations were as described and used before (Ottman, et al., 2017). Analysis of the expression profiles was performed with an in-house analysis pipeline (Koehorst, et al., 2016), including Bowtie2

(Galaxy Tool Version 0.6) for the mapping of reads against the reference genome (Langmead and Salzberg, 2012), htseq-count (Galaxy Tool Version 0.6.1galaxy1) to extract count tables per gene (Anders, et al., 2015) and DESeq2 (Galaxy Tool Version 2.1.8.0) for the analysis of differential expression (Love, et al., 2014).

Results

Medium composition for optimal growth and therapeutic applications of *A. muciniphila*

From our improved metabolic model we concluded that *A. muciniphila* has a necessity for L-threonine and GlcNAc to support growth (van der Ark, et al., 2017). Moreover, this model also predicted growth on glucose in the presence of these additions. Hence, we aimed to omit mucin from the bicarbonate-buffered mineral medium currently used to grow *A. muciniphila* media (Derrien, et al., 2004) and added glucose and GlcNAc in different ratios as well as L-threonine and L-proline. The latter was added as mucin is known to contain large amounts of proline. However, the specific growth rate on this PT medium was rather low and amounted to 0.06 h^{-1} (Table 1). Hence, to call for rapid growth we added protein hydrolysate plant origin (Table 1). The addition of soy protein hydrolysate resulted in a high growth rate of 0.53 h^{-1} exceeding that of *A. muciniphila* on mucin, which is approximately 0.41 h^{-1} (Derrien, et al., 2004, Ottman, et al., 2017). Since the soy protein hydrolysate is derived from a plant source, it is an acceptable food-grade nitrogen source and applicable on a large scale. Moreover, as the growth rate on soy medium was higher than that on mucin and high cell densities were obtained, we decided to focus on this food-grade medium for further studies.

Table 1. Growth rate of *A. muciniphila* on soy and PT media, with GlcNAc and glucose as carbon sources. The ratio between acetate and propionate produced on each medium is in the last column

Medium	Growth rate (h^{-1})	st.dev	Acetate/propionate ratio
Soy peptone 16g/L (soy medium)			
Glu GlcNAc	0.53	0.05	0.92
Thr 6g/L, Pro 6g/L (PT medium)			
GlcNAc	0.04	0.02	1.46
Glu GlcNAc	0.06	0.04	1.07

The different media tested showed no differences in fermentation profiles, when the same sugars were added to the growth medium. The ratio between acetate and propionate was found to be 1:1 when grown on equimolar quantities of glucose and GlcNAc, and 3:2 to 2:1

when only GlcNAc was added (Table 1) The addition of glucose to the growth medium increased the amount of propionate by a factor ~1.5, while the amount of acetate is reduced only ~0.9 fold. This is mainly due to the use of GlcNAc for fermentation, which results in the release of one acetate per GlcNAc molecule.

Cell morphology changes in different media

The cell shape of *A. muciniphila* has been described as an oval shaped bacterium of approximately 1 um in length (Derrien, et al., 2004). We observed aberrant cell shapes when growing *A. muciniphila* in PT medium or soy medium. When grown on mucus medium, the cells were nearly exclusive around 1 µm and oval shaped. When *A. muciniphila* is cultured on soy medium, the cell morphology became less uniform. Cells were elongated and even a 'tripod' cell was observed (Figure 1A). The latter was the case when cells were cultured in soy medium with glucose and only 1 mM of GlcNAc was added. Besides, the cells also showed possible compartmentalisation inside the elongated cells (Figure 1A). When *A. muciniphila* was grown on PT medium, cell elongations of up to 50 µm were observed (Figure 1B).

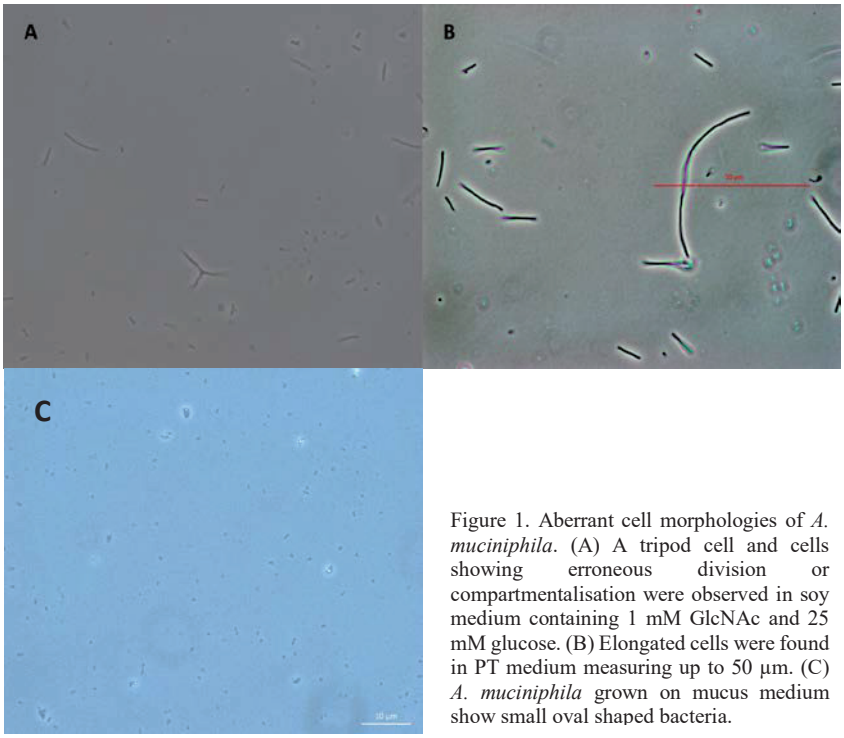

Figure 1. Aberrant cell morphologies of *A. muciniphila*. (A) A tripod cell and cells showing erroneous division or compartmentalisation were observed in soy medium containing 1 mM GlcNAc and 25 mM glucose. (B) Elongated cells were found in PT medium measuring up to 50 µm. (C) *A. muciniphila* grown on mucus medium show small oval shaped bacteria.

To visualise the compartmentalisation of cells inside the elongated structures, we employed SEM (Figure 2). The images show that the elongated bacteria can be divided in two subgroups. One group with cell internally subdivided in compartments, the other group with cells elongated without visual subdivisions. These observations suggest that the regulation of cell division or cell shape is disturbed in the studied media.

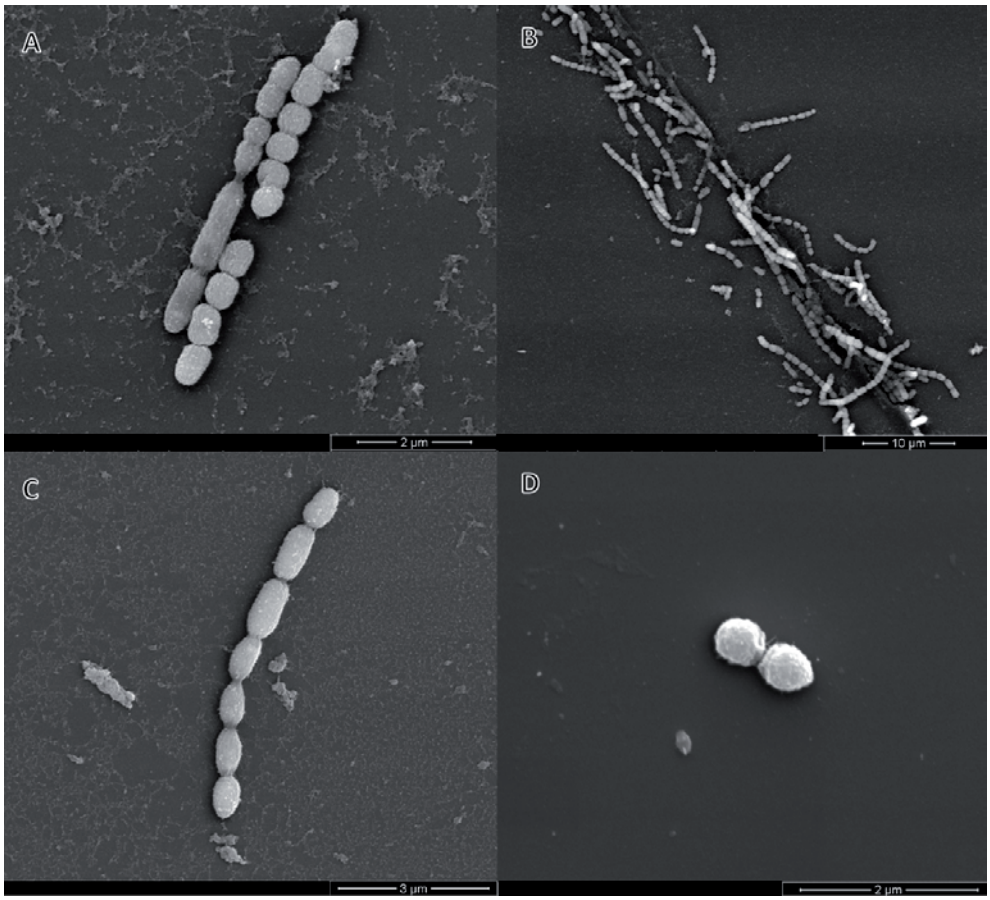

Figure 2. Scanning electron micrographs of *A. muciniphila* cultured on soy medium (A, B and C). The cells are elongated or do not divide properly. Normal shaped cells were observed in mucus medium (D).

The cell length of bacteria grown in soy medium and mucus medium was measured to quantify the visual differences in length. We found that *A. muciniphila* cells grown on soy medium (n cells = 251) were larger compared to cells grown on mucus medium (n cells =

160) (p-value < 0.01), with an average cell length of 1.3 (±0.80) µm and 0.8 (±0.25) µm respectively (Figure 3).

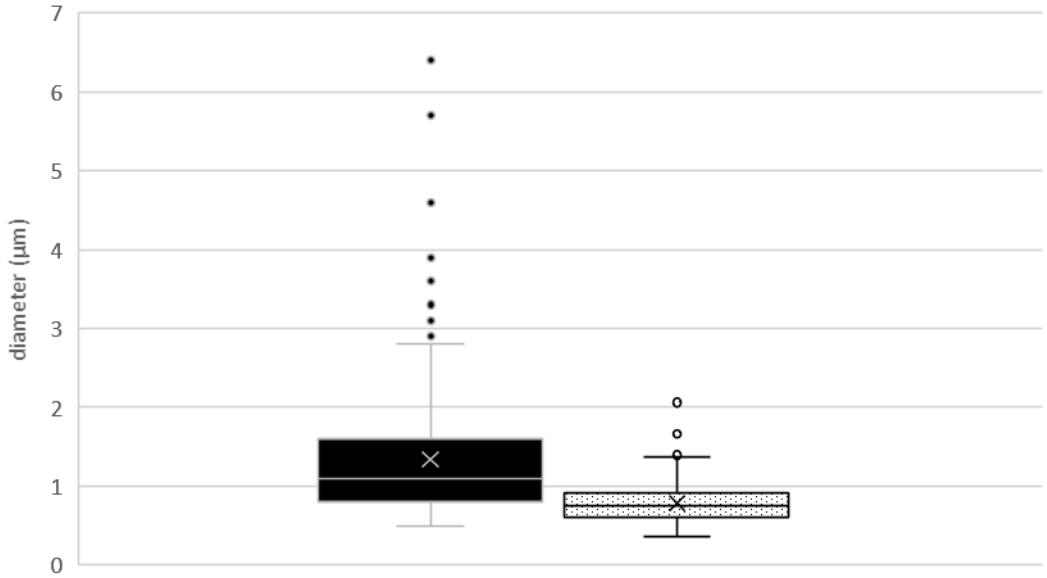

Figure 3. Cell length of cells grown in soy medium (black, left) and mucus medium (white dotted, right). The average cell length in soy medium is significantly larger compared to mucus medium.

Gene expression in defined and undefined media

Using RNAseq analysis we compared the expression profile of *A. muciniphila* cultured on the soy medium with that obtained on mucus medium to study the cause of changes in cell morphology and pinpoint possible anabolic adaptations. A total of 133 genes was found to be differentially expressed between soy and mucus medium, out of a total 2138 genes predicted by the *A. muciniphila* genome (Table S1, Figure 4). Of these differentially expressed genes, 40 have no annotated function. The analysed samples cluster together with growth on different samples, allowing comparison of gene expression profiles (Figure S1).

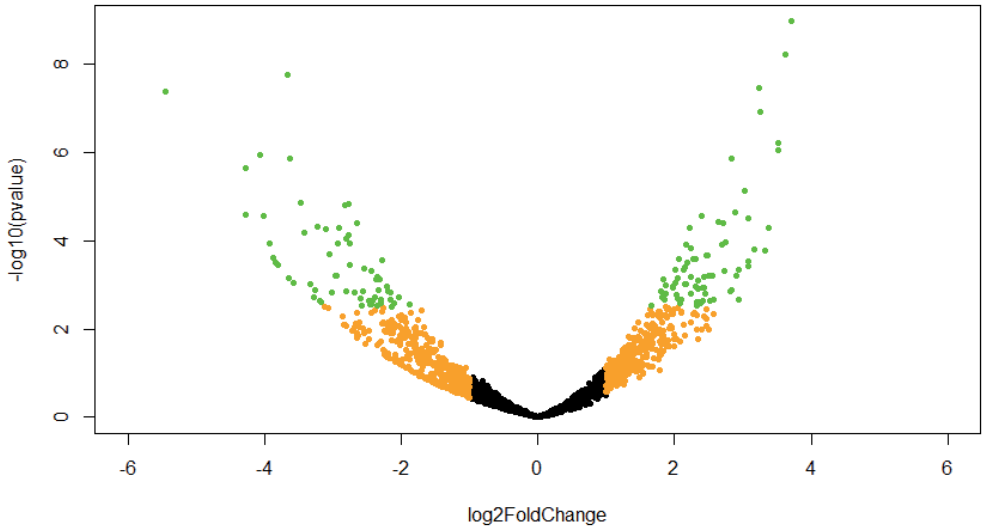

Figure 4. Volcano plot of all *A. muciniphila* genes expressed in soy medium versus mucus medium. Green dots represent the genes that are significantly different in expression between soy and mucus grown cells.

When *A. muciniphila* was cultured on soy medium, the cells were found to be elongated. The cell shape determining protein MreB (Amuc_0540) was upregulated 8.9 fold in soy medium. Other regulated genes coding for proteins involved in cell division code for CcmA (Amuc_1317) and MraZ (Amuc_0649), which are both also 4-6 fold upregulated (Table 2). Other genes homologues to genes described to be involved in cell shape and cell division were not significantly regulated (Table 2).

Table 2. Genes homologues to genes described to be involved in cell shape regulation and cell division, in order of ascending q-value. Genes that are differentially expressed (q-value < 0.05) in green.

Locus tag	Annotation (NCBI)	2log fold change	q-value
Amuc_0540	rod shape-determining protein MreB	3.16	0.01
Amuc_1317	Integral membrane protein CcmA involved in cell shape determination	2.19	0.01
Amuc_0649	Cell division protein MraZ	2.73	0.02
Amuc_0348	Cell division protein FtsH (EC 3.4.24.-)	2.00	0.11
Amuc_0514	Cell division protein FtsI [Peptidoglycan synthetase] (EC 2.4.1.129)	1.37	0.15
Amuc_1052	Cell division trigger factor (EC 5.2.1.8)	1.05	0.33
Amuc_1176	Cell division inhibitor	-1.17	0.41
Amuc_2076	Cell division protein FtsK	0.47	0.69
Amuc_0662	Cell division protein FtsQ	-0.57	0.71
Amuc_1558	Intramembrane protease RasP/YluC, implicated in cell division based on FtsL cleavage	-0.28	0.84
Amuc_0658	Cell division protein FtsW	0.31	0.87
Amuc_0152	Cell division protein FtsZ (EC 3.4.24.-)	0.23	0.89
Amuc_0153	Cell division protein FtsA	0.15	0.94
Amuc_0652	Cell division protein FtsI [Peptidoglycan synthetase] (EC 2.4.1.129)	0.03	0.99

Because the sugars present in the medium could influence the expression profiles of genes involved in polysaccharide degradation, we mined for regulation of those genes from our data. An upregulation of a fucosidase (Amuc_0146) and a galactosidase (Amuc_1666) was observed in mucus medium, represented by a negative fold change as compared to growth in soy medium (Table *3*). A higher expression of genes belonging to the glycoside hydrolase families 109, 20 and 98 was found in soy medium. These hydrolases are usually involved in GlcNAc or GalNAc degradation.

Table 3. Genes involved in polysaccharide degradation that are significantly regulated, ordered by q-value, with Uniprot annotations.

Locus tag	2log fold change	q-value	Annotation (Uniprot)
Amuc_0017	3.62	0.00	Glycosyl hydrolase family 109 protein 1 (EC 3.2.1.-)
Amuc_1666	-3.62	0.00	Beta-galactosidase (EC 3.2.1.23) (Lactase)
Amuc_2136	2.83	0.00	Glycoside hydrolase, family 20, catalytic core
Amuc_0146	-2.77	0.00	Alpha-L-fucosidase (EC 3.2.1.51)
Amuc_1438	2.27	0.01	Glycosyl hydrolase family 98 putative carbohydrate binding module
Amuc_0920	1.97	0.03	Glycosyl hydrolase family 109 protein 2 (EC 3.2.1.-)

Finally, we studied the gene expression profiles of genes possibly involved in host interactions, such as the Amuc_1100 and its predicted gene cluster involved in the production of the outer membrane located type IV pilus secretin Amuc_1098 (PilQ). The expression of this gene was 1.6 times higher in soy medium when compared to mucus medium. No significant differences (q-value >0.05) were found in the expression of the whole gene cluster Amuc_1098-Amuc_1102, which was previously identified as possibly involved in host signalling (Ottman, et al., 2017).

Table 4. Expression of genes possibly involved in host signalling.

Locus tag	Annotation (Ottman, et al., 2016); NCBI)	2Log fold change	q-value
Amuc_1098	outer membrane located pilus secretin (PilQ)	1.6	0.06
Amuc_1099	hypothetical protein	2.4	0.10
Amuc_1100	hypothetical protein	0.2	0.89
Amuc_1101	cell division protein FtsA/ Type IV pilus biogenesis protein PilM	0.5	0.73
Amuc_1102	hypothetical protein	0.0	0.99

Influence of growth medium on *A. muciniphila* efficacy in preclinical trials

To study the influence of medium composition on *A. muciniphila* therapeutic efficiency, we supplemented *A. muciniphila* grown on mucus or soy medium to mice fed a high-fat diet (HFD). We measured the weight gain and fat mass gain of these groups compared to mice fat a control chow diet (ND) and mice fed a HFD, which received a placebo treatment. After daily gavages for 5 weeks, the diet-induced fat mass gain was reduced by about 50% in both groups treated with *A. muciniphila* (Figure 5A). Similarly, the body mass gain was also reduced by both *A. muciniphila* grown on mucus and soy medium (Figure 5B).

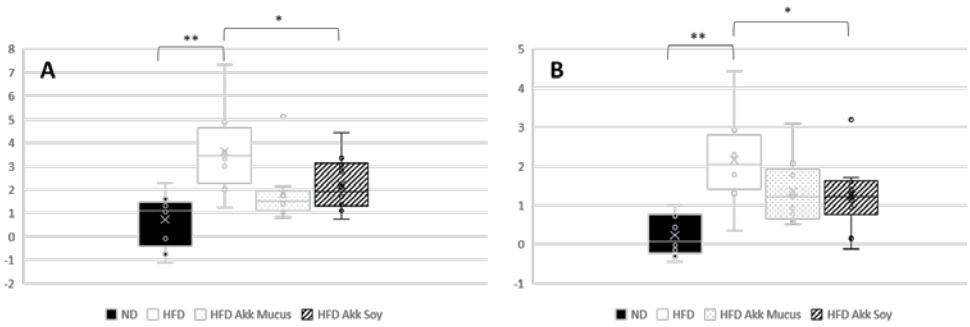

Figure 1. Fat mass gain of mice with ND, HFD and supplemented with *A. muciniphila* grown on mucus and soy (A). Weight gain of mice with ND, HFD and supplemented with *A. muciniphila* grown on mucus and soy (B). The fat mass gain and weight gain are reduced with supplementation of *A. muciniphila*. *P < 0.05; **P < 0.001. No significant differences between HFD Akk Mucus and HFD Akk Soy.

Discussion

We have shown that *A. muciniphila* can be optimally cultured in the previously described minimal medium with the addition of soy protein hydrolysate. The growth rate of *A. muciniphila* in the soy medium was found to be slightly higher when compared to that in the original mucus medium, with a growth rate of 0.53 h^{-1} and 0.41 h^{-1}, respectively. Previously, it was shown that *A. muciniphila* could be cultured with a low growth rate on a basal medium with high amounts of casein tryptone, without the addition of GlcNAc (Ottman et al., 2017). This may be possible by the presence of glycosylated casein molecules that may contribute to an alternative carbon and energy source. Mucins in the mucus media contain a plethora of glycan structures, including galactose, GlcNAC, mannose, fucose and others. During the

development of the minimal medium (van der Ark, et al., 2017), we found that the co-addition of glucose and GlcNAc increased the growth rate. Therefore, it is likely that the addition of more and different sugars could even further increase the growth rate.

Remarkably, we observed an altered morphology of *A. muciniphila* cells grown on soy media as compared to that found on mucin medium. Cells were in general approximately 1.5 times longer than when grown on mucus medium. An even further altered cell morphology was found when cells were grown on the PT medium. This could be a consequence of various factors, including protein source, ratio between glucose and GlcNAc, or growth rate. Further studies are needed to differentiate between those possibilities and address the exact morphology of *A. muciniphila* when grown in the human intestinal tract.

The upregulation of the gene coding for MreB could explain the differences in cell morphology, because an increase of this protein increases the cell length (Jones, et al., 2001, Figge, et al., 2004). The other two significantly upregulated genes are CcmA (Amuc_1317) and MraZ (Amuc_0649). CcmA is involved in the determination of cell shape, by influencing peptidoglycan cross-linking in *Helicobater pylori,* and likely requires an cytoskeleton protein such as MreB for positioning. For the determination of cell shape in *H. pylori,* the role of CcmA is linked to genes coding for Csd1-3, which have no known homologues in *A. muciniphila* (Sycuro, et al., 2010, Typas, et al., 2011). Therefore, the function of CcmA in *A. muciniphila* might be regulated differently in the bacterium. CcmA could act as cytoskeleton scaffold involved in peptidoglycan synthesis as secondary function (Hay, et al., 1999).

The cell division genes of *A. muciniphila* were identified before, and include FtsQAZ (Pilhofer, et al., 2008). It has been found that the localization of the cell division protein cluster is different in *A. muciniphila*, where the gene *ftsQ* is not followed by genes encoding other members of the FTS-protein family, but by a homologue of the *recA* gene (Pilhofer, et al., 2008). The function of MraZ in the cell division process is likely to be a transcriptional regulator (Eraso, et al., 2014). The protein function has been characterised in *E. coli,* in which it regulates the division and cell wall (*cdw*) gene cluster and it was found to be associated with DNA in the nucleoid. In *A. muciniphila,* the *mraZ* gene is located upstream of the peptidoglycan synthesis gene cluster. None of the genes involved in this cluster (Amuc_0650-0661) was found to be up or down regulated in this study (Table S1). These findings are in line with previous findings that the overexpression of the *mraZ* gene leads to

filamentation of the cells and even cell death (Eraso, et al., 2014). The combination of upregulated MreB, CcmA and MraZ is likely to result in cells with filamentous phenotypes and low division rates. The effect on morphology could be caused by adjusted signalling for cell division, which is partly dependent on peptidoglycan formation and hydrolysis (Keep, et al., 2006, Typas, et al., 2011). As shown in previous research (van der Ark, et al., 2017), the peptidoglycan formation of *A. muciniphila* is likely to follow an alternative route, with the UDP-GlcNAc precursors being formed directly from GlcNAc. A misbalance between GlcNAc and glucose in metabolism could change the formation kinetics of the cell membrane and thereby the cell division signalling.

Additionally, the function of gene Amuc_1101 is annotated as FtsA. However, recent insight suggests it could rather have the function of the pili-associated protein PilM as it is located in close proximity to the gene for the type IV pilus secretin *pilQ* (Amuc_1098) (Ottman, et al., 2016). This alternative annotation is also reflected in Table 4 and a previous proteomics study, where the protein encoded by this gene was located on the outer membrane (Ottman, et al., 2017). The gene upstream of this putative *ftsA/pilM* gene, is the gene coding for a hypothetical protein on locus Amuc_1100, and its product was found to be involved in host signalling (Plovier, et al., 2017). We found no significant differences in the expression profiles of this gene. Therefore, we hypothesized that the cultivation of *A. muciniphila* on soy medium has no influence on the efficacy of bacteria in preclinical trials. Indeed, there was no observed difference between the efficacy of the two treatments in terms of body mass gain and fat mass gain. Thereby we confirmed the applicability of soy medium for intervention studies and clinical trials. Further clinical trials are needed to investigate the efficacy of soy medium grown *A. muciniphila* in humans and the first results indicate that there are no safety issues (Plovier et al., 2017).

Conclusion

We have shown that *A. muciniphila* can be efficiently grown in a synthetic medium devoid of animal-derived compounds. Cells grown on the newly developed synthetic medium showed morphological changes that could be explained by upregulation of cell shape determining genes when the global *A. muciniphila* expression was compared to that when grown in the original mucus medium. The expression of genes that are potentially involved

in host signalling were not found to be influenced by cultivation in the synthetic medium. Finally, there were no observed differences between the therapeutic efficacy of cells grown in mucus or synthetic medium in preclinical mice trials.

Acknowledgements

The study was funded by the SIAM gravitation grant 024.002.002 of the Netherlands Organization for Scientific Research. We would like to thank Sebastian Hornung for support in transcriptome analysis.

References

1 Anders, S., Pyl, P.T., and Huber, W. (2015) HTSeq--a Python framework to work with high-throughput sequencing data, *Bioinformatics* **31**: 166-169.
2 Andriantsoanirina, V., Allano, S., Butel, M.J., and Aires, J. (2013) Tolerance of Bifidobacterium human isolates to bile, acid and oxygen, *Anaerobe* **21**: 39-42.
3 Bui, T.P.N., Ritari, J., Boeren, S., de Waard, P., Plugge, C.M., and de Vos, W.M. (2015) Production of butyrate from lysine and the Amadori product fructoselysine by a human gut commensal, *Nature Communications* **6**.
4 Chang, C.P., and Liew, S.L. (2013) Growth Medium Optimization for Biomass Production of a Probiotic Bacterium, Lactobacillus rhamnosus ATCC 7469, *Journal of Food Biochemistry* **37**: 536-543.
5 Derrien, M., Belzer, C., and de Vos, W.M. (2016) Akkermansia muciniphila and its role in regulating host functions, *Microb Pathog*.
6 Derrien, M., Vaughan, E.E., Plugge, C.M., and de Vos, W.M. (2004) Akkermansia muciniphila gen. nov., sp nov., a human intestinal mucin-degrading bacterium, *Int J Syst Evol Microbiol* **54**: 1469-1476.
7 Dinan, T.G., Stanton, C., and Cryan, J.F. (2013) Psychobiotics: a novel class of psychotropic, *Biol Psychiatry* **74**: 720-726.
8 Eraso, J.M., Markillie, L.M., Mitchell, H.D., Taylor, R.C., Orr, G., and Margolin, W. (2014) The Highly Conserved MraZ Protein Is a Transcriptional Regulator in Escherichia coli, *J Bacteriol* **196**: 2053-2066.
9 Everard, A., Belzer, C., Geurts, L., Ouwerkerk, J.P., Druart, C., Bindels, L.B., et al. (2013) Cross-talk between Akkermansia muciniphila and intestinal epithelium controls diet-induced obesity, *Proc Natl Acad Sci U S A* **110**: 9066-9071.
10 Figge, R.M., Divakaruni, A.V., and Gober, J.W. (2004) MreB, the cell shape-determining bacterial actin homologue, co-ordinates cell wall morphogenesis in Caulobacter crescentus, *Mol Microbiol* **51**: 1321-1332.
11 Flint, H.J., Duncan, S.H., Scott, K.P., and Louis, P. (2007) Interactions and competition within the microbial community of the human colon: links between diet and health, *Environ Microbiol* **9**: 1101-1111.
12 Gomez-Gallego, C., Pohl, S., Salminen, S., De Vos, W.M., and Kneifel, W. (2016) Akkermansia muciniphila: a novel functional microbe with probiotic properties, *Benef Microbes* **7**: 571-584.
13 Guinane, C.M., and Cotter, P.D. (2013) Role of the gut microbiota in health and chronic gastrointestinal disease: understanding a hidden metabolic organ, *Therap Adv Gastroenterol* **6**: 295-308.
14 Hay, N.A., Tipper, D.J., Gygi, D., and Hughes, C. (1999) A novel membrane protein influencing cell shape and multicellular swarming of Proteus mirabilis, *J Bacteriol* **181**: 2008-2016.
15 Heenan, C.N., Adams, M.C., Hosken, R.W., and Fleet, G.H. (2002) Growth Medium for Culturing Probiotic Bacteria for Applications in Vegetarian Food Products, *LWT - Food Science and Technology* **35**: 171-176.
16 Heinken, A., Khan, M.T., Paglia, G., Rodionov, D.A., Harmsen, H.J., and Thiele, I. (2014) Functional metabolic map of Faecalibacterium prausnitzii, a beneficial human gut microbe, *J Bacteriol* **196**: 3289-3302.
17 Higuchi, M., Yamamoto, Y., and Kamio, Y. (2000) Molecular biology of oxygen tolerance in lactic acid bacteria: Functions of NADH oxidases and Dpr in oxidative stress, *J Biosci Bioeng* **90**: 484-493.
18 Hill, C., Guarner, F., Reid, G., Gibson, G.R., Merenstein, D.J., Pot, B., et al. (2014) Expert consensus document. The International Scientific Association for Probiotics and Prebiotics consensus statement on the scope and appropriate use of the term probiotic, *Nat Rev Gastroenterol Hepatol* **11**: 506-514.
19 Hur, K.Y., and Lee, M.S. (2015) Gut Microbiota and Metabolic Disorders, *Diabetes Metab J* **39**: 198-203.

20 Jones, L.J., Carballido-Lopez, R., and Errington, J. (2001) Control of cell shape in bacteria: helical, actin-like filaments in Bacillus subtilis, *Cell* **104**: 913-922.
21 Kanai, T., Mikami, Y., and Hayashi, A. (2015) A breakthrough in probiotics: Clostridium butyricum regulates gut homeostasis and anti-inflammatory response in inflammatory bowel disease, *J Gastroenterol* **50**: 928-939.
22 Keep, N.H., Ward, J.M., Cohen-Gonsaud, M., and Henderson, B. (2006) Wake up! Peptidoglycan lysis and bacterial non-growth states, *Trends Microbiol* **14**: 271-276.
23 Khan, M.T., Duncan, S.H., Stams, A.J., van Dijl, J.M., Flint, H.J., and Harmsen, H.J. (2012) The gut anaerobe Faecalibacterium prausnitzii uses an extracellular electron shuttle to grow at oxic-anoxic interphases, *ISME J* **6**: 1578-1585.
24 Koehorst, J.J., van Dam, J.C., van Heck, R.G., Saccenti, E., Dos Santos, V.A., Suarez-Diez, M., and Schaap, P.J. (2016) Comparison of 432 Pseudomonas strains through integration of genomic, functional, metabolic and expression data, *Sci Rep* **6**: 38699.
25 Kumar, H., Salminen, S., Verhagen, H., Rowland, I., Heimbach, J., Banares, S., et al. (2015) Novel probiotics and prebiotics: road to the market, *Curr Opin Biotechnol* **32**: 99-103.
26 Lagier, J.C., Khelaifia, S., Alou, M.T., Ndongo, S., Dione, N., Hugon, P., et al. (2016) Culture of previously uncultured members of the human gut microbiota by culturomics, *Nat Microbiol* **1**.
27 Langmead, B., and Salzberg, S.L. (2012) Fast gapped-read alignment with Bowtie 2, *Nature Methods* **9**: 357-359.
28 Love, M.I., Huber, W., and Anders, S. (2014) Moderated estimation of fold change and dispersion for RNA-seq data with DESeq2, *Genome Biol* **15**: 550.
29 Mattila-Sandholm, T., Myllärinen, P., Crittenden, R., Mogensen, G., Fondén, R., and Saarela, M. (2002) Technological challenges for future probiotic foods, *International Dairy Journal* **12**: 173-182.
30 Nichols, D., Cahoon, N., Trakhtenberg, E.M., Pham, L., Mehta, A., Belanger, A., et al. (2010) Use of ichip for high-throughput in situ cultivation of "uncultivable" microbial species, *Appl Environ Microbiol* **76**: 2445-2450.
31 Ottman, N., Davids, M., Suarez-Diez, M., Boeren, S., Schaap, P.J., Martins Dos Santos, V.A.P., et al. (2017) Genome-scale model and omics analysis of metabolic capacities of Akkermansia muciniphila reveal a preferential mucin-degrading lifestyle, *Appl Environ Microbiol*.
32 Ottman, N., Huuskonen, L., Reunanen, J., Boeren, S., Klievink, J., Smidt, H., et al. (2016) Characterization of Outer Membrane Proteome of Akkermansia muciniphila Reveals Sets of Novel Proteins Exposed to the Human Intestine, *Front Microbiol* **7**: 1157.
33 Ottman, N., Reunanen, J., Meijerink, M., Pietila, T.E., Kainulainen, V., Klievink, J., et al. (2017) Pili-like proteins of Akkermansia muciniphila modulate host immune responses and gut barrier function, *PLoS One* **12**: e0173004.
34 Ouwerkerk, J.P., Aalvink, S., Belzer, C., and de Vos, W.M. (2016a) Akkermansia glycaniphila sp. nov., an anaerobic mucin-degrading bacterium isolated from reticulated python faeces, *Int J Syst Evol Microbiol* **66**: 4614-4620.
35 Ouwerkerk, J.P., Aalvink, S., Belzer, C., and De Vos, W.M. (2017) Preparation and preservation of viable Akkermansia muciniphila cells for therapeutic interventions, *Benef Microbes* **8**: 163-169.
36 Ouwerkerk, J.P., van der Ark, K.C., Davids, M., Claassens, N.J., Robert Finestra, T., de Vos, W.M., and Belzer, C. (2016b) Adaptation of Akkermansia muciniphila to the oxic-anoxic interface of the mucus layer, *Appl Environ Microbiol*.
37 Pilhofer, M., Rappl, K., Eckl, C., Bauer, A.P., Ludwig, W., Schleifer, K.H., and Petroni, G. (2008) Characterization and evolution of cell division and cell wall synthesis genes in the bacterial phyla Verrucomicrobia, Lentisphaerae, Chlamydiae, and Planctomycetes and phylogenetic comparison with rRNA genes, *J Bacteriol* **190**: 3192-3202.
38 Plovier, H., Everard, A., Druart, C., Depommier, C., Van Hul, M., Geurts, L., et al. (2017) A purified membrane protein from Akkermansia muciniphila or the pasteurized bacterium improves metabolism in obese and diabetic mice, *Nat Med* **23**: 107-113.
39 Quevrain, E., Maubert, M.A., Michon, C., Chain, F., Marquant, R., Tailhades, J., et al. (2016) Identification of an anti-inflammatory protein from Faecalibacterium prausnitzii, a commensal bacterium deficient in Crohn's disease, *Gut* **65**.

40 Ritari, J., Salojarvi, J., Lahti, L., and de Vos, W.M. (2015) Improved taxonomic assignment of human intestinal 16S rRNA sequences by a dedicated reference database, *Bmc Genomics* **16**.
41 Santer, M. (2010) Joseph Lister: first use of a bacterium as a 'model organism' to illustrate the cause of infectious disease of humans, *Notes Rec R Soc Lond* **64**: 59-65.
42 Swidsinski, A., Dorffel, Y., Loening-Baucke, V., Theissig, F., Ruckert, J.C., Ismail, M., et al. (2011) Acute appendicitis is characterised by local invasion with Fusobacterium nucleatum/necrophorum, *Gut* **60**: 34-40.
43 Sycuro, L.K., Pincus, Z., Gutierrez, K.D., Biboy, J., Stern, C.A., Vollmer, W., and Salama, N.R. (2010) Relaxation of peptidoglycan cross-linking promotes Helicobacter pylori's helical shape and stomach colonization, *Cell* **141**: 822-833.
44 Teusink, B., Wiersma, A., Molenaar, D., Francke, C., Vos, W.M., Siezen, R.J., and Smid, E.J. (2006) Analysis of growth of Lactobacillus plantarum WCFS1 on a complex medium using a genome-scale metabolic model, *J Biol Chem* **281**.
45 Typas, A., Banzhaf, M., Gross, C.A., and Vollmer, W. (2011) From the regulation of peptidoglycan synthesis to bacterial growth and morphology, *Nature Reviews Microbiology* **10**: 123-136.
46 Udayappan, S., Manneras-Holm, L., Chaplin-Scott, A., Belzer, C., Herrema, H., Dallinga-Thie, G.M., et al. (2016) Oral treatment with Eubacterium hallii improves insulin sensitivity in db/db mice **2**: 16009.
47 van der Ark, K.C., Aalvink, S., Plovier, H., Cani, P.D., Belzer, C., and De Vos, W.M. (2017) Model-driven design of a minimal medium for Akkermansia muciniphila confirms mucus adaptation, ***In press***.
48 Wang, L., Christophersen, C.T., Sorich, M.J., Gerber, J.P., Angley, M.T., and Conlon, M.A. (2011) Low relative abundances of the mucolytic bacterium Akkermansia muciniphila and Bifidobacterium spp. in feces of children with autism, *Appl Environ Microbiol* **77**: 6718-6721.

Supplementary information

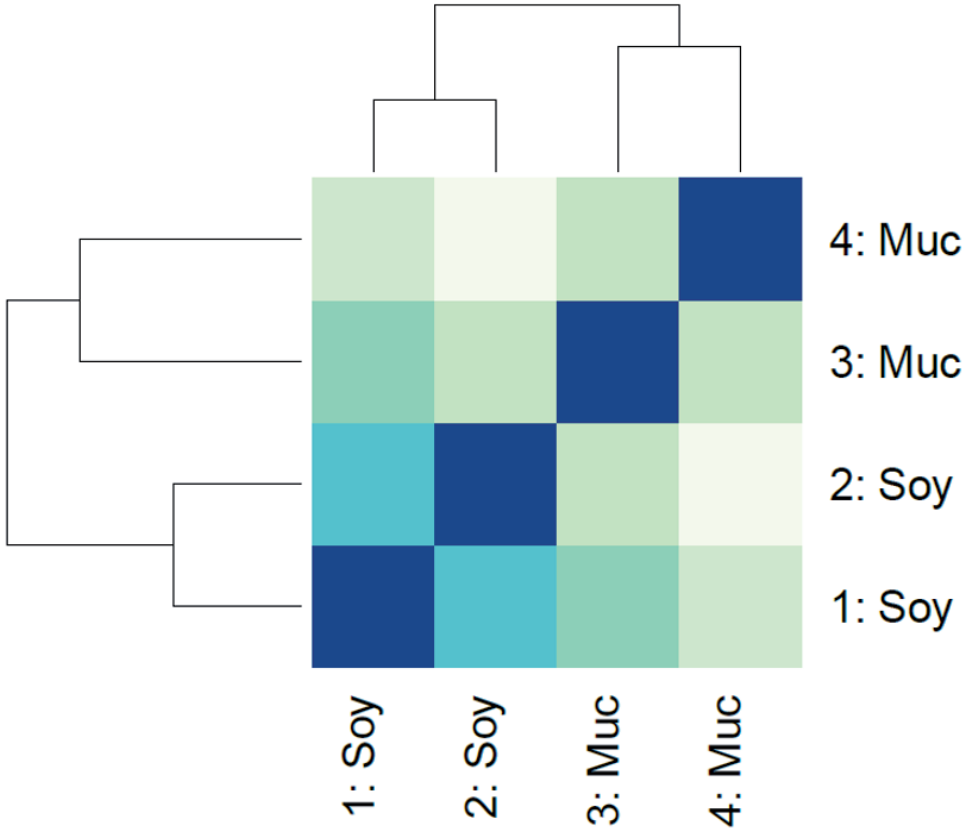

Figure S1 Sample-to-sample distance of RNA sequencing results by medium type. Both soy and mucus samples cluster together, with a higher similarity between soy samples.

Table S1 Genes up- or downregulated in soy versus mucus medium. A positive value means upregulated in soy medium. NCBI annotation.

Locus tag	Annotation	2log fold change	q-value
Amuc_1602	hypothetical protein	3.7	0.00
Amuc_0017	oxidoreductase domain-containing protein	3.6	0.00
Amuc_1677	type III restriction protein res subunit	-3.7	0.00
Amuc_1068	Methionine adenosyltransferase	3.2	0.00

Amuc_1711	hypothetical protein	-5.4	0.00
Amuc_2046	hypothetical protein	3.3	0.00
Amuc_1896	histone family protein DNA-binding protein	3.5	0.00
Amuc_1495	3-dehydroquinate dehydratase	3.5	0.00
Amuc_1115	integrase	-4.1	0.00
Amuc_1666	glycoside hydrolase family 2	-3.6	0.00
Amuc_2136	Glycoside hydrolase, family 20, catalytic core	2.8	0.00
Amuc_1304	phosphate ABC transporter permease	-4.3	0.00
Amuc_2053	hypothetical protein	3.0	0.00
Amuc_0146	alpha-L-fucosidase	-2.8	0.00
Amuc_1002	Carboxymuconolactone decarboxylase	-3.5	0.00
Amuc_1335	Bacteriophage capsid protein-like protein	-2.8	0.00
Amuc_0627	hypothetical protein	2.4	0.00
Amuc_1305	binding-protein-dependent transporters inner membrane component	-4.3	0.00
Amuc_1717	hypothetical protein	2.9	0.00
Amuc_1958	hypothetical protein	-4.0	0.00
Amuc_2038	PUR-alpha/beta/gamma DNA/RNA-binding protein	3.1	0.00
Amuc_0200	methylmalonyl-CoA epimerase	2.6	0.00
Amuc_0643	hypothetical protein	-2.6	0.00
Amuc_1069	S-adenosyl-L-homocysteine hydrolase	2.7	0.00
Amuc_0955	ribosome-binding factor A	3.4	0.00

Amuc_1088	ferrous iron transport protein B	2.2	0.00
Amuc_1298	sulfate adenylyltransferase, large subunit	-2.9	0.00
Amuc_1405	group 1 glycosyl transferase	-3.2	0.00
Amuc_0963	ABC transporter	-3.1	0.00
Amuc_2045	hypothetical protein	-3.4	0.01
Amuc_1167	hypothetical protein	-2.8	0.01
Amuc_1340	hypothetical protein	-2.8	0.01
Amuc_1560	hypothetical protein	2.7	0.01
Amuc_0107	hydrophobe/amphiphile efflux-1 (HAE1) family transporter	-2.8	0.01
Amuc_0233	L-threonine 3-dehydrogenase	2.7	0.01
Amuc_1005	aldo/keto reductase	-3.9	0.01
Amuc_1074	sulfatase	2.2	0.01
Amuc_1300	adenylylsulfate reductase	-2.9	0.01
Amuc_0025	hypothetical protein	2.2	0.01
Amuc_0540	rod shape-determining protein MreB	3.2	0.01
Amuc_0174	hypothetical protein	3.3	0.01
Amuc_1303	phosphate ABC transporter ATPase	-3.1	0.01
Amuc_0794	hypothetical protein	2.5	0.01
Amuc_2072	rubrerythrin	2.5	0.01
Amuc_0085	thiamine biosynthesis protein ThiS	-3.9	0.01
Amuc_0841	argininosuccinate lyase	2.3	0.01
Amuc_1438	glycosyl hydrolase family protein	2.3	0.01

Amuc_1766	family 2 glycosyl transferase	2.1	0.01
Amuc_0037	amino acid permease	-2.3	0.01
Amuc_0383	30S ribosomal protein S15	3.1	0.01
Amuc_1317	hypothetical protein	2.2	0.01
Amuc_1148	hypothetical protein	-3.8	0.01
Amuc_1157	beta-lactamase	-2.8	0.01
Amuc_1379	ABC transporter	3.1	0.01
Amuc_0956	translation initiation factor IF-2	2.2	0.02
Amuc_1348	phage tape measure protein	-2.5	0.02
Amuc_0403	ABC transporter	2.0	0.02
Amuc_0927	30S ribosomal protein S8	2.1	0.02
Amuc_2075	hypothetical protein	2.9	0.02
Amuc_0649	MraZ protein	2.7	0.02
Amuc_0602	hypothetical protein	-2.4	0.02
Amuc_0149	metallophosphoesterase	-2.3	0.02
Amuc_0215	hypothetical protein	2.2	0.02
Amuc_0414	phosphoheptose isomerase	2.5	0.02
Amuc_0967	RNP-1 like RNA-binding protein	2.9	0.02
Amuc_1336	peptidase S49	-3.0	0.02
Amuc_1358	hypothetical protein	-3.0	0.02
Amuc_1533	indole-3-glycerol-phosphate synthase	2.5	0.02

Amuc_0026	hypothetical protein	2.4	0.02
Amuc_0536	hypothetical protein	2.0	0.02
Amuc_1332	hypothetical protein	-3.6	0.02
Amuc_1159	serine/threonine protein kinase	-2.3	0.02
Amuc_0774	major facilitator superfamily protein	-2.4	0.02
Amuc_1597	polyprenyl synthetase	1.8	0.02
Amuc_1205	50S ribosomal protein L9	2.3	0.02
Amuc_2123	hypothetical protein	2.0	0.03
Amuc_1334	hypothetical protein	-3.6	0.03
Amuc_0984	succinate dehydrogenase/fumarate reductase iron-sulfur subunit	2.2	0.03
Amuc_1849	hypothetical protein	-3.3	0.03
Amuc_1903	hypothetical protein	2.2	0.03
Amuc_1246	hypothetical protein	1.9	0.03
Amuc_1676	Eco57I restriction endonuclease	-2.2	0.03
Amuc_0920	oxidoreductase domain-containing protein	2.0	0.03
Amuc_1044	50S ribosomal protein L1	2.3	0.03
Amuc_1266	hypothetical protein	2.4	0.03
Amuc_1639	hypothetical protein	2.4	0.03
Amuc_1786	hypothetical protein	2.0	0.03
Amuc_2141	hypothetical protein	2.3	0.03
Amuc_1697	protein tyrosine phosphatase	2.8	0.03
Amuc_1956	ybaK/ebsC protein	-3.3	0.03

Amuc_0603	hypothetical protein	-2.3	0.03
Amuc_0490	hypothetical protein	-2.2	0.03
Amuc_1531	anthranilate synthase	2.8	0.03
Amuc_1630	RpiB/LacA/LacB family sugar-phosphate isomerase	1.8	0.03
Amuc_1926	cytochrome c assembly protein	-2.8	0.03
Amuc_2096	polysaccharide biosynthesis protein	-2.6	0.03
Amuc_1114	outer membrane autotransporter barrel domain-containing protein	-2.2	0.03
Amuc_0323	phage transcriptional regulator, AlpA	-2.7	0.03
Amuc_1996	hypothetical protein	-3.0	0.03
Amuc_0925	KOW domain-containing protein	2.4	0.03
Amuc_1256	ribonuclease P protein component	2.2	0.03
Amuc_0172	hypothetical protein	1.9	0.03
Amuc_1418	phosphoglycerate kinase	2.0	0.03
Amuc_0362	hypothetical protein	1.8	0.04
Amuc_0545	hypothetical protein	-2.0	0.04
Amuc_1112	hypothetical protein	-3.3	0.04
Amuc_1343	hypothetical protein	-2.4	0.04
Amuc_0830	potassium-transporting ATPase subunit A	-2.6	0.04
Amuc_2177	Preprotein translocase subunit SecA	2.0	0.04
Amuc_0297	30S ribosomal protein S3	2.9	0.04
Amuc_0335	ABC transporter	1.9	0.04

Amuc_1293	hypothetical protein	-2.3	0.04
Amuc_1368	hypothetical protein	2.6	0.04
Amuc_1417	glyceraldehyde-3-phosphate dehydrogenase, type I	2.1	0.04
Amuc_1377	DnaB domain-containing protein helicase domain-containing protein	-2.4	0.04
Amuc_1930	transporter permease	-2.5	0.04
Amuc_0712	hypothetical protein	-3.2	0.04
Amuc_1365	hypothetical protein	2.4	0.04
Amuc_1899	flavodoxin/nitric oxide synthase	2.5	0.04
Amuc_2173	Redoxin domain-containing protein	2.3	0.04
Amuc_1372	hypothetical protein	-3.2	0.04
Amuc_0628	hypothetical protein	2.4	0.04
Amuc_0675	hypothetical protein	-2.1	0.04
Amuc_0913	ATP/cobalamin adenosyltransferase	2.4	0.04
Amuc_1668	ATPase AAA	-2.3	0.04
Amuc_0985	succinate dehydrogenase flavoprotein subunit	2.1	0.04
Amuc_0371	two component regulator propeller domain-containing protein	-1.9	0.05
Amuc_1931	transporter permease	-2.5	0.05
Amuc_1349	hypothetical protein	-2.4	0.05
Amuc_1515	major facilitator superfamily protein	-2.4	0.05
Amuc_1613	NADH dehydrogenase (ubiquinone) 24 kDa subunit	2.3	0.05
Amuc_0694	hypothetical protein	1.7	0.05
Amuc_1169	hypothetical protein	-2.1	0.05

CHAPTER 5

Adaptation of *Akkermansia muciniphila* to the oxic–anoxic interface of the mucus layer

Kees C.H. van der Ark*, Janneke P. Ouwerkerk*, Mark Davids, Nico J Claassens, Teresa Robert Finestra, Willem M. de Vos and Clara Belzer

(*) Contributed equally

This chapter was previously published as:

Adaptation of Akkermansia muciniphila to the oxic-anoxic interface of the mucus layer, *Applied And Environmental Microbiology*, 2016, 82:23 11 6983-6993, Ouwerkerk, J.P.*, **van der Ark, K.C.***, Davids, M., Claassens, N.J., Robert Finestra, T., de Vos, W.M., and Belzer, C.

Abstract

Akkermansia muciniphila colonizes the mucus layer of the gastrointestinal tract where the organism can be exposed to the oxygen that diffuses from epithelial cells. To understand how *A. muciniphila* is able to survive and grow at this oxic-anoxic interface, its oxygen tolerance, response and reduction capacities were studied. *A. muciniphila* was found to be oxygen-tolerant. On top of this, under aerated conditions, *A. muciniphila* showed significant oxygen reduction capacities and its growth rate and yield were increased as compared to strict anaerobic conditions. Transcriptome analysis revealed an initial oxygen stress response upon exposure to oxygen. Hereafter, genes related to respiration were expressed, including those coding for the cytochrome bd complex, which can function as terminal oxidase. The functionality of *A. muciniphila* cytochrome bd genes was proven by successfully complementing the cytochrome-deficient *Escherichia coli* strain ECOM4. We conclude that *A. muciniphila* can use oxygen when present at nanomolar concentrations.

Introduction

The gastrointestinal (GI) tract harbors a rich and diverse microbial community, which has proven to play a role in host health and physiology (Flint, et al., 2012). This microbial community is not in direct contact with epithelial cells, in between is a thin layer of host-derived mucus. The outer layer of mucus is colonized with microbes that differ in composition from the luminal microbiota (Swidsinski, et al., 2002, Zoetendal, et al., 2002). The mucin glycans are used by some bacteria as growth substrates resulting in the production of short chain fatty acids (SCFAs) (Manach, et al., 2004). To the host the SCFAs are important modulators of gut health (Manach, et al., 2004). To the microbial community SCFAs are a necessary waste product, the production process of SCFAs is required to maintain the redox balance in the cell, as it can restore the NAD^+/NADH ratio (van Hoek and Merks, 2012).

One member of the mucosa-associated microbiota is *Akkermansia muciniphila*, a mucin-degrading specialist that can use mucin as sole carbon and nitrogen source (Derrien, et al., 2004). *A. muciniphila* is associated with a healthy GI tract as its abundance is inversely correlated with several GI tract related disorders (Belzer and de Vos, 2012). Moreover, it has been shown that *A. muciniphila* has immune-stimulatory capacities, stimulates host mucin production, increases the mucus layer thickness (Derrien, et al., 2004, Derrien, et al., 2011, Everard, et al., 2013, Reunanen, et al., 2015), and possibly strengthens the intestinal barrier function (Derrien, et al., 2011, Shin, et al., 2014). On top of this a causal role between *A. muciniphila* in the protection against high-fat-diet-induced obesity in mice was reported (Everard, et al., 2013) and its abundance has been identified as potential prognostic marker for predicting the success of dietary interventions for diabetes (Dao, et al., 2015).

A. muciniphila was initially described as a strict anaerobe (Derrien, et al., 2004). However more recently, it was reported that *A. muciniphila* can tolerate low amounts of oxygen (Reunanen, et al., 2015). The oxygen that diffuses from the gastrointestinal epithelial cells is thought to be one of the factors that keep strictly anaerobic commensal microbiota at a distance (Van den Abbeele, et al., 2011, Khan, et al., 2012). However, several mucosa-associated bacteria have developed strategies to cope with low levels of oxygen (Espey, 2013).

Many microorganisms have to build up mechanisms to protect themselves against oxidative stress, with enzymes such as catalase and superoxide dismutase, small proteins like thioredoxin and glutaredoxin, and molecules such as glutathione (Cabiscol, et al., 2000). Some molecules are constitutively present and help to maintain an intracellular reducing environment or to scavenge chemically reactive oxygen species (ROS). Among these molecules are non-enzymatic antioxidants such as NADPH and NADH. However, enzymes such as superoxide dismutases (SOD), catalases and hydroperoxidases are under transcriptional regulation and can decrease the steady-state levels of ROS.

Since the adaptation of *A. muciniphila* to the oxygen levels in the mucus layer has not been studied, we used an integrated physiological, genetic and biochemical approach to characterize the oxygen response of this mucosal symbiont. Herein we show that *A. muciniphila* is able to survive and grow at nanomolar levels of oxygen, exposes a complex transcriptional response to oxygen, and contains a functional cytochrome bd complex that could be used as terminal oxidase.

Materials and methods

Growth conditions *A. muciniphila*

A. muciniphila Muc^T (CIP 107961^T) was grown in a bicarbonate-buffered basal medium (Derrien, et al., 2004) with a pH of 6.5-7.0, supplemented with 0.5% (w/v) hog gastric mucin (Type III; Sigma-Aldrich, St. Louis, MO, USA), as described previously (Miller and Hoskins, 1981). On plates, *A. muciniphila* was grown on the same mucin-based medium supplemented with 0.8% agar (Oxoid, Baringstoke, UK) further referred to as mucin-based plates (Derrien, et al., 2004). The correlation of optical density at 600 nm (OD600) to counted colony-forming units (CFU) on plates was determined to be $4.0x10^8$ CFU per ml for an OD600 of 1.0.

Oxygen survival and tube experiment

A fully-grown culture was exposed to ambient air and incubated at 37˚C while shaking. Survival rate was determined in fourfold over a period of 48 hours. Series of 10-fold dilutions were made and 2 µl of each dilution was spotted on mucin-based plates.

To test for growth at different oxygen concentrations, gas tube experiments were performed, essentially as described previously (Khan, et al., 2012). For this purpose a 1% inoculum of a

mucin-grown culture was mixed with 20 ml of either molten mucin- based medium supplemented with 0.8% agar (~40 °C). Medium was poured into glass tubes under strict anaerobic conditions and sealed with a metal cap trough which ambient air could diffuse. Hereafter, the tubes were placed in ambient air. The oxygen penetration was measured by the pink-to-colorless turning point of the resazurin color indicator (Sigma-Aldrich) while growth was observed by the turbidity in the tube. The experiments were repeated at leas 3 times.

Fermentor growth of *A. muciniphila*

Bacterial cultures were grown in two parallel 1.2 l fermentors (Bio Console ADI1025 and Bio Controller ADI 1010, Applikon Biotechnology B.V., Delft, The Netherlands) using 0.67 l medium. The pH was controlled at 7.2, stirring at 50 rpm, initial gas flow N_2/CO_2 (80/20%) of 2 l/h, and the temperature was set at 37˚C. The mucin-medium used was slightly altered replacing the phosphate buffer with a 40mM MOPS buffer (Carl Roth Gmbh, Karlsruhe, Germany), and supplemented with 0.25% hog gastric mucin (Type III; Sigma-Aldrich, St. Louis, MO, USA) as sole carbon and nitrogen source (Plugge, 2005). Hereafter, the medium was sparged with N_2/CO_2 to remove all oxygen from the medium. A 0.2 l/h gas flow of ambient air was applied to the medium to measure the oxygen uptake rate of the medium without *A. muciniphila*, after which the medium was made anaerobic again using N_2/CO_2 at 2 l/h. A 1% *A. muciniphila* inoculum was used to inoculate the fermentors after which growth was monitored by measuring the OD600 over a period of 27 h. At an optical density of 0.1, one of the fermentors was switched to 0.2 l/h of ambient airflow while the other remained under 2 l/h N_2/CO_2 flow. Samples for transcriptome and metabolic analyses were taken as described below.

To determine heme dependent oxygen reduction, *A. muciniphila* was grown in a heme deprived synthetic medium using five parallel fermentors (Dasgip-Eppendorf). Hemin (Sigma Aldrich) was added in three fermentors at a concentration of 2ug/ml. Oxygen was introduced at 0.2 l/h at an OD600 of 1 to one fermentor with hemin containing medium and to one fermentor with hemin deprived medium. The remaining fermentors were used as controls.

Metabolic analysis

To determine the production of metabolites, 1.5 ml of bacterial cultures were centrifuged and the supernatant was stored at −20°C. Short Chain Fatty Acids (SCFAs) were determined by

High-Performance Liquid Chromatography (HPLC) as previously described (van Gelder, et al., 2012). Total protein concentrations were determined by Pierce BCA protein assay kit (Thermo Scientific, Rockford, USA) and Qubit® (Life Technologies, Eugene, USA) according to manufacturer's protocols. The concentration of proteins determined to be 32 mg/l at an OD600 of 0.1. Metabolic data were analyzed with the student t-test and the Mann-Whitney test. Two-tailed *P* values of <0.05 were considered statistically significant.

RNA sequencing and transcriptome analysis

Cells were collected under N_2 flow, and immediately centrifuged (4,800 Xg, 5 min, 4°C). Cell pellets were directly suspended into Trizol® Reagent (Ambion, Life Technologies, Carlsbad, CA, USA) and stored at −80°C until RNA was purified.

Total RNA was isolated by a method combining the Trizol® Reagent and the RNeasy Mini kit (QIAGEN GmbH, Hilden, Germany), essentially as described previously (Chomczynski, 1993, Zoetendal, et al., 2006). Genomic DNA was removed by on-column DNase digestion step during RNA purification (DNase I recombinant, RNase-free, Roche Diagnostics GmbH, Mannheim, Germany). Yield and RNA quality were assessed using the Experion™ RNA StdSens Analysis Kit in combination with the Experion™ System (Bio-Rad Laboratories, Inc., Hercules, CA, USA). Depletion of rRNA was performed using the Ribo-Zero™ Kit for bacteria (Epicentre, Madison, WI, USA) according to manufacturer's instructions. The success of the rRNA depletion step was checked using the Experion™ RNA StdSens Analysis Kit in combination with the Experion™ System. Library construction for whole-transcriptome sequencing (RNA-Seq) was done by ScriptSeq™ v2 RNA-Seq Library Preparation Kit in combination with ScriptSeq™ Index PCR primers (Epicentre, Madison, WI, USA) according to the manufacturer's instructions.

The barcoded cDNA libraries were sent to BaseClear (Leiden, The Netherlands), where they were pooled and 50 bp sequencing (single end reads) was performed on two lanes using the Illumina HiSeq2500 platform in combination with the TruSeq Rapid SBS and TruSeq Rapid SR Cluster Kits (Illumina, San Diego, USA).

Reads were mapped to the genome of *A. muciniphila* with Bowtie2 v2.2.1 (Langmead and Salzberg, 2012) using default settings and BAM files were converted with SAMtools v0.1.19 (Li, et al., 2009). BEDTools v2.17.0 was used to determine the read count for each protein-

coding region (Quinlan and Hall, 2010). Only reads with a minimum 30% length overlap and mapped on the correct strand were counted. Differential gene expression was assessed using edgeR (Robinson, et al., 2010) with default trimmed mean of M-values (TMM) settings. Sequences have been deposited under ArrayExpress accession E-MTAB-5111.

Cloning of *A. muciniphila* cytochrome bd

The cytochrome bd genes (Amuc_1694 and Amuc_1695) were amplified from genomic DNA using the following primers: Rev_1694 AGATCACTCGAGAAAGGATCCTCAGTAACTGTGTTCGTTGAGCTGGA and FW_1695 TGAACTAGATCTTTTAAGAAGGAGATATACATATGGACGATCCGGTCTTATTAT CCC. The PCR reaction was done with Phusion polymerase (Thermo Scientific, Waltham, MA, USA). The PCR reaction conditions were as follows: denaturation at 96°C for 5 min followed by 35 cycles of a denaturation step at 96°C for 10s, an annealing step at 59°C for 30 s and an extension step at 72°C for 1 min, and one final extension step at 72°C for 8 min. The PCR product was cloned into plasmid pBbA5c (Addgene plasmid #35281) containing an IPTG-inducible PlacUV5 promoter, a terminator, p15a origin of replication and a chloramphenicol resistance marker (Lee, et al., 2011). For this purpose, the PCR product and the destination vector were digested with BglII and XhoI (FastDigest, Thermo Scientific, Waltham, MA, USA) after which they were ligated with T4 ligase (Thermo Scientific, Waltham, MA, USA) overnight at 15˚C. 2 µl of the ligation mixture was used directly to transform *Escherichia coli* NEB5α (New England Biolabs, Ipswich, MA, USA) chemical competent cells according to manufacturer's instructions. Transformants were selected on plates with LB agar with 25 µg/ml chloramphenicol (Oxoid, Baringstoke, UK) and incubated overnight at 37˚C. The resulting vector pBbA5c-AmuCytbd was confirmed by Sanger sequencing.

Transformation of *E. coli* ECOM4

Electrocompetent cells of the cytochrome deficient, kanamycin resistant *E. coli* ECOM4 (Portnoy, et al., 2010), kindly provided by Prof. Bernhard Ø. Palsson, were prepared by inoculating with 1% of an overnight *E. coli* ECOM4 pre-culture (OD600 of 0.6-0.7) in 1 l M9 medium (Sigma-Aldrich Chemie, Steinheim, Germany) with 25 µg/l kanamycin (Carl Roth Gmbh, Karlsruhe, Germany) and grown at 37˚C shaking at 180 rpm until exponential

phase (OD600 of 0.3-0.4). The bacterial culture was cooled down on ice for 15 min and centrifuged (5,000 Xg, 15 min, 4˚C); cells were washed twice with 400 ml of cold demi-water, once with 10 ml of icecold 10% (v/v) glycerol and resuspended in 2 ml of 10% glycerol. Finally, 80 µl aliquots were prepared and stored at -80˚C for later transformation.

Competent *E. coli* ECOM4 cells were transformed with pBbA5c-AmuCytbd using electroporation in a 2mm electroporation cuvette at the following settings: 2500 V, 200 Ω and 25 µF (ECM630 Precision Pulse, Harvard Apparatus, Inc., Holliston, USA). Immediately after, 1 ml of SOC medium (0.5 g/l NaCl, 20g/l tryptone, 5 g/l yeast extract, 2.5 ml/l KCl, 2.03 g/l $MgCl_2 \cdot 6H_2O$), 3.60 g/l glucose) was added and cells were recovered for 1 hour at 37˚C. The transformed cells were then plated on LB agar plates with appropriate antibiotics (20 µg/ml kanamycin and 25 µg/ml chloramphenicol). to select for ECOM4-AmuCytbd cells

Growth of *E. coli* ECOM4-AmuCytbd and metabolic profiling

E. coli ECOM4 and ECOM4-AmuCytbd strains were grown on M9 medium (Sigma-Aldrich Chemie, Steinheim, Germany) with 20 µg/ml kanamycin and 25 µg/ml chloramphenicol, at 37˚C while shaking at 180 rpm. For metabolic analysis, cells were grown in pre-cultured, after which equal cell amounts were inoculated in M9 medium containing 18 mM glucose, either induced with the tested optimal concentration (data not shown) of 25 µM IPTG (Fischer Scientific, Fair Lawn, USA), or without inducer. Samples were taken over a period of 50 h, growth was determined measuring optical density (OD600) and HPLC analysis was done as described for *A. muciniphila* samples.

Spectra of cytochrome bd

Erlenmeyer flasks containing 500 ml M9 medium were inoculated with *E. coli* ECOM4 and *E. coli* ECOM4-Amucytbd with and without IPTG. Cells were collected at the end of the exponential phase by centrifugation (4,800 Xg, 10 min). *A. muciniphila* cells were grown in 200mL cultures in anaerobic bottles. Pellets of *E. coli* ECOM4 (Amucytbd) and *A. muciniphila* were dissolved in 1 ml lysis buffer (50 mM Tris-HCl pH 8, 1 mM EDTA, 150 mM NaCl, 1mM DDT, 0.5 mM PMSF, 1% dodecylmaltoside) and lysed by 2 passages through a French press (SPHC, Stansted Fluid Power Ltd, Essex, UK) at 16.000 psi or 4 times 30 seconds sonication at output 3.5. Cell debris was removed by centrifugation (10,500 Xg, 10 min). Spectra were measured by UV-2501PC (Shimadzu corporation, Kyoto, Japan) at 380-700 nm and solutions were reduced using 50 mM sodium dithionite.

Results

Oxygen tolerance and oxygen reduction of *A. muciniphila*

To test oxygen tolerance, survival of *A. muciniphila* cells was measured after exposure to ambient air. Based on CFU counts, *A. muciniphila* cells were able to survive up to 48 hours in ambient air. The viability had dropped to 25% after 24 hours and was only 1% after 48 hours (Figure 1A). To test the oxygen reduction capacity of *A. muciniphila*, the penetration depth of oxygen was measured in a gas tube assay based on the turning point of a redox indicator (resazurin). The oxygenated zone was deeper in non-inoculated tubes (10.0 ± 1.0 mm) compared to the tubes where *A. muciniphila* was growing (5.0 ± 1.0 mm) (Figure 1B).

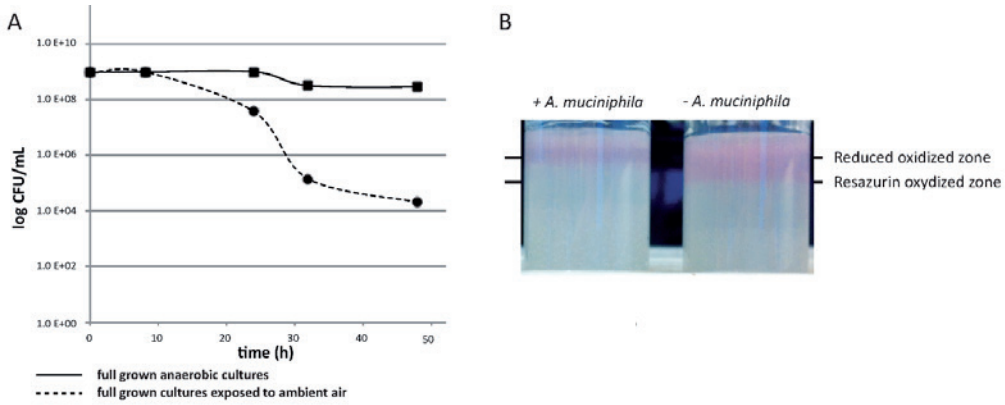

Figure 1. (A) Survival of *A. muciniphila* after exposure to oxygen over time. 1% of survival was measured during 48 hours exposure to ambient air (---) while in anaerobic cultures were still >90% were viable ( ). Points depict the average of 4 replicates. B) Growth of *A. muciniphila* in the tube assay. Left a control tube. Right an *A. muciniphila* inoculated tube. The lowest line indicates the resazurin oxidized zone in the control tube, the upper line indicates the reduced oxidized zone in the tube where *A. muciniphila* was growing A representative picture of 4 repeats is shown.

A. muciniphila shows enhanced growth under aerated conditions

The growth of *A. muciniphila* at aerated conditions was investigated in a fermentor system controlled for temperature and pH. Both dissolved oxygen concentration (dO2%) and redox (mV) were measured throughout the experiment. Before growing *A. muciniphila* in the fermentor system, a control fermentor (negative control) was run to measure the increase in redox potential and oxygen diffusion by switching the gas flow from an N_2 flow of 2.0 l/h to an ambient airflow of 0.2 l/h (Figure 2C). Hereafter, experiments were run in two parallel fermenters, at T1 (the beginning of the exponential phase at OD600 ≈ 0.1, grey-shaded area in Figure 2) one of the two fermentors was switched to an ambient airflow of 0.2 l/h (aerated

fermentor) and the other fermentor was kept under strict anaerobic conditions (anaerobic fermentor). At T1, the redox potential showed an increase after the introduction of ambient air (Figure 2B); this increase, however, declined and the redox potential was lowered again until *A. muciniphila* reached stationary phase pointing towards the potential use of oxygen as final electron acceptor. The oxygen concentration remained under our detection level of 0.1% dO_2 during the complete growth curve of *A. muciniphila* and only increased in stationary phase (Figure 2B).

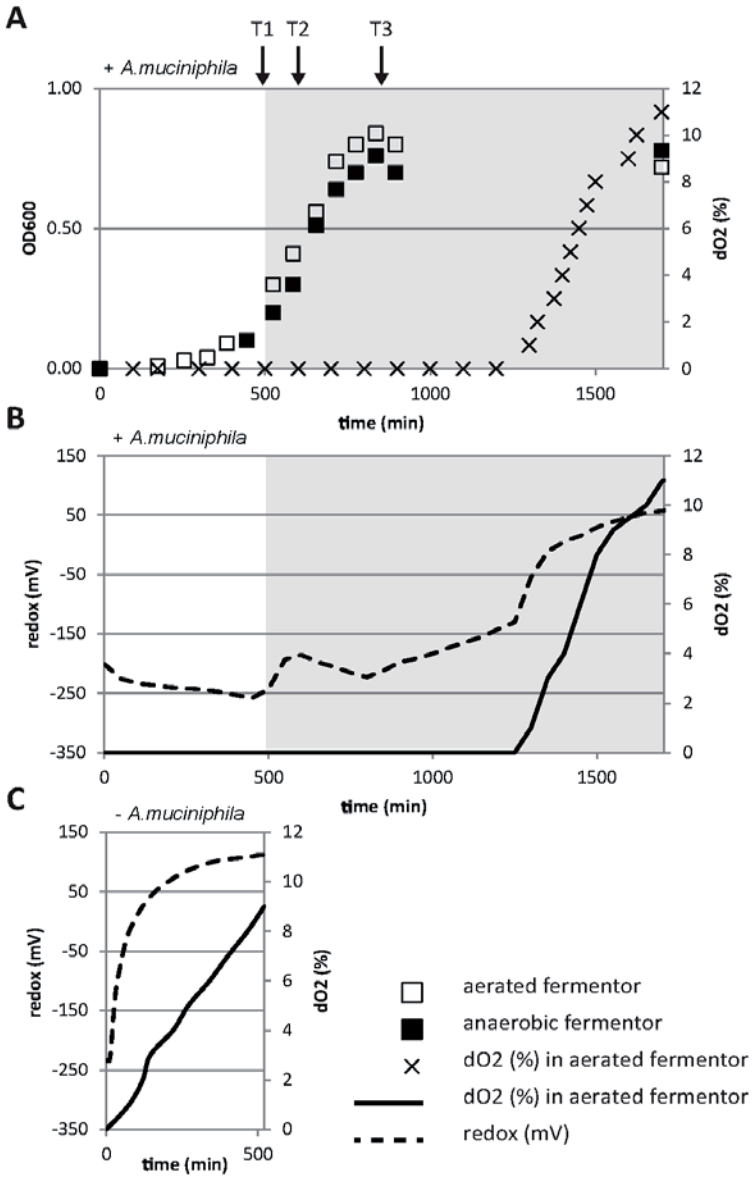

Figure 2. Growth, oxygen concentration and redox potential of *A. muciniphila* in aerated fermentor system. (A) Growth of *A. muciniphila* measured by OD600 in the aerated and anaerobic fermentor, and the dissolved oxygen concentration (dO2) in the aerated fermentor. Grey-shaded area indicates switch to ambient airflow of 0.2 l/h. (B) Redox potential (mV) (---) and the oxygen concentration (dO2%) (—) during the growth of *A. muciniphila* in the aerated fermentor. Grey-shaded area indicates switch to ambient airflow of 0.2 l/h. (C) Redox potential (mV) (---) and the oxygen concentration (dO2%) (—) of the negative control (without *A. muciniphila*). Figures show solely one experiment but are representative for all four experiments performed.

Under aerated conditions a significantly higher growth rate (*P*=0.02) and significantly higher OD600 (*P*=0.05) at the end-exponential phase were measured (Figure 3B, C). The fermentation profile of *A. muciniphila* consisted of acetate, propionate, and small amounts of 1,2-propanediol, typical for growth in mucin-based medium (Figure 3A)(38). Under aerated conditions however, the ratio of acetate to propionate was altered from 1.2 to 1.5 (*P*=0.03) (Figure 3D), suggesting an altered fermentation pathway.

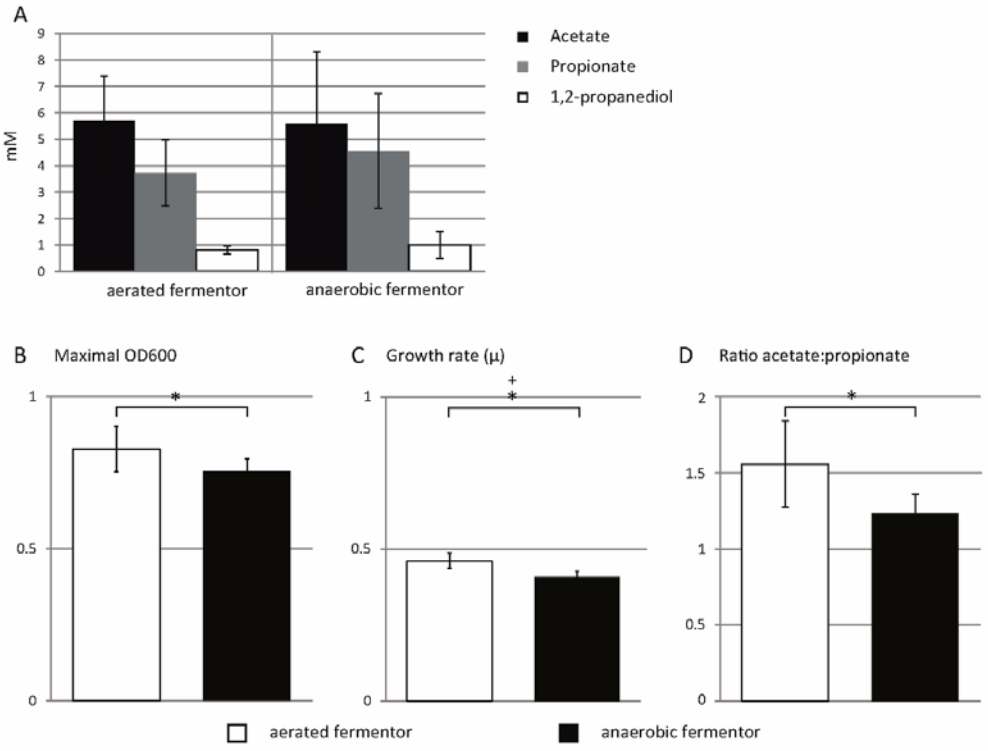

Figure 3. Growth and physiology of *A. muciniphila* in the aerated fermentor system. (A) SCFA production profile of *A. muciniphila* at stationary phase including acetate, propionate, and 1,2-propanediol. (B) Maximal OD600 reached during growth in the aerated fermentor and the anaerobic fermentor. (C) Growth rate (μ) based on the OD600 during the exponential growth phase in the aerated fermentor and the anaerobic fermentor. (D) Ratio of the production of acetate to the production of propionate per fermentor run in the aerated fermentor and the anaerobic fermentor. Bars represent the mean of n=4, error bars represent the standard deviation (SD). (*) Indicates significant difference using the two-tailed student T-test. B p=0.05; C p=0.02; D p=0.03. (+) Indicates significant using the one-tailed Mann-Whitney Test (p=0.03).

The minimal oxygen-reducing capacity of *A. muciniphila* under the given fermentor conditions was calculated based on the oxygen uptake rate in the negative control and the protein concentration of *A. muciniphila* cultures. The increase in oxygen concentration of the

negative control was calculated to be 69.4±31.9 mU/l (mU is defined as nanomole substrate per minute). This calculation is based on the difference between the increase in oxygen concentration of the negative control (dO2% in Figure 2C) and the increase in oxygen concentration of the *A. muciniphila* grown fermentor (dO2% in Figure 2B) for all four experiments. The oxygen reduction capacity of *A. muciniphila* was determined to be 2.26±0.99 mU/mg total protein (n=4).

Initial transcriptional response of *A. muciniphila* to aerated conditions is dominated by oxygen stress response

The transcriptome of *A. muciniphila* was determined by RNAseq analysis for both aerated and anaerobic fermentor conditions at the beginning of exponential phase (before aeration) (T1), during mid-exponential phase (T2), and at end-exponential phase of growth (T3) (black arrows in Figure 2A). All genes that differed significantly between the conditions can be found in Table S1. At T1 (before aeration) both parallel fermentors had identical gene expression profiles (Figure 4A). Comparing the aerated to the non-aerated fermentor at T2 (mid-exponential) resulted in 38 genes that were expressed significantly different (Figure 4B). During this initial transcriptional response a total of 26 genes were significantly upregulated due to the presence of oxygen. Only 18 of the genes are annotated of which 6 were annotated as potential oxygen stress related genes: superoxide dismutase; hydroperoxidase; entericidin EcnAB, homologous to the EcnAB of *E. coli* that is involved in the stress response (Bishop, et al., 1998); rubrerythrin, previously implied in the protection from oxidative damage in sulfate-reducing bacteria (Zhou, et al., 2011); excinuclease, controlling for potential ROS-mediated DNA damage; and a family 2 glycosyl transferase, part of the capsular polysaccharide biosynthesis pathway upregulated to potentially protect the cells against the presence of oxygen (Table 1). Also one potential oxidoreductase, and six genes that are broadly categorized as potential growth phase dependent were significantly upregulated (Table 1). Twelve genes were significantly downregulated under aerated conditions. Five of these genes encode for the assimilatory sulfate reduction pathway (Figure 4B, Table 1). The expression of the oxygen stress-related genes, after the initial oxygen response, was assessed by comparing the aerated fermentor at T2 and T3. The expression of these genes did not further increase significantly, except for hydroperoxidase (Table S1).

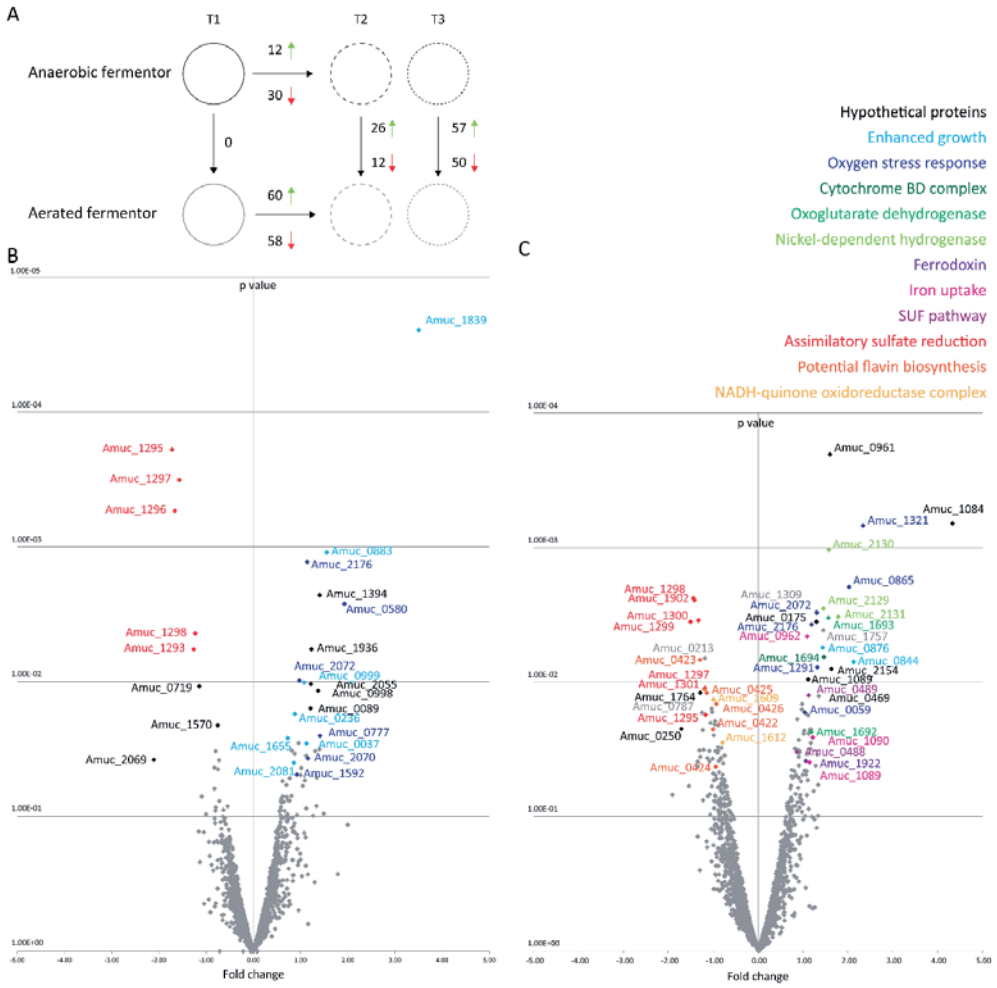

Figure 4. Differentially expressed genes of *A. muciniphila* under aerated conditions. (A) Schematic representation of the significant differentially expressed genes between aerated and non-aerated conditions at the different time points. A red arrow indicate downregulated genes, a green indicates upregulated genes. (B) Volcano plot of the aerated fermentor versus the non-aerated fermentor at T2. (C) Volcano plot of the aerated fermentor versus the non-aerated fermentor at T3. The p-values were determined using edgeR (Robinson, et al., 2010) with default trimmed mean of M-values (TMM) settings (significant differences of gene expression between all conditions can be found in Table S1).

Table 3. Oxygen responsive genes that are significant differentially expressed between aerated and non-aerated fermentor at T2 and T3. Only genes that are involved in oxygen metabolism are included in this table, all other differentially expressed genes can be found in Table S1.

Gene or pathway	Gene number	Fold change T2	Fold change T3	Potential mechanism
T2 aerated vs non aerated fermetner				
amino acid permease	**Amuc_0037**	2.19	**2.13**	**Enhanced growth**
ion transport 2 domain-containing protein	**Amuc_0236**	1.84	**0.79**	**Enhanced growth**
Entericidin EcnAB	**Amuc_0580**	3.82	**0.94**	**Response to starvation conditions**
short-chain dehydrogenase/reductase SDR	**Amuc_0777**	2.66	**2.30**	**Oxidoreductase**
cupin barrel domain containing protein	**Amuc_0883**	1.08	**1.96**	**Enhanced growth**
sigma 54 modulation protein/ribosomal protein S30EA	**Amuc_0999**	2.11	**1.33**	**Enhanced growth**
superoxide dismutase	**Amuc_1592**	1.90	**1.22**	**$2\ O^- + 2\ H+ \rightarrow H2O2$**
sulfatase	**Amuc_1655**	1.66	**0.54**	**Sulfate cleavage from mucin protein for enhanced growth**
heavy metal translocating P-type ATPase	**Amuc_1839**	11.39	**1.68**	**Enhanced growth**
hydroperoxidase	**Amuc_2070**	2.23	**1.90**	**$2\ H2O2 \rightarrow 2\ H2O + O2$**
rubrerythrin	**Amuc_2072**	1.97	**2.48**	**Stress response**
family 2 glycosyl transferase	**Amuc_2081**	1.81	**1.18**	**Capsular polysaccharide biosynthesis pathway upregulated potentially to protect against the oxygen presence**
excinuclease	**Amuc_2176**	2.21	**2.29**	**To control for potential ROS mediated DNA damage**

Assimilatory sulfate reduction (Amuc_1294 - Amuc_1301)	**Amuc_1293**	-2.40	**-1.35**	**Not functional due to high redox potential**
	Amuc_1295	-3.30	**-2.25**	
	Amuc_1296	-3.17	**-1.87**	
	Amuc_1297	-2.96	**-2.27**	
	Amuc_1298	-2.35	**-2.67**	
T3 aerated vs non-aerated fermentor				
Suf pathway (Amuc_0486 - Amuc_0489)	**Amuc_0488**	**1.20**	1.82	**Iron uptake [Fe-S]**
	Amuc_0489	**1.17**	2.18	
oxoglutarate dehydrogenase (Amuc_1692 - Amuc_1693)	**Amuc_1692**	**1.61**	2.28	**Potential read-trough of transcript**
	Amuc_1693	**1.65**	2.96	
cytochrome bd complex (Amuc_1694 - Amuc_1695)	**Amuc_1694**	**0.91**	2.77	**Aerobic respiration**
Feo iron transporter (Amuc_1089 - Amuc_1090)	**Amuc_1089**	**0.88**	2.22	**Iron uptake**
	Amuc_1090	**0.75**	2.33	
nickel-dependent hydrogenase (Amuc_2128 - Amuc_2132)	**Amuc_2129**	**1.41**	2.74	**Oxygen tolerant hydrogenase that might use the H2 present at its ecological niche**
	Amuc_2130	**1.32**	2.98	
	Amuc_2131	**1.78**	3.46	
ATPase AAA	**Amuc_0059**	**1.26**	2.05	**UvrB/UvrC protein; ATPase binding domain; part of NER. To control for potential ROS mediated DNA damage**
Phosphopyruvate hydratase	**Amuc_0844**	**2.65**	4.37	**Involved in glycolysis, enhanced growth**

heavy metal translocating P-type ATPase	**Amuc_0876**	**1.63**	2.72	**Enhanced growth**
alkyl hydroperoxide reductase	**Amuc_1321**	**1.25**	5.06	**ROS scavenger**
ferodoxin	**Amuc_1922**	**1.01**	2.09	**Iron uptake**
rubrerythrin	**Amuc_2072**	**1.97**	2.48	**Stress response**
excinuclease	**Amuc_2176**	**2.21**	2.29	**To control for potential ROS mediated DNA damage**
Potential flavin biosynthesis (Amuc_0421 - Amuc_1426)	**Amuc_0422**	**-1.15**	-2.00	**Electron sink**
	Amuc_0423	**-1.51**	-2.45	
	Amuc_0424	**-1.26**	-1.92	
	Amuc_0425	**-1.08**	-2.20	
	Amuc_0426	**-1.40**	-1.91	
Assimilatory sulfate reduction (Amuc_1294 - Amuc_1301)	**Amuc_1295**	**-3.30**	-2.25	**Redox to high to be functional**
	Amuc_1297	**-2.96**	-2.27	
	Amuc_1298	**-2.35**	-2.67	
	Amuc_1299	**-1.74**	-2.83	
	Amuc_1300	**-1.51**	-2.51	
	Amuc_1301	**-1.05**	-2.28	
NADH-quinone oxidoreductase complex (Amuc_1604 - Amuc_1614)	**Amuc_1609**	**-1.28**	-1.98	**Not essential in the electron transport from NADH to oxygen in a mutant E. coli strain**
	Amuc_1612	**-1.14**	-1.72	
Menaquinone pathway	**Amuc_1017**	**-1.56**	-2.43	**Menaquinone pathway**

End-exponential transcriptional response of *A. muciniphila* to aerated conditions points towards respiration using cytochrome bd as terminal oxidase

Comparing the aerated to the non-aerated fermentor at T3 (end-exponential) resulted in 107 significantly altered genes (Figure 4C, Table S1). During this end-exponential transcriptional response, a total of 57 genes were significantly upregulated under aerated conditions. As well as at T2 a series of oxygen stress related genes was upregulated (Figure 4C, Table 1). Three major gene clusters were significantly upregulated under aerated conditions: (i) a cluster involved in iron transport including the Feo iron transporters; (ii) a respiratory gene cluster including oxoglutarate dehydrogenase subunits and its adjacent gene cytochrome d ubiquinol oxidase subunit II, and (iii) a nickel-dependent hydrogenase cluster, from which 3 out of 5 genes were significantly oxygen induced, pointing towards the use of cytochrome bd as terminal oxidase. The cytochrome bd ubiquinol oxidase subunit I, although abundantly present in the transcriptome, showed no transcriptional induction by oxygen. However, when comparing the expression of the cytochrome bd subunits in the aerated fermentor at T2 and T3, we see that both subunits have an increased expression over time in aerated conditions (Table S1). At T3, both the SUF pathway, and the ferredoxin gene were significantly upregulated and are potentially involved in electron transfer. In addition, two genes broadly categorized as potential growth phase dependent genes were significantly upregulated under aerated conditions (Figure 4C, Table 1). A total of 50 genes were significantly downregulated under aerated conditions (Table S1) and included the following 3 major gene clusters: (i) the assimilatory sulfate reduction, (ii) the potential flavin biosynthesis, and (iii) the NADH-quinone oxidoreductase complex (Figure 4C, Table 1).

Cytochrome bd genes of *A. muciniphila* restore respiration in the cytochrome-deficient mutant *Escherichia coli* ECOM4

Under aerated conditions *A. muciniphila* showed both slightly increased growth (Figure 3) and oxygen reduction capacities of 2.26±0.99 mU/mg total protein, pointing towards the potential use of oxygen as final electron acceptor. Moreover, the *A. muciniphila* genome contains the genes for cytochrome bd subunits I (Amuc_1695) and II (Amuc_1694) and the gene coding for subunit II was significantly upregulated under aerated conditions (Figure 4). To test if the *A. muciniphila* cytochrome bd genes encode a functional cytochrome bd complex that can be used for respiration, we complemented the cytochrome-deficient *E. coli*

ECOM4 with the pBbA5c-AmuCytbd expressing the genes for cytochrome bd subunits I (Amuc_1695) and II (Amuc_1694) of *A. muciniphila*, resulting in strain ECOM4-AmuCytbd. As previously shown by Portnoy et al. (Portnoy, et al., 2010), there was no production of acetate by the cytochrome-deficient *E. coli* ECOM4 under oxic conditions, in contrast to the parental strain *E. coli* MG1655, which produces ample amounts of acetate (Portnoy, et al., 2010). However, in the strain ECOM4-amuCytbd, expressing the *A. muciniphila* cytochrome bd genes, the acetate production is partly restored upon induction with IPTG (3.2 ± 0.8 mM) and slightly lower without induction (2.2 ± 0.4 mM) (Table 2). Moreover, the growth yield increased from an OD600 of 0.18 ± 0.04 to 0.43 ± 0.03 in this complemented strain (Table 2).

Table 4. Acetate production of ECOM4-AmuCytbd, ECOM4 and wild type *E. col*i MG1655. A negative control of M9 medium without bacteria was included (-). Values represent mean (SD), n=3. Data with different superscript letters are significantly different are significantly different using 2-tailed student t-test.

Strain	**ECOM4-AmuCytbd**		**ECOM4**
IPTG concentration	**25 µM**	**0 µM**	**25 µM**
Acetate (mM)	3.3 (0.8)[a]	2.2 (0.4)[a]	0.0 (0.0)[b]
Yield (OD600)	0.4 (0.0)[c]	0.4 (0.0)[c]	0.2 (0.0)[d]

Cytochrome bd is present and functional in *A. muciniphila*

Finally, the presence of the cytochrome bd complex of *A. muciniphila* was confirmed by spectra showing a small peak at 560 nm, and a larger peak at 430nm, indicating the presence of cytochromes (Figure 5A). The presence of the cytochrome bd complex in the complemented strain ECOM4-AmuCytbd was confirmed using an spectrum measurement that showed a major peak at 430nm, which is in line with the Soret peak of cytochrome bd (Figure 5B), as previously described (Borisov, 2008, Bloch, et al., 2009). To determine if the oxygen reduction was heme and thus cytochrome bd dependent, three parallel fermentors containing medium with and without hemin were used. Without bacteria, there was no difference observed in dO% between a fermentor with heme and a fermentor without heme (10.5±0.2 %). In the presence of *A. muciniphila* without hemin, the oxygen concentration reached an average saturation of 1.1±0.2% in the first 400min of aeration. With hemin, the same amount of cells was able to directly and completely reduce the oxygen, preventing accumulation of oxygen in the system. The saturation remained constant at 0.1±0.0% (Figure S3).

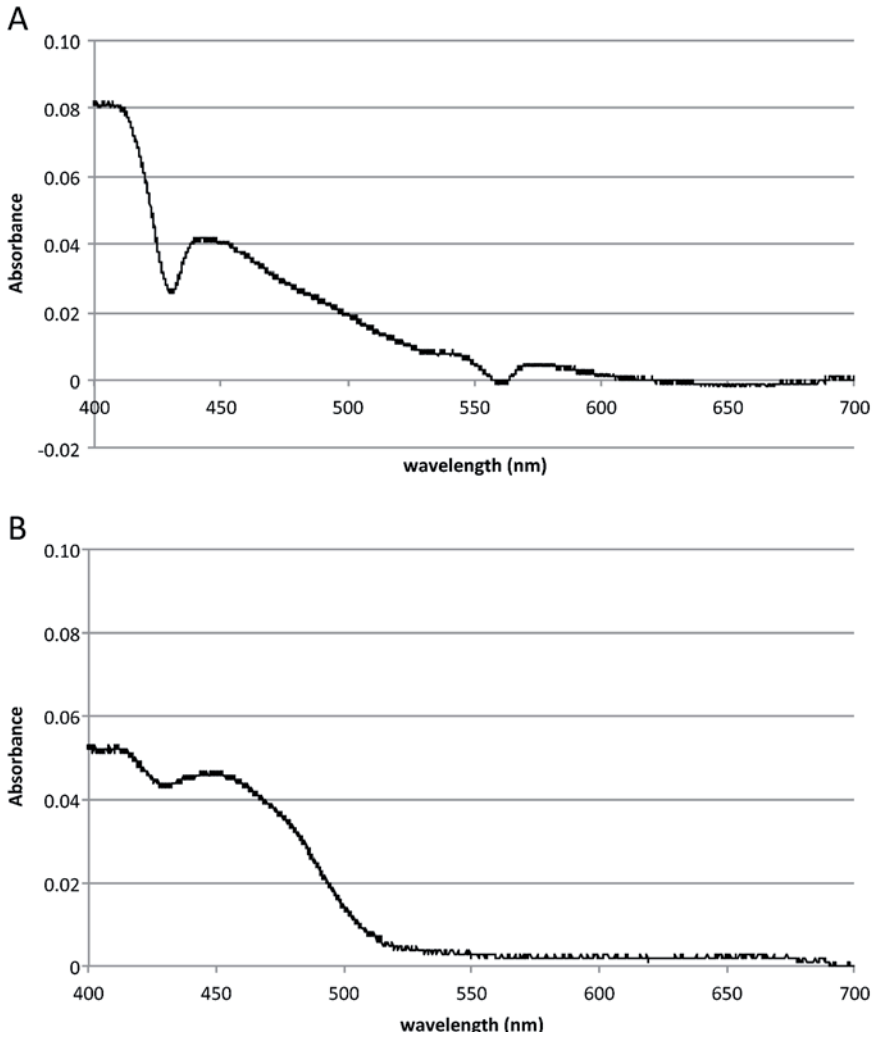

Figure 5. Cytochrome bd complex of *A. muciniphila*. (A) Spectrum of *A. muciniphila* cell free extract. Spectrum shows the oxidized spectrum minus the dithionate-reduced spectrum. (B) Spectrum of *E. coli* ECOM4-AmuCytbd cell free extract minus the ECOM4 cell free extract spectrum. The baseline is set for absorbance at 700 nm. Both spectra show a similar pattern at 430nm.

Discussion

A. muciniphila is known to colonize the oxic-anoxic interface of the mucus layer. Using an integrated physiological, genetic and transcriptomic approach the oxygen response of *A. muciniphila* was addressed and shown to be highly complex, effective, and to involve a functional respiratory complex. Analysis of the global transcriptional response identified 137 genes involved in the reaction to oxygen and other formed ROS (Table S1). This could testify for an adaptation of *A. muciniphila* to continuous exposure to these products in its natural habitat. Moreover, we also observed the effective use of oxygen in a rudimentary respiratory chain involving a cytrochrome bd complex, indicating that *A. muciniphila* is capable of competing with other strict anaerobes that may colonize the mucosal layer.

The oxygen survival of *A. muciniphila* is in line with anaerobic gut colonizers such as *Bacteroides fragilis* and *Bifidobacterium adolescentis*, which were still viable after 48 hours of ambient air exposure (Rolfe, et al., 1978). As previously described for gut colonizers *Faecalibacterium prausnitzii* (Khan, et al., 2012) and *B. fragilis* (Baughn and Malamy, 2004), *A. muciniphila* had enhanced growth at the oxic-anoxic interphase as shown in the gas tube assay (Figure 1B). The presence of riboflavin or other vitamins did not affect the observed growth ring (data not shown). Therefore, a riboflavin dependent extracellular electron shuttle as was proposed for the enhanced growth *F. prausnitzii* at the oxic-anoxic interface, is probably not present in *A. muciniphila*. For *B. fragilis* cytochrome bd oxidase was shown to be essential for growth at nanomolar oxygen concentrations (Baughn and Malamy, 2004). The genes for cytochrome bd subunits I (Amuc_1695) and II (Amuc_1694) are present in *A. muciniphila* and we confirmed their presence by spectral measurements. We also showed the functional relevance of the cytochrome bd complex by the lower oxygen reduction capacity in heme-deprived medium. The bacteria were only able to fully reduce the oxygen when heme was supplemented. Evolutionary, the *A. muciniphila* cytochrome bd genes are closest related to that of some aerobic members of the Verrucomicrobia, including *Verrucomicrobium spinosum*, and *Opitutus tarae*. The presence of the cytochrome bd genes in *A. muciniphila* might therefore be conserved during adaptation to the intestinal environment.

Apart from oxygen tolerance, the oxygen reduction capacity of *A. muciniphila* was demonstrated in the gas tube assay, and quantified in the fermentor system to be at least 2.26

mU/mg total protein. This lower limit of oxygen conversion capacity of *A. muciniphila* is less than previously characterized anaerobic bacteria that employ the cytochrome bd, including *B. fragilis* (9 nmole/min/mg total protein) and *Moorella thermoacetica* (29.8 nmole/min/mg protein) (Baughn and Malamy, 2004, Das, et al., 2005). However, *A. muciniphila* is clearly able to reduce nanomolar concentrations of oxygen. Given the actual concentrations of oxygen in the mucus layer, which has been estimated to be 15 mmHg (~210 nM) (Espey, 2013), we speculate that *A. muciniphila* can take advantage of these nanomolar concentrations in its ecological niche to compete with other strict anaerobes. The cytochrome bd complex was described to be essential in intestinal colonization of mice as was reported using respiratory mutants of *E. coli* (Jones, et al., 2007) and *B. fragilis* (Baughn and Malamy, 2004). Hence, it is tempting to suggest that *A. muciniphila* might need the cytochrome bd in initial colonization of its host as well.

The mechanism behind the oxygen response was investigated by analyzing the transcriptional response of *A. muciniphila* under aerated condition in the fermentor system. Two different responses to oxygen could be distinguished: the detoxification of oxygen and the use of oxygen in aerobic respiration. A variety of mechanisms could explain the upregulated and downregulated genes after aeration at both T2 (mid-exponential) and T3 (end-exponential phase) (Table 1). The detoxification of oxygen is reflected in the initial transcriptional response of *A. muciniphila*. Both superoxide dismutase (Amuc_1592), and hydroperoxidase (Amuc_2070) are upregulated to scavenge the ROS. Oxygen also induced the transcription of both rubrytrin genes of *A. muciniphila*, previously shown to be upregulated as well in the acute murine colitis model where there is an increase of ROS in the GI tract (Berry, et al., 2012). In conclusion, *A. muciniphila* harbors an arsenal of genes to detoxify oxygen that are significantly upregulated under aerated conditions. However this does not explain the observed enhanced growth and the shift towards higher acetate to propionate ratio.

The transcriptome of *A. muciniphila* at the end-exponential phase points towards the use of oxygen in aerobic respiration mediated by cytochrome bd. As the energy yield of aerobic respiration is higher than fermentation, this might be the reason for the enhanced growth we observed under aerated conditions (Figure 4) (Lechardeur, et al., 2011). The cytochrome d ubiquinol oxidase (subunit II) (Amuc_1694) was significantly upregulated, while subunit I (Amuc_1695), although abundantly present in the transcriptome, showed no transcriptional

induction by oxygen (both T2 and T3). To be functional, the cytochrome bd complex needs to be coupled to an NADH dehydrogenase to recycle its menaquinone and produce NAD^+ (Figure 6). *A. muciniphila* harbors a NADH hydrogenase complex consisting of the following 13 genes: Amuc_1604-Amuc_1614, Amuc_1551, and Amuc_2157-Amuc_2158. While the first gene cluster was downregulated under aerated conditions, the other genes were slightly (~1.5 fold) upregulated, though not significantly. Moreover, this NADH hydrogenase complex belongs to the NADH dehydrogenase type I (Baranova, et al., 2007), which has been shown not to be essential in the electron transport from NADH to oxygen in a mutant *E. coli* strain (Tran, et al., 1997). Therefore, we screened the genome for another potential NADH dehydrogenase and found that Amuc_1809 might be a candidate. Although abundantly expressed at all tested conditions, Amuc_1809 was slightly upregulated under aerated conditions at T2 (1.1 fold upregulated) and T3 (1.3 fold upregulated), not significantly. Hence, this NADH dehydrogenase might operate in conjunction with the cytochrome bd complex to use oxygen as final electron acceptor.

The enhanced growth under aerated conditions was observed together with a marginal but significant shift towards a higher acetate to propionate ratio. As cytochrome bd uses oxygen as final electron acceptor, resulting in the production of H_2O and NAD^+ (Figure 6); to maintain the NAD^+:NADH ratios, the extra NAD^+ production needs to be balanced by additional NADH regeneration. Therefore, the metabolism might shift from propionate, where net 2 NADH are oxidized to 2 NAD^+, towards acetate production, where 1 NAD^+ is reduced to 1 NADH (simplified schematic representation in Figure S2). More acetate production will lead towards more ATP production as well. As acetate is a more oxidized fermentation product, more electrons are released from pyruvate and donated to NAD^+ leading to the production of more NADH. The NADH can be oxidized and the electrons can be transferred back to oxygen via an NADH dehydrogenase, menaquinones and cytochrome bd. Due to the change in acetate to propionate ratio, more ATP and NADH can be generated, leading to a slightly increased growth rate and yield, as observed in our fermentor experiments. This was confirmed by increased growth and acetate production of ECOM4-AmuCytbd (Table 2), and its presence in *A. muciniphila* was confirmed by spectral measurements (Figure 5).

The cytochrome bd complex is likely to involve iron-containing hemes as cofactor. Both Feo iron transporters (Amuc_1089-Amuc_1090) predicted to be involved in Fe^{2+} transport were significantly upregulated under aerated conditions. This might point towards increased iron uptake to allow incorporation of the iron-containing heme cofactors in the cytochrome bd. All known members of the bd-family of oxygen reductases most commonly use ubiquinol or menaquinol as substrate (Borisov, et al., 2011). *A. muciniphila* is predicted to harbor the complete pathway to produce menaquinones (Figure S1). However, one gene (Amuc_1017) was significantly downregulated at T3 while the other 8 were not significantly altered under aeration condition.

Taken together, we showed that a subunit of cytochrome bd complex is transcriptionally induced under aerated conditions and its presence in *A. muciniphila* was confirmed by spectrum measurements. The genes for both Feo iron transporters were significantly upregulated to potentially employ the iron-consisting-heme cofactors of the cytochrome bd. The oxygen conversion capacity of *A. muciniphila* is lower compared previously characterized cytochrome bd of two other bacteria (Baughn and Malamy, 2004, Das, et al., 2005), yet it clearly possesses the ability to reduce oxygen. Finally, the functionality of the cytochrome bd complex of *A. muciniphila* was confirmed by the increased growth and the acetate production of ECOM4-AmuCytbd. On top of this *A. muciniphila* had a lower oxygen reduction capacity in absence of heme. Therefore we propose the following mechanism (Figure 6): *A. muciniphila* uses the cytochrome bd complex coupled to an unidentified NADH dehydrogenase (possible candidate Amuc_1809) to use oxygen as final electron acceptor. The use of oxygen as final electron acceptor by cytochrome bd oxidase shifts the metabolic process towards higher acetate to propionate ratio, resulting in more ATP and NADH and eventually leading to an slightly increased growth rate and yield. In its ecological niche *A. muciniphila* might use this additional energy to outcompete strict anaerobes in the mucus layer.

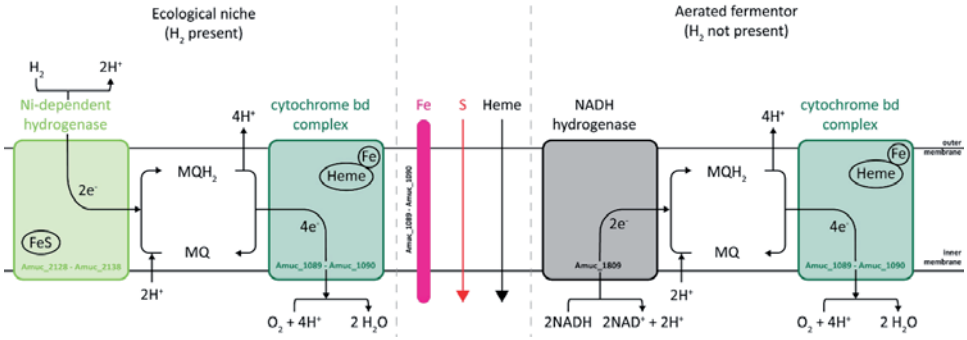

Figure 6. Schematic representation of aerobic respiration by *A. muciniphila* under nanomolar oxygen concentrations.

Acknowledgments

We are grateful to Prof. B. Ø Palsson for providing the ECOM4 strain, and to Prof. J.D. Keasling for the pBbA5c plasmid. The work was supported by ERC Advanced Grant 250172 - MicrobesInside from the European Research Council and the Netherlands Organization for Scientific Research (Spinoza Award and SIAM Gravity Grant 024.002.002) to WMdV.

References

1 Baranova, E.A., Morgan, D.J., and Sazanov, L.A. (2007) Single particle analysis confirms distal location of subunits NuoL and NuoM in *Escherichia coli* complex I, *Journal of structural biology* **159**: 238-242.

2 Baughn, A.D., and Malamy, M.H. (2004) The strict anaerobe Bacteroides fragilis grows in and benefits from nanomolar concentrations of oxygen, *Nature* **427**: 441-444.

3 Belzer, C., and de Vos, W.M. (2012) Microbes inside--from diversity to function: the case of *Akkermansia*, *The ISME journal* **6**: 1449-1458.

4 Berry, D., Schwab, C., Milinovich, G., Reichert, J., Ben Mahfoudh, K., Decker, T., et al. (2012) Phylotype-level 16S rRNA analysis reveals new bacterial indicators of health state in acute murine colitis, *The ISME journal* **6**: 2091-2106.

5 Bishop, R.E., Leskiw, B.K., Hodges, R.S., Kay, C.M., and Weiner, J.H. (1998) The entericidin locus of *Escherichia coli* and its implications for programmed bacterial cell death, *Journal of molecular biology* **280**: 583-596.

6 Bloch, D.A., Borisov, V.B., Mogi, T., and Verkhovsky, M.I. (2009) Heme/heme redox interaction and resolution of individual optical absorption spectra of the hemes in cytochrome bd from *Escherichia coli*, *Biochimica et biophysica acta* **1787**: 1246-1253.

7 Borisov, V.B. (2008) Interaction of bd-type quinol oxidase from *Escherichia coli* and carbon monoxide: heme d binds CO with high affinity, *Biochemistry (Mosc)* **73**: 14-22.

8 Borisov, V.B., Gennis, R.B., Hemp, J., and Verkhovsky, M.I. (2011) The cytochrome bd respiratory oxygen reductases, *Biochimica et biophysica acta* **1807**: 1398-1413.

9 Cabiscol, E., Tamarit, J., and Ros, J. (2000) Oxidative stress in bacteria and protein damage by reactive oxygen species, *Int Microbiol* **3**: 3-8.

10 Chomczynski, P. (1993) A reagent for the single-step simultaneous isolation of RNA, DNA and proteins from cell and tissue samples, *Biotechniques* **15**: 532-534, 536-537.

11 Dao, M.C., Everard, A., Aron-Wisnewsky, J., Sokolovska, N., Prifti, E., Verger, E.O., et al. (2015) *Akkermansia muciniphila* and improved metabolic health during a dietary intervention in obesity: relationship with gut microbiome richness and ecology, *Gut*.

12 Das, A., Silaghi-Dumitrescu, R., Ljungdahl, L.G., and Kurtz, D.M., Jr. (2005) Cytochrome bd oxidase, oxidative stress, and dioxygen tolerance of the strictly anaerobic bacterium *Moorella thermoacetica*, *Journal of bacteriology* **187**: 2020-2029.

13 Derrien, M., Van Baarlen, P., Hooiveld, G., Norin, E., Muller, M., and de Vos, W.M. (2011) Modulation of mucosal immune response, tolerance, and proliferation in mice colonized by the mucin-degrader *Akkermansia muciniphila*, *Frontiers in microbiology* **2**: 166.

14 Derrien, M., Vaughan, E.E., Plugge, C.M., and de Vos, W.M. (2004) *Akkermansia muciniphila* gen. nov., sp. nov., a human intestinal mucin-degrading bacterium, *International journal of systematic and evolutionary microbiology* **54**: 1469-1476.

15 Espey, M.G. (2013) Role of oxygen gradients in shaping redox relationships between the human intestine and its microbiota, *Free radical biology & medicine* **55**: 130-140.

16 Everard, A., Belzer, C., Geurts, L., Ouwerkerk, J.P., Druart, C., Bindels, L.B., et al. (2013) Cross-talk between Akkermansia muciniphila and intestinal epithelium controls diet-induced obesity, *Proc Natl Acad Sci U S A* **110**: 9066-9071.

17 Flint, H.J., Scott, K.P., Louis, P., and Duncan, S.H. (2012) The role of the gut microbiota in nutrition and health, *Nat Rev Gastroenterol Hepatol* **9**: 577-589.

18 Jones, S.A., Chowdhury, F.Z., Fabich, A.J., Anderson, A., Schreiner, D.M., House, A.L., et al. (2007) Respiration of *Escherichia coli* in the mouse intestine, *Infection and immunity* **75**: 4891-4899.

19 Khan, M.T., Duncan, S.H., Stams, A.J., van Dijl, J.M., Flint, H.J., and Harmsen, H.J. (2012) The gut anaerobe *Faecalibacterium prausnitzii* uses an extracellular electron shuttle to grow at oxic-anoxic interphases, *The ISME journal* **6**: 1578-1585.

20 Langmead, B., and Salzberg, S.L. (2012) Fast gapped-read alignment with Bowtie 2, *Nature Methods* **9**: 357-359.

21 Lechardeur, D., Cesselin, B., Fernandez, A., Lamberet, G., Garrigues, C., Pedersen, M., et al. (2011) Using heme as an energy boost for lactic acid bacteria, *Curr Opin Biotechnol* **22**: 143-149.

22 Lee, T.S., Krupa, R.A., Zhang, F., Hajimorad, M., Holtz, W.J., Prasad, N., et al. (2011) BglBrick vectors and datasheets: A synthetic biology platform for gene expression, *Journal of biological engineering* **5**: 12.
23 Li, H., Handsaker, B., Wysoker, A., Fennell, T., Ruan, J., Homer, N., et al. (2009) The Sequence Alignment/Map format and SAMtools, *Bioinformatics* **25**: 2078-2079.
24 Manach, C., Scalbert, A., Morand, C., Remesy, C., and Jimenez, L. (2004) Polyphenols: food sources and bioavailability, *The American journal of clinical nutrition* **79**: 727-747.
25 Miller, R.S., and Hoskins, L.C. (1981) Mucin degradation in human colon ecosystems. Fecal population densities of mucin-degrading bacteria estimated by a "most probable number" method, *Gastroenterology* **81**: 759-765.
26 Plugge, C.M. (2005) Anoxic media design, preparation, and considerations, *Methods Enzymol* **397**: 3-16.
27 Portnoy, V.A., Scott, D.A., Lewis, N.E., Tarasova, Y., Osterman, A.L., and Palsson, B.O. (2010) Deletion of genes encoding cytochrome oxidases and quinol monooxygenase blocks the aerobic-anaerobic shift in *Escherichia coli* K-12 MG1655, *Applied and environmental microbiology* **76**: 6529-6540.
28 Quinlan, A.R., and Hall, I.M. (2010) BEDTools: a flexible suite of utilities for comparing genomic features, *Bioinformatics* **26**: 841-842.
30 Reunanen, J., Kainulainen, V., Huuskonen, L., Ottman, N., Belzer, C., Huhtinen, H., et al. (2015) Akkermansia muciniphila Adheres to Enterocytes and Strengthens the Integrity of the Epithelial Cell Layer, *Appl Environ Microbiol* **81**: 3655-3662.
31 Robinson, M.D., McCarthy, D.J., and Smyth, G.K. (2010) edgeR: a Bioconductor package for differential expression analysis of digital gene expression data, *Bioinformatics* **26**: 139-140.
32 Rolfe, R.D., Hentges, D.J., Campbell, B.J., and Barrett, J.T. (1978) Factors related to the oxygen tolerance of anaerobic bacteria, *Applied and environmental microbiology* **36**: 306-313.
33 Shin, N.R., Lee, J.C., Lee, H.Y., Kim, M.S., Whon, T.W., Lee, M.S., and Bae, J.W. (2014) An increase in the Akkermansia spp. population induced by metformin treatment improves glucose homeostasis in diet-induced obese mice, *Gut* **63**: 727-735.
34 Swidsinski, A., Ladhoff, A., Pernthaler, A., Swidsinski, S., Loening-Baucke, V., Ortner, M., et al. (2002) Mucosal flora in inflammatory bowel disease, *Gastroenterology* **122**: 44-54.
35 Tran, Q.H., Bongaerts, J., Vlad, D., and Unden, G. (1997) Requirement for the proton-pumping NADH dehydrogenase I of Escherichia coli in respiration of NADH to fumarate and its bioenergetic implications, *European Journal of Biochemistry* **244**: 155-160.
36 Van den Abbeele, P., Van de Wiele, T., Verstraete, W., and Possemiers, S. (2011) The host selects mucosal and luminal associations of coevolved gut microorganisms: a novel concept, *FEMS microbiology reviews* **35**: 681-704.
37 van Gelder, A.H., Aydin, R., Alves, M.M., and Stams, A.J. (2012) 1,3-Propanediol production from glycerol by a newly isolated Trichococcus strain, *Microbial Biotechnology* **5**: 573-578.
38 van Hoek, M.J., and Merks, R.M. (2012) Redox balance is key to explaining full vs. partial switching to low-yield metabolism, *BMC Syst Biol* **6**: 22.
39 Zhou, J.Z., He, Q., Hemme, C.L., Mukhopadhyay, A., Hillesland, K., Zhou, A.F., et al. (2011) How sulphate-reducing microorganisms cope with stress: lessons from systems biology, *Nature Reviews Microbiology* **9**: 452-466.
40 Zoetendal, E.G., Booijink, C.C., Klaassens, E.S., Heilig, H.G., Kleerebezem, M., Smidt, H., and de Vos, W.M. (2006) Isolation of RNA from bacterial samples of the human gastrointestinal tract, *Nature protocols* **1**: 954-959.
41 Zoetendal, E.G., von Wright, A., Vilpponen-Salmela, T., Ben-Amor, K., Akkermans, A.D., and de Vos, W.M. (2002) Mucosa-associated bacteria in the human gastrointestinal tract are uniformly distributed along the colon and differ from the community recovered from feces, *Applied and environmental microbiology* **68**: 3401-3407.

Supplementary Information

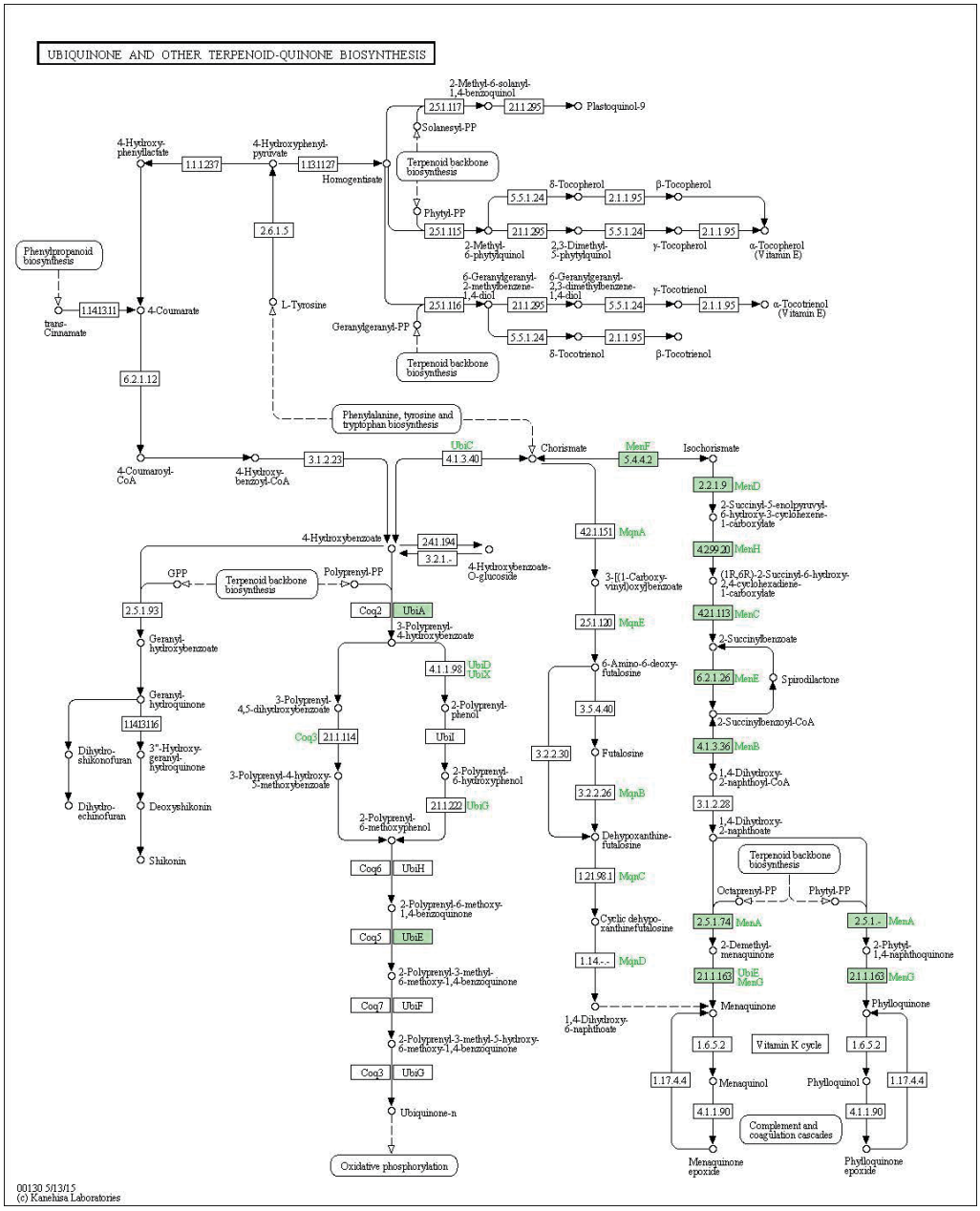

Figure S1. Menaquinol pathway. This figure illustrates the Menoquinol pathway as proposed by KEGG. Colored genes are present in *A. muciniphila* Muc^{T}.

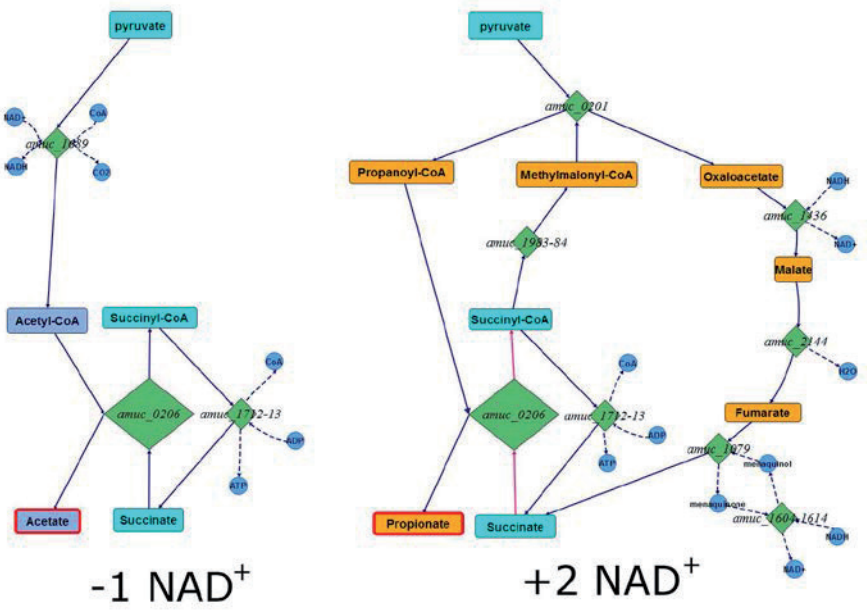

Figure S2. Simplified schematic representation of the metabolic pathways propionate and acetate (NAD+ pool) of *A. muciniphila*. Pyruvate to propionate results in netto 2 oxidized NADH to 2 NAD+, while pyruvate to acetate production results in netto 1 reduced NAD+.

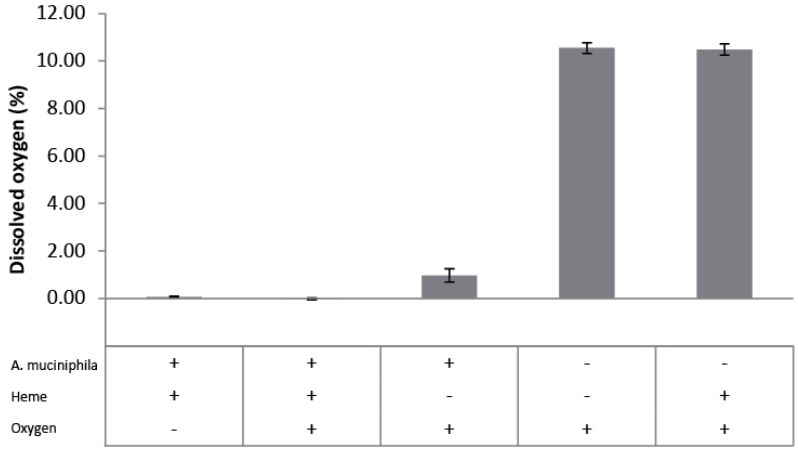

Figure S3. Heme depended oxygen reduction. The oxygen was completely reduced when heme was present (aerobic fermentor + heme) and accumulated when no heme was present (aerobic fermentor – heme). The anaerobic fermentor was included to determine the influence of heme. The negative control fermentors without bacteria and with and without heme showed no difference in dissolved oxygen concentration.

Table S1. Significantly altered genes between all tested conditions

T1vsT2_no_O2

Gene code	Annotation	2log FC	2log CPM	PValue
Amuc_0037	amino acid permease	1.03	9.57	2.85E-02
Amuc_0038	glutaminase	1.18	8.97	1.68E-02
Amuc_0089	hypothetical protein	1.44	7.19	3.89E-03
Amuc_0101	hypothetical protein	-1.29	14.74	4.25E-02
Amuc_0239	hypothetical protein	-1.12	5.05	3.67E-02
Amuc_0242	pseudouridine synthase	-0.78	10.15	2.28E-02
Amuc_0259	hypothetical protein	-1.05	6.67	3.38E-02
Amuc_0266	50S ribosomal protein L32	-0.86	8.06	4.85E-02
Amuc_0330	hypothetical protein	-1.13	9.17	9.20E-03
Amuc_0410	hypothetical protein	1.03	4.21	4.38E-02
Amuc_0468	DeoR family transcriptional regulator	-0.84	8.62	2.29E-02
Amuc_0469	N-acetyltransferase GCN5	-1.04	9.10	1.92E-02
Amuc_0504	hypothetical protein	0.75	6.62	4.67E-02
Amuc_0566	hypothetical protein	-1.66	2.63	1.57E-02
Amuc_0580	entericidin EcnAB	-1.31	8.16	3.10E-02
Amuc_0606	hypothetical protein	-1.43	7.69	1.30E-02
Amuc_0691	thioredoxin	-0.84	10.35	4.79E-02
Amuc_0748	riboflavin biosynthesis protein RibF	-0.74	7.49	4.26E-02
Amuc_0753	glycosyl transferase family protein	0.80	7.34	4.68E-02
Amuc_0819	multi antimicrobial extrusion protein MatE	-1.22	7.51	3.30E-02
Amuc_0976	hypothetical protein	-0.85	7.69	8.90E-03
Amuc_1022	G-D-S-L family lipolytic protein	0.74	7.77	3.02E-02
Amuc_1087	hypothetical protein	-2.70	6.04	3.46E-02
Amuc_1137	hypothetical protein	-0.93	7.06	4.75E-02
Amuc_1363	hypothetical protein	-1.00	8.97	2.59E-02
Amuc_1364	hypothetical protein	-1.10	9.28	1.33E-02
Amuc_1386	dihydropteroate synthase	-1.00	6.83	1.24E-02
Amuc_1409	hypothetical protein	-1.54	12.23	1.21E-02
Amuc_1430	50S ribosomal protein L31	-0.97	9.98	1.02E-02
Amuc_1508	hypothetical protein	1.98	0.56	1.09E-02
Amuc_1529	hypothetical protein	-1.09	9.42	5.54E-03

Amuc_1531	anthranilate synthase	0.97	9.01	7.01E-03
Amuc_1540	50S ribosomal protein L36	-1.09	10.25	1.07E-02
Amuc_1567	methylated-DNA--protein-cysteine methyltransferase	-0.84	6.78	1.10E-02
Amuc_1593	hypothetical protein	0.75	6.06	4.54E-02
Amuc_1679	Xylose isomerase domain-containing protein TIM barrel	0.78	6.21	4.79E-02
Amuc_1717	hypothetical protein	-0.94	11.51	2.78E-02
Amuc_1790	PDZ/DHR/GLGF domain-containing protein	0.75	6.54	3.16E-02
Amuc_1896	histone family protein DNA-binding protein	-1.31	11.34	9.73E-03
Amuc_1899	flavodoxin/nitric oxide synthase	-1.24	8.82	9.58E-03
Amuc_1936	hypothetical protein	-1.30	9.84	2.44E-03
Amuc_2072	rubrerythrin	-1.09	9.02	2.72E-03

T1vsT2_O2

Gene code	Annotation	2logFC	2logCPM	PValue
Amuc_0016	hypothetical protein	1.02	12.90	4.84E-02
Amuc_0037	amino acid permease	2.16	9.57	6.76E-06
Amuc_0038	glutaminase	-1.34	8.97	1.73E-04
Amuc_0089	hypothetical protein	2.65	7.19	9.65E-08
Amuc_0130	hypothetical protein	1.33	4.14	4.30E-02
Amuc_0131	hypothetical protein	1.70	3.97	2.71E-03
Amuc_0204	sodium ion-translocating decarboxylase subunit beta	0.66	9.01	4.58E-02
Amuc_0213	glutamyl-tRNA(Gln) amidotransferase subunit B	-0.79	10.09	3.76E-02
Amuc_0220	hydrophobe/amphiphile efflux-1 (HAE1) family transporter	-2.10	9.32	8.69E-04
Amuc_0236	Ion transport 2 domain-containing protein	0.95	7.04	5.38E-03
Amuc_0237	arsenate reductase-like protein	0.65	8.11	3.47E-02
Amuc_0267	hypothetical protein	-0.73	10.97	4.23E-02

Amuc_0270	shikimate kinase	-1.00	8.85	1.11E-02
Amuc_0271	30S ribosomal protein S16	-1.14	9.45	1.68E-02
Amuc_0275	preprotein translocase subunit YajC	-0.86	10.48	2.10E-02
Amuc_0327	hypothetical protein	-1.57	9.96	2.79E-02
Amuc_0328	hypothetical protein	-1.19	11.38	4.94E-02
Amuc_0330	hypothetical protein	-1.72	9.17	7.01E-04
Amuc_0372	glutamate decarboxylase	1.22	11.79	7.61E-03
Amuc_0384	Maltose O-acetyltransferase	0.62	7.40	4.86E-02
Amuc_0469	N-acetyltransferase GCN5	-1.04	9.10	1.92E-02
Amuc_0485	50S ribosomal protein L27	-0.94	9.05	3.41E-02
Amuc_0583	hypothetical protein	-1.29	6.30	2.56E-02
Amuc_0606	hypothetical protein	-1.46	7.69	1.11E-02
Amuc_0632	family 2 glycosyl transferase	-0.68	7.73	3.73E-02
Amuc_0677	hypothetical protein	0.66	7.05	3.80E-02
Amuc_0687	outer membrane autotransporter barrel domain-containing protein	-1.15	11.64	1.16E-04
Amuc_0717	amino acid permease	0.86	8.64	1.70E-02
Amuc_0748	riboflavin biosynthesis protein RibF	-0.76	7.49	3.77E-02
Amuc_0767	hypothetical protein	1.09	7.65	2.60E-03
Amuc_0772	phosphoglycerate mutase	1.15	8.95	1.74E-03
Amuc_0773	acyltransferase 3	0.69	7.14	3.59E-02
Amuc_0777	short-chain dehydrogenase/reductase SDR	2.51	6.92	3.49E-05
Amuc_0778	hypothetical protein	0.83	6.04	4.84E-02
Amuc_0803	coagulation factor 5/8 type domain-containing protein	0.87	9.38	1.62E-02
Amuc_0818	adenosylhomocysteinase	-0.83	7.14	3.20E-02
Amuc_0819	multi antimicrobial extrusion protein MatE	-1.28	7.51	2.48E-02
Amuc_0868	beta-N-acetylhexosaminidase	0.74	7.29	3.14E-02
Amuc_0882	hypothetical protein	1.34	12.90	4.17E-03
Amuc_0883	hypothetical protein	1.38	9.10	1.47E-03
Amuc_0907	hypothetical protein	-1.26	9.19	3.09E-02

Amuc_0925	KOW domain-containing protein	-0.93	10.99	4.35E-02
Amuc_0947	biotin/lipoyl attachment domain-containing protein	0.70	7.78	3.24E-02
Amuc_0998	hypothetical protein	1.28	7.62	9.53E-03
Amuc_1090	FeoA family protein	-0.88	9.43	4.82E-02
Amuc_1107	ATP phosphoribosyltransferase	-0.98	11.20	3.17E-02
Amuc_1141	glycosyl transferase family protein	1.76	6.93	1.46E-02
Amuc_1176	hypothetical protein	-0.76	8.59	8.01E-05
Amuc_1177	lipocalin family protein	1.39	6.25	9.40E-04
Amuc_1196	hypothetical protein	-0.90	7.77	1.67E-02
Amuc_1213	hypothetical protein	-1.53	10.91	5.35E-04
Amuc_1229	hypothetical protein	-0.80	11.64	4.14E-02
Amuc_1293	hypothetical protein	-1.79	6.81	6.33E-05
Amuc_1294	sulfite reductase	-1.45	11.21	3.11E-03
Amuc_1295	binding-protein-dependent transporters inner membrane component	-2.08	10.99	4.19E-06
Amuc_1296	ABC transporter	-1.88	9.96	5.47E-05
Amuc_1297	substrate-binding protein of aliphatic sulfonate ABC transporter	-2.01	10.18	2.19E-06
Amuc_1298	sulfate adenylyltransferase, large subunit	-1.72	10.77	4.30E-05
Amuc_1299	sulfate adenylyltransferase subunit 2	-1.25	10.39	6.08E-03
Amuc_1300	adenylylsulfate reductase	-0.85	10.96	3.33E-02
Amuc_1342	hypothetical protein	1.08	10.14	4.64E-02
Amuc_1363	hypothetical protein	-0.99	8.97	2.83E-02
Amuc_1364	hypothetical protein	-1.16	9.28	9.50E-03
Amuc_1365	hypothetical protein	-1.52	9.52	6.28E-03
Amuc_1368	hypothetical protein	-1.22	8.45	9.89E-03
Amuc_1381	ABC transporter	0.86	6.46	1.83E-02
Amuc_1394	hypothetical protein	1.20	7.82	4.38E-03
Amuc_1409	hypothetical protein	-1.20	12.23	4.84E-02
Amuc_1451	hypothetical protein	-0.97	8.25	6.97E-03

Amuc_1497	hypothetical protein	1.04	8.19	3.51E-02
Amuc_1529	hypothetical protein	-1.10	9.42	5.08E-03
Amuc_1540	50S ribosomal protein L36	-0.86	10.25	4.27E-02
Amuc_1594	NCAIR mutase-like protein	0.77	6.24	4.66E-02
Amuc_1602	hypothetical protein	0.93	8.25	2.62E-02
Amuc_1613	NADH dehydrogenase (ubiquinone) 24 kDa subunit	-0.81	9.83	3.93E-02
Amuc_1674	hypothetical protein	1.16	4.70	4.30E-02
Amuc_1676	Eco57I restriction endonuclease	-1.11	7.50	2.81E-02
Amuc_1684	TonB-dependent receptor	0.72	7.88	4.36E-02
Amuc_1692	2-oxoglutarate dehydrogenase, E2 subunit, dihydrolipoamide succinyltransferase	1.02	7.77	1.53E-02
Amuc_1693	2-oxoglutarate dehydrogenase, E1 subunit	0.99	9.86	1.70E-02
Amuc_1717	hypothetical protein	-1.30	11.51	2.65E-03
Amuc_1743	hypothetical protein	0.98	7.43	8.84E-03
Amuc_1770	AsnC family transcriptional regulator	-0.83	9.13	2.02E-02
Amuc_1812	alpha-amylase	1.89	10.22	5.33E-05
Amuc_1838	hypothetical protein	-1.04	7.93	4.40E-03
Amuc_1839	heavy metal translocating P-type ATPase	3.19	7.44	1.31E-05
Amuc_1870	Alpha-glucosidase	-0.77	9.54	2.61E-02
Amuc_1896	histone family protein DNA-binding protein	-1.39	11.34	6.39E-03
Amuc_1904	hypothetical protein	1.42	5.93	4.38E-03
Amuc_1914	restriction modification system DNA specificity domain	-0.87	9.25	4.02E-02
Amuc_1990	pyrroline-5-carboxylate reductase	0.76	5.90	4.00E-02
Amuc_2015	thiamine-phosphate pyrophosphorylase	-1.91	9.49	8.48E-04
Amuc_2016	Hydroxyethylthiazole kinase	-0.94	9.55	2.54E-02
Amuc_2035	hypothetical protein	1.31	5.04	3.25E-02

Amuc_2038	PUR-alpha/beta/gamma DNA/RNA-binding protein	-0.90	10.64	2.56E-02
Amuc_2051	glutamate dehydrogenase	-0.98	10.01	2.27E-02
Amuc_2053	hypothetical protein	-1.04	8.02	1.03E-02
Amuc_2055	hypothetical protein	1.18	9.20	6.54E-03
Amuc_2058	hypothetical protein	1.13	6.15	1.59E-02
Amuc_2060	hypothetical protein	0.95	6.42	2.67E-02
Amuc_2061	hypothetical protein	1.28	4.07	2.91E-02
Amuc_2070	hydroperoxidase II	-0.95	10.78	8.61E-05
Amuc_2078	capsular polysaccharide biosynthesis protein	0.87	9.28	2.26E-02
Amuc_2079	PHP domain-containing protein	1.15	6.07	3.06E-02
Amuc_2080	sugar transferase	1.37	7.19	1.63E-03
Amuc_2081	family 2 glycosyl transferase	1.05	6.65	7.28E-03
Amuc_2082	group 1 glycosyl transferase	0.94	7.07	1.31E-02
Amuc_2084	group 1 glycosyl transferase	1.16	6.54	1.15E-02
Amuc_2085	hypothetical protein	1.55	5.56	2.67E-03
Amuc_2088	group 1 glycosyl transferase	1.21	4.75	4.48E-02
Amuc_2093	family 2 glycosyl transferase	1.15	4.42	2.35E-02
Amuc_2094	family 2 glycosyl transferase	0.88	4.65	4.71E-02
Amuc_2129	nickel-dependent hydrogenase large subunit	0.97	9.03	1.10E-02
Amuc_2130	cytochrome B561	0.96	8.73	1.00E-02
Amuc_2131	hydrogenase maturation protease	1.31	6.72	5.55E-03
Amuc_2132	hydrogenase nickel incorporation protein HypA	1.02	5.39	1.77E-02
Amuc_2141	hypothetical protein	-0.92	9.89	2.68E-02
Amuc_2176	excinuclease ABC subunit A	0.90	8.75	5.75E-03

T2_O2vsT2_no_O2

Gene code	Annotation	2logFC	2logCPM	PValue
Amuc_0037	amino acid permease	1.13	9.57	2.88E-02
Amuc_0089	hypothetical protein	1.21	7.19	1.58E-02
Amuc_0236	Ion transport 2 domain-containing protein	0.88	7.04	1.73E-02
Amuc_0342	OsmC family protein	0.81	6.76	3.25E-02
Amuc_0580	entericidin EcnAB	1.93	8.16	2.65E-03
Amuc_0687	outer membrane autotransporter barrel domain-containing protein	1.31	11.64	3.28E-02
Amuc_0719	hypothetical protein	-1.14	9.81	1.08E-02
Amuc_0777	short-chain dehydrogenase/reductase SDR	1.41	6.92	2.53E-02
Amuc_0844	Phosphopyruvate hydratase	1.40	8.27	3.18E-02
Amuc_0882	hypothetical protein	1.00	12.90	4.94E-02
Amuc_0883	hypothetical protein	1.56	9.10	1.10E-03
Amuc_0998	hypothetical protein	1.37	7.62	1.17E-02
Amuc_0999	sigma 54 modulation protein/ribosomal protein S30EA	1.08	10.76	1.02E-02
Amuc_1016	hypothetical protein	-0.82	6.43	4.36E-02
Amuc_1176	hypothetical protein	0.88	8.59	3.43E-02
Amuc_1177	lipocalin family protein	0.96	6.25	2.85E-02
Amuc_1255	hypothetical protein	-0.72	7.52	3.83E-02
Amuc_1293	hypothetical protein	-1.26	6.81	5.75E-03
Amuc_1295	binding-protein-dependent transporters inner membrane component	-1.72	10.99	1.90E-04
Amuc_1296	ABC transporter	-1.66	9.96	5.41E-04
Amuc_1297	substrate-binding protein of aliphatic sulfonate ABC transporter	-1.56	10.18	3.19E-04
Amuc_1298	sulfate adenylyltransferase, large subunit	-1.23	10.77	4.39E-03
Amuc_1394	hypothetical protein	1.41	7.82	2.28E-03
Amuc_1570	hypothetical protein	-0.76	7.92	2.11E-02
Amuc_1592	Superoxide dismutase	0.92	9.77	4.91E-02

Amuc_1655	sulfatase	0.73	8.98	2.62E-02
Amuc_1812	alpha-amylase	1.02	10.22	4.37E-02
Amuc_1839	heavy metal translocating P-type ATPase	3.51	7.44	2.46E-05
Amuc_1904	hypothetical protein	1.12	5.93	3.56E-02
Amuc_1936	hypothetical protein	1.24	9.84	5.74E-03
Amuc_2015	thiamine-phosphate pyrophosphorylase	-0.75	9.49	4.47E-02
Amuc_2055	hypothetical protein	1.22	9.20	1.04E-02
Amuc_2069	hypothetical protein	-2.11	3.59	3.80E-02
Amuc_2070	hydroperoxidase II	1.16	10.78	3.71E-02
Amuc_2072	rubrerythrin	0.98	9.02	9.80E-03
Amuc_2081	family 2 glycosyl transferase	0.86	6.65	4.01E-02
Amuc_2111	ErfK/YbiS/YcfS/YnhG family protein	-0.80	8.57	3.29E-02
Amuc_2176	excinuclease ABC subunit A	1.14	8.75	1.29E-03

T3_O2vsT3_no_O2

Gene code	Annotation	2logFC	2logCPM	PValue
Amuc_0038	glutaminase	1.32	8.97	3.47E-02
Amuc_0059	ATPase AAA	1.04	11.25	1.68E-02
Amuc_0175	PDZ/DHR/GLGF domain-containing protein	1.30	8.86	3.57E-03
Amuc_0213	glutamyl-tRNA(Gln) amidotransferase subunit B	-1.18	10.09	6.68E-03
Amuc_0250	hypothetical protein	-1.71	8.08	2.23E-02
Amuc_0252	hypothetical protein	-1.02	7.89	1.67E-02
Amuc_0270	shikimate kinase	-0.95	8.85	3.27E-02
Amuc_0291	valyl-tRNA synthetase	-0.89	9.57	2.10E-02
Amuc_0337	prephenate dehydrogenase	0.82	6.99	3.14E-02
Amuc_0360	hypothetical protein	1.12	8.92	2.42E-02
Amuc_0422	3,4-dihydroxy-2-butanone 4-phosphate synthase	-1.00	9.48	2.25E-02
Amuc_0423	6,7-dimethyl-8-ribityllumazine synthase	-1.29	6.90	6.87E-03
Amuc_0424	NusB antitermination factor	-0.94	7.59	4.26E-02

Amuc_0425	signal recognition particle-docking protein FtsY	-1.14	7.15	1.21E-02
Amuc_0426	radical SAM enzyme, Cfr family	-0.93	9.11	1.46E-02
Amuc_0436	HAD-superfamily hydrolase	-0.90	8.49	3.38E-02
Amuc_0439	30S ribosomal protein S13	-1.03	9.91	1.58E-02
Amuc_0445	GTP-binding protein YchF	-0.97	8.61	2.08E-02
Amuc_0463	Phosphopantothenoylcysteine decarboxylase	-0.81	7.30	3.09E-02
Amuc_0469	N-acetyltransferase GCN5	1.35	9.10	1.28E-02
Amuc_0475	methyltransferase	0.81	6.76	4.60E-02
Amuc_0485	50S ribosomal protein L27	-1.00	9.05	4.80E-02
Amuc_0488	FeS assembly protein SufB	0.87	9.43	3.33E-02
Amuc_0489	SufBD protein	1.13	9.26	1.26E-02
Amuc_0533	hypothetical protein	-0.89	7.79	3.24E-02
Amuc_0534	phosphoribosylformylglycinamidine synthase II	-0.79	9.89	4.91E-02
Amuc_0556	FmdB family regulatory protein	1.11	5.23	3.44E-02
Amuc_0573	3'-5' exonuclease	-0.88	9.20	3.85E-02
Amuc_0616	protein serine/threonine phosphatase	1.09	7.42	4.60E-02
Amuc_0642	tRNA delta(2)-isopentenylpyrophosphate transferase	-1.13	5.44	3.68E-02
Amuc_0650	S-adenosyl-methyltransferase MraW	0.75	9.03	4.51E-02
Amuc_0760	hypothetical protein	-0.95	7.28	4.94E-02
Amuc_0775	thioesterase	1.28	7.60	4.20E-02
Amuc_0787	rhomboid family protein	-1.25	9.21	1.69E-02
Amuc_0844	Phosphopyruvate hydratase	2.13	8.27	7.11E-03
Amuc_0850	RNA methyltransferase, TrmA family	-0.78	7.96	4.04E-02
Amuc_0865	rubrerythrin	2.03	9.33	1.97E-03
Amuc_0868	beta-N-acetylhexosaminidase	0.92	7.29	3.25E-02
Amuc_0876	heavy metal translocating P-type ATPase	1.45	8.47	5.57E-03

Amuc_0888	MerR family transcriptional regulator	0.99	6.48	4.90E-02
Amuc_0955	ribosome-binding factor A	-1.21	9.71	3.21E-02
Amuc_0961	hypothetical protein	1.61	8.11	2.03E-04
Amuc_0962	4Fe-4S ferredoxin	1.10	7.63	4.60E-03
Amuc_0983	YD repeat protein	1.18	10.61	2.85E-02
Amuc_0988	TatD-related deoxyribonuclease	0.98	7.03	1.61E-02
Amuc_1017	hypothetical protein	-1.28	7.25	3.61E-02
Amuc_1030	cupin	-1.08	5.44	3.27E-02
Amuc_1084	hypothetical protein	4.33	7.04	6.64E-04
Amuc_1089	FeoA family protein	1.15	10.63	3.98E-02
Amuc_1090	FeoA family protein	1.22	9.43	2.58E-02
Amuc_1145	hypothetical protein	-0.98	10.22	2.49E-02
Amuc_1177	lipocalin family protein	1.15	6.25	2.27E-02
Amuc_1187	Alpha-galactosidase	1.04	9.85	4.58E-02
Amuc_1211	N-acetylmuramoyl-L-alanine amidase family 2 protein	0.91	7.15	3.60E-02
Amuc_1219	hypothetical protein	-1.35	9.65	4.26E-02
Amuc_1222	oligopeptide transporter	-0.75	8.69	3.53E-02
Amuc_1250	carbamoyl-phosphate synthase small subunit	-0.88	8.15	2.08E-02
Amuc_1290	hypothetical protein	1.02	9.17	2.42E-02
Amuc_1291	surface layer protein	1.32	7.32	7.79E-03
Amuc_1295	binding-protein-dependent transporters inner membrane component	-1.17	10.99	1.75E-02
Amuc_1297	substrate-binding protein of aliphatic sulfonate ABC transporter	-1.18	10.18	1.11E-02
Amuc_1298	sulfate adenylyltransferase, large subunit	-1.42	10.77	2.47E-03
Amuc_1299	sulfate adenylyltransferase subunit 2	-1.50	10.39	3.57E-03
Amuc_1300	adenylylsulfate reductase	-1.33	10.96	3.49E-03
Amuc_1301	cysteine synthase A	-1.19	11.38	1.13E-02
Amuc_1309	aldose 1-epimerase	1.30	8.74	3.02E-03

Amuc_1310	17 kDa surface antigen	0.91	9.36	2.70E-02
Amuc_1321	alkyl hydroperoxide reductase	2.34	10.72	6.90E-04
Amuc_1343	hypothetical protein	-1.30	7.46	3.23E-02
Amuc_1408	chaperonin GroEL	0.91	12.13	4.18E-02
Amuc_1412	hypothetical protein	0.85	10.64	4.93E-02
Amuc_1517	ECF subfamily RNA polymerase sigma-24 subunit	0.86	7.61	3.19E-02
Amuc_1537	outer membrane autotransporter barrel domain-containing protein	1.12	11.00	1.77E-02
Amuc_1609	4Fe-4S ferredoxin	-0.99	8.25	1.36E-02
Amuc_1612	NADH dehydrogenase (quinone)	-0.79	9.51	2.83E-02
Amuc_1653	Ribulose-phosphate 3-epimerase	-0.84	7.02	3.81E-02
Amuc_1654	leucyl-tRNA synthetase	-0.89	10.73	3.05E-02
Amuc_1692	2-oxoglutarate dehydrogenase, E2 subunit, dihydrolipoamide succinyltransferase	1.19	7.77	2.35E-02
Amuc_1693	2-oxoglutarate dehydrogenase, E1 subunit	1.57	9.86	3.34E-03
Amuc_1694	cytochrome d ubiquinol oxidase, subunit II	1.47	7.92	6.53E-03
Amuc_1757	phosphotransferase system, phosphocarrier protein HPr	1.45	9.97	4.13E-03
Amuc_1764	hypothetical protein	-1.28	7.66	1.20E-02
Amuc_1776	hypothetical protein	1.09	9.66	1.74E-02
Amuc_1777	von Willebrand factor type A	1.19	12.17	2.25E-02
Amuc_1780	hypothetical protein	0.93	7.67	3.35E-02
Amuc_1814	hypothetical protein	-1.34	5.86	3.92E-02
Amuc_1843	hypothetical protein	1.17	6.11	3.16E-02
Amuc_1901	metallophosphoesterase	-1.23	8.28	2.28E-02
Amuc_1902	hypothetical protein	-1.44	10.54	2.39E-03
Amuc_1903	hypothetical protein	-1.06	9.13	2.02E-02
Amuc_1922	ferredoxin	1.07	11.13	3.88E-02

Amuc_1960	PA14 domain-containing protein	1.07	6.59	4.92E-02
Amuc_1965	aspartate kinase	-0.82	8.72	3.67E-02
Amuc_1972	HhH-GPD family protein	-0.86	7.24	4.69E-02
Amuc_1985	hypothetical protein	0.88	9.05	1.89E-02
Amuc_2051	glutamate dehydrogenase	-1.01	10.01	3.73E-02
Amuc_2054	hypothetical protein	-1.08	6.15	3.90E-02
Amuc_2072	rubrerythrin	1.31	9.02	3.07E-03
Amuc_2111	ErfK/YbiS/YcfS/YnhG family protein	-0.95	8.57	1.96E-02
Amuc_2120	hypothetical protein	1.12	7.78	9.56E-03
Amuc_2129	nickel-dependent hydrogenase large subunit	1.46	9.03	2.85E-03
Amuc_2130	cytochrome B561	1.58	8.73	1.04E-03
Amuc_2131	hydrogenase maturation protease	1.79	6.72	3.28E-03
Amuc_2136	Glycoside hydrolase, family 20, catalytic core	0.98	10.15	1.47E-02
Amuc_2148	beta-N-acetylhexosaminidase	1.03	7.62	2.30E-02
Amuc_2154	hypothetical protein	1.64	8.54	8.00E-03
Amuc_2176	excinuclease ABC subunit A	1.19	8.75	3.74E-03

T2_O2vsT3_O2		logFC	logCPM	Pvalue
Amuc_1901	metallophosphoesterase	3.08	8.26	4.06E-10
Amuc_1301	cysteine synthase A	-2.83	11.36	2.56E-09
Amuc_0439	30S ribosomal protein S13	-2.35	9.90	4.13E-09
Amuc_2051	glutamate dehydrogenase	-2.75	9.97	7.89E-09
Amuc_1654	leucyl-tRNA synthetase	-2.28	10.72	1.38E-08
Amuc_0422	3,4-dihydroxy-2-butanone 4-phosphate synthase	-2.40	9.47	3.21E-08
Amuc_0616	protein serine/threonine phosphatase	3.31	7.53	4.94E-08
Amuc_0485	50S ribosomal protein L27	-2.61	9.02	2.19E-07
Amuc_2111	ErfK/YbiS/YcfS/YnhG family protein	-2.13	8.55	2.56E-07
Amuc_0573	3'-5' exonuclease	-2.47	9.20	2.67E-07
Amuc_1612	NADH dehydrogenase (quinone)	-1.81	9.50	3.25E-07

Amuc_0534	phosphoribosylformylglycinamidine synthase II	-2.02	9.89	5.40E-07
Amuc_0426	radical SAM enzyme, Cfr family	-2.08	9.11	7.06E-07
Amuc_1694	cytochrome d ubiquinol oxidase, subunit II	2.43	7.89	8.05E-07
Amuc_0469	N-acetyltransferase GCN5	2.64	9.19	1.71E-06
Amuc_1089	FeoA family protein	-2.20	10.61	5.91E-06
Amuc_1965	aspartate kinase	-1.95	8.72	6.30E-06
Amuc_1609	4Fe-4S ferredoxin	-1.96	8.26	7.61E-06
Amuc_1300	adenylylsulfate reductase	-2.06	10.95	1.62E-05
Amuc_1090	FeoA family protein	-1.95	9.40	2.76E-05
Amuc_1653	Ribulose-phosphate 3-epimerase	-2.04	7.03	3.22E-05
Amuc_0213	glutamyl-tRNA(Gln) amidotransferase subunit B	-1.83	10.08	3.57E-05
Amuc_0983	YD repeat protein	1.96	10.61	5.16E-05
Amuc_0425	signal recognition particle-docking protein FtsY	-2.09	7.16	5.49E-05
Amuc_0955	ribosome-binding factor A	1.93	9.67	6.45E-05
Amuc_1693	2-oxoglutarate dehydrogenase, E1 subunit	1.79	9.86	0.000112
Amuc_1250	carbamoyl-phosphate synthase small subunit	-1.53	8.16	0.00015
Amuc_0424	NusB antitermination factor	-1.97	7.61	0.000152
Amuc_1299	sulfate adenylyltransferase subunit 2	-1.95	10.38	0.000317
Amuc_1295	binding-protein-dependent transporters inner membrane component	-1.56	10.95	0.000418
Amuc_0291	valyl-tRNA synthetase	-1.35	9.58	0.00063
Amuc_1960	PA14 domain-containing protein	1.71	6.57	0.000742
Amuc_1177	lipocalin family protein	1.71	6.30	0.001103
Amuc_0270	shikimate kinase	1.16	8.84	0.002179
Amuc_0436	HAD-superfamily hydrolase	1.30	8.51	0.002239

Amuc_1692	2-oxoglutarate dehydrogenase, E2 subunit, dihydrolipoamide succinyltransferase	1.49	7.77	0.002355
Amuc_1298	sulfate adenylyltransferase, large subunit	-1.38	10.75	0.003355
Amuc_0423	6,7-dimethyl-8-ribityllumazine synthase	-1.55	6.91	0.003563
Amuc_0962	4Fe-4S ferredoxin	1.12	7.65	0.003785
Amuc_0868	beta-N-acetylhexosaminidase	1.18	7.30	0.003817
Amuc_0038	glutaminase	1.57	8.96	0.003836
Amuc_0850	RNA methyltransferase, TrmA family	-1.26	7.96	0.00386
Amuc_0888	MerR family transcriptional regulator	1.49	6.50	0.004756
Amuc_1310	17 kDa surface antigen	0.95	9.37	0.008482
Amuc_1222	oligopeptide transporter	0.90	8.70	0.009872
Amuc_0445	GTP-binding protein YchF	-1.13	8.62	0.010741
Amuc_1297	substrate-binding protein of aliphatic sulfonate ABC transporter	-1.18	10.15	0.013182
Amuc_1537	outer membrane autotransporter barrel domain-containing protein	1.09	11.03	0.013917
Amuc_1922	ferredoxin	-0.97	11.10	0.019463
Amuc_1321	alkyl hydroperoxide reductase	1.12	10.64	0.027838
Amuc_0175	PDZ/DHR/GLGF domain-containing protein	0.77	8.84	0.045832
Amuc_1517	ECF subfamily RNA polymerase sigma-24 subunit	0.76	7.62	0.050143
Amuc_1309	aldose 1-epimerase	0.79	8.76	0.062443
Amuc_1757	phosphotransferase system, phosphocarrier protein HPr	0.83	9.97	0.064148
Amuc_1291	surface layer protein	0.82	7.30	0.065961
Amuc_0787	rhomboid family protein	0.80	9.19	0.072646
Amuc_2129	nickel-dependent hydrogenase large subunit	0.68	9.01	0.097101

Amuc_1030	cupin	-0.86	5.46	0.13556
Amuc_2148	beta-N-acetylhexosaminidase	0.61	7.60	0.13709
Amuc_2072	rubrerythrin	-0.60	9.01	0.140012
Amuc_1211	N-acetylmuramoyl-L-alanine amidase family 2 protein	0.59	7.14	0.145489
Amuc_1408	chaperonin GroEL	0.54	12.13	0.148913
Amuc_1972	HhH-GPD family protein	-0.70	7.25	0.150375
Amuc_0642	tRNA delta(2)-isopentenylpyrophosphate transferase	0.82	5.47	0.176493
Amuc_0463	Phosphopantothenoylcysteine decarboxylase	-0.49	7.31	0.236391
Amuc_1777	von Willebrand factor type A	0.48	12.16	0.273026
Amuc_2131	hydrogenase maturation protease	0.47	6.69	0.384665
Amuc_0876	heavy metal translocating P-type ATPase	-0.38	8.46	0.421573
Amuc_0337	prephenate dehydrogenase	-0.26	6.99	0.512197
Amuc_0865	rubrerythrin	0.30	9.28	0.546694
Amuc_2130	cytochrome B561	0.24	8.71	0.546999
Amuc_0775	thioesterase	-0.33	7.59	0.556213
Amuc_2176	excinuclease ABC subunit A	-0.20	8.76	0.598361
Amuc_0650	S-adenosyl-methyltransferase MraW	-0.16	9.02	0.622332
Amuc_0988	TatD-related deoxyribonuclease	0.18	7.02	0.625398
Amuc_0489	SufBD protein	-0.18	9.24	0.628164
Amuc_0556	FmdB family regulatory protein	0.22	5.24	0.685003
Amuc_1187	Alpha-galactosidase	0.14	9.83	0.732847
Amuc_0059	ATPase AAA	-0.10	11.23	0.783478
Amuc_2136	Glycoside hydrolase, family 20, catalytic core	-0.10	10.14	0.78636
Amuc_0844	Phosphopyruvate hydratase	-0.16	8.23	0.804343
Amuc_0488	FeS assembly protein SufB	-0.09	9.43	0.814634
Amuc_0475	methyltransferase	-0.09	6.78	0.843837

CHAPTER 6

Encapsulation of the therapeutic microbe *Akkermansia muciniphila* in a double emulsion enhances survival in simulated gastric conditions

Kees C. H. van der Ark, Avis Dwi Wahyu Nugroho, Claire Berton-Carabin, Che Wang, Clara Belzer, Willem M. de Vos and Karin Schroen

This chapter was previously published as:

Encapsulation of the therapeutic microbe Akkermansia muciniphila in a double emulsion enhances survival in simulated gastric conditions. *Food Research International,* 2017, **Kees C.H. van der Ark**, Avis Dwi Wahyu Nugroho, Claire Berton-Carabin, Che Wang, Clara Belzer, Willem M. de Vos, Karin Schroen (In Press)

Abstract

There is considerable attention for developing *Akkermansia muciniphila* as a new therapeutic microbe since it has shown to prevent diet-induced obesity and type 2 diabetes in mice. However, *A. muciniphila* is sensitive to gastric conditions such as low pH and oxygen. Therefore, we explored the possibility of encapsulating *A. muciniphila* in a water-in-oil-in-water (W/O/W) double emulsion, to allow for protection during gastric passage and subsequent release in the small intestine. The bacteria were efficiently encapsulated in the inner emulsion droplets and remained entrapped during *in vitro* gastric digestion. The cells were then released in the simulated intestinal phase of the *in vitro* system. The viability of encapsulated cells was found to be higher when compared to cells dispersed in buffer, that had been subjected to similar mechanical process as the one conducted to prepare the emulsion systems. Surprisingly, the viability of the processed cells was even higher than that of the cells dispersed in buffer without processing, likely due to shear-induced stress tolerance. To conclude, encapsulation in a double emulsion seems to be a promising strategy to protect *A. muciniphila* during gastric passage in oral formulations.

Introduction

The influence of the gut microbiota on human health has been studied extensively during the past decades. Correlations have been found between microbiota composition and diseases, including but not limited to type 2 diabetes, metabolic syndrome and ulcerative colitis (Clemente, et al., 2012, Marchesi, et al., 2016). Recently, treatments aiming to change the microbiota composition were employed to fight infections. Faecal transplants by intubation were used to treat chronic infections caused by *Clostridium difficile* with high effectiveness (van Nood, et al., 2013). However, the mode of action of these treatments is poorly understood due to the undefined composition of the faecal matter (van Nood, et al., 2013).

In the last year, specific bacterial species from the microbiota have been identified as potential probiotics or even therapeutic microbes (Plovier, et al., 2016, Quevrain, et al., 2016, Udayappan, et al., 2016) that could be used to treat or prevent specific diseases. An important species is the gut bacterium *Akkermansia muciniphila*, the presence and abundance of which has been reported to inversely correlate with body weight, gut permeability and inflammation (Wang, et al., 2011, Everard, et al., 2013). This human mucus colonizer was found to be not only important for obesity development and associated metabolic disorders, but also for influencing the host's general health and physiology. Recently, the administration of *A. muciniphila* by gavage was found to protect mice from diet-induced obesity (Everard, et al., 2013, Plovier, et al., 2016). Moreover, *A. muciniphila* was found to be safe for use in humans (Plovier, et al., 2016). Incorporating this functional microbe in food products or medicine could be the starting point for obesity and type 2 diabetes prevention; however, the application of *A. muciniphila* may be challenged by its sensitivity to low pH, shear, and oxygen (Derrien, et al., 2004, Ouwerkerk, et al., 2016). Besides, survival or growth of *A. muciniphila* in the presence of bile salts has not been documented yet.

To protect *A. muciniphila* during gastric passage, an effective encapsulation system is needed. Probiotics have commonly been encapsulated in various ways to increase shelf life, viability and targeted delivery (Anal and Singh, 2007), although many of these techniques impose high stress on the bacteria. For example, spray drying causes high osmotic pressure, and exposure to oxygen. Additionally, the high temperatures used in spray drying could either reduce bacterial viability and denature proteins that are of importance in probiotic efficacy (Plovier, et al., 2016). Extrusion is used for encapsulation in alginate beads, resulting in

particles of 2 to 5 mm; the most important limitation of extrusion being susceptibility of the alginate beads to damage (Krasaekoopt, et al., 2003, Solanki, et al., 2013).

In the current study we used W/O/W emulsions for encapsulation (Su, et al., 2008), which are oil globules, containing small aqueous droplets that are dispersed in an aqueous continuous phase (Leal-Calderon, et al., 2012). The internal aqueous droplets can serve as an entrapping reservoir for *A. muciniphila* because of its small size of ~1 µm. Besides, dedicated emulsification was preferred for *A. muciniphila* because of the rather mild process conditions. Encapsulation of *A. muciniphila* in the inner droplets of double water-in-oil-in-water (W/O/W) emulsions may give protection from adverse external conditions, and also allow targeted delivery in the intestine, as was found for the probiotic *Lactobacillus rhamnosus* that had a higher relative viability (10-100 fold) after gastric digestions compared to the control (Shima, et al., 2006, Pimentel-Gonzalez, et al., 2009). However, *L. rhamnosus* has a high acid resistance and can survive an acidity of pH 2.5 (Corcoran, et al., 2005), whereas *A. muciniphila* is unable to grow at a pH below 5.5 (Derrien, et al., 2004), and needs to be better protected.

The application of W/O/W emulsions is challenging due to the many factors that can contribute to their physical instability. They often consist of large and polydisperse droplets that have a strong tendency for flocculation, creaming and coalescence (Benichou, et al., 2004, van der Graaf, et al., 2005). In addition, it is difficult to retain the encapsulated matter within the water phase; release may occur as a result of concentration gradients and osmotic pressure difference (Benichou, et al., 2004), especially during storage. Bacteria-sized particles can even be expelled by coalescence of the inner water phase with the outer water phase. So, localisation of the entrapped bacteria in the W/O/W emulsion during gastric simulation and stabilization of the emulsion itself is imperative. Furthermore, an oil-based emulsion is needed to allow for the release of bacteria after gastric passage, because the oil is degraded by bile upon entering the small intestine.

In this study, we encapsulated *A. muciniphila* (or fluorescently-labelled particle analogues) in the inner water droplets of double W/O/W emulsions produced via a mild homogenization technique developed in our labs. First, the morphology and physical stability of the emulsions were assessed. Subsequently, we investigated the localisation of bacteria analogues within

the emulsions, and finally the survival rate of *A. muciniphila*, when emulsions were subjected to storage and simulated gastrointestinal conditions.

Materials and Methods

Media preparation of *A. muciniphila*

Liquid culture of *A. muciniphila* Muc^T (CIP 107961^T) was prepared in anoxic basal media as described previously (Derrien, et al., 2004). The basal media was supplemented with 20 g/L tryptone (Oxoid Ltd, UK) and 4 g/L L-threonine (Sigma-Aldrich, USA). A mixture of 250 mM glucose (D(+)-glucose monohydrate, Merck, Germany) and N-acetyl-D-glucosamine (purity ≥99%, Sigma-Aldrich, USA) was added by 10% v/v as the carbon source. Media were filled into serum bottles sealed with butyl-rubber stoppers and aluminium crimp caps under anaerobic conditions provided by a gas phase of 182 kPa (1.5 atm) N_2/CO_2.

For the total viable count (TVC), Brain Heart Infusion (BHI) mucin agar was prepared containing 10 g agar (bacteriological agar no. 1), Oxoid Ltd, UK), 37 g BHI (Becton, Dickinson & Co, Belgium), 0.5 g L-cysteine hydrochloride monohydrate (Sigma-Aldrich, USA), 1 mL rezasurin, and 5 g commercial hog gastric mucin (Type III ; Sigma, Saint Louis, USA) per litre medium. BHI mucin agar was kept in 2 anaerobic atmosphere generation bags (AnaeroGen™, Oxoid Ltd, UK) at minimum one day before use and one fresh bag was used during incubation.

Cultivation and preparation of concentrated glycerol stocks of *A. muciniphila*

Cultivation of *A. muciniphila* liquid culture was done in anoxic medium by inoculating 1% v/v of 2 days pre-culture. Incubation was done at 37 °C for 2-3 days until late exponential phase. Cells were harvested by centrifugation at 10,000 g for 10 minutes and washed twice in buffer A (Phosphate Buffered Saline (PBS), 10 mM pH 7.4 with additional NaCl: 0.2 g/l KCl, 0.23 g/L KH_2PO_4, 2 g/L NaCl, 1.15 g/L Na_2HPO_4). The harvested cells were then added by 1:1 (v/v) ratio to anaerobic vials containing 50% v/v glycerol in water. Cells were preserved at -80 °C until use. One vial was thawed and counted by TVC as the reference concentration for all other experiments. For the use at non-microbiological laboratory, the cells were pasteurised at 68 °C in a water bath for 30 minutes prior to use, to render them inactive.

Preparation and characterisation of double emulsions

Before use, both rotor-stator homogenizer and premix emulsification system were cleaned and filled with 1% halamid (Chloramine-T, Boom B.V., The Netherlands) solution for 10 minutes. The system was emptied and refilled with sterile water to wash the remaining halamid. Water-in-oil (W_1/O) emulsion (3:7, v/v) was firstly prepared by combining a freshly prepared solution of 10^9 CFU/mL *A. muciniphila* in PBS 10 mM + 2 g/L NaCl with 1% w/v PGPR (Givaudan, Switzerland) in sunflower oil (C1000, The Netherlands) in 50 mL conical centrifuge tube. The glycerol stocks used throughout the project were thawed only once and were not refrozen. The water and oil mixture was homogenized with a rotor-stator homogenizer (Ultraturrax T-18, IKA, Germany) at 4400 RPM for 6 minutes with manual up-and-down moving every minute to ensure uniform homogenization.

Afterward, the resulting primary emulsion was added to the outer water phase containing 1% w/v sodium caseinate (sodium caseinate S 80% purity, DMV international, The Netherlands) in PBS 10 mM + 2 g/L NaCl that had been stirred overnight. The volume fraction of W_1/O emulsion was 10% of the total double emulsion volume. A coarse double emulsion was first made with the rotor-stator homogenizer at 3400 RPM for 6 minutes, prior to emulsification with a premix column at 4 bar (pressurized CO_2) for 5 passes. The procedure was similar to that used in previous work (Sahin, et al., 2014), except that it was carried out without nickel sieve and glass beads. The obtained double emulsion was kept in a 1 L bottle sealed with butyl-rubber stoppers and aluminium screw cap under anaerobic condition. A total volume of 300 mL double emulsions was made per batch.

All preparations were done in triplicate; the primary and double emulsions were characterized for droplet morphology and droplet size distribution. Droplet morphology was observed using bright field confocal microscope at 400X magnification. A volume of 4 µL sample was used for all microscopy preparations throughout the project unless stated otherwise. For each sample, the droplet size distribution was measured in triplicate using a light scattering instrument (Mastersizer 2000, Malvern, UK) with the values indicated in Table S1 (Supplementary materials and methods). The window glass pair was cleaned with soap and ethanol air every 3 to 4 measurements to ensure accurate detection.

In case of measurement of double emulsions containing living bacteria, measurement was done using 15 microscopy images processed by automated image analysis software (ImageJ

1.49o) and MS. Excel 2010 (Supplementary material). All values of droplet size were expressed as volume-weighted mean diameter (D [4, 3]). The following formula (Eq. 1) was used for the calculation of D [4, 3] in MS. Excel:

$$D(4,3) = \frac{\sum n_i d_i^4}{\sum n_i d_i^3} \quad (1)$$

where n_i is expressed as the number of particles in each size-class per unit volume of emulsion, while d_i is the diameter of the particles in each size-class. The width of the distribution (Span) was determined as follows (Eq. 2):

$$Span = \frac{d(0.9) - d(0.1)}{d(0.5)} \quad (2)$$

where $d(0.1)$, $d(0.5)$ and $d(0.9)$ are the sizes below which 10%, 50% and 90% of the particles are counted, respectively.

Alternatively, the program ImageJ was used to analyse 15 microscopy images. First, the image was converted to black and white, after which the threshold was adjusted to show the desired droplets. Additionally, outliers were removed to exclude small primary emulsion droplets. Finally, the particles with a radius of 10 µm to infinity and a circularity of 0.50 – 1.00 were analysed. The output was used to calculate the D [4, 3] according to equation (1).

The osmotic pressure on the droplets exerted by the outer water phase was calculated by using the Van 't Hoff equation:

$$\Pi = n \times C \times R \times T \quad (3)$$

In which Π is the osmotic pressure, T in Kelvin, R the gas constant, C the concentration of the compounds, and n the amount of dissociated compounds.

Bacterial viability and emulsion stability during storage

A freshly prepared double emulsion loaded with bacteria was stored in anaerobic serum bottles with a N_2/CO_2 headspace and in aerobic conical centrifugation tubes. The same was done with an equal amount of bacteria in 10 mM PBS buffer as a control. Each bottle contained 10 mL of liquid. After these treatments, the samples were kept in the fridge at 4˚C and samples were taken at 0, 2 , 24 , 48 and 72 hours. At each time point, 0.5 mL sample of

the experimental group and the control group were taken under sterile conditions. To count the viable cells, the double emulsions underwent centrifugation steps (10,000 g for 10 min) to break down the emulsion and fully separate the oil layer and water layer (water phases 1 and 2). The complete sample was mixed with a vortex agitator for 10 seconds to suspend the bacteria. Serial dilutions (10^{-1} to 10^{-7}) were made of each sample in PBS. Spots of 2 µL were made from each dilution on BHI-mucin-agar plates, prepared as described above. The plates were incubated for two days at 37 ˚C.

The droplet size distribution, morphology, and encapsulation efficiency were set as standards to evaluate the physical properties of the double emulsion systems. The double emulsions were stored at 4 °C for 96 hours for the stability tests, and samples were taken at 0, 1, 2, 4, 24, 48, and 96 hours. The whole set of experiments was conducted twice and each experiment contained two parallel cultures for each condition.

Localisation and encapsulation efficiency of bacteria and fluorescent particles

Double emulsions were prepared with hydrophilic fluorescent particles (FluoSpheres® 1 µm F-13081, maximum emission wavelength 505 nm, ThermoFisher Scientific, USA) or pasteurized biomass which was labelled by 0.3% v/v of 3.34 mM SYTO9 (λ_{em} 608 nm, ThermoFisher Scientific, USA). The double emulsions were subjected to simulated digestion (see detailed procedure below) and samples were observed under fluorescence microscope. Green light (λ = 540 nm) was used for the excitation.

The encapsulation efficiency was calculated based on the average of 30 random microscopic images (400x magnification) from samples stored for different time periods.

The encapsulation efficiency was calculated as follows (Eq. 4):

$$\text{Encapsulation efficiency (\%)} = \frac{1}{30}\sum_{i=1}^{30} a_i = \frac{1}{30}(\mathrm{a}_1 + \mathrm{a}_2 + \cdots + \mathrm{a}_n) \quad (4)$$

where

$$\mathrm{a}_i = \frac{\text{number of fluorescent particles entrapped in inner water droplets}}{\text{total number of fluorescent particles in view}} \quad (5)$$

Simulated digestion test

The international consensus of standardized static in vitro digestion method by Minekus et al. (Minekus, et al., 2014) was applied with some modifications (Table S2 Supplementary material). The tests were done in chemostat bioreactors (DASGIP® Parallel Bioreactor System, Eppendorf, Germany), each with a total volume of 500 mL. The gastric test was done at pH 3.0, 37 °C, 2 hours, and 100 RPM agitation with 0.2% w/v pepsin (from porcine gastric mucosa 3200–4500 U mg^{-1} protein, Sigma, USA), diluted in simulated gastric fluid (SGF) pH 6.0 (Table S3 Supplementary material). The intestinal test was done at pH 7.0, 37 °C, 2 hours, and 100 RPM agitation with 0.48% w/v porcine bile extract (B8631, Sigma-Aldrich, USA) and 0.22% w/v pancreatin (from porcine pancreas, 8X USP specification, Sigma-Aldrich, USA).

Potassium hydroxide (3 M) and sulfuric acid (0.5 M) were used to control the pH during the experiment. Dissolved oxygen was programmed for gradual decrease during 2 hours gastric test until anaerobic conditions were reached and maintained during the intestinal phase. Pure nitrogen was used to alter the atmospheric composition in the vessels. Samples were taken before and after each digestion stage, kept on ice and observed by phase contrast confocal microscopy at 400x. Each microscope slide was prepared just before observation to keep droplets intact. For viable cell counts, the double emulsions were disrupted by centrifugation at 10,000 g for 10 minutes prior to TVC plating on BHI mucin.

All equipment and materials were sterilized except the enzyme solutions. Additional antibiotics were added with final concentration of 5 µg/mL vancomycin hydrochloride (>900 µg/mg, AcrosOrganics, Belgium) and 50 µg/mL kanamycin sulfate (Sigma–Aldrich, USA) during the digestion test and in BHI-mucin-agar to avoid contamination and growth of undesired cells. Both processed and unprocessed cells dispersed in PBS were tested as control. In the former case, a bacterial suspension in PBS buffer was subjected to the same mechanical treatment as applied for preparing the double emulsions, i.e., 2 treatments with the rotor-stator homogenizer, followed by the premix column emulsification step.

Further analysis and blanks

Zeta potential of sodium-caseinate-stabilized droplets at different pH

In order to assess the effect of pH changes on the behaviour of oil droplets coated with sodium caseinate, additional (simple O/W) emulsions were prepared by mixing sunflower oil (10% volume fraction) with 1% sodium caseinate in PBS + 2 g/L NaCl, which was set at different pH values (1, 3, 5, 7, and 9). The mixture was homogenized at 6000 RPM for 10 minutes. The charge of the resulting emulsion droplets was analysed using Malvern Zetasizer Nano S (Malvern, UK). Prior to analysis, samples were diluted 10 times with deionized water. The measurement was done 3 times for each sample with an equilibration time of 300 s.

Utilization and resistance of bile extract

Pre-culture of *A. muciniphila* was added at 1% v/v to anoxic tryptone media containing different concentration of porcine bile extract (0.05%, 0.1%, 0.5% and 1%, Bile extract porcine, Sigma-Aldrich, USA) . All media were supplemented with 10% v/v of a 125 mM n-acetylglucosamine and 125 mM glucose solution. Each treatment was done in duplicate. The culture was incubated at 37 °C and optical density at 600 nm was measured. Anoxic tryptone medium with sugars was used as the positive control.

Statistical analyses

The cell survival during digestion tests for both treatments (i.e., encapsulated bacteria and control) was analysed using two-way ANOVA on SPSS Statistics (version 23, IBM). One-way ANOVA was used to compare the protection in the gastric test. A Student's t-test in Microsoft Excel 2010 was used to compare the methods to measure droplets size. The analysis of cell release was also done using a paired t-test. Significant differences were considered at the level of $p \leq 0.05$. Standard errors of means were obtained and are shown as error bars in figures and tables.

Results and Discussion

Droplet size characterisation

An important prerequisite for developing the double emulsion delivery system was that the inner water droplets should be large enough to allow encapsulation of *A. muciniphila* cells, which have a size of 0.6 – 1.0 μm (Derrien, et al., 2004). Therefore, the preparation conditions for the primary (W/O) emulsions were chosen such that water droplets (W_1) of around 3.5

µm (Table 1 and Figure 1) were obtained, which is suitable to accommodate single or paired cells of *A. muciniphila*.

Table 1 Average volume weighted mean diameter (D[4,3]) of inner water droplets (W_1) and oil droplets (O) over 4-day storage at 4° C.

Droplets	W_1	O			
Time (h)	0	0	24	48	96
Average D[4,3] (µm)	3.50±0.30	15.11±0.6	24.00±0.9	24.74±1.3	25.13±1.5
Span	1.33±0.12	1.50±0.04	1.73±0.06	1.60±0.01	1.62±0.07

The fraction of primary emulsion in the total emulsion was chosen such that a high load of bacteria per gram of emulsion was obtained as presented in Table S4. Quite remarkably, the oil droplet diameter increased in 24 hours from 15 µm to a stable value of around 24-25 µm (Table 1). The diameter increased by a 1.6 factor, which is equivalent to a 4.6 swelling factor (defined as the ratio of droplet volume at time *t* to droplet volume at *t*=0). This swelling was consistently observed in various trials of the present study (See Supplementary data Figure S1 and Figure S2). The shift of the distribution of droplet size diameter can be seen in Figure 1. All distributions were overall monomodal and normal.

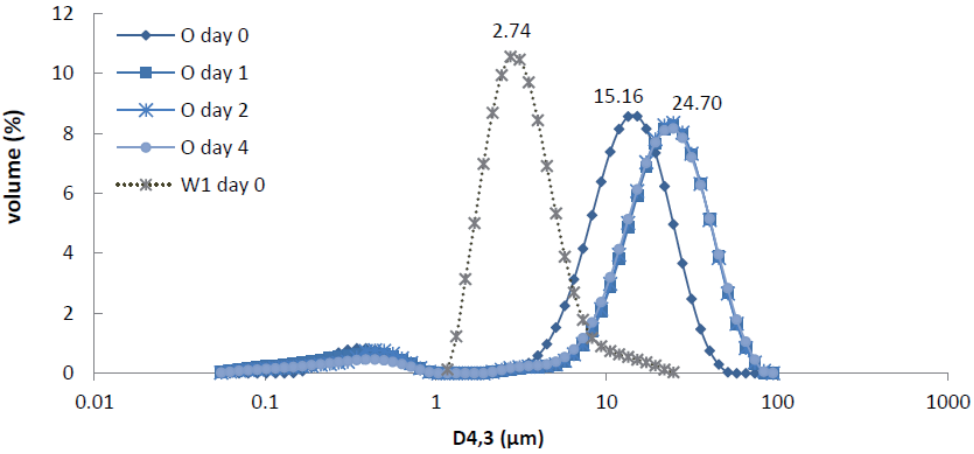

Figure 1. Droplet size distribution of inner water droplets (W_1) in the primary W/O emulsion, and of oil droplets (O) in the double emulsion over 4 day storage at 4 °C.

Both coalescence of oil droplets or water diffusion from outer to inner water phase (swelling) would result in larger droplet diameters. Such a diffusion process was previously shown to occur in comparable double emulsions (Eisinaite, et al., 2016). Although swelling has been shown to be one of the main challenges for the application of double emulsions, it can sometimes be used on purpose to, e.g., increase the emulsion's viscosity post-preparation (Leal-Calderon, et al., 2012, Bahtz, et al., 2015). According to Yan and Pal (Yan and Pal, 2001), water transfer from the external to the internal water phase is mainly caused by osmotic pressure differences that cause rapid swelling. In the present work, the inner and outer water phases were formulated from the same PBS buffer (A); the only differences being sodium caseinate (1% w/v) added to the outer water phase, while the inner water phase contained glycerol stock of bacteria. Based on the following assumptions: final concentration of glycerol in W_1 phase approximately 85.5 mM, sodium related to caseinate was 1.3%, and bacterial cells having the same osmotic pressure as the used buffer, the total osmotic pressure difference was calculated to be 1.96×10^2 Pa. Following Leal-Calderon et al. (Leal-Calderon, et al., 2012), we calculated an induced swelling of a factor or 1.2, while we experimentally determined 4.6 from the oil droplet size. This indicates that also coalescence occurred, and that both effects contributed to the observed increase in droplet size over 24 h.

Encapsulation efficiency and viability

Encapsulation efficiency of double emulsions

The encapsulation efficiency of bacteria was emulated by the use of 1 μm fluorescent particles and calculated with Eq. 4. We found a high initial particle encapsulation efficiency of 97.5%, which decreased to 89.6% after 4 days. As such relatively large hydrophilic particles are unlikely to migrate through the oil phase, the observed decrease was most probably caused by release of inner droplets (W_1) into the outer water phase (W_2), but please note that encapsulation efficiency remained high, and particle release was minimal. When using non-labelled cells, it was found that colonies on BHI-mucus plates were only observed after breaking the emulsion with centrifugation. If the emulsion was not broken, no colonies were observed. This indicates that all viable cell were encapsulated.

Viability during storage

Double emulsions loaded with cells were stored for 3 days in both anaerobic and aerobic conditions. For both conditions, a control was included, consisting of cells simply dispersed

in PBS. After one day, only cells stored anaerobically and dispersed in PBS showed no decrease in viability. After two days, the viability decreased in all conditions, but the viability in the PBS buffer remained high under anaerobic conditions (Figure 2). For the conditions used, no statistical differences were found between any of the end points ($p>0.12$).

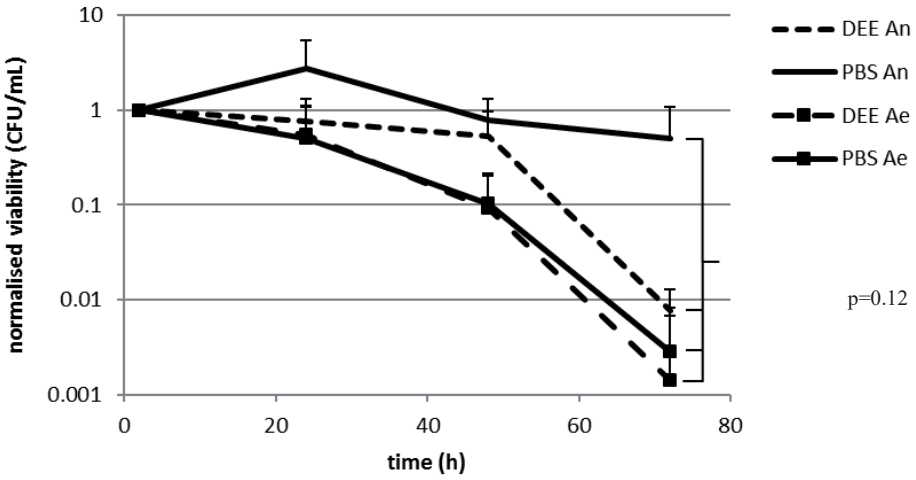

Figure 2. The viability of *A. muciniphila* during storage while encapsulated in a double emulsion or freely dispersed in PBS (DEE = Double Emulsion Encapsulated, PBS = free dispersed in PBS, An = anaerobic, Ae= aerobic). The data were normalised to the viability after two hours. Only the bacteria stored anaerobically in PBS show no decrease in viability over 72h, but the differences were not significant, p=0.12.

Digestive tests

Emulsion morphology during in vitro gastric digestion

Droplet morphology changes in each stage of the simulated digestion, shown in Figure 3. In this series of experiments, the double emulsions had an initial diameter of 17.7 ± 0.3 µm. The microscopic appearance of the double emulsions just after preparation is shown in Figure 3a. When brought into contact with pepsin and electrolytes, the droplets flocculated, which can be seen in Figure 3b. To be complete, immediately after sample addition the pH of the simulated gastric fluid (SGF) increased from pH 3.0 to pH 4.9-5.5, before the system went back to a pH value of 3.0, and this can explain the immediate occurrence of droplet flocculation (as also further explained in the supporting material, Figure S3). Briefly, at pH 5 the zeta potential is low, and electrostatic repulsion between droplets is minimal. Besides, the presence of calcium and other metal ions in the gastric fluid may enhance droplet flocculation through electrostatic screening (Parker and Dalgleish, 1981, Hunt and Dalgleish,

1996, Dickinson, 2010), and calcium bridges may form at low pH with the phosphoseryl residues of α-casein and β-casein. Furthermore, porcine pepsin will hydrolyse caseinate leading to destabilization and coalescence of the double emulsions, since the smaller peptides have a different affinity for the interface (Nik, et al., 2010). After 2 hours exposure to gastric fluid, large oil droplets were present with various morphology as can be seen in Figure 3c, with inner water droplets still present.

At the end of the gastric test, the digestion was shifted to intestinal conditions, and emulsion droplets having a diameter of 10 μm could barely be seen after 2 h (Figure 3d); the few remaining oil droplets seemed nearly depleted from inner droplets. The disappearance of oil droplets was expected, since 70-90% of the fat is hydrolysed in the small intestine of the human body (Maldonado-Valderrama, et al., 2008). Bile salts aid lipolysis by competitively displacing protein emulsifier (Vinarov, et al., 2012), and thus allowing lipase and colipase to adsorb on the lipid surface and carry out lipolysis (Maldonado-Valderrama, et al., 2011), irrespective of droplet size (Begley, et al., 2005).

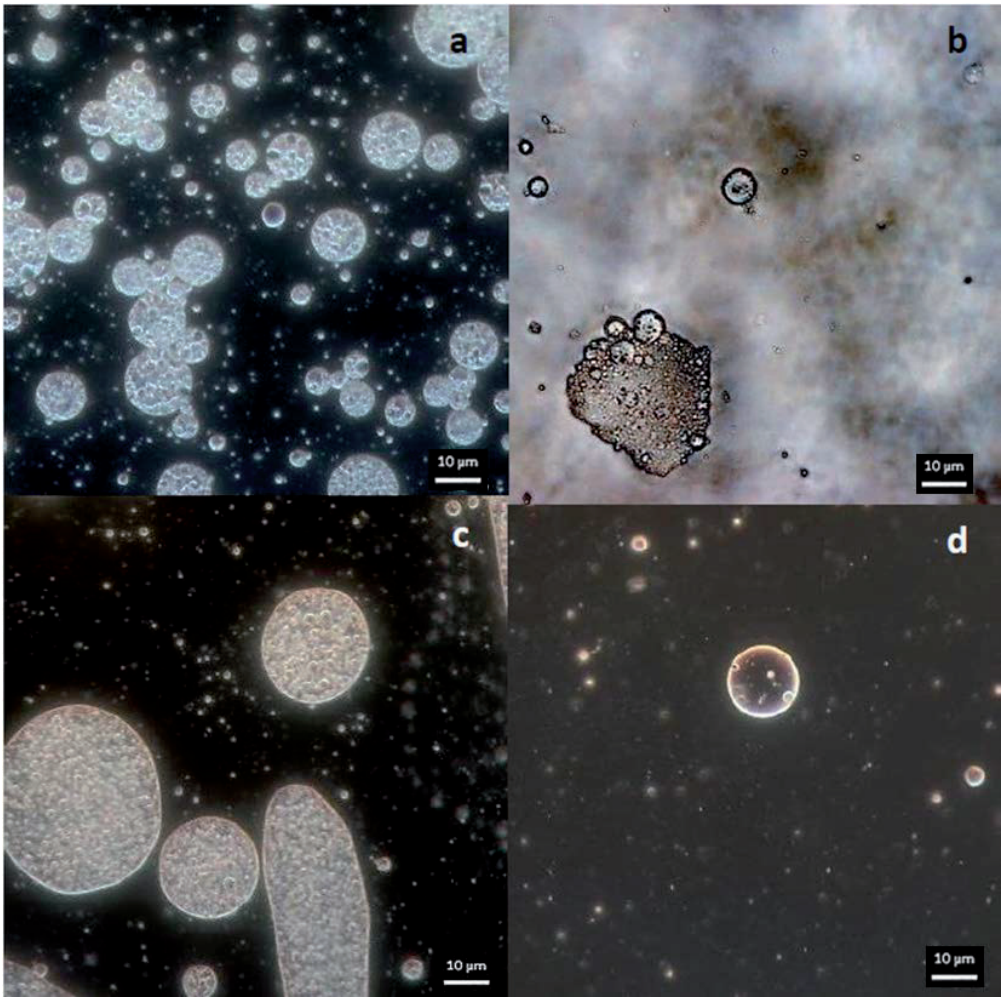

Figure 3. Double emulsion droplet morphology in stages of the simulated gastrointestinal digestion observed at 400X magnification using phase contrast microscopy (a) before digestion (b) flocculation after immediate contact with gastric fluid, (c) after 2 hours gastric conditions (d) after 2h intestinal condition. Bar is 10 µm.

Localisation of entrapped particles and *A. muciniphila* cells during gastric passage

To investigate localisation within the double emulsion when subjected to digestive conditions, a test was done using fluorescently-labelled bacteria (Figure 4). Right after preparation, cells were observed in the inner water phase (Figure 4a), and during the gastric phase (see Figure 4b), the cells remained there even though the oil globules were coalescing. In this phase, contact of bacterial cells and gastric fluid was minimized, which is very important to create a protective effect (see encapsulation section). The oil droplets that appear

as opaque spheres during the intestinal phase (Figure 4c), did not contain labelled bacteria but the continuous phase of the digested emulsion did.

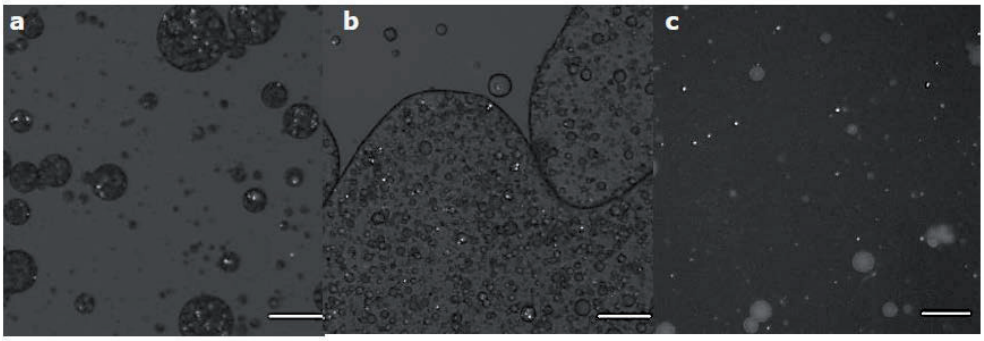

Figure 4. Double emulsions with fluorescence-labelled cells during each stage of simulated digestion (a) before digestion (b) after gastric phase (c) after intestinal phase. The bar represents 20 μm. Cells were observed as white dots. Oil globules that don't contain cells show up as opaque spheres.

The release of cells was confirmed by total viable cell counting of samples obtained after the intestinal phase (with and without breaking the emulsion), and the total numbers of bacteria were shown to be similar ($p > 0.05$; Figure 5). This also indicates that most cells were released at the end of the intestinal phase, given their sensitivity to the digestive conditions used.

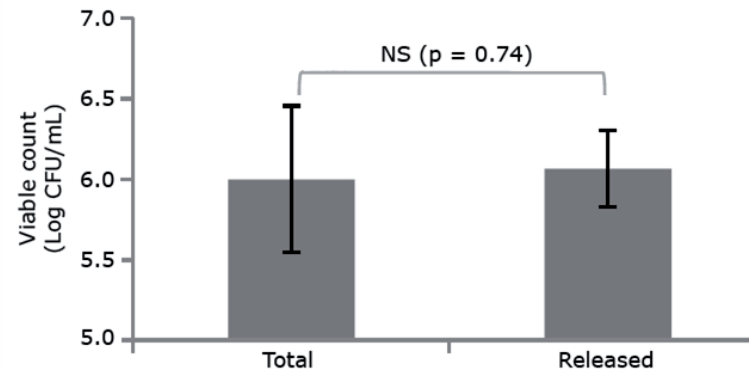

Figure 5. The viability of released *A. muciniphila* after in vitro digestion. The total amount of cells was obtained by breaking the emulsion, the released fraction by directly plating the digestate. There is no observed difference ($p = 0.74$) between the total amount and released bacteria.

Increased viability of encapsulated A. muciniphila during gastric passage

A. muciniphila survival was tested throughout simulated digestion using double emulsions and appropriate controls (freely dispersed cells in PBS buffer that have received the same processing as the double emulsion or are only dispersed (Figure 6). The relative viability of the non-encapsulated bacteria in the gastric juice (2 hours) decreased by more than 100-fold,

and only 0.4% of the control bacteria survived. The non-processed bacteria showed an even higher loss of viability in the gastric phase since only 0.02% survived. On the other hand, the bacteria encapsulated in the double emulsion were more resistant to the gastric phase, leading to an equivalent survival of 6.6%. All differences are significant ($p<0.05$), also after the intestinal phase during which the viability increased for both controls in PBS, but further decreased for the encapsulated bacteria. This could be due to the delayed exposure to bile that may stimulate the growth of *A. muciniphila* (see Figure S4).

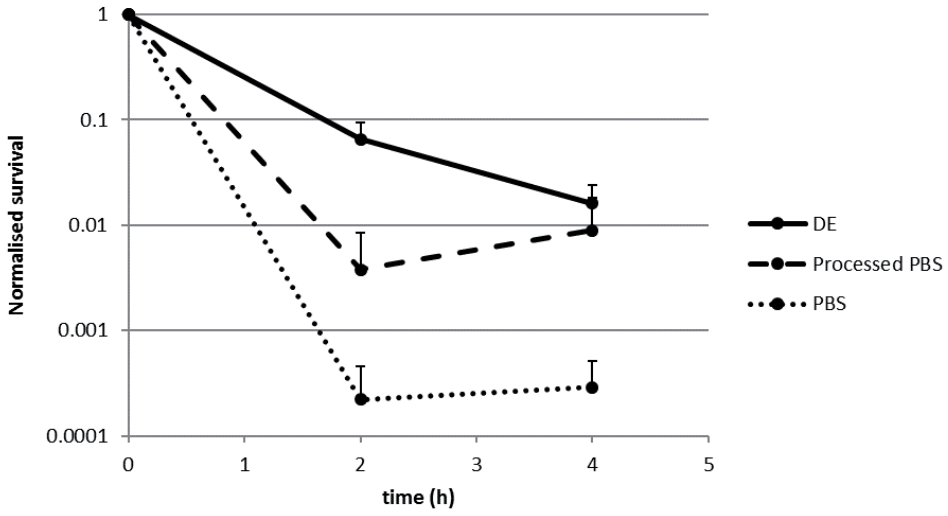

Figure 6. The normalised survival of *A. muciniphila* after 2 hours incubation in gastric juice and subsequent 2 hours incubation in intestinal fluid. Bacteria encapsulated in a double emulsion (DE, full line) had a higher survival than bacteria that were mechanically processed in PBS (dashed line). The lowest survival was obtained for bacteria that were only dispersed in PBS (dotted line). Error bars indicate standard deviation, only positive values are indicated.

Other researchers have reported the use of double emulsion microencapsulation for probiotic species. Similar results were observed with *Lactobacillus acidophilus* (Shima, et al., 2006) in which encapsulation at inner phase volume ratios between 0.03 and 0.45 resulted in 10-100 times higher survival after 2 hours gastric testing. Double emulsion encapsulation of *L. rhamnosus* (Pimentel-Gonzalez, et al., 2009) also exhibited approximately 100 times higher survival difference compared to control. However, this higher survivability cannot be directly compared to those of *A. muciniphila,* mainly due to different sensitivity to dissolved oxygen (Jyoti, et al., 2004, Talwalkar and Kailasapathy, 2004), (Ouwerkerk, et al., 2016). It is known that oxygen, other gases and small non-electrolyte solutes can diffuse through oil and

membranes (Walter and Gutknecht, 1986), and the resulting stress may have induced tolerance in the cells which could explain the difference between processed and non-processed cells dispersed in PBS (den Besten, et al., 2010, Abee, et al., 2011).

Conclusion

We have shown that the viability of *A. muciniphila* after passage through an *in vitro* gastric system is enhanced by its encapsulation in a double emulsion. Upon addition of the emulsion to gastric conditions, the oil droplets flocculate, but the bacteria remain entrapped inside the inner water phase. Upon the introduction of intestinal liquid, the emulsion is digested and the bacteria are released. Hence, double emulsions seems to be promising systems for encapsulation and targeted intestinal delivery of health-promoting bacteria.

References

1 Abee, T., Wels, M., de Been, M., and den Besten, H. (2011) From transcriptional landscapes to the identification of biomarkers for robustness, *Microbial Cell Factories* **10**.

2 Anal, A.K., and Singh, H. (2007) Recent advances in microencapsulation of probiotics for industrial applications and targeted delivery, *Trends in Food Science & Technology* **18**: 240-251.

3 Bahtz, J., Gunes, D.Z., Hughes, E., Pokorny, L., Riesch, F., Syrbe, A., et al. (2015) Decoupling of mass transport mechanisms in the stagewise swelling of multiple emulsions, *Langmuir* **31**: 5265-5273.

4 Begley, M., Gahan, C.G.M., and Hill, C. (2005) The interaction between bacteria and bile, *FEMS Microbiol Rev* **29**: 625-651.

5 Benichou, A., Aserin, A., and Garti, N. (2004) Double emulsions stabilized with hybrids of natural polymers for entrapment and slow release of active matters, *Adv Colloid Interface Sci* **108-109**: 29-41.

6 Clemente, J.C., Ursell, L.K., Parfrey, L.W., and Knight, R. (2012) The impact of the gut microbiota on human health: an integrative view, *Cell* **148**: 1258-1270.

7 Corcoran, B.M., Stanton, C., Fitzgerald, G.F., and Ross, R.P. (2005) Survival of probiotic lactobacilli in acidic environments is enhanced in the presence of metabolizable sugars, *Appl Environ Microbiol* **71**: 3060-3067.

8 den Besten, H.M.W., Arvind, A., Gaballo, H.M.S., Moezelaar, R., Zwietering, M.H., and Abee, T. (2010) Short- and Long-Term Biomarkers for Bacterial Robustness: A Framework for Quantifying Correlations between Cellular Indicators and Adaptive Behavior, *PLoS One* **5**.

9 Derrien, M., Vaughan, E.E., Plugge, C.M., and de Vos, W.M. (2004) Akkermansia muciniphila gen. nov., sp nov., a human intestinal mucin-degrading bacterium, *Int J Syst Evol Microbiol* **54**: 1469-1476.

10 Dickinson, E. (2010) Flocculation of protein-stabilized oil-in-water emulsions, *Colloids and Surfaces B-Biointerfaces* **81**: 130-140.

11 Eisinaite, V., Juraite, D., Schroen, K., and Leskauskaite, D. (2016) Preparation of stable food-grade double emulsions with a hybrid premix membrane emulsification system, *Food Chem* **206**: 59-66.

12 Everard, A., Belzer, C., Geurts, L., Ouwerkerk, J.P., Druart, C., Bindels, L.B., et al. (2013) Cross-talk between Akkermansia muciniphila and intestinal epithelium controls diet-induced obesity, *Proc Natl Acad Sci U S A* **110**: 9066-9071.

13 Hunt, J.A., and Dalgleish, D.G. (1996) The effect of the presence of KCl on the adsorption behaviour of whey protein and caseinate in oil-in-water emulsions, *Food Hydrocolloids* **10**: 159-165.

14 Jyoti, B.D., Suresh, A., and Venkatesh, K.V. (2004) Effect of preculturing conditions on growth of Lactobacillus rhamnosus on medium containing glucose and citrate, *Microbiological Research* **159**: 35-42.

15 Krasaekoopt, W., Bhandari, B., and Deeth, H. (2003) Evaluation of encapsulation techniques of probiotics for yoghurt, *International Dairy Journal* **13**: 3-13.

16 Leal-Calderon, F., Homer, S., Goh, A., and Lundin, L. (2012) W/O/W emulsions with high internal droplet volume fraction, *Food Hydrocolloids* **27**: 30-41.

17 Maldonado-Valderrama, J., Wilde, P., Macierzanka, A., and Mackie, A. (2011) The role of bile salts in digestion, *Advances in Colloid and Interface Science* **165**: 36-46.

18 Maldonado-Valderrama, J., Woodward, N.C., Gunning, A.P., Ridout, M.J., Husband, F.A., Mackie, A.R., et al. (2008) Interfacial characterization of beta-lactoglobulin networks: Displacement by bile salts, *Langmuir* **24**: 6759-6767.

19 Marchesi, J.R., Adams, D.H., Fava, F., Hermes, G.D., Hirschfield, G.M., Hold, G., et al. (2016) The gut microbiota and host health: a new clinical frontier, *Gut* **65**: 330-339.

20 Minekus, M., Alminger, M., Alvito, P., Ballance, S., Bohn, T., Bourlieu, C., et al. (2014) A standardised static in vitro digestion method suitable for food - an international consensus, *Food & Function* **5**: 1113-1124.

21 Nik, M.M., Wright, A.J., and Corredig, M. (2010) Interfacial design of protein-stabilized emulsions for optimal delivery of nutrients, *Food & Function* **1**: 141-148.

22 Ouwerkerk, J.P., van der Ark, K.C., Davids, M., Claassens, N.J., Robert Finestra, T., de Vos, W.M., and Belzer, C. (2016) Adaptation of Akkermansia muciniphila to the oxic-anoxic interface of the mucus layer, *Appl Environ Microbiol*.
23 Parker, T.G., and Dalgleish, D.G. (1981) Binding of Calcium-Ions to Bovine Beta-Casein, *Journal of Dairy Research* **48**: 71-76.
24 Pimentel-Gonzalez, D.J., Campos-Montiel, R.G., Lobato-Calleros, C., Pedroza-Islas, R., and Vernon-Carter, E.J. (2009) Encapsulation of Lactobacillus rhamnosus in double emulsions formulated with sweet whey as emulsifier and survival in simulated gastrointestinal conditions, *Food Research International* **42**: 292-297.
25 Plovier, H., Everard, A., Druart, C., Depommier, C., Van Hul, M., Geurts, L., et al. (2016) A purified membrane protein from Akkermansia muciniphila or the pasteurized bacterium improves metabolism in obese and diabetic mice, *Nat Med*.
26 Quevrain, E., Maubert, M.A., Michon, C., Chain, F., Marquant, R., Tailhades, J., et al. (2016) Identification of an anti-inflammatory protein from Faecalibacterium prausnitzii, a commensal bacterium deficient in Crohn's disease, *Gut* **65**: 415-425.
27 Sahin, S., Sawalha, H., and Schroën, K. (2014) High throughput production of double emulsions using packed bed premix emulsification, *Food Research International* **66**: 78-85.
28 Shima, M., Morita, Y., Yamashita, M., and Adachi, S. (2006) Protection of Lactobacillus acidophilus from the low pH of a model gastric juice by incorporation in a W/O/W emulsion, *Food Hydrocolloids* **20**: 1164-1169.
29 Solanki, H.K., Pawar, D.D., Shah, D.A., Prajapati, V.D., Jani, G.K., Mulla, A.M., and Thakar, P.M. (2013) Development of microencapsulation delivery system for long-term preservation of probiotics as biotherapeutics agent, *Biomed Res Int* **2013**.
30 Su, J.H., Flanagan, J., and Singh, H. (2008) Improving encapsulation efficiency and stability of water-in-oil-in-water emulsions using a modified gum arabic (Acacia (sen) SUPER GUM (TM)), *Food Hydrocolloids* **22**: 112-120.
31 Talwalkar, A., and Kailasapathy, K. (2004) The role of oxygen in the viability of probiotic bacteria with reference to L. acidophilus and Bifidobacterium spp, *Curr Issues Intest Microbiol* **5**: 1-8.
32 Udayappan, S., Manneras-Holm, L., Chaplin-Scott, A., Belzer, C., Herrema, H., Dallinga-Thie, G.M., et al. (2016) Oral treatment with Eubacterium hallii improves insulin sensitivity in db/db mice **2**: 16009.
33 van der Graaf, S., Schroen, C.G.P.H., and Boom, R.M. (2005) Preparation of double emulsions by membrane emulsification - a review, *Journal of Membrane Science* **251**: 7-15.
34 van Nood, E., Vrieze, A., Nieuwdorp, M., Fuentes, S., Zoetendal, E.G., de Vos, W.M., et al. (2013) Duodenal infusion of donor feces for recurrent Clostridium difficile, *N Engl J Med* **368**: 407-415.
35 Vinarov, Z., Tcholakova, S., Damyanova, B., Atanasov, Y., Denkov, N.D., Stoyanov, S.D., et al. (2012) Effects of emulsifier charge and concentration on pancreatic lipolysis: 2. Interplay of emulsifiers and biles, *Langmuir* **28**: 12140-12150.
36 Walter, A., and Gutknecht, J. (1986) Permeability of Small Nonelectrolytes through Lipid Bilayer-Membranes, *Journal of Membrane Biology* **90**: 207-217.
37 Wang, L., Christophersen, C.T., Sorich, M.J., Gerber, J.P., Angley, M.T., and Conlon, M.A. (2011) Low relative abundances of the mucolytic bacterium Akkermansia muciniphila and Bifidobacterium spp. in feces of children with autism, *Appl Environ Microbiol* **77**: 6718-6721.
38 Yan, J., and Pal, R. (2001) Osmotic swelling behavior of globules of W/O/W emulsion liquid membranes, *Journal of Membrane Science* **190**: 79-91.

Supplementary Information

Supplementary Materials and Methods

Table S1 Optical index values used in droplets size distribution measurement

Emulsion	Refractive index of dispersed phase	Absorption index of dispersed phase	Refractive index of dispersant
W1/O	1.333	0.01	1.469
W1/O/W2	1.465	0.01	1.333

Table S2 Conditions and components of simulated digestion model. Composition of SGF and SIF is given in Table S3

			Example			
Phase	**Conditions**	**Solutions**	**Stock concentration**	**Vol. Stock**	**Conc. In SGF**	
Gastric	pH 3, 37˚C, mixed, gradual oxygen decrease to 0%	Simulated Gastric Fluid (SGF)*	1.25x	187.5 mL	1x	**SGF:emulsion = 1:1**
		Double emulsion	-	250 mL	-	
		Porcine pepsin	0.1 g/mL	40 mL	0.8%	
		$CaCl_2$ (add to pepsin)	0.3 M	125 µL	0.075 mM	
		H_2SO_4	0.5M	-	Equiv. pH3.0	
		water	-	17.5 mL	-	
		Total volume reactions		500 mL		
Stopping	Incubated on ice, 10 min	NaOH	0.5 M		Equiv. pH 6.5-7	For gastric phase sampling
Intestinal	pH 7, 37˚C, mixed, anaerobic	Simulated Intestinal Fluid (SIF)*	1.25x	137.5 mL	1x	**SIF:emulsion= 1:1**
		Gastric chyme	-	250 mL	-	
		NaOH	3 M	-	Equiv. pH 7.0	

	Porcine pancreatin	8 mg/mL	62.5 mL	1 mg/mL
	Porcine bile	68.75 mg/mL	31.25 mL	10 mM
	$CaCl_2$ (add to bile)	0.3 M	250 µL	0.3 mM
	water	-	16.5 mL	
	Total volume reaction		500 mL	
Stopping	Incubate on ice, 10 min			

Table S3 Composition of SGF and SIF

	Stock		**SGF** (pH 3)		**SIF** (pH 7)	
Constituent	**Stock Concentration**		**Vol. of stock**	**Conc. in SGF**	**Vol. of stock**	**Conc. in SIF**
	(g/L)	**(mol/L)**	**(mL)**	**(mmol/L)**	**(mL)**	**(mmol/L)**
KCl	37.3	0.5	25.875	6.9	17	6.8
KH_2PO_4	68	0.5	3.375	0.9	2	0.8
$NaHCO_3$	84	1	46.875	25	106.25	85
NaCl	117	2	44.25	47.2	24	38.4
$MgCl_2(H2O)_6$	30.5	0.15	1.5	0.1	2.75	0.33
$(NH_4)2CO_3$	48	0.5	1.875	0.5	-	-
NaOH		1	-	-	-	-
HCl		6	4.875	15.6	1.75	8.4
Water			**Make up to 1500 ml**		**Make up to 1000mL**	

Supplementary Results

A. muciniphila load in double emulsions

Table S4 Calculation of *A. muciniphila* load and inner water droplets per gram of double emulsions with different fractions of dispersed phase (with loading 10^9 *A. muciniphila*/ml in W1). The bacterial load increases with the increase of fraction of primary emulsion.

Fraction of W1 in primary emulsion	**Fraction of primary emulsion in double emulsion**	**Number of Akkermansia/g double emulsion**	**Number of inner water droplets/g double emulsion**
25	10	2.5×10^6	7.5×10^8
30	10	3.0×10^6	9.0×10^8
30	30	9.0×10^6	2.7×10^9
40	30	1.2×10^7	3.6×10^9

Morphology and droplet sizes of double emulsions

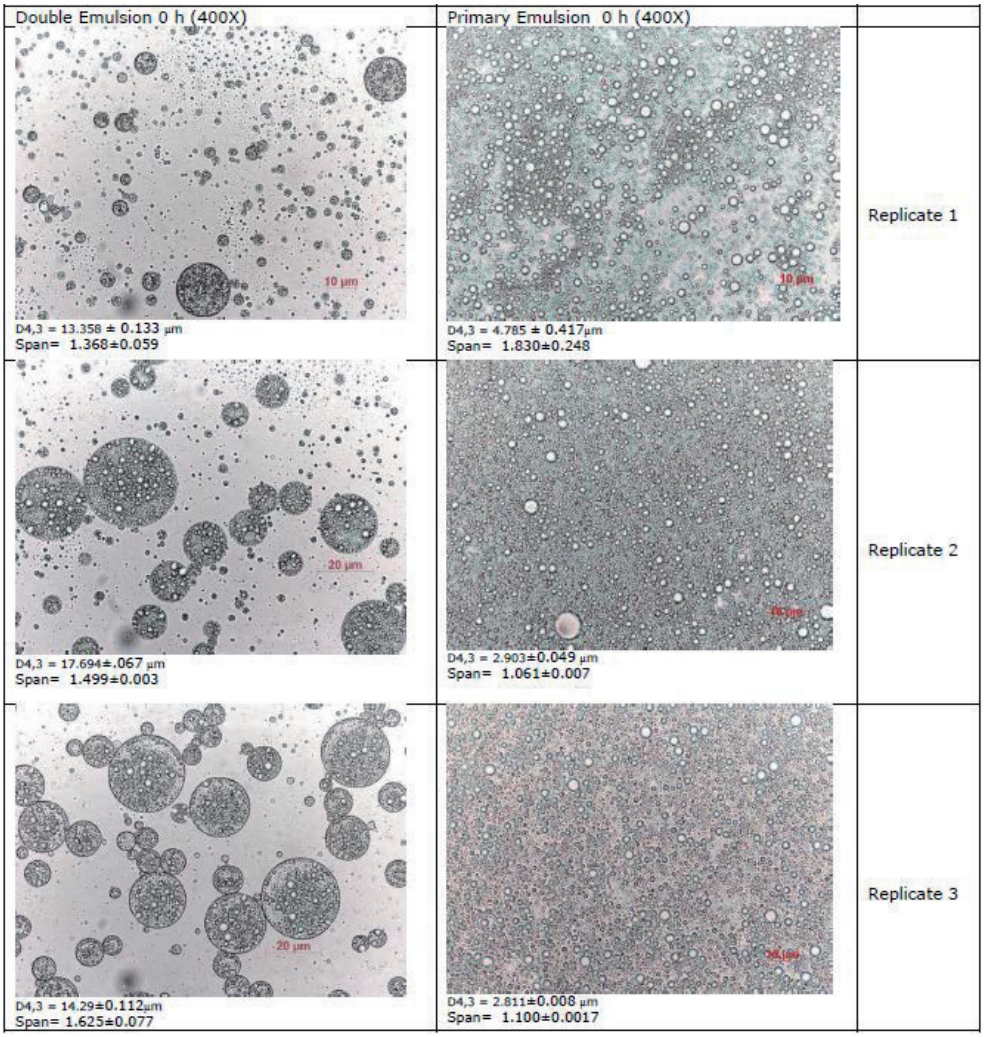

Figure S1. Morphology and droplet sizes of double emulsions at t=0

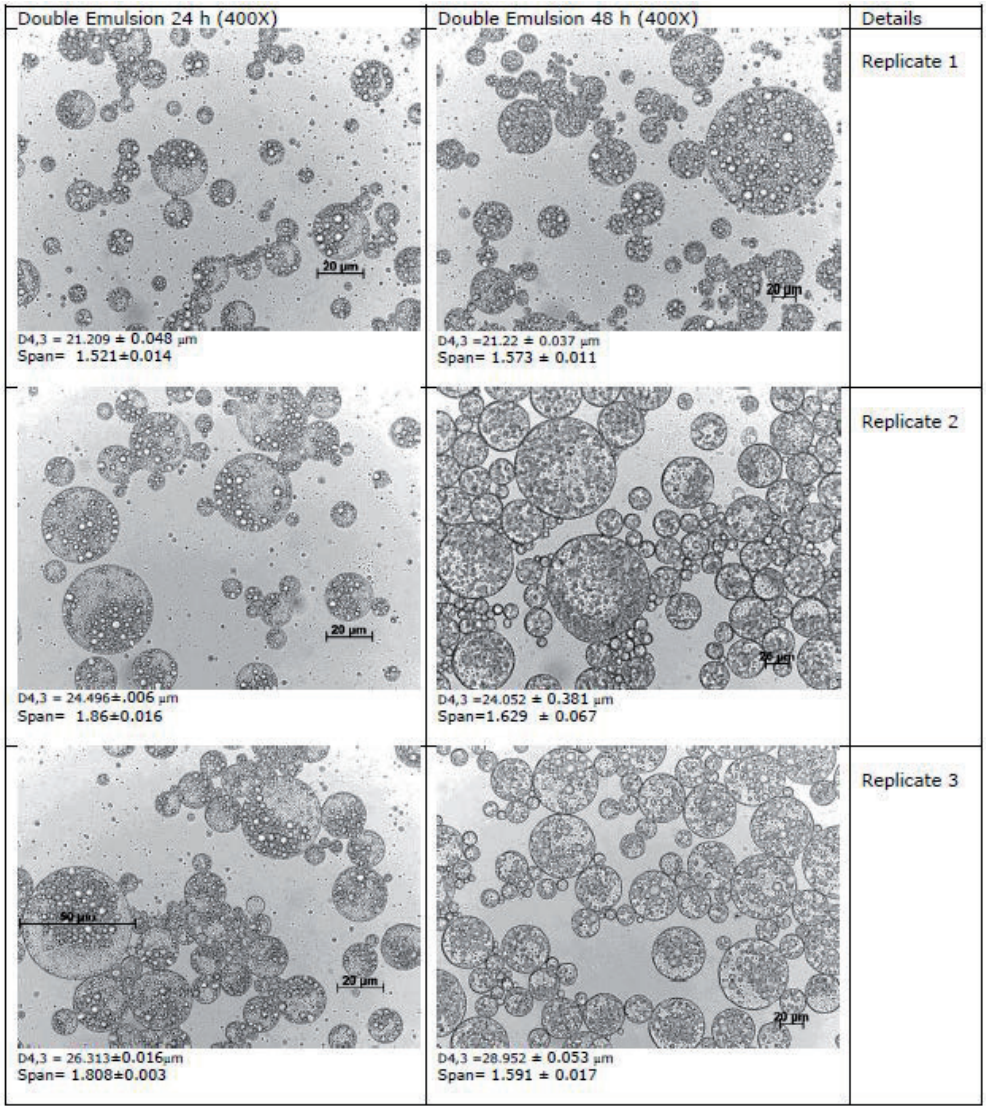

Figure S2. Morphology and droplet sizes of double emulsions after 24 hours and 48 hours

Emulsion stability under changing pH conditions

The stability of protein-stabilized emulsions is heavily influenced by the droplet surface charge (Xu, Wu, & Xu, 2007), and often ±30 mV is accepted as the threshold for stable emulsions (Everett, 1988). The emulsion is subjected to a low pH in the gastric system, therefore the physical stability of oil droplets was investigated by measuring the zeta potential

of sodium caseinate-stabilized simple emulsions at various pH. As can be seen in Figure S3, sodium caseinate can contribute to stable emulsions when the pH values are above 6.0. Below pH 6.0, the zeta potential increased and reached 0 mV at the isoelectric point (IEP = pH 4.5) which is close to the IEP of native casein (pH 4.6) (Liu, Cui, Mao, & Guo, 2012). The zeta potential then became positive below the IEP, but it never reached higher than +30 mV in the measured pH range, therefore below pH 6.0 flocculation of oil droplets could be expected.

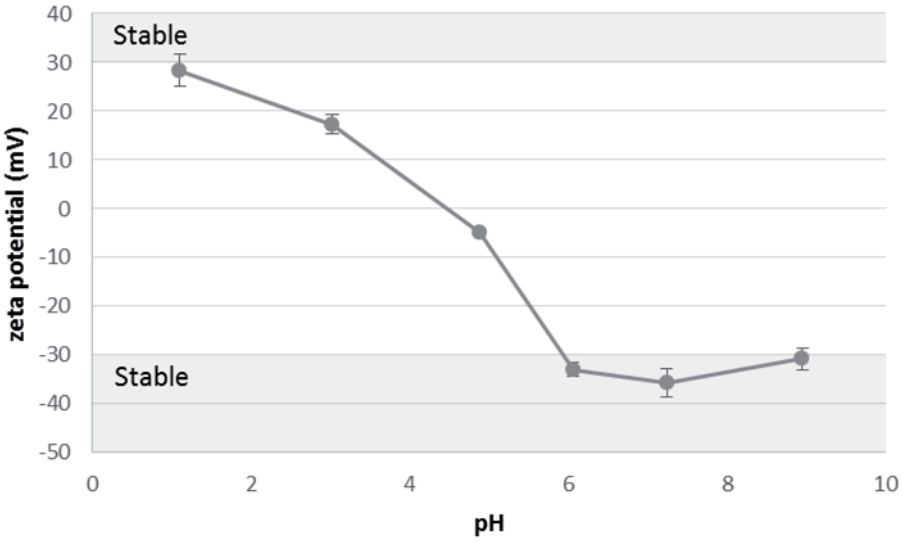

Figure S3. Zeta potential of oil droplets stabilized by sodium caseinate. Values are mean ± standard deviations from triple measurements. The areas highlighted in grey indicate stable conditions.

Growth of *A. muciniphila* on bile

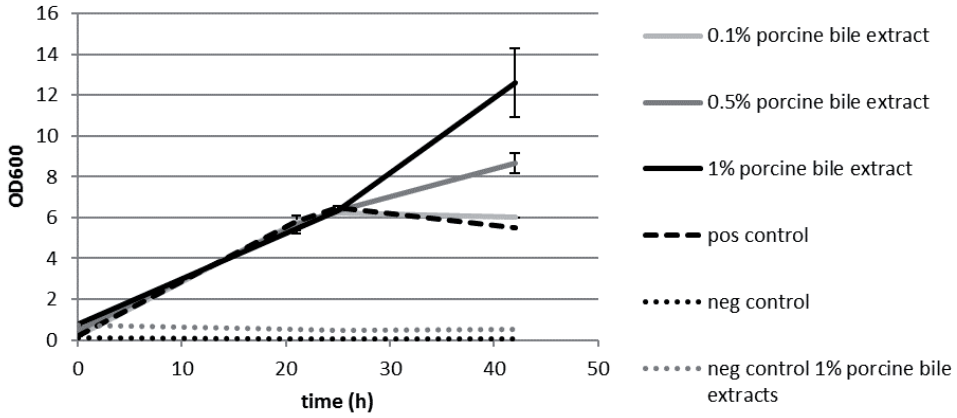

Figure S4 Growth of *A. muciniphila* on medium supplemented with 0.1%, 0.5% and 1% porcine bile extract. Normal growth was observed in the medium without supplemented bile extract (dashed line – no bile added), while growth was increased by porcine bile extract (full lines). No growth was observed in the negative controls (dotted line – no *A. muciniphila* cells added).

Supplementary References

Everett, D. H. (1988). *Basic Principles of Colloid Science* London: The Royal Society of Chemistry.

Liu, Y., Cui, Y. J., Mao, H. Y., & Guo, R. (2012). Calcium Carbonate Crystallization in the Presence of Casein. *Crystal Growth & Design, 12* (10), 4720-4726.

Xu, R. L., Wu, C. F., & Xu, H. Y. (2007). Particle size and zeta potential of carbon black in liquid media. *Carbon, 45* (14), 2806-2809.

CHAPTER 7

General Discussion

General Discussion

This thesis describes detailed studies on the growth, metabolism and application of *Akkermansia muciniphila,* a symbiont colonizing the human gut. The aims of this thesis were to investigate the growth requirements of *A. muciniphila* for the development of a minimal medium, a synthetic medium free from animal components and viable delivery to the host. These aims were defined based on the need for a detailed physiological characterization of *A. muciniphila* and developing mechanistic insight into interactions between *A. muciniphila* and the host.

Causality and using genome-scale metabolic models in gut microbiota research

The bacterial composition in our gut has been subjected to many studies over the past decade, showing a great variety of correlations between bacterial groups and parameters of health (De Vos and De Vos, 2012). It has been well established that the intestinal bacteria can influence food digestion as well as affect immune and metabolic regulation. On the other hand, the intestinal bacterial composition and activity can be modulated by diet as well as medication (Actis, et al., 2014, Lee and Ko, 2014, Roopchand, et al., 2015, Zoetendal and Vos, 2014). It is expected that more research will focus on establishing the causality and molecular details of the bacteria-host interactions by thorough mechanistic and human interventions studies. Detailed studies of cultured representatives of bacteria involved in the correlations with health and disease is among the first prerequisites, as described in chapter 2 (van der Ark, et al., 2017).

To obtain unambiguous causative relations and detailed mechanistic insight in bacteria-host interactions, several microbiota-based therapies are currently applied. The least specific interventions are exploiting faecal microbiota transplantations (FMT) or influencing the abundance of bacterial species by prebiotic and other dietary compounds (Anhe, et al., 2015, Gibson, et al., 2017, Gupta, et al., 2016, Roopchand, et al., 2015). Recent insights and developments allow more specific interventions, which can result in mechanistic insights. These studies include the administration of cultured bacteria or derivatives in human subjects or patients. Another way is the specific suppression or inactivation of bacteria by the use of bacteriophages. The different therapies may have variable efficacies in clinical trials. It has been widely established that dietary interventions can change the microbiota (Cotillard, et al., 2013, Dao, et al., 2016), but have not been found to cure diseases (Vieira, et al., 2016).

In some cases, the use of presently known probiotic bacteria has found to provide a positive influence on the prevention or development of a disease or metabolic disorders but convincing and robust evidence is lacking (Vieira, et al., 2016). These cases included studies using specific probiotic strains (Derrien and van Hylckama Vlieg, 2015), including bifidobacteria (Tojo, et al., 2014) and lactobacilli (Wang, et al., 2015). The use of other potential beneficial bacteria in intervention studies is limited to mouse models and include members of the natural microbiota and possible therapeutic microbes, such as *Eubacterium hallii* (Udayappan, et al., 2016), *Faecalibacterium prausnitzii* (Rossi, et al., 2015), *Butyricicoccus pullicaecorum* (Eeckhaut, et al., 2014), *Clostridium butyricum* (Kanai, et al., 2015), and *A. muciniphila* (Everard, et al., 2013, Plovier, et al., 2017). From all different intervention studies, only FMT has shown to be functional in curing several diseases, including recurrent *Clostridium difficile* infection (de Vos, 2013, van Nood, et al., 2013).

Next to these preclinical studies, cause-effect studies in human are essential to further advance the field and provide the necessary basis for performing mechanistic studies. For this purpose, cultured bacteria are needed that can be used in human interventions.

In chapter 2 we provide a thorough description on predicting growth medium parameters of bacteria based on their genomes, providing insight on how pure cultures can be optimally grown. Based on whole genome sequences, predictions can be made on organism autotrophies for example by identifying the synthesis pathways for e.g. amino acids that are present and absent. The genome sequences can also be used to create genome-scale metabolic models (GEMs). These GEMs can be used to study the metabolic capacities of a bacterium and thereby aid in defining a minimal medium. Based on these minimal media, a systems cycle can be initiated to improve the GEM: predictions by the GEM can be validated using the minimal medium, after which the new discoveries can be implemented in the GEM again, resulting in altered predictions and an improved GEM. The GEM can subsequently be used to generate new hypotheses. Moreover, with an improved GEM, novel phenotypes can be better predicted. The possible phenotypes combined with data on niche composition, including bacterial communities, can be used to predict *in vivo* functionality. It is worth notifying that the present predictions are limited to interactions based on metabolites, and do not include immunomodulation by proteins.

The GEMs have various limitations, including their dependence on (appropriate) annotation, the inability to include proteins or peptides, and the failure to predict immunomodulation that all could underestimate the role of bacteria in gut health. Multiple studies have found interactions between bacterial species and the host, including *A. muciniphila* and *F. prausnitzii* (Plovier, et al., 2017, Quevrain, et al., 2016).

In spite of the above-described shortcomings, GEMs are still a valuable tool in helping to understand the role of the microbiota. Also without the incorporation of immunomodulation in GEMs, it was recently shown that GEMs can be used to design dietary interventions in humans (Shoaie, et al., 2015). As described above, the host diet has influence on the microbial composition and the degradation of dietary components by bacteria has influence on host health. Such research is possible only by understanding the behaviour of the microbes.

The use of the *A. muciniphila* GEM to design a minimal medium

An initial GEM for *A. muciniphila* was constructed based on the full genome annotation and validated using non-defined media (Ottman, et al., 2017). This GEM was updated and used in chapter 3 to support the design of a minimal and synthetic medium for the effective growth of *A. muciniphila*. We confirmed the prediction of L-threonine essentiality for the growth of *A. muciniphila*, whereas the sugar-degrading capabilities were generally predicted correctly. However the model required optimization to fully understand the metabolism of *A. muciniphila.* To discover misinterpretations of metabolism by the model, it is important to also understand the steps taken in the construction of the model. One of the important steps in creating a functional model is the use of gap-filling algorithms (Henry, et al., 2010, Orth and Palsson, 2010). These algorithms, as the name suggests, fill gaps in the metabolic pathways that are not predicted in the initial draft model. These gaps can be caused by wrong annotation of genes or the absence of annotated genes with the assumption that the functionality should be present. In case of such an incorrect annotation, or assumed presence of functionality, the gap filling does not result in mistakes in the model, but just fill gaps. However, if the filled gaps represent reactions that are really absent in the genome of the organism, it leads to erroneous predictions. The latter was the case for the wrongly filled gap in the conversion of fructose-6-phosphate (Fru6P) to glucosamine-6-phosphate (GlcN6P), mediated by the enzyme GlcN6P synthase GlmS in the *A. muciniphila* GEM. The filling of this gap led to the prediction that glucose could be used as carbon source and converted into

GlcN6P via Fru6P. We showed in chapter 3 that is was not the case, because the only enzyme mediating the conversion between Fru6P and GlcN6P in *A. muciniphila*, named NagB, was found to prefer the reaction in the direction of Fru6P. Hence, it was discovered that N-acetylglucosamine (GlcNAc) or N-acetylgalactosamine (GalNAc) cannot be synthesized de novo from glucose and hence are essential for the growth of *A. muciniphila*, and thus need to be present in the growth medium. The composition of the developed media was therefore mainly based on the supplementation of GlcNAc or GalNAc.

The genome of *A. muciniphila* predicts the presence of peptidoglycan and recently it was demonstrated that *A. muciniphila* does produce this important cell-wall component using chemical microbiology (T Sminia PhD thesis: Probing the bacterial cell wall with chemical biology tools - 2017). The absence of GlmS is unique for bacteria that produce peptidoglycan and its precursor uridine diphosphate (UDP)-GlcNAc (Figure 1) (Barreteau, et al., 2008). The constant availability of GlcNAc and GalNAc provided by the host resulted in an effective way of UDP-GlcNAc synthesis. The synthesis of UDP-GlcNAc usually involves the subsequent phosphorylation, amination and acetylation of glucose to yield the same end product. This normally requires one glutamine for amination and one acetyl-CoA for acetylation. Both steps require ATP, one for the synthesis of glutamine for amination of Fru6P (Harper, et al., 2010), and one for the synthesis of acetyl-CoA (Kumari, et al., 2000) (Figure 1). In the case of *A. muciniphila,* GlcNAc is readily provided by the host via the produced mucus. This makes the synthesis of GlcN6P a redundant function in *A. muciniphila,* which could have resulted in the loss of the gene or its function. The shortcut in UDP-GlcNAc synthesis reduces the need of approximately 2 ATP per UDP-GlcNAc synthesized, which gives *A. muciniphila* a competitive advantage over other mucolytic bacteria that need to synthesize UDP-GlcNAc via GlcN6P (Figure 1).

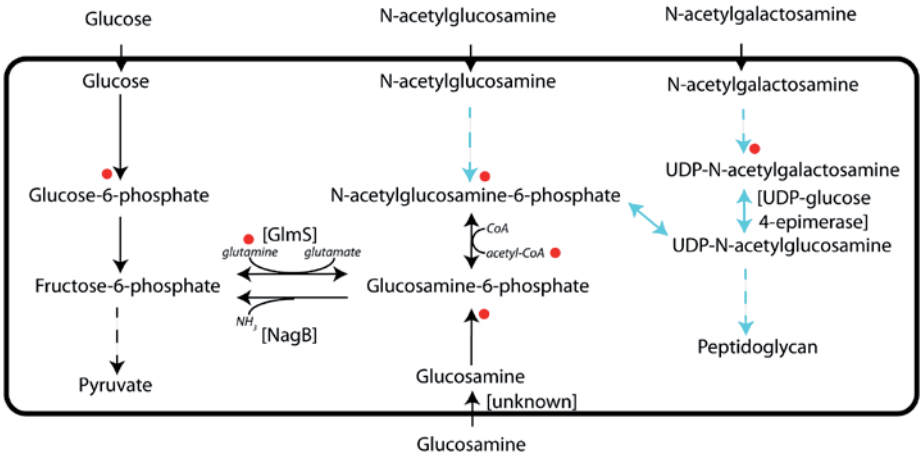

Figure 1. Overview of GlcNAc, glucose, glucosamine and GalNAc utilization and the conversion from GlcN6P to Fru6P. The peptidoglycan shortcut is indicated by blue arrows. Enzymes and transporter between [ ] and co-metabolites are indicated only when required. Dotted arrows indicate multiple reactions. A red dot indicates the consumption of 1 ATP for the production of this substrate at the indicated reaction.

Besides the growth on GlcNAc, we also found similar growth on GalNAc and limited growth on glucosamine (GlcN). Both GlcN and GalNAc degradation were not predicted by the initial model, but observed upon the addition to the minimal medium. Apparently, GalNAc can replace GlcNAc in the minimal medium and hence we assigned an epimerase (UDP-glucose 4-epimerase encoded by the gene on locus Amuc_1125 or Amuc_0029) that potentially mediated the reaction (Figure 1). The degradation of GlcN is predicted to be possible with the addition of a transport reaction, which is not yet annotated in the *A. muciniphila* genome. Therefore, the inability to reach high growth rates and optical densities on this sugar is likely due to limited transport.

The use of GlcNAc directly for peptidoglycan synthesis is mediated by the formation of UDP-GlcNAc. The subsequent use of UDP-GlcNAc for peptidoglycan synthesis is common in all peptidoglycan-forming bacteria (Barreteau, et al., 2008). The conversion between GlcNAc-1P and UDP-GlcNAc is mediated by the uridyltransferase GlmU, encoded by the gene on locus Amuc_0814. The preceding phosphorylation of GlcNAc could be mediated by N-acetylhexosamine 1-kinase, encoded by the gene on locus Amuc_0030, directly adjacent to one of the genes for UDP-glucose 4-epimerase on locus Amuc_0029. These genes indicate the direct use of GlcNAc in peptidoglycan formation (Uehara and Park, 2004). The operon-like structure of the genes for N-acetylhexosamine 1-kinase and UDP-glucose 4-epimerase

could be a lead for the incorporation of GalNAc residues in the cell wall. The use of GalNAc in cell wall polysaccharides has been described before (Leoff, et al., 2008).

The minimal medium was composed based on the previously described CP mineral medium, with the omission of ammonium (Plugge, 2005). To sustain growth for *A. muciniphila*, only GlcNAc (or GalNAc) and L-threonine need to be added. The omission of ammonium indicates that either L-threonine of GlcNAc could serve as nitrogen source. Vitamins, including B12, were added during the experiments. It was described before that vitamin B12 is an important cofactor in the methylmalonyl pathway for the conversion of succinate to propionate (Ottman, et al., 2017). Although not essential for growth, vitamin B12 is important for propionate production, and thereby optimal utilization of the provided sugars in terms of energy gain.

The growth of *A. muciniphila* on minimal medium is approximately 0.08 h^{-1}, depending on the applied combination of sugars. This is around 20% of the growth rate obtained for *A. muciniphila* grown on mucus, which has a doubling time of around 1.5 h (equals a growth rate of 0.46 h^{-1}). Enrichment of the minimal medium with glucose, as predicted by the GEM and shown *in vitro*, increases the growth rate 1.5 fold, from ~0.08 h^{-1} on GlcNAc only to ~0.12 h^{-1} on GlcNAc with the addition of glucose. We expect that the development of this medium paved the road for future physiological studies of *A. muciniphila* and its application as therapeutic microbe.

Combining the GEM with the minimal medium would allow the prediction and verification of physiological properties and phenotypes of *A. muciniphila*. This includes the production of γ-aminobutyric acid (GABA) and the reaction to oxygen as discussed below, but also predictions on interspecies interactions. It was shown that *A. muciniphila* is a keystone species in gut microbiota composition (Arumugam, et al., 2011, Shetty, et al., 2017). This data can be used to determine the co-occurrence of this species with other bacterial species (Shetty, et al., 2017). A function we expect to find in species correlated with the presence of *A. muciniphila* is sulphate reduction. This is expected because of the presence of a dozen sulfatase genes in the genome of *A. muciniphila* (van Passel, et al., 2011), the described sulfatase activity in the supernatant (Derrien, et al., 2004), and presence of sulfate on mucins (Johansson, et al., 2011). The release of sulfate by *A. muciniphila* could be used by sulfate-reducing bacteria (SRB), such as *Desulfovibrio piger* to produce hydrogen sulfide. Hydrogen

sulfide is a mediator in the gut-brain axis (Schicho, et al., 2006). Finally, it could be possible for *A. muciniphila* to use the hydrogen sulfide to produce cysteine, which in turn is used to reduce oxygen. Even though we were not able to prove this hypothesis *in vitro*, such interactions are common in the gut, and are an important contributor to the microbiota composition.

The capacity of *A. muciniphila* to utilize mucus-derived components and its physiological characteristics are indicative of a high degree of adaptation of this microbe to the mucosal environment. The oxygen respiration (discussed below) and the use of GlcNAc in anabolism and catabolism results in the efficient use of available compounds. There are more microbes that show mucolytic capabilities, such as *Bacteroides fragilis.* This anaerobic bacterium is also able to reduce oxygen (Baughn and Malamy, 2004), and can degrade mucus, but is not associated to health in the same way as *A. muciniphila.* Like *A. muciniphila*, *B. fragilis* is also able to remove sialic acid residues from human derived polysaccharides (Godoy, et al., 1993). However, *B. fragilis* was found to be associated with the onset of colorectal cancer in rats and with colorectal cancer development in human (Boleij, et al., 2015, Wu, et al., 2009). From all *Bacteroides* species, *B. fragilis* is most commonly associated with adverse effects (Wexler, 2007). The outcome of competition in the mucus layer between species can be determined by differences in the composition of the mucus layer (Li, et al., 2015). Imposing the conditions found the in mucus layer on GEMs of mucolytic bacteria could be used to predict the outcome of the competition, and ultimately interventions to steer the bacterial composition and diversity of the mucus layer.

Growing *A. muciniphila* for therapeutic applications

The anaerobic preparations of *A. muciniphila* used for the first mouse trials have been described recently (Ouwerkerk, et al., 2017). Further development of the medium and growth conditions for *A. muciniphila* building on an improved GEM for clinical trials is discussed in chapter 4 of this thesis. The minimal medium was supplemented with soy peptone and glucose to increase the growth yield and growth rate. During the medium development, we also investigated the growth on casein digests. We found that the addition of a tryptic digest of casein yield the highest growth rate. As discussed above, the growth rate of *A. muciniphila* on non-mucus medium could be improved by enriching the medium. This was indeed the case after the addition of more complex nitrogen sources. The growth rate on medium

supplemented with soy or casein protein digests reaches the same rate as on mucus medium, ~0.3-0.8 h^{-1}, depending on the type of peptide and sugars present in the medium.

The good growth of *A. muciniphila* on glucose with high concentrations of only tryptone, as described previously (Ottman, et al., 2017a) could be due to the presence of glycosylated casein fractions that may serve as a glycan substrates for growth. These casein glycans contain, like mucosal glycans, different sugar residues, including GalNAc, mannose and galactose in mucin (Johansson, et al., 2011) and galactose and GalNAc in kappa-casein (Neelima, et al., 2013) and GlcNAc, GalNAc, galactose, fucose and mannose in lactoferrin (O'Riordan, et al., 2014). The increased yield and growth rate on casein-derived tryptone can be explained by the presence of these glycans. Combined with the knowledge about growth on different sugars described in chapter 3 and in previous studies (Derrien, et al., 2004, Ottman, et al., 2017a), we hypothesise that the addition of different types of monosaccharides can further increase growth rate and yield. These sugars could include fucose and galactose besides the already used glucose, GlcNAc and GalNAc.

The comparison of growth rate and yield between mucus medium, tryptone medium and soy medium is complicated by the changes in morphology of the bacteria and the opacity of mucus medium. Due to the elongated cell morphology in especially soy medium, the relation between cell number and optical density changes. In general, larger cell scatter more light increasing the optical density and thereby increasing the perceived growth rate of the soy medium (Volkmer and Heinemann, 2011). The suspension of mucus in medium invokes a starting optical density (OD600) of around 0.7, while the other medium types generally not exceed an OD600 of 0.1. Therefore, the measurement of the net increase of OD600 for mucus medium might underestimate the actual growth yield and rate. This is then caused by the supposed degradation of mucus. To determine the real increase of cell density, quantitative PCR or determination of CFUs could be applied.

We showed that the changes in growth medium have no significant effect on therapeutic efficacy in mice. The expression profile of genes involved in cell shape and division suggested that the cells were not dividing normally, which could result in cell death, as discussed in chapter 4. Impaired growth of the bacteria could have an influence on the colonisation properties of the bacteria, resulting in reduced long-term effects. These effects are not incorporated in the study design, because mice are sacrificed at the end of the trial,

and supplemented with bacteria each day during the trial. Therefore, long-term effect studies are required for optimal use of *A. muciniphila* potential. The growth medium would need to be adjusted to decrease cell size if the therapeutic potential is impaired indeed. This could be done by studying the influence of different sugar compositions in the medium, to mimic the glycan composition of mucin. It remains to be established how the changed cellular morphology affects the metabolic impact and colonization capacity of *A. muciniphila* in mice or human.

***A. muciniphila* oxygen reduction capacities**

The niche adaptation of *A. muciniphila* is not only manifested in the GlcNAc-mediated mucin dependency, but also in the oxygen tolerance of *A. muciniphila*, as discussed in chapter 5. While initially *A. muciniphila* has been described as a strict anaerobe, we observed that this bacterium is capable of reducing low amounts of oxygen and use it for respiration. The mechanism that is employed by *A. muciniphila* to reduce oxygen resembles the mechanism used by *E. coli* at low oxygen tensions (Belevich, et al., 2005). It uses cytochrome bd to mediate the transfer of electrons to oxygen, and also utilizes oxygen detoxification systems, such as catalase and oxygen dismutase to reduce excess of oxygen and other reactive oxygen species (ROS). The need for heme as a cofactor for respiratory growth was only found after the growth on mucus-free medium to which haemin was added, which shows the importance of the development of defined media for the study of bacterial physiology. The knowledge on oxygen resistance has been used in the preparation of bacteria for intervention studies. We found that the reduction of viability was not significant in the first 24 hours of exposure to ambient oxygen pressure, and therefore the collection and formulation of the bacteria did not require strictly anaerobic conditions to maintain a high viability.

The discovery of oxygen reduction and respiration redefines *A. muciniphila* not to be strict anaerobic bacterium. However, *A. muciniphila* does also not fit in the category of facultative aerobic bacteria, because it cannot tolerate ambient oxygen levels. *A. muciniphila* is also not an microaerophilic bacterium, because that would hold that a dissolved oxygen concentration below 2-10% is a prerequisite for growth (Willey, 2008). This is not the case with *A. muciniphila*. The growth of *A. muciniphila* is not impaired in the absence of oxygen. Therefore, we would like to classify *A. muciniphila* as a facultative microaerophilic bacterium.

Oxygen resistance or reduction by cytochromes is a widespread trait among probiotics and gut bacteria. In the genus of *Bifidobacteria,* there is a wide distribution in oxygen sensitivity. *B. adolescentis* had no observed viability after 48 hours exposure to oxygen in ambient air, while 91% of *B. bifidum* cells survived the exposure (Andriantsoanirina, et al., 2013). Oxygen reduction in a range of lactic acid bacteria has been found to involve a heme-containing cytochrome bd complex and menaquinones (Brooijmans, et al., 2009). The mucus-degrading *Bacteroides fragilis* also employs a cytochrome bd containing electron transport chain very similar to *A. muciniphila,* which also is likely to utilize quinones (Baughn and Malamy, 2004). Also other presumed strictly anaerobic gut bacteria show some mechanism of oxygen resistance or reduction. For example, an external electron shuttle has described to be used by *F. prausnitzii* to reduce oxygen (Khan, et al., 2012).

The oxygen concentrations in the gut show a steep decrease starting at the epithelial barrier towards the centre of the gut (Albenberg, et al., 2014, Espey, 2013). This oxygen gradient is important in shaping the gut microbiota, but is not constant over time (Espey, 2013). The presence of oxygen and reactive oxygen species (ROS) in the gut is also influenced by gut health. Upon damage or inflammation of the epithelial cells, more ROS and oxygen diffuse into the gut, and the production of ROS increases upon the entry of polymorphonuclear neutrophils (PMNs) on the inflamed site (Mittal, et al., 2014). Loss of gut barrier function also inhibits the secretion of mucus, reducing the nutrient availability for *A. muciniphila.* Distortion of the gut ecosystem by inflammation results in changes of the microbiota composition (Boulange, et al., 2016, Ijssennagger, et al., 2015, Turner, 2009), which might explain widespread correlations found between colonic inflammations and gut microbiota. Characterization of cultured microbiota in terms of oxygen tolerance is therefore important to understand the influence of the host on the microbiota composition and vice versa.

Many of the characterized gut bacteria show some adaptation to the presence of oxygen. It is generally assumed that the anaerobic bacteria account for over 90% of the microbiota (Eckburg, et al., 2005, Maier, et al., 2014). The presence of oxygen in the host and the leakage of oxygen into the gut (Figure 2), and its isolation from other anaerobic ecosystems, make it favourable for bacteria to have some degree of oxygen tolerance to survive and colonize this ecosystem.

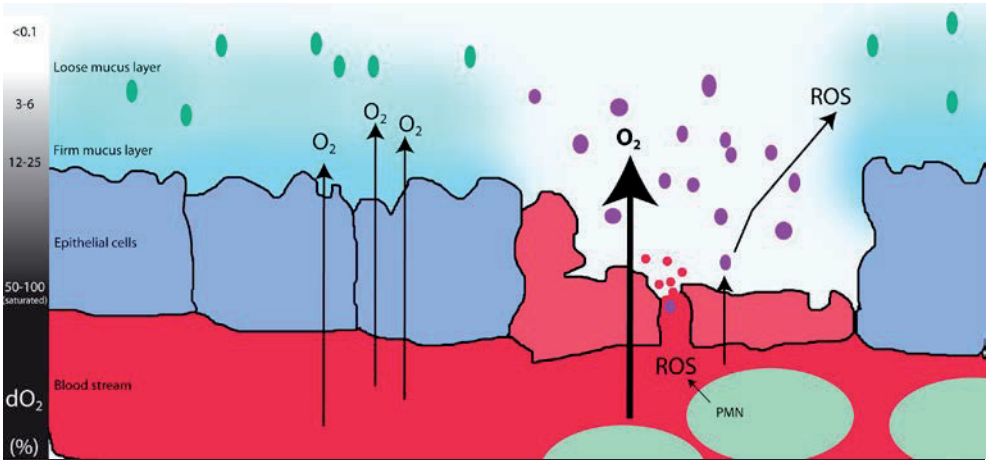

Figure 2. Overview of the niche of *A. muciniphila* (green ovals). Upon inflammation, increased amounts of oxygen and ROS enter the gut from the blood stream. This inhibits the growth of oxygen sensitive bacteria, and changes the bacterial composition, allowing pathogens to enter the blood stream (purple). Polymorphonuclear neutrophils (PMNs) produce more ROS to counter infection. Oxygen concentrations as percentage of saturation after (Espey, 2013).

The first steps in genetic modification of *A. muciniphila*

The need for detailed physiological studies of intestinal bacteria in general and *A. muciniphila* in specific has been well recognized. To study the physiology and its impact on molecular mechanisms, it is helpful to be able to modify the genetic content. In studying *A. muciniphila*-host interactions, deletion or overexpression of the Amuc_1100 gene would provide final proof of its signalling function (Ottman, et al., 2017b, Plovier, et al., 2017), and deletion of the cytochrome bd subunits should yield an oxygen sensitive strain. Mucus utilization could be studied by deleting the glycosidases and sulfatases, and growth of *A. muciniphila* on glucose could be achieved by expressing a functional GlmS gene. This gene is missing in the synthesis pathway of GlcN6P, as discussed above.

Hence, we have studied the options to make *A. muciniphila* genetically accessible. Firstly, we utilized random transposon insertion, as described previously for the species *Verrucromicrobium spinosum* (Domman, et al., 2011). The use of this technique relied on the simultaneous transformation of a genetic element, the transposon, with the required protein to insert the genetic element, the transposase. This method did not yield any modified colonies of *A. muciniphila*.

The challenges in developing a genetic toolbox for *A. muciniphila* are numerous. Firstly, the limited amount of applicable antibiotics is limited due to the resistance of *A. muciniphila*.

Secondly, it was a challenge to determine whether the applied transformation protocols would allow the translocation of DNA over the cell membrane. Thirdly, after successful translocation of DNA, it is unknown whether the plasmid is replicated inside the cell.

We investigated the availability of antibiotics for transformation to be able to use selection markers. The selected markers used in the experiments should invoke resistance against tetracycline and chloramphenicol, used at 10 µg/mL and 25 µg/mL respectively. These antibiotic concentrations in agar fully inhibited growth of *A. muciniphila,* in contrast to what was described before, possibly due to application of the antibiotics inside the agar instead of diffusion from a strip on top of the agar plates. (Ouwerkerk, 2016). The promoters used for these antibiotic resistance genes are optimized for use in *E. coli,* so they might not confer resistance to *A. muciniphila.* To determine the translocation of DNA over the cell membrane, we transformed fluorescently labelled plasmids and traced these plasmids upon transformation by electroporation (see Figure 3). The technique showed the successful translocation of plasmid DNA into the cell. Hence, the first two of the three above-mentioned problems were addressed, which will help in the further development of a genetic system. The lack of knowledge on plasmid replication could be solved by gene insertion into the genome by homologous recombination.

Recombination of DNA can be inhibited by the degradation of DNA upon entry in the cell. *A. muciniphila* codes for several restriction modification systems that are able to degrade foreign DNA (van Passel, et al., 2011). Additionally, *A. muciniphila* encodes a CRISPR-Cas system, which could be employed for genetic modification (Selle and Barrangou, 2015), but also degrades the DNA upon entry into the cell when the right spacer sequence is present in the translocated DNA. Characterisation of the protospacer adjacent motif would be required for the prevention of DNA degradation or utilization of the system for genetic modification (Jiang, et al., 2013).

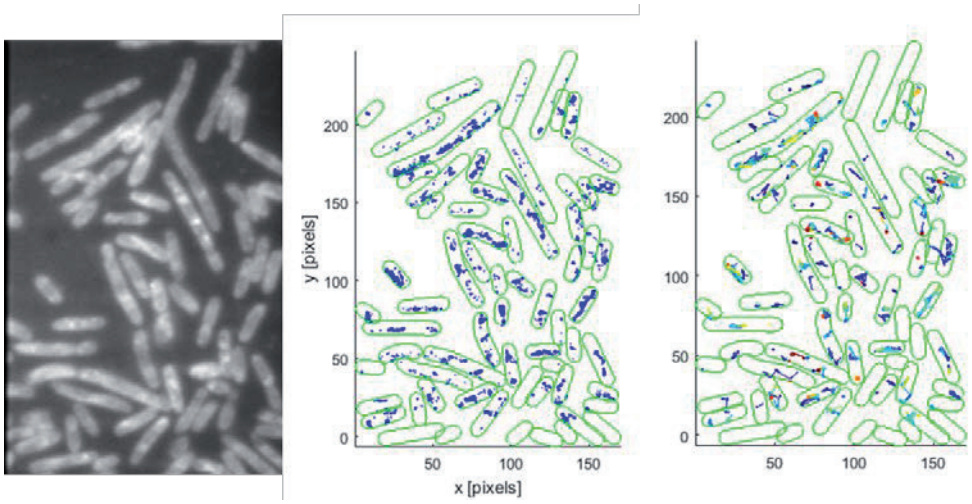

Figure 3. Image of labelled plasmids in *A. muciniphila* traced after electroporation. The bacteria were visualised (left) after which the location of fluorescence was determined (middle) and tracked over time (right). (Image obtained in collaboration with Jan Groen, Sharon Geerlings and Marnix Vlot, Microbiology, Wageningen University and Research, 2017).

Alternatively, we approached the issue from the ecological perspective. We assumed that *A. muciniphila*, like other bacteria, can be infected by bacteriophages. In fact, the *A. muciniphila* genome contains several prophages or remnants thereof, indicating the presence of bacteriophages in this gut symbiont. Such bacteriophages, by definition, are able to transfer their genetic content, either DNA or RNA, into the bacterial cell. By using the inherent infecting capabilities of bacteriophages, it would be possible to modify the genetic content of *A. muciniphila.* The isolated bacteriophage should be sequenced and characterized to identify possible functions such as integrases to develop possible vectors for transformation or transfection (Oram, et al., 2007). Subsequent modification of the phage DNA could lead to specific knock-ins or recombinant deletions from the *A. muciniphila* genome. A prerequisite for using the phage for genetic engineering, is the presence of an in vitro packaging system or a second host, which is genetically accessible. The bacteriophage DNA can be adjusted and used to transform the second host, after which the second host can produce new phage particle. These particles could be used to modify the *A. muciniphila* genome.

To obtain bacteriophages, we filtered faecal samples that were previously shown to have a high relative abundance of *A. muciniphila*, because a high relative abundance increases the chance of the presence of a bacteriophage for the target species (Manrique, et al., 2017,

Weinbauer, 2004). Subsequent plaque assays and enrichment of potential bacteriophage in liquid medium resulted in the discovery of a potential bacteriophage for *A. muciniphila,* which was only observed using electron microscopy, see Figure 4.

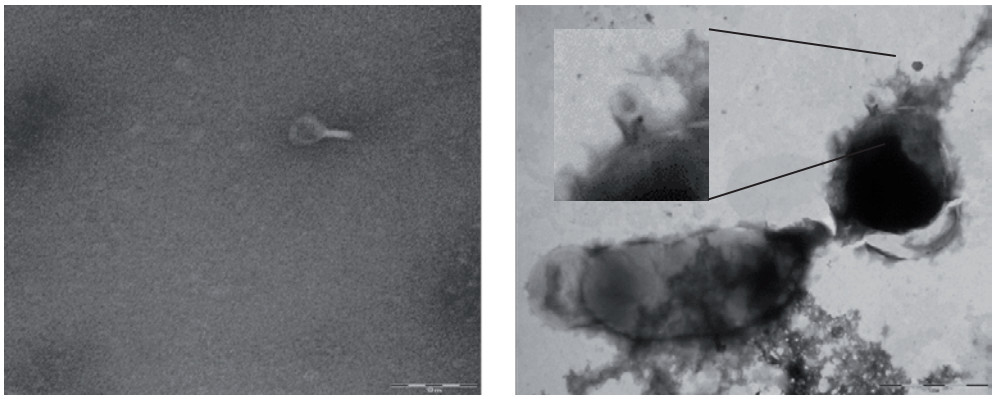

Figure 4. Electronmicrographs of potential bacteriophages isolated from faecal samples and enriched in *A. muciniphila* cultures. A single phage-like particle with 100 nm scale (left) and a phage-like particle attached to an *A. muciniphila* cell with 1 µm scale (right). (Image obtained in collaboration with Sharon Geerlings and Yifan Zhu, Microbiology, Wageningen University and Research, 2017).

Potential health-promoting functions of *A. muciniphila*

Different modes of interaction between *A. muciniphila* and the host have been described. *A. muciniphila* produces the SCFA acetate and propionate (Derrien, et al., 2004). These compounds are known to fuel enterocytes and are involved in immune and metabolic signalling (Andoh, 2016). Propionate is known to increase the gut transit speed, while acetate decreases this (Kolmeder and de Vos, 2017). Propionate also decreases satiety (Kolmeder and de Vos, 2017). As described in chapters 3, 4 and 5 of this thesis, the ratio between acetate and propionate is influenced by the sugars present in the medium, the addition of oxygen and the presence of vitamin B12. An increase of glucose in the medium also increases the production of propionate. The presence of oxygen also increases the production of propionate. The reduction of oxygen also decreases the toxicity of this compound for other bacteria and increases fermentative conditions, which could lead to butyrate production.

The production of SCFA is the result of mucin degradation. It is expected that the degradation of mucin by *A. muciniphila* would decrease the thickness of the mucus layer. This layer forms a barrier between the colonic content and the host and thereby prevents infections (Hansson, 2012). However, the presence of *A. muciniphila* was found to be associated with an increased

thickness of the mucus layer (Everard, et al., 2013), and possibly increase the gut barrier function (Reunanen, et al., 2015, Schneeberger, et al., 2015). This could be caused by the increase of mucin-producing goblet cells upon administration of *A. muciniphila* (Shin, et al., 2014).

The direct interaction of *A. muciniphila* with the host is not only mediated by secreted compounds, but also by an immunomodulation protein. This protein was identified to be Amuc_1100*, a pili-like protein that induces a the NF-κB pathway via the induction of TLR-2 and TLR-4 signalling *in vitro* (Ottman, et al., 2017b). The efficacy of this protein was confirmed in an intervention study in mice. The protein showed to have a similar effect as the administration of viable or pasteurized *A. muciniphila* (Plovier, et al., 2017). In addition to the interpretations and predictions of the GEM described in this thesis and the above described interactions, some other observations can be made regarding the possible functionality of *A. muciniphila.* Recent observations considering the gut-brain axis indicate that the compound γ-aminobutyric acid (GABA) is an important signalling molecule in this trans-host connection (Dinan, et al., 2013). In humans, GABA is an inhibitory neurotransmitter, which presence has influence on epileptic episodes (Petroff, 2002), anxiety and depression (Dinan, et al., 2013, Schousboe and Waagepetersen, 2007). The effect of GABA is counteracted by glutamate from which it is synthesized (Petroff, 2002). The bacterial GABA synthesis pathway is used for deacidification of the cytosol (Feehily and Karatzas, 2013). In this pathway, glutamate is converted to GABA by glutamate decarboxylase (GAD) with pyridoxal-5'-phosphate (PLP) as cofactor (Dhakal, et al., 2012). In this reaction, a proton is bound to glutamate and exported over the cell membrane with GABA, see Figure 5 (Dhakal, et al., 2012). The genes in this pathway are also annotated in the genome of *A. muciniphila,* including the required transporter and glutamate decarboxylase encoded by genes on locus amuc_0037 and amuc_0372, respectively. GABA production by *A. muciniphila* has not yet been shown *in vitro* but could be tested by the addition of glutamate and PLP to the minimal medium. Interestingly, correlations have been shown between *A. muciniphila* abundance, anxiety and GABA receptor upregulation in mice (Burokas, et al., 2017).

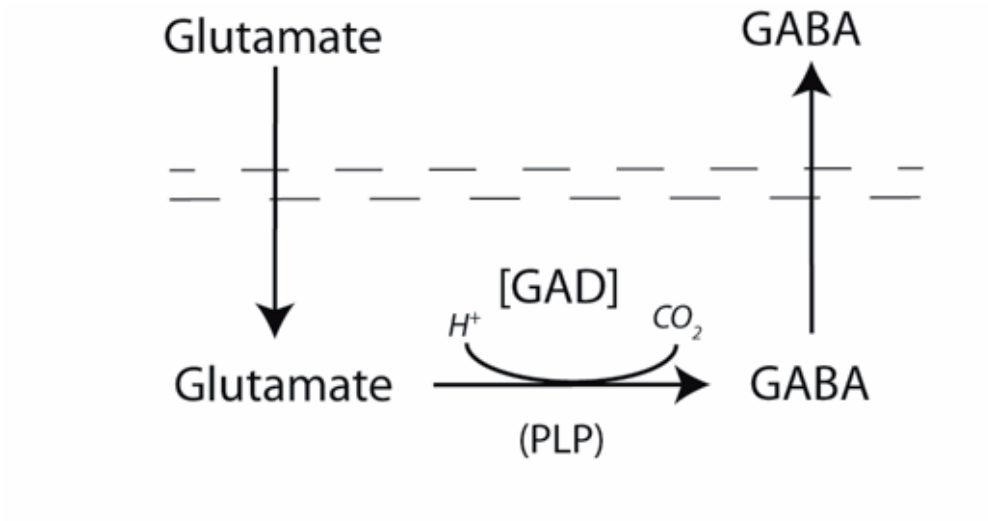

Figure 5. Overview of the GABA production pathway. Dashed lines indicate cell membrane. The enzyme glutamate decarbocylase (GAD) is indicated between [ ], cofactor pyridoxal-5'-phosphate (PLP) is indicated between ( ).

For the host, GABA has a completely different function, as it can be detected by specific GABA receptors. It functions as a neurotransmitter and relieves anxiety. Combining the potential GABA production by *A. muciniphila,* an increased relative abundance in mice that have a reduced anxiety upon addition of GOS/FOS, with increased expression of GABA receptors in mice, it could be speculated that *A. muciniphila* is one of the undiscovered psychobiotics (Dinan, et al., 2013).

Administration of viable *A. muciniphila*

In chapter 6 we described the application of a double emulsion system for the viable delivery of *A. muciniphila* to the small intestine. We used an *in vitro* digestive model simulating the stomach and first part of the small intestine with the addition of bile. In this system, we showed that *A. muciniphila* has a significant higher survival rate when encapsulated in a double emulsion than the control of non-encapsulated bacteria in PBS. A challenge in encapsulating bacteria is the available space for bacteria in the inner water phase. As shown in chapter 6, the size of *A. muciniphila* varies in the different media that were used. Therefore, we used a medium based on a tryptic digest of casein for the cultivation of bacteria for encapsulation, instead of the clinical applicable soy medium. The casein medium showed

smaller cells compared to soy medium, which allowed encapsulation in the inner water droplets that have an average size of 5 µm. The decrease of viability during simulated digestion with the encapsulation in a double emulsion is about 100-fold. This could be improved by enhancing the buffer capacity of the inner water phase to increase the protection against the acid in the stomach. Additionally, a boost can be given to the bacteria upon release by co-encapsulating nutrients that are required for growth. This could be a cocktail of mucosal sugars, especially including GlcNAc. The supplementation of nutrients could also be achieved by incorporating glycoproteins in the emulsification process, although that might influence the stability of the emulsion itself. For enhanced protection during formulation and gastric passage, it might be beneficial to add cysteine as antioxidant in the encapsulation procedure as previously employed for *F. prausnitzii* (Khan, et al., 2014).

The importance of viable delivery of *A. muciniphila* is debatable, because pasteurized cells and *A. muciniphila* protein Amuc_1100* have a similar effect in preclinical mouse trials (Plovier, et al., 2017). All treatments reduced the effect of a high fat diet on the metabolism of the mice, including fat mass gain and weight gain. The application of the bacteria, both viable and pasteurized, and purified proteins in this preclinical trial was done by gavage. This implies that the applied treatments were not exposed to saliva and the full volume of the treatment is added to the stomach at once, possibly resulting in a lower acidity. The exposure to bile is also different in mice compared to humans. Therefore, it might be worthwhile investigating also the delivery of pasteurized cells and proteins encapsulated in a double emulsion. The low acidity in the stomach can have a destabilizing influence on the protein Amuc_1100*. Additionally, it is vulnerable for degradation by active proteases and peptidases, which are secreted throughout the GI tract (Antalis, et al., 2007). When the efficacy of protein Amuc_1100*, viable bacteria and pasteurized bacteria in mice was tested, the above discussed similar results were obtained for the mediation of diet induced obesity and associated biomarkers and gut barrier function. However, longitudinal effects and effects on other non-metabolic diseases were not tested. Also the long-term effect of *A. muciniphila* colonisation by live bacteria was not studied, although persistent strain colonisation after FMT or probiotic ingestion is not always shown and differs between studies (Li, et al., 2016, Segers and Lebeer, 2014). A combination of *A. muciniphila* strains might increase the colonization efficiency and therapeutic efficacy, as was also described for various probiotics (Timmerman, et al., 2004).

The mode and matrix for administration have influence on the functionality of probiotics (Ranadheera, et al., 2010). In the presented research, we only studied the application of a single type of double emulsion system based on sunflower oil. Alternative encapsulation methods have been applied for probiotic lactic acid bacteria, as briefly discussed in chapter 6. Many other administration matrices can be considered, such as ingestion of lyophilized bacteria, frozen bacteria in glycerol or formulation in food products. The two most important challenges in encapsulating probiotics are the shear imposed during processing, and upscaling of the process itself. Besides emulsification, there is one other technique which has been employed for the encapsulation of probiotics and that lives up to both challenges, which is extrusion (Solanki, et al., 2013). For this purpose, mainly alginate is used to form the extruded particles containing bacteria. This technique could be tested for *A. muciniphila* as well, but it is not possible to predict to what extent it will protect this bacterium and what the influence of the final product will be. A possible drawback of using extrusion is the sensory mouthfeel if the product particles exceed 100 µm and the low cfu/g material (Iravani, et al., 2015, Kailasapathy, 2009, Khosravi Zanjani, et al., 2014). In the end, *A. muciniphila* should also taste good.

Bile resistance of *A. muciniphila*

In the chapter 6 on the delivery in a double emulsion system, we found that *A. muciniphila* viability increased with the incubation in porcine bile extract. The viability of non-encapsulated bacteria increased during the incubation in the intestinal phase, where bile is present. We further investigated the bile resistance of *A. muciniphila*, and found that the resistance on the used porcine bile extract is not replicated for ox bile or purified bile salts (Figure 6). For porcine bile, there was no inhibition found with the addition of 1% (w/v). Both ox bile and purified bile salts show inhibition with the addition of 0.5% (w/v). This can be caused by the differences in extraction methods, purification and composition of the bile extract used.

The used bile salts (Sigma, Bile salts for Microbiology) are a mixture of purified cholic acid sodium salt and deoxycholic sodium salt (Noriega, et al., 2004). The Ox-bile (Sigma, Ox bile, dehydrated, purified for microbiology) used in the experiment is a dehydrated form of bile, therefore also containing more impurities. The porcine bile extract (Sigma, Bile extract porcine) is suggested to be used for the determination of bile acid resistance by the

manufacturer. The differences of composition between bovine and porcine bile have been described to be mainly in the hydroxylation of the glycine conjugates and tauro conjugates (Coleman, et al., 1979).

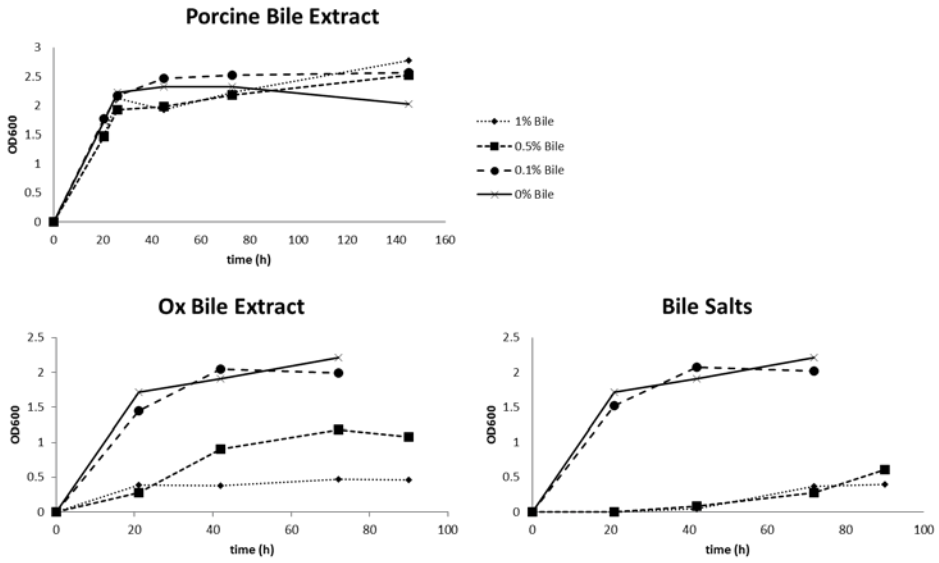

Figure 6. Growth of *A. muciniphila* grown in soy medium with the addition of porcine bile extract, ox bile extract or purified bile salts at 0%, 0.1%, 0.5% and 2% (w/v). Data shown are averages of duplicates. Symbols in legend account for all bile types.

The mechanism of protection against bile is not known for *A. muciniphila.* A putative bile acid transporter gene is annotated in the genome on locus Amuc_0139, and if expressed could be involved in export of bile acid, thereby reducing the effects inside the cell, but not on the cell wall. Alternatively, an external polysaccharide layer could protect against the effect of bile, as previously described in *Lactobacillus* and *Bifidobacterium* (Fanning, et al., 2012, Ruiz, et al., 2013).

Conclusion and future expectations for applications of *A. muciniphila*

In this thesis we have shown that *A. muciniphila* can be cultivated for human applications. We have also improved the GEM of this microbe and found that L-threonine and either GlcNAc or GalNAc are essential ingredients for growth, which can be applied in medical applications. We have shown that *A. muciniphila* is a facultative microaerophilic bacterium that can use oxygen as electron acceptor. Finally, we have ensured that it can be applied in a double emulsion to improve viable delivery to the gut.

Mouse intervention and human correlation studies have resulted in the hypothesis that *A. muciniphila* could have a positive effect on human health. The mechanism by which *A. muciniphila* confers it beneficial properties are described to vary from immunomodulation by Amuc_1100* (Ottman, et al., 2017b, Plovier, et al., 2017), the production of SCFA (Belzer and de Vos, 2012, Ottman, et al., 2017a) and maybe GABA production as hypothesized above. The genome of *A. muciniphila* also contains over 600 genes with unknown function. Each of these genes could represent a possible mediator between humans and *A. muciniphila.* If the modification of the genome becomes possible, it could be possible to make a random transposon library (van Opijnen and Camilli, 2013). This library can be used for intervention study for *in vivo* study of functional genes.

Besides applying bacteria, or parts of it, the abundance of *A. muciniphila* could also be increased in the host by food additives. The addition of a GOS/FOS mixture to mice has shown to increase the relative abundance of *A. muciniphila* in mice (Burokas, et al., 2017). For the growth of *A. muciniphila* in humans, it could be helpful to identify additional food additives that increase the abundance, on top of previously described polyphenols and capsaicin (Baboota, et al., 2014, Roopchand, et al., 2015). These additives should be indigestible fibres that contain GlcNAc residues, which may be combined with glutamate and PLP for GABA production.

Before GABA production can be induced *in vivo,* it should be produced *in vitro.* Using the minimal medium developed for *A. muciniphila* will prove to be critical in this study and in further elucidating the physiology of *A. muciniphila.*

The final challenges in applying *A. muciniphila* as therapeutic agent are correct dosing, population wide application and long term safety. The research described in this thesis, especially the development of suitable growth media, has made these type of clinical studies possible. If *A. muciniphila* is the therapeutic microbe it promises to be, we expect to receive confirmation soon as a human trial is ongoing (Plovier et al., 2017; see clinicaltrials.gov).

References

1 Actis, P., Maalouf, M.M., Kim, H.J., Lohith, A., Vilozny, B., Seger, R.A., and Pourmand, N. (2014) Compartmental Genomics in Living Cells Revealed by Single-Cell Nanobiopsy, *Acs Nano* **8**: 546-553.
2 Albenberg, L., Esipova, T.V., Judge, C.P., Bittinger, K., Chen, J., Laughlin, A., et al. (2014) Correlation between intraluminal oxygen gradient and radial partitioning of intestinal microbiota, *Gastroenterology* **147**: 1055-1063 e1058.
3 Andoh, A. (2016) Physiological Role of Gut Microbiota for Maintaining Human Health, *Digestion* **93**: 176-181.
4 Andriantsoanirina, V., Allano, S., Butel, M.J., and Aires, J. (2013) Tolerance of Bifidobacterium human isolates to bile, acid and oxygen, *Anaerobe* **21**: 39-42.
5 Anhe, F.F., Roy, D., Pilon, G., Dudonne, S., Matamoros, S., Varin, T.V., et al. (2015) A polyphenol-rich cranberry extract protects from diet-induced obesity, insulin resistance and intestinal inflammation in association with increased Akkermansia spp. population in the gut microbiota of mice, *Gut* **64**: 872-883.
6 Antalis, T.M., Shea-Donohue, T., Vogel, S.N., Sears, C., and Fasano, A. (2007) Mechanisms of disease: protease functions in intestinal mucosal pathobiology, *Nat Clin Pract Gastroenterol Hepatol* **4**: 393-402.
7 Arumugam, M., Raes, J., Pelletier, E., Le Paslier, D., Yamada, T., Mende, D.R., et al. (2011) Enterotypes of the human gut microbiome, *Nature* **473**: 174-180.
8 Baboota, R.K., Murtaza, N., Jagtap, S., Singh, D.P., Karmase, A., Kaur, J., et al. (2014) Capsaicin-induced transcriptional changes in hypothalamus and alterations in gut microbial count in high fat diet fed mice, *J Nutr Biochem* **25**: 893-902.
9 Barreteau, H., Kovac, A., Boniface, A., Sova, M., Gobec, S., and Blanot, D. (2008) Cytoplasmic steps of peptidoglycan biosynthesis, *FEMS Microbiol Rev* **32**: 168-207.
10 Baughn, A.D., and Malamy, M.H. (2004) The strict anaerobe Bacteroides fragilis grows in and benefits from nanomolar concentrations of oxygen, *Nature* **427**: 441-444.
11 Belevich, I., Borisov, V.B., Konstantinov, A.A., and Verkhovsky, M.I. (2005) Oxygenated complex of cytochrome bd from Escherichia coli: stability and photolability, *Febs Letters* **579**: 4567-4570.
12 Belzer, C., and de Vos, W.M. (2012) Microbes inside-from diversity to function: the case of Akkermansia, *Isme Journal* **6**: 1449-1458.
13 Boleij, A., Hechenbleikner, E.M., Goodwin, A.C., Badani, R., Stein, E.M., Lazarev, M.G., et al. (2015) The Bacteroides fragilis Toxin Gene Is Prevalent in the Colon Mucosa of Colorectal Cancer Patients, *Clinical Infectious Diseases: An Official Publication of the Infectious Diseases Society of America* **60**: 208-215.
14 Boulange, C.L., Neves, A.L., Chilloux, J., Nicholson, J.K., and Dumas, M.E. (2016) Impact of the gut microbiota on inflammation, obesity, and metabolic disease, *Genome Medicine* **8**: 42.
15 Brooijmans, R., Smit, B., Santos, F., van Riel, J., de Vos, W.M., and Hugenholtz, J. (2009) Heme and menaquinone induced electron transport in lactic acid bacteria, *Microbial Cell Factories* **8**: 28.
16 Burokas, A., Arboleya, S., Moloney, R.D., Peterson, V.L., Murphy, K., Clarke, G., et al. (2017) Targeting the Microbiota-Gut-Brain Axis: Prebiotics Have Anxiolytic and Antidepressant-like Effects and Reverse the Impact of Chronic Stress in Mice, *Biol Psychiatry*.
17 Coleman, R., Iqbal, S., Godfrey, P.P., and Billington, D. (1979) Membranes and bile formation. Composition of several mammalian biles and their membrane-damaging properties, *Biochemical Journal* **178**: 201-208.
18 Cotillard, A., Kennedy, S.P., Kong, L.C., Prifti, E., Pons, N., Le Chatelier, E., et al. (2013) Dietary intervention impact on gut microbial gene richness, *Nature* **500**: 585-588.
19 Dao, M.C., Everard, A., Aron-Wisnewsky, J., Sokolovska, N., Prifti, E., Verger, E.O., et al. (2016) Akkermansia muciniphila and improved metabolic health during a dietary intervention in obesity: relationship with gut microbiome richness and ecology, *Gut* **65**: 426-436.
20 de Vos, W.M. (2013) Fame and future of faecal transplantations--developing next-generation therapies with synthetic microbiomes, *Microbial Biotechnology* **6**: 316-325.

21 Derrien, M., and van Hylckama Vlieg, J.E. (2015) Fate, activity, and impact of ingested bacteria within the human gut microbiota, *Trends Microbiol* **23**: 354-366.
22 Derrien, M., Vaughan, E.E., Plugge, C.M., and de Vos, W.M. (2004) Akkermansia muciniphila gen. nov., sp nov., a human intestinal mucin-degrading bacterium, *Int J Syst Evol Microbiol* **54**: 1469-1476.
23 Dhakal, R., Bajpai, V.K., and Baek, K.H. (2012) Production of gaba (gamma - Aminobutyric acid) by microorganisms: a review, *Braz J Microbiol* **43**: 1230-1241.
24 Dinan, T.G., Stanton, C., and Cryan, J.F. (2013) Psychobiotics: a novel class of psychotropic, *Biol Psychiatry* **74**: 720-726.
25 Domman, D.B., Steven, B.T., and Ward, N.L. (2011) Random transposon mutagenesis of Verrucomicrobium spinosum DSM 4136(T), *Arch Microbiol* **193**: 307-312.
26 Eckburg, P.B., Bik, E.M., Bernstein, C.N., Purdom, E., Dethlefsen, L., Sargent, M., et al. (2005) Diversity of the human intestinal microbial flora, *Science* **308**: 1635-1638.
27 Eeckhaut, V., Ducatelle, R., Sas, B., Vermeire, S., and Van Immerseel, F. (2014) Progress towards butyrate-producing pharmabiotics: Butyricicoccus pullicaecorum capsule and efficacy in TNBS models in comparison with therapeutics, *Gut* **63**: 367.
28 Espey, M.G. (2013) Role of oxygen gradients in shaping redox relationships between the human intestine and its microbiota, *Free Radical Biology and Medicine* **55**: 130-140.
29 Everard, A., Belzer, C., Geurts, L., Ouwerkerk, J.P., Druart, C., Bindels, L.B., et al. (2013) Cross-talk between Akkermansia muciniphila and intestinal epithelium controls diet-induced obesity, *Proc Natl Acad Sci U S A* **110**: 9066-9071.
30 Fanning, S., Hall, L.J., Cronin, M., Zomer, A., MacSharry, J., Goulding, D., et al. (2012) Bifidobacterial surface-exopolysaccharide facilitates commensal-host interaction through immune modulation and pathogen protection, *Proc Natl Acad Sci U S A* **109**: 2108-2113.
31 Feehily, C., and Karatzas, K.A. (2013) Role of glutamate metabolism in bacterial responses towards acid and other stresses, *J Appl Microbiol* **114**: 11-24.
32 Gibson, G.R., Hutkins, R., Sanders, M.E., Prescott, S.L., Reimer, R.A., Salminen, S.J., et al. (2017) Expert consensus document: The International Scientific Association for Probiotics and Prebiotics (ISAPP) consensus statement on the definition and scope of prebiotics, *Nat Rev Gastroenterol Hepatol* **14**: 491-502.
33 Godoy, V.G., Dallas, M.M., Russo, T.A., and Malamy, M.H. (1993) A role for Bacteroides fragilis neuraminidase in bacterial growth in two model systems, *Infection and Immunity* **61**: 4415-4426.
34 Gupta, S., Allen-Vercoe, E., and Petrof, E.O. (2016) Fecal microbiota transplantation: in perspective, *Therap Adv Gastroenterol* **9**: 229-239.
35 Hansson, G.C. (2012) Role of mucus layers in gut infection and inflammation, *Curr Opin Microbiol* **15**: 57-62.
36 Harper, C.J., Hayward, D., Kidd, M., Wiid, I., and van Helden, P. (2010) Glutamate dehydrogenase and glutamine synthetase are regulated in response to nitrogen availability in Myocbacterium smegmatis, *BMC Microbiol* **10**: 138.
37 Henry, C.S., DeJongh, M., Best, A.A., Frybarger, P.M., Linsay, B., and Stevens, R.L. (2010) High-throughput generation, optimization and analysis of genome-scale metabolic models, *Nat Biotechnol* **28**: 977-U922.
38 Ijssennagger, N., Belzer, C., Hooiveld, G.J., Dekker, J., van Mil, S.W., Muller, M., et al. (2015) Gut microbiota facilitates dietary heme-induced epithelial hyperproliferation by opening the mucus barrier in colon, *Proc Natl Acad Sci U S A* **112**: 10038-10043.
39 Iravani, S., Korbekandi, H., and Mirmohammadi, S.V. (2015) Technology and potential applications of probiotic encapsulation in fermented milk products, *J Food Sci Technol* **52**: 4679-4696.
40 Jiang, W., Bikard, D., Cox, D., Zhang, F., and Marraffini, L.A. (2013) RNA-guided editing of bacterial genomes using CRISPR-Cas systems, *Nat Biotechnol* **31**: 233-239.
41 Johansson, M.E., Larsson, J.M., and Hansson, G.C. (2011) The two mucus layers of colon are organized by the MUC2 mucin, whereas the outer layer is a legislator of host-microbial interactions, *Proc Natl Acad Sci U S A* **108 Suppl 1**: 4659-4665.

42 Kailasapathy, K. (2009) Encapsulation technologies for functional foods and nutraceutical product development, *CAB Reviews: Perspectives in Agriculture, Veterinary Science, Nutrition and Natural Resources* **4**: 1-19.
43 Kanai, T., Mikami, Y., and Hayashi, A. (2015) A breakthrough in probiotics: Clostridium butyricum regulates gut homeostasis and anti-inflammatory response in inflammatory bowel disease, *J Gastroenterol* **50**: 928-939.
44 Khan, M.T., Duncan, S.H., Stams, A.J., van Dijl, J.M., Flint, H.J., and Harmsen, H.J. (2012) The gut anaerobe Faecalibacterium prausnitzii uses an extracellular electron shuttle to grow at oxic-anoxic interphases, *ISME J* **6**: 1578-1585.
45 Khan, M.T., van Dijl, J.M., and Harmsen, H.J. (2014) Antioxidants keep the potentially probiotic but highly oxygen-sensitive human gut bacterium Faecalibacterium prausnitzii alive at ambient air, *PLoS One* **9**: e96097.
46 Khosravi Zanjani, M.A., Ghiassi Tarzi, B., Sharifan, A., and Mohammadi, N. (2014) Microencapsulation of Probiotics by Calcium Alginate-gelatinized Starch with Chitosan Coating and Evaluation of Survival in Simulated Human Gastro-intestinal Condition, *Iran J Pharm Res* **13**: 843-852.
47 Kolmeder, C.A., and de Vos, W.M. (2017) Gut health and the personal microbiome. In: *Nutrigenomics and Proteomics in Health and Disease*: John Wiley & Sons, Ltd. 201-219.
48 Kumari, S., Beatty, C.M., Browning, D.F., Busby, S.J., Simel, E.J., Hovel-Miner, G., and Wolfe, A.J. (2000) Regulation of acetyl coenzyme A synthetase in Escherichia coli, *J Bacteriol* **182**: 4173-4179.
49 Lee, H., and Ko, G. (2014) Effect of metformin on metabolic improvement and gut microbiota, *Appl Environ Microbiol* **80**: 5935-5943.
50 Leoff, C., Saile, E., Sue, D., Wilkins, P., Quinn, C.P., Carlson, R.W., and Kannenberg, E.L. (2008) Cell wall carbohydrate compositions of strains from the Bacillus cereus group of species correlate with phylogenetic relatedness, *J Bacteriol* **190**: 112-121.
51 Li, H., Limenitakis, J.P., Fuhrer, T., Geuking, M.B., Lawson, M.A., Wyss, M., et al. (2015) The outer mucus layer hosts a distinct intestinal microbial niche, *Nat Commun* **6**: 8292.
52 Li, S.S., Zhu, A., Benes, V., Costea, P.I., Hercog, R., Hildebrand, F., et al. (2016) Durable coexistence of donor and recipient strains after fecal microbiota transplantation, *Science* **352**: 586-589.
53 Maier, E., Anderson, R.C., and Roy, N.C. (2014) Understanding how commensal obligate anaerobic bacteria regulate immune functions in the large intestine, *Nutrients* **7**: 45-73.
54 Manrique, P., Dills, M., and Young, M.J. (2017) The Human Gut Phage Community and Its Implications for Health and Disease, *Viruses* **9**.
55 Mittal, M., Siddiqui, M.R., Tran, K., Reddy, S.P., and Malik, A.B. (2014) Reactive oxygen species in inflammation and tissue injury, *Antioxid Redox Signal* **20**: 1126-1167.
56 Neelima, Sharma, R., Rajput, Y.S., and Mann, B. (2013) Chemical and functional properties of glycomacropeptide (GMP) and its role in the detection of cheese whey adulteration in milk: a review, *Dairy Sci Technol* **93**: 21-43.
57 Noriega, L., Gueimonde, M., Sanchez, B., Margolles, A., and de los Reyes-Gavilan, C.G. (2004) Effect of the adaptation to high bile salts concentrations on glycosidic activity, survival at low PH and cross-resistance to bile salts in Bifidobacterium, *Int J Food Microbiol* **94**: 79-86.
58 O'Riordan, N., Kane, M., Joshi, L., and Hickey, R.M. (2014) Structural and functional characteristics of bovine milk protein glycosylation, *Glycobiology* **24**: 220-236.
59 Oram, M., Woolston, J.E., Jacobson, A.D., Holmes, R.K., and Oram, D.M. (2007) Bacteriophage-based vectors for site-specific insertion of DNA in the chromosome of Corynebacteria, *Gene* **391**: 53-62.
60 Orth, J.D., and Palsson, B.O. (2010) Systematizing the generation of missing metabolic knowledge, *Biotechnol Bioeng* **107**: 403-412.
61 Ottman, N., Davids, M., Suarez-Diez, M., Boeren, S., Schaap, P.J., Martins Dos Santos, V.A.P., et al. (2017a) Genome-scale model and omics analysis of metabolic capacities of Akkermansia muciniphila reveal a preferential mucin-degrading lifestyle, *Appl Environ Microbiol*.

62 Ottman, N., Reunanen, J., Meijerink, M., Pietila, T.E., Kainulainen, V., Klievink, J., et al. (2017b) Pili-like proteins of Akkermansia muciniphila modulate host immune responses and gut barrier function, *PLoS One* **12**: e0173004.
63 Ouwerkerk, J.P. (2016) Akkermansia species : phylogeny, physiology and comparative genomics. Wageningen: Wageningen University.
64 Ouwerkerk, J.P., Aalvink, S., Belzer, C., and De Vos, W.M. (2017) Preparation and preservation of viable Akkermansia muciniphila cells for therapeutic interventions, *Benef Microbes* **8**: 163-169.
65 Petroff, O.A. (2002) GABA and glutamate in the human brain, *Neuroscientist* **8**: 562-573.
66 Plovier, H., Everard, A., Druart, C., Depommier, C., Van Hul, M., Geurts, L., et al. (2017) A purified membrane protein from Akkermansia muciniphila or the pasteurized bacterium improves metabolism in obese and diabetic mice, *Nat Med* **23**: 107-113.
67 Plugge, C.M. (2005) Anoxic media design, preparation, and considerations, *Methods Enzymol* **397**: 3-16.
68 Quevrain, E., Maubert, M.A., Michon, C., Chain, F., Marquant, R., Tailhades, J., et al. (2016) Identification of an anti-inflammatory protein from Faecalibacterium prausnitzii, a commensal bacterium deficient in Crohn's disease, *Gut* **65**.
69 Ranadheera, R.D.C.S., Baines, S.K., and Adams, M.C. (2010) Importance of food in probiotic efficacy, *Food Research International* **43**: 1-7.
70 Reunanen, J., Kainulainen, V., Huuskonen, L., Ottman, N., Belzer, C., Huhtinen, H., et al. (2015) Akkermansia muciniphila Adheres to Enterocytes and Strengthens the Integrity of the Epithelial Cell Layer, *Appl Environ Microbiol* **81**: 3655-3662.
71 Roopchand, D.E., Carmody, R.N., Kuhn, P., Moskal, K., Rojas-Silva, P., Turnbaugh, P.J., and Raskin, I. (2015) Dietary Polyphenols Promote Growth of the Gut Bacterium Akkermansia muciniphila and Attenuate High-Fat Diet-Induced Metabolic Syndrome, *Diabetes* **64**: 2847-2858.
72 Rossi, O., Khan, M.T., Schwarzer, M., Hudcovic, T., Srutkova, D., Duncan, S.H., et al. (2015) Faecalibacterium prausnitzii Strain HTF-F and Its Extracellular Polymeric Matrix Attenuate Clinical Parameters in DSS-Induced Colitis, *PLoS One* **10**: e0123013.
73 Ruiz, L., Margolles, A., and Sanchez, B. (2013) Bile resistance mechanisms in Lactobacillus and Bifidobacterium, *Front Microbiol* **4**: 396.
74 Schicho, R., Krueger, D., Zeller, F., Von Weyhern, C.W.H., Frieling, T., Kimura, H., et al. (2006) Hydrogen Sulfide Is a Novel Prosecretory Neuromodulator in the Guinea-Pig and Human Colon, *Gastroenterology* **131**: 1542-1552.
75 Schneeberger, M., Everard, A., Gomez-Valades, A.G., Matamoros, S., Ramirez, S., Delzenne, N.M., et al. (2015) Akkermansia muciniphila inversely correlates with the onset of inflammation, altered adipose tissue metabolism and metabolic disorders during obesity in mice, *Sci Rep* **5**: 16643.
76 Schousboe, A., and Waagepetersen, H.S. (2007) GABA: homeostatic and pharmacological aspects, *Prog Brain Res* **160**: 9-19.
77 Segers, M.E., and Lebeer, S. (2014) Towards a better understanding of Lactobacillus rhamnosus GG--host interactions, *Microbial Cell Factories* **13 Suppl 1**: S7.
78 Selle, K., and Barrangou, R. (2015) Harnessing CRISPR-Cas systems for bacterial genome editing, *Trends Microbiol* **23**: 225-232.
79 Shetty, S.A., Hugenholtz, F., Lahti, L., Smidt, H., and de Vos, W.M. (2017) Intestinal microbiome landscaping: insight in community assemblage and implications for microbial modulation strategies, *FEMS Microbiol Rev* **41**: 182-199.
80 Shin, N.R., Lee, J.C., Lee, H.Y., Kim, M.S., Whon, T.W., Lee, M.S., and Bae, J.W. (2014) An increase in the Akkermansia spp. population induced by metformin treatment improves glucose homeostasis in diet-induced obese mice, *Gut* **63**: 727-735.
81 Shoaie, S., Ghaffari, P., Kovatcheva-Datchary, P., Mardinoglu, A., Sen, P., Pujos-Guillot, E., et al. (2015) Quantifying Diet-Induced Metabolic Changes of the Human Gut Microbiome, *Cell Metabolism* **22**: 320-331.
82 Solanki, H.K., Pawar, D.D., Shah, D.A., Prajapati, V.D., Jani, G.K., Mulla, A.M., and Thakar, P.M. (2013) Development of microencapsulation delivery system for long-term preservation of probiotics as biotherapeutics agent, *Biomed Res Int* **2013**.

83 Timmerman, H.M., Koning, C.J., Mulder, L., Rombouts, F.M., and Beynen, A.C. (2004) Monostrain, multistrain and multispecies probiotics--A comparison of functionality and efficacy, *Int J Food Microbiol* **96**: 219-233.
84 Tojo, R., Suarez, A., Clemente, M.G., de los Reyes-Gavilan, C.G., Margolles, A., Gueimonde, M., and Ruas-Madiedo, P. (2014) Intestinal microbiota in health and disease: role of bifidobacteria in gut homeostasis, *World J Gastroenterol* **20**: 15163-15176.
85 Turner, J.R. (2009) Intestinal mucosal barrier function in health and disease, *Nat Rev Immunol* **9**: 799-809.
86 Udayappan, S., Manneras-Holm, L., Chaplin-Scott, A., Belzer, C., Herrema, H., Dallinga-Thie, G.M., et al. (2016) Oral treatment with Eubacterium hallii improves insulin sensitivity in db/db mice **2**: 16009.
87 Uehara, T., and Park, J.T. (2004) The N-acetyl-D-glucosamine kinase of Escherichia coli and its role in murein recycling, *J Bacteriol* **186**: 7273-7279.
88 van der Ark, K.C.H., van Heck, R.G.A., Martins Dos Santos, V.A.P., Belzer, C., and de Vos, W.M. (2017) More than just a gut feeling: constraint-based genome-scale metabolic models for predicting functions of human intestinal microbes, *Microbiome* **5**: 78.
89 van Nood, E., Vrieze, A., Nieuwdorp, M., Fuentes, S., Zoetendal, E.G., de Vos, W.M., et al. (2013) Duodenal infusion of donor feces for recurrent Clostridium difficile, *N Engl J Med* **368**: 407-415.
90 van Opijnen, T., and Camilli, A. (2013) Transposon insertion sequencing: a new tool for systems-level analysis of microorganisms, *Nature Reviews Microbiology* **11**: 435-442.
91 van Passel, M.W., Kant, R., Zoetendal, E.G., Plugge, C.M., Derrien, M., Malfatti, S.A., et al. (2011) The genome of Akkermansia muciniphila, a dedicated intestinal mucin degrader, and its use in exploring intestinal metagenomes, *PLoS One* **6**: e16876.
92 Vieira, A.T., Fukumori, C., and Ferreira, C.M. (2016) New insights into therapeutic strategies for gut microbiota modulation in inflammatory diseases, *Clin Transl Immunology* **5**: e87.
93 Volkmer, B., and Heinemann, M. (2011) Condition-dependent cell volume and concentration of Escherichia coli to facilitate data conversion for systems biology modeling, *PLoS One* **6**: e23126.
94 Wang, J., Tang, H., Zhang, C., Zhao, Y., Derrien, M., Rocher, E., et al. (2015) Modulation of gut microbiota during probiotic-mediated attenuation of metabolic syndrome in high fat diet-fed mice, *ISME J* **9**: 1-15.
95 Weinbauer, M.G. (2004) Ecology of prokaryotic viruses, *FEMS Microbiol Rev* **28**: 127-181.
96 Wexler, H.M. (2007) Bacteroides: the good, the bad, and the nitty-gritty, *Clinical Microbiology Reviews* **20**: 593-621.
97 Willey, J.M.S., L M; Woolverton, C J (2008) *Prescott, Harley, and Klein's Microbiology*: McGraw-Hill, 1088.
98 Wu, S., Rhee, K.J., Albesiano, E., Rabizadeh, S., Wu, X., Yen, H.R., et al. (2009) A human colonic commensal promotes colon tumorigenesis via activation of T helper type 17 T cell responses, *Nat Med* **15**: 1016-1022.
99 Zoetendal, E.G., and Vos, W.M. (2014) Effect of diet on the intestinal microbiota and its activity, *Curr Opin Gastroenterol* **30**.

Summary

In chapter 1 of this thesis, we provide background knowledge about the gut microbiota in general and *A. muciniphila* specifically. The gut harbors a complex ecosystem in which many bacteria, both beneficial and pathogens, thrive. These bacteria have a profound influence on host health, but their presence is in turn influenced by the host. Factors that influence microbial composition are diet, host health, age, gender, and environment in general. The mucosal niche that *A. muciniphila* lives in is characterized by its close proximity to the host epithelial cells. The mucus secreted by the host cells can serve as the sole carbon and nitrogen source for this bacterium. The potential importance of *A. muciniphila* as a member of the intestinal microbiota comes from the fact that *A. muciniphila* is reversely correlated with several diseases and reduce the fat mass gain of mice fed a high fat diet.

In chapter 2 we describe the use of genome-scale metabolic models to further understand the genetic and metabolic potential of microbiota members, as well as potential phenotypes and influence on the host. We emphasize the importance of culturing bacteria and provide an outline in which GEMs are used to aid in the development of minimal culture media. GEMs have been instrumental in the development of minimal media for microbiota members including *Faecalibacterium prausnitzii* and probiotic lactic acid bacteria. When it is possible to grow bacteria in pure cultures, it is also possible to study the phenotype of these bacteria. GEMs can be used to predict the phenotypes of bacteria under changing conditions. This includes the interaction with other bacteria, which makes it possible to make multispecies models. The construction and interpretation of these models is complicated, but not impossible. Multispecies GEMs have been successfully employed to predict the influence of diet on the host and of complex bacterial communities on the health of the host.

The use of GEMs for the development of minimal media was applied in chapter 3. The minimal medium described in this chapter was developed based on a previously defined GEM. We found that the essential components of *A. muciniphila* medium are L-threonine and either N-acetylglucosamine (GlcNAc) or N-acetylgalactosamine (GalNAc). The GEM accurately predicted the essentiality of L-threonine for *A. muciniphila* growth. However, it did not predict the essentiality of GlcNAc or GalNAc. We found that the enzyme mediating the reaction between fructose-6-phosphate and glucosamine-6-phostphate, an important first

step in peptidoglycan formation. The enzyme annotated for this function, NagB, was characterized and found to prefer the deaminating reaction. This finding was incorporated in the GEM, which resulted in the correct prediction of GlcNAc essentiality as well.

The composition of the minimal medium was used to develop an animal component free medium as described in chapter 4. The addition of soy derived peptides increased the growth rate an yield, and the omission of animal components makes the cultured bacteria applicable in humans. We observed morphology changes upon cultivation with soy peptides with light and scanning electron microscopy. The cells were significantly longer when compared to the mucus grown. To identify changes of *A. muciniphila* cultured on soy enriched medium compared to mucus medium, we applied transcriptome analysis. We found that there were changes in the expression of genes involved in the determination of cell shape and cell division, including the rod shape determining protein MreB. Upregulation of this gene is generally associated with cell elongation. We also analyzed the expression of the gene Amuc_1100, which was found to be involved in host signaling previously. There was no significant alteration in the expression of this genes, or genes in the associated gene cluster. To confirm the applicability of the soy medium to grow *A. muciniphila* for medical applications, we applied both mucus medium grown and soy medium grown bacteria in a preclinical mouse trial. We found no significant differences in the efficacy of both groups on the fat mass gain and general weight gain of mice fed a high fat diet.

In chapter 5 we zoom in on the oxygen tolerance of the anaerobic bacterium *A. muciniphila.* We discovered that *A. muciniphila* is able to tolerate ambient air for 24 hours. Subsequently, we investigated influence of small amounts of oxygen on *A. muciniphila* growth. The addition of oxygen increased the growth rate and yield, with small changes in the acetate:propionate ratio. This indicated that the oxygen was used as electron acceptor. By using transcriptome analysis we identified a candidate cytochrome bd, which could mediate respiration with oxygen as electron acceptor. We expressed the two subunits of this cytochrome in the cytochrome deficient *Escherichia coli* ECOM4. The metabolism of this transgenic *E. coli* ECOM4-Cytbd was changed, resembling the native metabolism of *E. coli.* Finally, we proved that the oxygen reduction was at least partly heme dependent. With the addition and omission of heme in a heme deprived synthetic medium, we observed the partial loss of oxygen reduction capacity.

In chapter 6 of this thesis, we describe a method for protecting *A. muciniphila* during ingestion. We encapsulated the cell in a water in oil in water double emulsion. We determined the changes of the emulsion during simulated digestion tests. The emulsion coagulated into large oil droplets in the low pH phase simulating the stomach. During coagulation, the cell remained entrapped inside the emulsion. Upon entry of the intestinal phase with the presence of bile and pancreatic extracts, we observed digestion of the emulsion and release of the bacteria. We determined the survival of bacteria encapsulated in the double emulsion and compared it with the survival of cells freely dispersed in PBS. We found a 100 fold higher survival of the encapsulated cells. We concluded that the double emulsion could be an effective matrix for the viable delivery of *A. muciniphila.*

To conclude this thesis, we discussed all the findings in chapter 7. The application of *A. muciniphila* has been made possible by the development of the media described in this thesis. This allows detailed study of this bacterium *in vitro* and *in vivo*. The *in vivo* intervention studies are especially important in moving from correlations to causalities and mechanistic insight in the microbiome. We also provide a preview of what can be expected in future *A. muciniphila* research. A hypothesis is described for the production of the neurotransmitter γ-aminobutyric acid (GABA), based on the *A. muciniphila* GEM. GABA is a potential mediator in the gut-brain axis, which is currently being investigated intensely. We show the first steps that were taken in the development of a genetic system for *A. muciniphila*, with the possible isolation of a bacteriophage. The final steps required for the application of *A. muciniphila* as therapeutic microbe are described shortly, and are all within reach.

Samenvatting

In hoofdstuk 1 van deze thesis wordt de huidige kennis van de darmflora geïntroduceerd, gevolgd door de kennis over *Akkermansia muciniphila.* Het maagdarmstelsel is een complex ecosysteem waarin zowel goede als ziekteverwekkende bacteriën leven. Deze bacteriën hebben sterke invloed op de gezondheid van de gastheer, die op zijn beurt de samenstelling van de bacteriën beïnvloed. Factoren die invloed hebben op de microbiële compositie zijn dieet, gezondheid van de gastheer, leeftijd, geslacht, en de omgeving in het algemeen. De slijmlaag of mucus laag waar *A. muciniphila* leeft wordt gekenmerkt door de nabijheid van de darmcellen van de gastheer. De mucus dat wordt geproduceerd door de gastheer voorziet deze bacterie van zowel koolstof als stikstof. Het potentiele belang van *A. muciniphila* als onderdeel van de darmflora wordt veroorzaakt door de lage aanwezigheid van deze bacterie in mensen met verschillende ziektes. Daarnaast worden muizen die met een vetrijk dieet minder dik als ze *A. muciniphila* krijgen toegediend.

In hoofdstuk twee beschrijven we het gebruik van metabole modellen voor de studie van de genetische en metabole potentie van de darmflora soorten en fenotypen die invloed hebben op de gastheer. We benadrukken het belang van het groeien van bacteriën en voorzien in een kader waarbinnen de modellen gebruikt kunnen worden voor de ontwikkeling van minimale groei media. Metabole modellen zijn belangrijk geweest in de ontwikkeling van minimale media voor *Faecalibacterium prausnitzii*, en probiotische melkzuurbacteriën. Als het mogelijk is om bacteriën in reincultuur te groeien, is het ook mogelijk de fenotypen in verschillende condities te bestuderen. Dit maakt het ook mogelijk de interacties tussen soorten te bestuderen, waardoor metabole modellen met meerdere soorten gemaakt kunnen worden. Deze complexe modellen hebben succesvol bijgedragen aan het voorspellen van de invloed van dieet op de gastheer en op de darmflora.

Het gebruik van metabole modellen voor de ontwikkeling van minimaal groeimedium is toegepast in hoofdstuk 3. Het minimale medium dat in dit hoofdstuk beschreven wordt is gebaseerd op een bestaand metabool model. We ontdekten dat de suikers n-acetylglucosamine (GlcNAc) of n-acetylgalactosamine (GalNAc) en het aminozuur L-threonine de essentiële ingrediënten zijn voor de groei van *A. muciniphila.* Het metabole model voorspelde de noodzaak van L-threonine, maar niet de noodzaak van GlcNAc of GalNAc. We ontdekten dat een enzym ontbrak dat de omzetting van fructose-6-fosfaat naar

glucosamine-6-fostfaat mogelijk zou maken. Deze omzetting is een belangrijke stap in de synthese van peptidoglycaan. Het enige enzym dat deze functie zou kunnen vervullen, NagB, bleek een voorkeur te hebben voor de deaminerende richting van de reactie. Deze ontdekking was toegevoegd aan het metabole model, wat resulteerde in de correcte voorspelling voor de noodzaak van GlcNAc.

De samenstelling van het minimale medium is gebruikt voor de ontwikkeling van een groeimedium wat geen dierlijke componenten bevat, zoals beschreven in hoofdstuk 4. De toevoeging van soja eiwitten zorgde voor de toename van groei snelheid en opbrengst, en de omissie van dierlijke componenten maakt het medium geschikt voor de toepassing in mensen. We observeerden veranderingen in de morfologie van de bacteriën met lichtmicroscopie en elektronenmicroscopie. De cellen waren significant langer in vergelijking met bacteriën die gegroeid waren in mucus medium. Om te achterhalen waardoor deze verandering veroorzaakt wordt, hebben we transcriptie analyse toegepast. We ontdekten dat genen die betrokken zijn in de bepaling van de bacterie vorm anders tot expressie kwamen. Eén van deze genen was de staafvormig bepalend gen MreB. Een hogere expressie van dit gen wordt geassocieerd met een langere cel vorm. We hebben ook de expressie van het gen Amuc_1100 geanalyseerd, omdat dit gen belangrijk is in de communicatie met de gastheer. We ontdekten geen significante verschillen in de expressie van dit gen. Om te bevestigen dat het soja medium gebruikt kan worden voor medische toepassingen, hebben we de verschillen tussen bacteriën gegroeid in mucus medium en soja medium getest in muizen. We hebben geen significante verschillen gevonden tussen de muizen in de toename van vetmassa en lichaamsgewicht.

In hoofdstuk 5 beschrijven we de zuurstoftolerantie van de anaerobe bacterie *A. muciniphila.* We ontdekten dan *A. muciniphila* 24 uur lang zuurstof kan tolereren. Daarna onderzochten we de invloed van kleine hoeveelheden zuurstof op *A. muciniphila* groei. De toevoeging van zuurstof zorgt voor een toename van groei snelheid en opbrengst, met kleine verschillen in de acetaat:propionaat ratio. Dit wijst erop dat zuurstof wordt gebruikt als elektronen acceptor. Door gebruikt te maken van transcriptie analyse ontdekten we dat cytochroom bd gebruikt kan worden in de respiratie van zuurstof. We brachten de twee onderdelen van cytochroom bd tot expressie in *Escherichia coli* ECOM4. Het metabolisme van transgene *E. coli* ECOM4-Cytbd veranderde en leek meer op het originele *E. coli* metabolisme. Tot slot hebben we

bewezen dat de reductie van zuurstof ten minste deels afhankelijk is van haem. Met de toevoeging en omissie van haem in een synthetisch medium ontdekte we het gedeeltelijke verlies van de capaciteit om zuurstof te reduceren.

In hoofdstuk 6 van deze thesis beschrijven we een methode om *A. muciniphila* te beschermen tijden ingestie. We verpakten de bacteriën in een water in olie in water dubbele emulsie. We bepaalden de veranderingen van de emulsie tijdens een gesimuleerde vertering. De emulsie coaguleerde in grotere oliedruppels in de lage pH fase waarin de maag gesimuleerd werd. Tijdens deze fase bleven de cellen in de binnenste water fase van de emulsie. Nadat de emulsie werd blootgesteld aan gal en alvleesklier extracten, observeerden we de afbraak van de emulsie en de vrijlating van de cellen. We bepaalden de overleving van verpakte bacteriën in vergelijking met bacteriën in PBS. We ontdekten dat er 100 keer meer van de verpakte bacteriën de vertering overleefden. We concluderen dat een dubbele emulsie een effectieve matrix kan zijn voor de toepassing van *A. muciniphila.*

Om deze thesis af te sluiten bespraken we alle ontdekkingen on hoofdstuk 7. De toepassing van *A. muciniphila* is mogelijk gemaakt door de ontwikkeling van de groei media die beschreven zijn in deze thesis. Dit maakte het mogelijk deze bacterie in detail te bestuderen, zowel *in vivo* als *in vitro.* De *in vivo* interventiestudies zijn van speciaal belang voor de bepaling van causaliteit en verkrijgen van mechanistisch inzicht in de darmflora. We beschrijven ook wat er verwacht kan worden van onderzoek naar *A. muciniphila* in de toekomst. We hypothetiseren dat de neurotransmitter γ-aminobutyric acid (GABA) geproduceerd kan worden door *A. muciniphila.* GABA speelt een rol in de verbinding tussen de darmen en de hersenen, waar tegenwoordig veel onderzoek naar gedaan wordt. We beschrijven de eerste stappen die we genomen hebben in de genetische modificatie van *A. muciniphila*, met de mogelijke isolatie van een bacteriofaag. De laatste stappen die nog nodig zijn voor de toepassing van *A. muciniphila* zijn kort beschreven, en zouden op korte termijn realiseerbaar moeten zijn.

About the author

Cornelis Henricus (Kees) van der Ark, was born in Berkel en Rodenrijs, The Netherlands, on April 5th, 1988. He obtained his Bachelor of Science degree in biotechnology in 2012 and his Master of Science degree in medical biotechnology in 2013 at the Wageningen University and Research centre. During his study, Kees was a member of the student council and the central council of the Wageningen University and Research centre in the academic year 2009-2010. He was the team captain of the 2012 Wageningen iGEM team, which was rewarded with the price for the best presentation during the European competition and advanced to the world finals at the Massachusetts Institute of Technology.

Kees was given the opportunity to study the growth and application of *Akkermansia muciniphila* in an attempt to obtain his PhD degree by Dr. Clara Belzer and Prof. Dr. Willem M. de Vos, which resulted in the presented work. During this period, Kees remained involved in the iGEM competition as supervisor of the 2014 and 2016 Wageningen teams, which resulted in two second places in the world finals.

Picture by Sven Menschel

Currently, the author is employed at the Amsterdam Intitule for Global Health and Development and the Academic Medical Centre in Amsterdam. At the department of Medical Microbiology he is studying the zoonotic potential of the pig pathogen *Streptococcus suis*.

Acknowledgements

This thesis was not just the work of one, but of many. I would like to acknowledge the help I received and cooperation I enjoyed over the past years, starting at the beginning.

Clara and Willem, thank you for giving me the opportunity to perform research in your group. Your supervision and help during the past years have been essential in obtaining the results presented in this thesis. I appreciate the fast communication without losing the scientific focus. It was a pleasure working with you and I feel privileged to have been part of the A-team. The other members of this team I would like to thank as well. Noora and Janneke, without your help during the first years of my thesis, life would have been much harder. Steven, thank you for your help in the lab and in improving the setup of experiments. Especially the willingness to take over experiments at any time, or helping out with large experiments was much appreciated. I would also like to thank you and Hugo for being my paranymphs.

I would also like to acknowledge the work and input from the students that were involved in the research, also if the experiments didn't work out as expected. So, Tijs, Teresa, Tamirat, Wouter, Sharon, Avis and Che, thank you for all the help.

Most chapters presented in this thesis are the result of very fruitful and pleasant cooperation. Ruben, thank you for saving the review we ended up writing together. Nico, thank you for sharing your knowledge on the functional expression of transmembrane proteins. Tom, thank you for helping with running and repairing the fermentors. Hubert and Patrice, thank you for testing our favourite bacterium in mice and brining these experiments to the best result possible. Claire and Karin, thank you for taking initiative in our almost too easy cooperation and joining forces in getting the project to a good end. Maria and Peter, thank you for your much needed help in applying and improving the metabolic model.

I would also like to thank all members of the Molecular Ecology group for their feedback during group meetings.

Besides the work presented in this thesis, I was also involved as supervisor with the iGEM team. The results of the teams were amazing, and would not have been possible without the

enthusiasm of the team's students and supervisors. Thank you all for the wonderful discussions, ideas and presentations during these projects.

Finally, I would like to thank all friends and family for providing the needed distraction during the past years. Especially one person, who has been in the frontline and fortunately but not coincidentally understood the struggles of scientific research, deserves a special place. The final words are for you, thank you Marcelle.

List of Publications

Adaptation of Akkermansia muciniphila to the oxic-anoxic interface of the mucus layer, *Applied And Environmental Microbiology*, Ouwerkerk, J.P.*, **van der Ark, K.C**.*, Davids, M., Claassens, N.J., Robert Finestra, T., de Vos, W.M., and Belzer, C. (2016)

A purified membrane protein from Akkermansia muciniphila or the pasteurized bacterium improves metabolism in obese and diabetic mice, *Nature medicine* **23**: 107-113. Plovier, H., Everard, A., Druart, C., Depommier, C., Van Hul, M., Geurts, L., Chilloux, J., Ottman, N., Duparc, T., Lichtenstein, L., Myridakis, A., Delzenne, N. M., Klievink, J., Bhattacharjee, A., **van der Ark, C. H.**, Aalvink, S., Martinez, L. O., Dumas, M., Maiter, D., Loumaye, A., Hermans, M. P., Thissen, J.-P., Belzer, C., de Vos, W. M., Cani, P. D., et al. (2017)

More than just a gut feeling: Constraint-based genome-scale metabolic models for predicting functions of human intestinal microbes, *Microbiome, 2017* ***5****:78* **Kees C.H. van der Ark***, Ruben G.A. van Heck*, Vitor A. P. Martins Dos Santos, Clara Belzer, Willem M. de Vos (2017)

Encapsulation of the therapeutic microbe Akkermansia muciniphila in a double emulsion enhances survival in simulated gastric conditions. *Food Research International,* **Kees C. H. van der Ark**, Avis Dwi Wahyu Nugroho, Claire Berton-Carabin, Che Wang, Clara Belzer, Willem M. de Vos, Karin Schroen (2017)

Model-driven design of a minimal medium for Akkermansia muciniphila confirms mucus adaptation, *Microbial Biotechnology*, **van der Ark, K.C.,** Aalvink, S., Plovier, H., Cani, P.D., Belzer, C., and De Vos, W.M. (Submitted)

Overview of Completed training activities

Discipline specific activities - meetings

Gut Day, Gut Flora Foundation, Rotterdam, The Netherlands 2013

Gut Day, Gut Flora Foundation, Groningen, The Netherlands 2014

Gut Day, Gut Flora Foundation, Venlo, The Netherlands 2016

KNVM Scientific Spring meeting, KNVM, Arnhem, The Netherlands 2013

KNVM Scientific Spring meeting, KNVM, Arnhem, The Netherlands 2014

KNVM Scientific Spring meeting, KNVM, Arnhem, The Netherlands 2016

Finnish Gut Day, University of Helsinki, Helsinki, Finland 2013

FEMS 2017, 7th congress of European Microbiologists, FEMS, Valencia, Spain 2017

Discipline specific activities - courses

Genetics and physiology of food-associated micro-organisms, VLAG, Wageningen, The Netherlands 2016

The Intestinal Microbiome and Diet in Human and Animal Health, VLAG, Wageningen, The Netherlands 2014

General courses

VLAG PhD week, VLAG, Baarlo, The Netherlands 2013

Data Management, WGS/Library Wageningen UR, Wageningen, The Netherlands 2016

Scientific Writing, WGS / Wageningen in'to Languages, Wageningen, The Netherlands 2014

Philosophy and Ethics of Food Science and Technology, WGS, Wageningen, The Netherlands 2014

Career Orientation, WGS, Wageningen, Netherlands 2016

Optionals

Preparing Project Proposal, VLAG 2013

AIO/Postdoc meeting, Laboratory of Microbiology 2013-2017

Workgroup meetings MolEco, Laboratory of Microbiology 2013-2017

PhD Trip 2015, Laboratory of Microbiology, California, USA 2015

WEES seminars, WEES, Wageningen, Netherlands 2013-2014

Colophon

The research described in this thesis was financially supported the Advanced Research Grant 250172 (MicrobesInside) of the European Research Council and the Spinoza Award and the SIAM gravitation grant 024.002.002 of the Netherlands Organization for Scientific Research.

Printing: Digiforce, Vianen